ISSN 0110—3326

RESEARCH REPORT

DESIGN OF CONCRETE STRUCTURES

Joint University of Canterbury New Zealand Concrete Society Seminar

R. Park, T. Paulay, M. J. N. Priestley and L. Gaerty

July 1986 86-14

Department of Civil Engineering

University of Canterbury
Christchurch New Zealand

CALCULATIONS

ALAN M. REAY
CONSULTING ENGINEER
CHRISTCHURCH

PAGE
SECT
FILE
DATE

SHEAR WALLS

In determining overstength.

effective width of comp. flange = .5 h_w

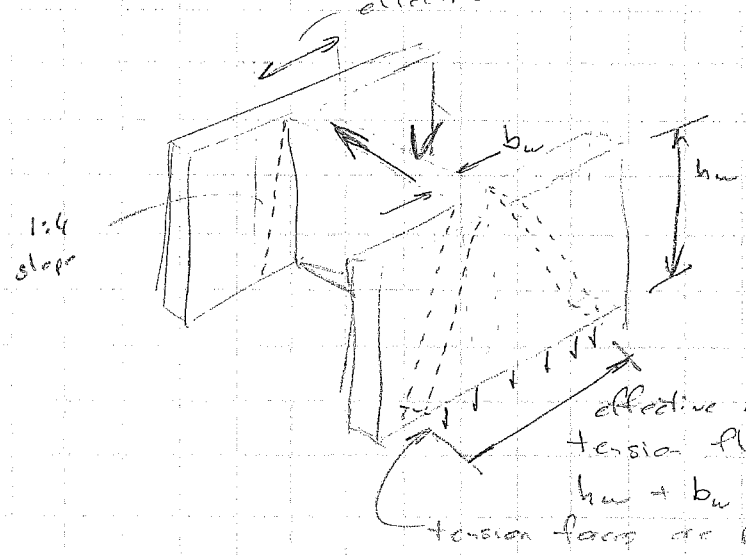

effective width of tension flange:
$h_w + b_w$

tension forces are spread up at at a slope of 1:2
Compression forces at $\frac{1}{2}$ this rate

DESIGN OF CONCRETE STRUCTURES

Joint University of Canterbury
New Zealand Concrete Society Seminar
Organised by the Department of Civil Engineering
of the University of Canterbury
Christchurch

July 9 to 11, 1986

The seminar offers a state-of-the-art covering of the design of concrete structures with particular emphasis on the requirements for seismic loading. Topics considered to be well established are covered only briefly during the seminar, while in the other areas, particularly where more recent research information has come to hand, an extended treatment is offered.

The seminar is planned to assist engineers to become more familiar with the New Zealand Standard Code of Practice for the Design of Concrete Structures NZS 3101:1982 and its applications. In some sessions of the seminar the presentations will be similar to those given in the seminars on NZS 3101:1982 organised in 1983 by the New Zealand Concrete Society. For this reason Technical Report No. 2 of the New Zealand Concrete Society, entitled "Applications of the New Zealand Standard Code of Practice for the Design of Concrete Structures, NZS 3101:1982", which includes a number of design examples, will be found useful.

This volume contains special notes which will be used in some of the sessions. The collection of papers, most of which have been published in different journals and conference proceedings, summarises findings of recently concluded research projects or presents up to date state-of-the-art reports in specific areas. The extensive bibliography provides opportunities for further studies.

Lecturers

R. Park, Professor of Civil Engineering
University of Canterbury, Christchurch

T. Paulay, Professor of Civil Engineering
University of Canterbury, Christchurch

M.J.N. Priestley, Reader in Civil Engineering
University of Canterbury, Christchurch

L. Gaerty, Assistant Director, New Zealand Concrete
Research Association, Porirua

CONTENTS

DUCTILE DESIGN APPROACH FOR REINFORCED CONCRETE FRAMES

R. Park

DUCTILE DESIGN APPROACH FOR REINFORCED CONCRETE FRAMES

Robert Park, M.EERI

In the design of multistorey moment-resisting reinforced concrete frames to resist severe earthquakes the emphasis should be on good structural concepts and detailing of reinforcement. Poor structural concepts can lead to major damage or collapse due to column sidesway mechanisms or excessive twisting as a result of soft storeys or lack of structural symmetry or uniformity. Poor detailing of reinforcement can lead to brittle connections, inadequate anchorage of reinforcement, or insufficient transverse reinforcement to prevent shear failure, premature buckling of compressed bars or crushing of compressed concrete. In the seismic provisions of the New Zealand concrete design code special considerations are given to the ratio of column flexural strength to beam flexural strength necessary to reduce the likelihood of plastic hinges forming simultaneously in the top and bottom of columns, the ratio of shear strength to flexural strength necessary to avoid shear failures in beams and columns at large inelastic deformations, the detailing of beams and columns for adequate flexural strength and ductility, and the detailing of beams, columns and beam-column joints for adequate shear resistance and bar anchorage. Differences exist between current United States and New Zealand code provisions for detailing beams and columns for ductility and for the design of beam-column joints.

1. INTRODUCTION

It is well known that when a structure responds elastically to ground motions during a severe earthquake, the maximum response acceleration may be several times the maximum ground acceleration and depends on the stiffness of the structure and the magnitude of the damping. For example, Fig. 1 shows the maximum acceleration response of a simple structure in the form of a single degree of freedom oscillator responding elastically to typical North American earthquake ground motions. Generally it is uneconomical to design a structure to

---

Department of Civil Engineering
University of Canterbury
Christchurch, New Zealand.

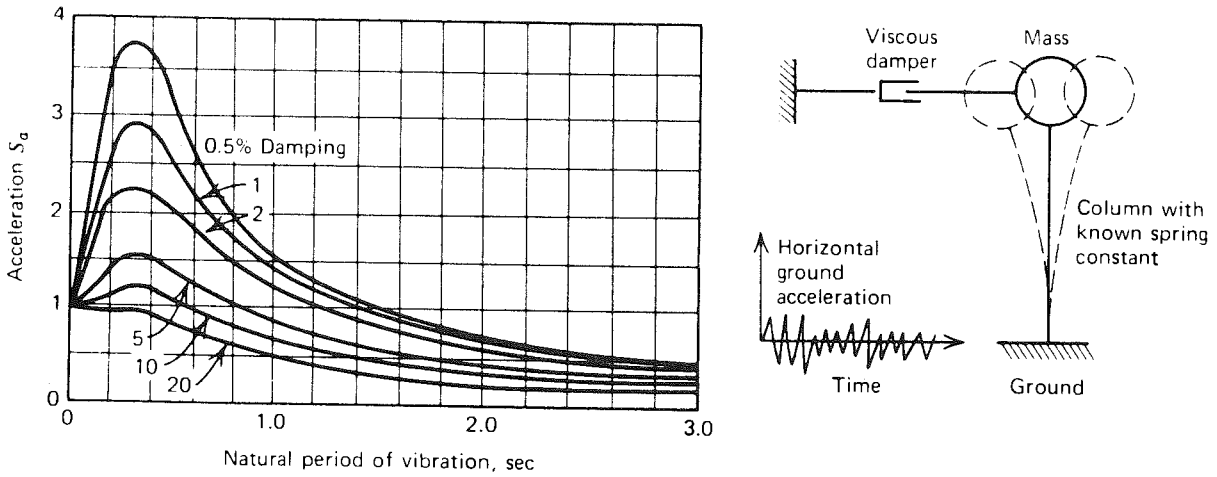

Figure 1 : Design Spectrum Giving Acceleration as a Function of Damping and Period of Vibration for a Single Degree of Freedom Oscillator Responding Elastically to Typical North American Earthquake Ground Motions.

respond in the elastic range to the greatest likely earthquake induced inertia forces. As a result, the design seismic horizontal forces recommended by codes are generally much less than the elastic response inertia forces induced by a major earthquake.

Experience has shown that structures designed to the level of seismic horizontal forces recommended by codes can survive major earthquake shaking. This apparent anomaly has been attributed mainly to the ability of well designed structures to dissipate seismic energy by inelastic deformations, helped by such other factors as reduced response due to decrease in stiffness and soil-structure interaction. Fig. 2 illustrates the lateral load-deflection response of an oscillator which is not strong enough to resist the full elastic response inertia load elastically and develops a plastic hinge with elasto-plastic characteristics. Because of the inelastic behaviour of the plastic

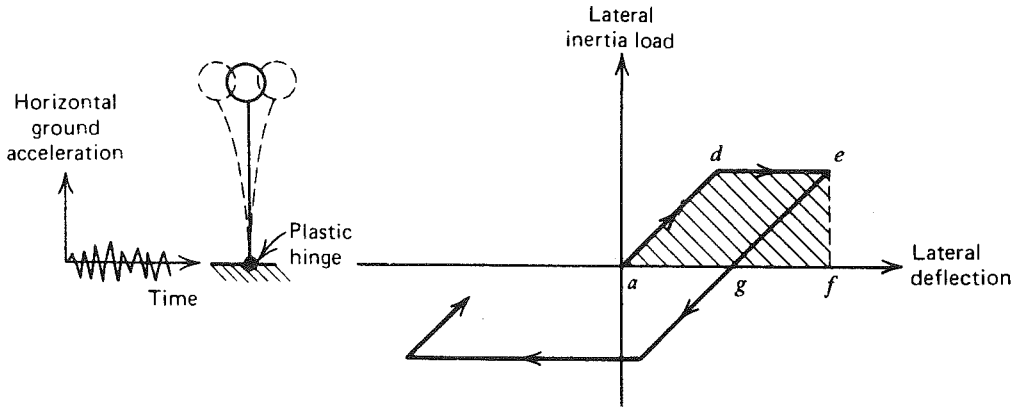

Figure 2 : Elasto-plastic Response of Ocillator to Earthquake Ground Motions.

hinge the maximum deflection of the elasto-plastic structure may not necessarily be much greater than that of the structure if behaving elastically. It is evident that use of the level of static seismic design loads recommended by codes implies that the critical regions of those members should have sufficient ductility to enable the structure to survive without collapse when subjected to several cycles of loading well into the inelastic range. This means avoiding all forms of brittle failure and achieving adequate ductility by flexural yielding of members.

The importance of good detailing of steel reinforcement in earthquake resistant reinforced concrete structures cannot be overemphasized. Significant protection against damage will be provided by carefully detailed reinforcement. As well as serving the normal function of providing resistance to tensile and compressive forces in concrete elements and their connections arising from bending, shear and normal forces, steel reinforcement is necessary to prevent compressed bars from buckling and to provide confinement to concrete in highly stressed areas of compression. Detailing should be based on a thorough understanding of the behaviour of reinforced concrete, thus ensuring that the requirements of all the internal forces in the structure are considered from the point of view of the serviceability, strength and ductility of the structure.

This paper will summarize developments in the ductile design approach for reinforced concrete frames subjected to seismic loading.

2. GENERAL PRINCIPLES OF DUCTILE DESIGN APPROACH

2.1 Design Strength and Ductility

It is evident that since it is generally uneconomical to design a structure to withstand the greatest likely earthquake without damage, the cost of providing strength must be weighed against the likely damage. The criteria for the level of loading of most seismic codes are as follows: buildings should be able to resist minor earthquakes without damage, to resist moderate earthquakes without structural damage but possibly with some nonstructural damage, and to resist major earthquakes without collapse but possibly with some structural and nonstructural damage. Hence the possibility of damage caused by a major earthquake is accepted, but not loss of life. The definitions of minor, moderate and major earthquakes vary from country to country. In many countries, for example New Zealand, only one level of earthquake load is considered in design, the level being that corresponding to a major earthquake.

In setting the levels of design static seismic loading, codes also have to consider the associated post-elastic deformations of the structure designed to that strength. Nonlinear dynamic analyses of code designed multistorey structures responding to typical major earthquake ground motions have given an indication of the order of post-elastic deformations, and hence the "ductility factor" required. However the number of variables involved in such analyses is so great that no more than qualitative statements concerning ductility demand can be made. For example, the type of ground motion has a considerable influence. Nevertheless some general conclusions can be drawn.

A measure of the ductility required of a structure is the displacement ductility factor μ defined as

$$\mu = \Delta_u/\Delta_y \qquad (1)$$

where Δ_u = maximum horizontal deflection of the structure during severe earthquake shaking, generally measured either at the top of the structure or at the point of action of the resultant horizontal seismic load.

Δ_y = horizontal deflection at that point of the structure at first yield.

A number of dynamic analyses have indicated that the maximum horizontal deflection reached by a structure, which is not strong enough to resist the full elastic response inertia load and yields with elasto-plastic load-deflection characteristics, may be approximately the same as that of a structure which is strong enough to respond in the elastic range. This "equal maximum deflection" response is illustrated in Fig. 3. The comparison is for structures with the same initial stiffness, the same percentage of critical viscous damping, and responding to the same major earthquake.

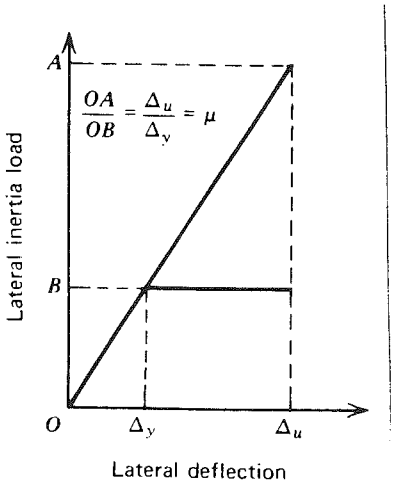

Figure 3 : Equal Maximum Deflection Response of Elastic and Elasto-plastic Structures to Earthquake Ground Motions.

Typically seismic codes assume an available displacement ductility factor of about μ = 3 to 5 for ductile frame structures and the design loads can be regarded as being approximately $1/\mu$ of the elastic response inertia loads. However the actual design spectrum used for seismic loading does not follow the exact shape of the spectrum shown in Fig. 1 but may be of trilinear or some other shape. Also the equal maximum displacement concept may not be particularly accurate for small periods of vibration. For small-period structures the maximum deflection reached during elasto-plastic response may be considerably greater than that reached during elastic response. Also the particular earthquake ground motion record will affect the comparison of elasto-plastic and elastic response. Hence the real displacement ductility demand on a structure may be quite different from code assumed values.

2.2 Structural Configuration

As far as possible the structural configuration of a building should have symmetry and uniformity.

The arrangement of the seismic load resisting elements in a building should, as nearly as is practicable, be located symmetrically about the

centre of mass of the building. This requirement is in order to minimize the torsional response of the structure during an earthquake. Unsymmetrical structural arrangements, for example, walls enclosing a service core at one end of the building only which is structurally connected to the remainder of the building, can result in significant twisting about the vertical axis of the building and hence lead to greater ductility demand on some parts of the structure than for symmetrical arrangements. Such twisting may become critical for the overall stability of the building. Furthermore, due to numerous uncertainties, the actual behaviour of an unsymmetrical building structure is difficult to predict, even with elaborate computer models. Note that the participation of nonstructural elements in the response of the structure may result in unexpected and undesirable torsional effects. The designer should endeavour to anticipate the influence of nonstructural elements on the response of the structure.

It is undesirable for discontinuities in stiffness and/or strength of the structural system to exist up the height of the building. For example, the absence of some vertical structural elements in one storey of a building can lead to a dangerous concentration of ductility demand in the remaining elements of the storey. Similarly, sudden variations in building plan dimensions up the height of the building can result in equally dangerous large local deformations.

There are many examples of severe earthquake damage occurring in reinforced concrete buildings as a result of poor structural configurations. Fig. 4a shows the Macuto Sheraton Hotel which suffered very severe structural damage during the 1967 Venezuela earthquake, as well as damage to tile infill walls [1]. The building had a poor structural feature - an abrupt change of stiffness from frames to structural walls above the mezzanine floor. This more flexible and less strong portion under the structural walls led to a concentration of inelastic strains and energy dissipation in this portion. Figs. 4b and c show typical compression and shear failures which occurred in the 1.1 m (43 in) diameter reinforced concrete columns under the shear walls. As another example, Fig. 5a shows part of the main building of the Olive View Hospital which suffered very severe damage during the 1971 San Fernando earthquake [2]. Structural walls were present in the upper storeys but were not present in the first storey. A sidesway mechanism developed in the columns of the first storey resulting in approximately a 0.6m (2 ft) permanent lateral deformation in the tops of those columns after the earthquake. Fig. 5a illustrates the deformations in the first storey. Fig. 5b indicates that the corner columns of that storey, which were only lightly tied, were insufficiently ductile to maintain their load carrying capacity at such large deformations. Fig. 5c shows that the spiral columns of that storey were able to preserve sufficient strength to prevent collapse, the circular spiral being able to effectively confine the concrete and prevent buckling of longitudinal bars. Again the more flexible and less strong portions under the structural walls led to a concentration of deformations in that storey of the building.

2.3 Interstorey Deflections

The horizontal deflection of a structure during an earthquake should not be so large as to cause extensive damage to nonstructural elements.

(a) The hotel building after the earthquake

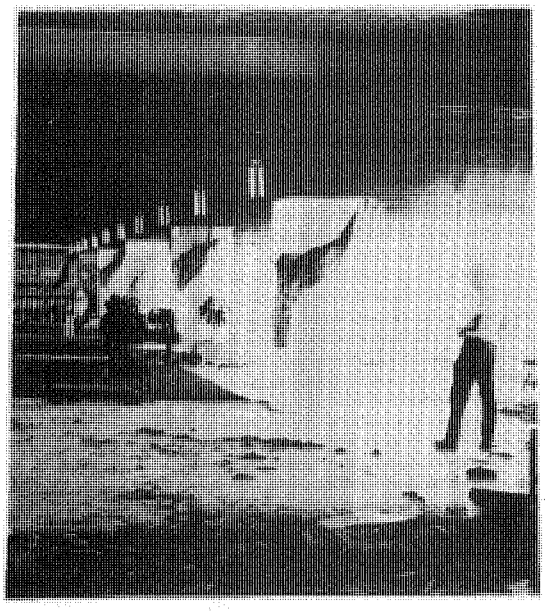

(b) View of failed columns at mezzanine level

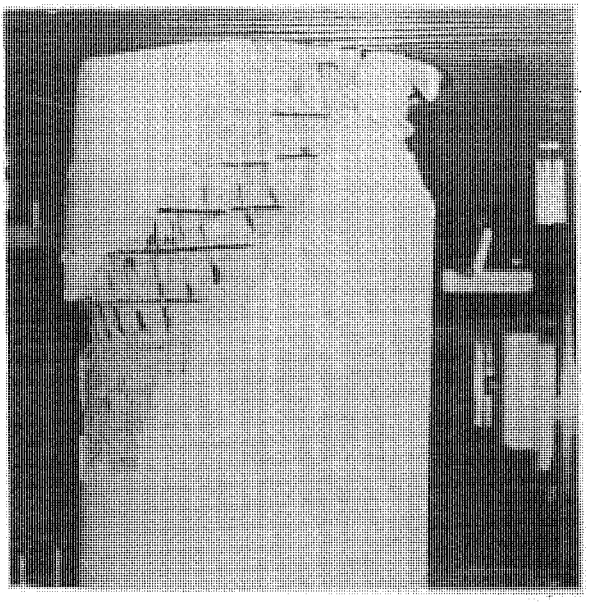

(c) Close up of damage to a column

Figure 4 : Damage to Macuto Sheraton Hotel Caused by the 1967 Venezuela Earthquake [1].

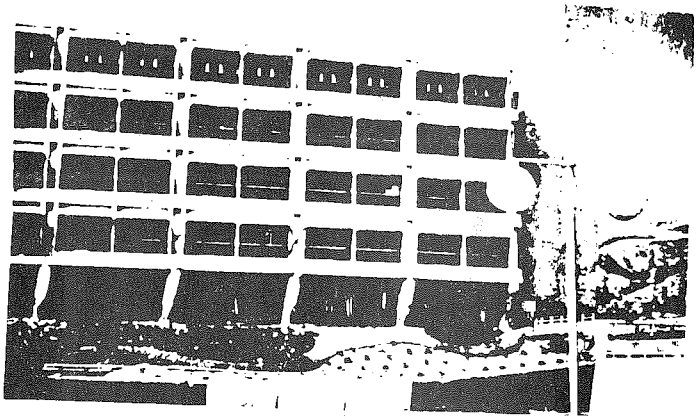

(a) A wing of the hospital building illustrating the sidesway deformations in the columns of the first storey

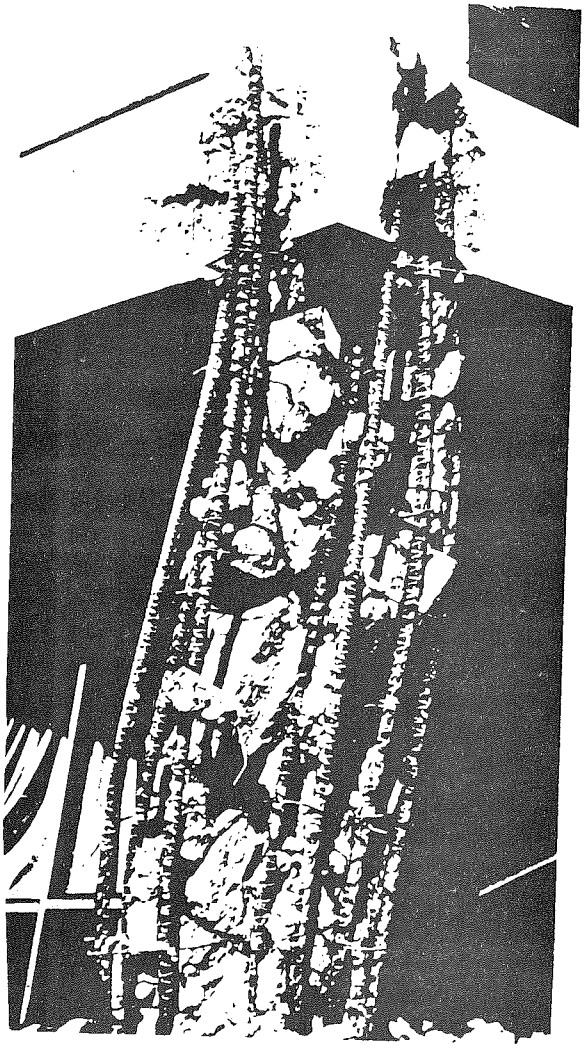

(b) Shattered column with inadequate tie reinforcement

(c) Core of spiral column maintaining load carrying capacity

Figure 5 : Damage to Olive View Hospital Building Caused by 1971 San Fernando Earthquake [2].

Also, large horizontal deflections result in high PΔ moments in the structure, where P is the column compressive load and Δ is the horizontal deflection of the column, which could lead to a significant reduction in the ability of the structure to resist further seismic loading. Codes normally place limits on the interstorey deflections to control damage and PΔ effects.

2.4 Achieving Adequate Ductility in Structural Systems

The exact characteristics of the earthquake ground motions that may occur at a given site cannot be predicted with certainty and the analytical modelling of some aspects of the behaviour of complete building structures is still open to question. Hence it is impossible to evaluate all aspects of the complete behaviour of a reinforced concrete building when subjected to very large seismic disturbances. Nevertheless it is possible to impart to the structure features that will ensure the most desirable behaviour. In terms of damage, strength and ductility (including energy dissipation) this means ensuring a desirable sequence in reaching the strengths of the various modes of resistance of the structure. It implies a desired heirarchy in the failure modes of the structure.

The rational approach for achieving this aim in earthquake resistant design is to chose the most suitable energy dissipating mechanism for the structure and to ensure by appropriate design procedures that yielding will occur only in the chosen manner during a severe earthquake. For reinforced concrete frames the best means of achieving energy dissipation is by flexural yielding at selected plastic hinges, since with proper design the plastic hinge positions can be made adequately ductile.

The ductility required at a plastic hinge in a yielding structure may be expressed by the curvature ductility factor ϕ_u/ϕ_y, where ϕ_u is the maximum curvature (rotation per unit length) at the critical section and ϕ_y is the curvature at the section at first yield. It should be emphasized that the required curvature ductility factor ϕ_u/ϕ_y at plastic hinge sections will generally be much greater than the required displacement ductility factor Δ_u/Δ_y value for the structure, since once yielding commences further displacement occurs mainly by rotation at the plastic hinges. This aspect of behaviour in the yield range is discussed further below.

For frames, mechanisms which involve flexural yielding at plastic hinges are shown in Fig. 6. If yielding commences in the columns of a frame before the beams, a column sidesway mechanism can form. In the worst case the plastic hinges may form in the columns in only one storey as in Fig. 6b, since the columns of the other storeys are stronger. Such a mechanism can make very large curvature ductility demands on the plastic hinges of the critical storey [3], particularly for tall buildings. The curvature ductility required at the plastic hinges of a column sidesway mechanism may be so large that it cannot be met and in that case collapse of the structure will occur. On the other hand if yielding commences in the beams before in the columns, a beam sidesway mechanism, as illustrated in Fig. 6c, will develop [3], which makes more moderate

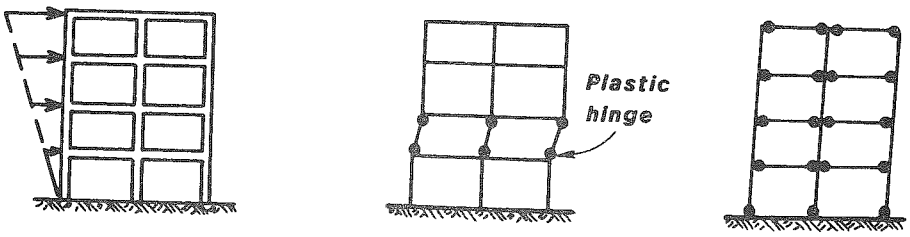

(a) Frame (b) Column sidesway mechanism (c) Beam sidesway mechanism

Figure 6 : Moment Resisting Frames With Horizontal Seismic Loading and Possible Mechanisms.

demands on the curvature ductility required at the plastic hinges in the beams and at the column bases. The curvature ductility demands at the plastic hinges of a beam sidesway mechanism can be met by careful detailing. Therefore for tall frames a beam sidesway mechanism is the preferred mode of inelastic deformation and a strong column-weak beam concept is advocated to ensure beam hinging. For frames with less than about three storeys, and for the top storey of tall frames, the curvature ductility required at the plastic hinges if a column sidesway mechanism develops is not particularly high. Hence for one and two storey frames, and in the top storey of taller frames, a strong beam-weak column concept can be permitted.

The required curvature ductility factor ϕ_u/ϕ_y which should be available at the plastic hinge locations in frames will depend on the many variables involved, such as the geometry of the members and the relative strengths of sections. This required ϕ_u/ϕ_y value for a particular frame can be calculated from the static collapse mechanism [3]. However it would appear that an available ϕ_u/ϕ_y of at least 3 should be provided at potential plastic hinge regions of regular frames, where μ is the required displacement ductility factor.

It should be appreciated that the static collapse mechanisms of Fig. 6 are idealised in that they involve possible behaviour under code type equivalent static seismic loading. The actual dynamic situation is different, due mainly to the effects of higher modes of vibration. Considerations such as in Fig. 6 can only be regarded as providing the designer with a reasonable feel for the situation. In important cases of some unusual structures it may be necessary to use time-history nonlinear dynamic analysis of the structure responding to severe earthquakes to obtain a better indication of the required curvature ductility at the critical plastic hinge sections.

3. NEW ZEALAND GENERAL SEISMIC DESIGN PROVISIONS

3.1 Introduction

The New Zealand general seismic design provisions are contained in a code for general structural design and design loadings for buildings [4]. This code was first published in 1976 and a second edition was

published in 1984. The code sets out the following general seismic design principles.

3.2 Adequate Ductility

Structural systems intended to dissipate energy by ductile flexural yielding should have adequate ductility. Adequate ductility may be considered to have been provided if all primary elements resisting seismic forces are detailed for ductility in accordance with the seismic provisions of the concrete design code [5].

An approximate criteria for adequate ductility, applicable to reasonably regular symmetrical frames without sudden changes in storey stiffness, given in the commentary of the code [4], is as follows: the building as a whole should be capable of deflecting laterally through at least eight load reversals so that the total horizontal deflection at the top of the main portion of the building under the design static seismic loading, calculated on the assumption of appropriate plastic hinges, is at least four times that at first yield, without the horizontal load carrying capacity of the building being reduced by more than 20%. The horizontal deflection at the top of the building at first yield can be taken as that when yield first occurs in any main structural element or that at the design static seismic load calculated on the assumption of elastic behaviour, whichever is the greater.

3.3 Capacity Design

Building frames designed for flexural ductile yielding should be the subject of "capacity design". In the capacity design of earthquake-resistant structures, energy-dissipating elements or mechanisms are chosen and suitably designed and detailed, and all other structural elements are then provided with sufficient reserve strength capacity to ensure that the chosen energy-dissipating mechanisms are maintained throughout the deformations that may occur.

3.4 Concurrent Earthquake Loading Effects

Columns, joints and foundations, which are part of two way frames, should be designed for concurrent earthquake load effects resulting from the simultaneous yielding of all beams in both directions.

3.5 Energy Dissipating Mechanisms

Ductile frames should be capable of dissipating seismic energy in a flexural mode at a significant number of plastic hinges in the beams, except that energy dissipation by column plastic hinge mechanisms is permitted in single or two-storey structures and in the top storey of multistorey structures. Apart from those specific cases, columns should be designed to have adequate strength to avoid column hinge mechanisms, taking into account possible distributions of column moments which may be different from that derived from elastic analysis with code static seismic loading applied and column loads appropriate to the simultaneous formation of plastic hinges in beams in several storeys.

3.6 Interstorey Deflections

For ductile frames in the worst seismic zone the horizontal deflection between two successive floors, computed for the design static seismic loading and assuming that the frame remains elastic, should not exceed 0.0032 of the storey height. In effect this means that, assuming the structure yields at the design static seismic loading, the permitted horizontal deflection at a displacement ductility factor of $\mu = 4$ is 1.3% of the storey height. The permitted interstorey deflection is less than this value if the nonstructural elements are not effectively separated from the structural elements.

4. NEW ZEALAND SEISMIC DESIGN PROVISIONS FOR DUCTILE REINFORCED CONCRETE FRAMES

4.1 Introduction

A considerable amount of research and development into the design of reinforced and prestressed concrete moment resisting frames and structural walls for seismic resistance has been conducted in New Zealand in recent years. The New Zealand seismic design provisions for ductile reinforced concrete frames are contained in a code for the design of concrete structures [5] published in 1982. The design provisions for gravity loading are based mainly on the 1977 building code of the American Concrete Institute. The seismic design provisions are based mainly on the research conducted in New Zealand and elsewhere. Papers resulting from deliberations of discussion groups [6,7,8] organised by the New Zealand National Society for Earthquake Engineering were used as a basis for the seismic provisions of the new code. The emphasis of the code is on good structural concepts and good detailing of reinforcement. It is also recognised that a proper assessment of the strength and ductility of a structure cannot be made using the working stress design method. It is required that the strength design method be used for seismic design.

The critical regions in frames to be designed for seismic resistance are illustrated in Fig. 7. The design actions at those regions and the design of the regions for adequate strength and ductility require the

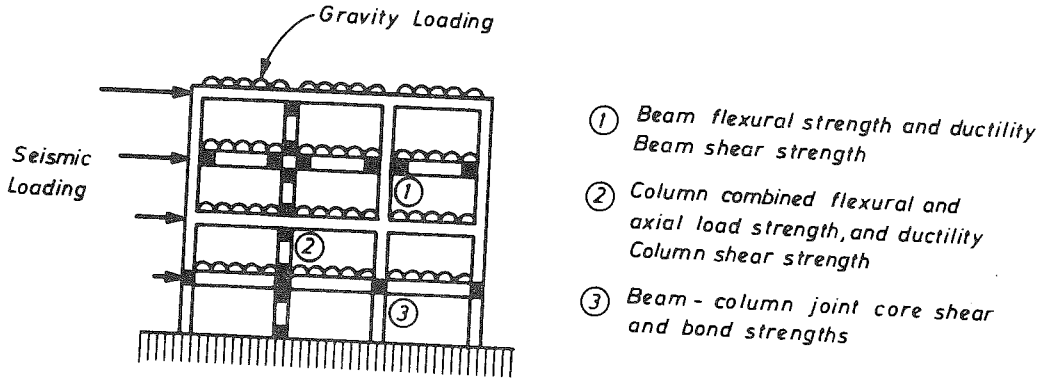

Figure 7 : Critical Regions in Frame Designed for Seismic Resistance.

particular attention of the designer.

The provisions of the concrete design code [5] for the seismic design of ductile reinforced concrete frames, and the background to those provisions, are outlined below.

4.2 Material Behaviour

4.2.1 Steel

Fig. 8 shows stress-strain curves measured for typical steel reinforcing bars under monotonic loading. In practice the actual yield strength of the steel will normally exceed the specified yield strength f_y. Also, in the plastic hinge regions the longitudinal reinforcement may reach strains in the order of 10 or more times the strain at first yield [3] and an increase in steel stress due to strain hardening may occur. The resulting increase in the flexural strength of beams in plastic hinge regions due to these two factors is of concern since it is accompanied by: (a) an increase in the shear forces in the members which could result in brittle failure, (b) an increase in the column moments which could cause a column sidesway mechanism, and (c) an increase in the shear forces in beam-column joints. A capacity design procedure is used to ensure that failure does not occur away from plastic hinge locations during a major earthquake.

In the capacity design procedure it is assumed that the plastic hinge regions develop their maximum likely flexural strength, referred to as "flexural overstrength". It is recommended that the flexural overstrength should be calculated assuming that the actual strength of the longitudinal reinforcing steel is $1.25f_y$ when f_y = 275 MPa (40 ksi) and $1.40f_y$ when f_y = 380 MPa (55 ksi), where f_y = specified yield strength of the reinforcing steel. These are the two grades of reinforcing steel in common use in New Zealand. The overstrength moment at plastic hinges takes into account both the actual steel yield strength being greater than specified and the effect of strain hardening at high strains. The higher overstrength factor for Grade 380 steel is due to the earlier strain hardening of that steel (see Fig. 8). The beams and joint shears and column actions used in design are the maximum likely values calculated on the basis of the overstrength beam actions.

Fig. 9a and b show stress-strain curves measured for reinforcing steel under cyclic loading. The "rounding" of the stress-strain curve during the loading reversals in the inelastic range due to the Bauschinger effect is of interest. This reduction in the tangent modulus of the steel at relatively low compressive stresses during reversed loading makes the buckling of compression steel more likely than would be expected in monotonic load tests. It is recommended that to prevent premature buckling of reinforcing bars during cycles of reversed loading the centre to centre spacing of transverse reinforcement restraining the longitudinal bars should not exceed six longitudinal bar diameters in the potential plastic hinge region of members.

Fig. 9a shows measured stress-strain behaviour for cyclic stressing with strain mainly in the tensile range. This cyclic strain history would

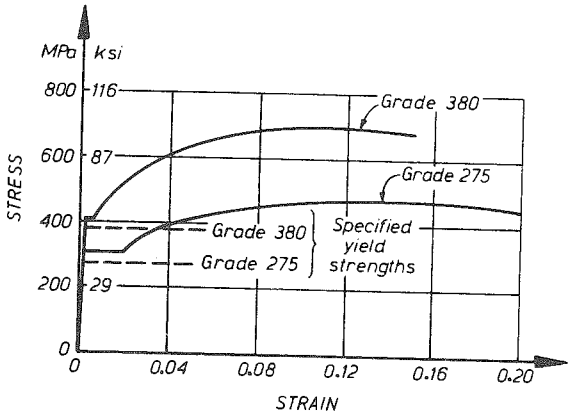

Figure 8 : Stress-Strain Relations for Typical Reinforcing Steel With Monotonic Loading.

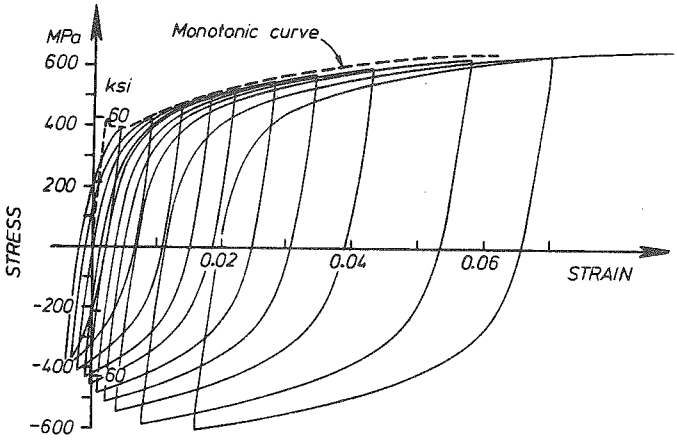

(a) Grade 380 ($f_y \geq 55$ ksi) reinforcing steel with unsymmetrical strain cycles.

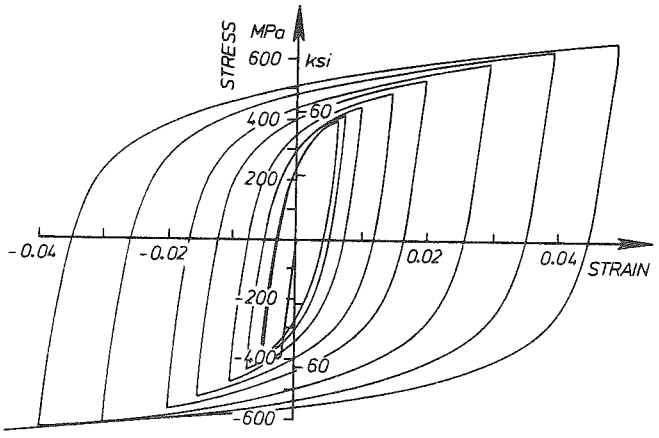

(b) Grade 380 ($f_y \geq 55$ ksi) reinforcing steel with symmetrical strain cycles.

Figure 9 : Stress-Strain Relations for Typical Reinforcing Steel With Cyclic Loading.

be typical of a longitudinal reinforcing bar in a beam during cyclic flexure where, since the neutral axis is close to the extreme compression fibre of the beam section, the steel strains in compression would be much smaller than the steel strains in tension. The stress-strain curve for monotonic loading is also shown in Fig. 9a. For the type of cyclic strain history shown in the figure it is evident that the monotonic stress-strain relation with origin at the original position gives a satisfactory envelope for the cyclic stress-strain behaviour of reinforcing steel in beams. Hence overstrength factors for beams can be based on monotonic stress-strain relations for the reinforcing steel.

Fig. 9b shows the results for cyclic stressing with gradually increasing symmetrical straining in the tension and compression range. This strain history would be typical of a longitudinal reinforcing bar in a building column during cyclic flexure with high axial load in which the neutral axis is close to mid-depth of the column section. The particular specimen in Fig. 9b was yielded in compression first. It is evident that symmetrical straining of the type shown in Fig. 9b results in a build up of steel stress to stress levels which are much greater than that given by the monotonic stress-strain curves with the origin in the original position. The build up of steel stress for this type of loading with increasing strain amplitudes is particularly high for steel which strain hardens early. Hence overstrength factors for columns used in design may need to be greater than those used for beams.

4.2.2 Concrete

In order to achieve ductile plastic hinge behaviour it is essential to avoid sudden failure of the concrete when it reaches its compressive strength. Concrete can be made to act in a ductile manner by providing adequate transverse confining reinforcement in the form of arrangements of spirals, hoops, stirrup ties or cross ties. The concrete becomes confined when at strains approaching the unconfined strength the transverse strains become very high and the concrete bears out against the transverse reinforcement which then applies a passive confining pressure. The strength and ductility of concrete is considerably improved by confinement. The confinement arises because of arching of the concrete between the transverse bars and the longitudinal bars. The cover concrete, including that concrete outside the arching forces, is not confined and will be lost as in the case of unconfined concrete.

It is evident from Fig. 10 that the confinement of concrete is improved if the transverse reinforcement is placed at relatively close spacing, and if there are a number of longitudinal bars well distributed around the column section and ties across the section, because then the arches between the bars are shallower and hence more of the concrete section is confined. It is recommended that in the potential plastic hinge regions of columns the centre to centre spacing of sets of transverse confining reinforcement should not exceed 0.2 of the smaller cross section dimension or 200 mm (7.9 in), whichever is smaller, and the spacing between tied longitudinal bars in columns with rectangular hoops should not exceed 200 mm (7.9 in).

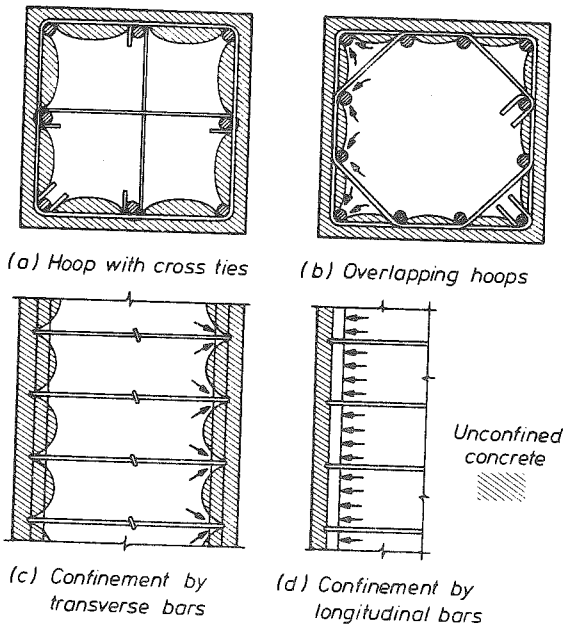

Figure 10 : Confinement of Concrete by Reinforcement.

4.3 Design of Beams

4.3.1 Beam Dimensions

To prevent lateral instability of beams, particularly after a reduction in stiffness resulting from cyclic flexure in the inelastic range, the dimensions of T and L beam members to which moments are applied at both ends should be such that

$$\ell_n/b_w \leqq 37 \qquad (2)$$

$$\ell_n h/b_w^2 \leqq 150 \qquad (3)$$

where ℓ_n = clear span, h = overall depth and b_w = width of web. For beams with rectangular cross sections the limitations on the right hand side of Eqs. 2 and 3 should be reduced to two-thirds of the values shown. These equations are approximations based on the theory for lateral instability of beams [3].

Also, to keep the longitudinal beam reinforcement reasonably close to the column core for effective moment transfer, the width of the beam web should not be more than the width of the column plus a distance each side of the column equal to one quarter of the overall depth of the column.

4.3.2 Design Moments

The design moments in beams should be calculated by elastic frame analysis for the code seismic and gravity loadings and the factored (ultimate) load combinations. Moment redistribution from the derived moment envelope may be used to gain a more advantageous design moment envelope and thus allow a more efficient design of the beam. The amount of moment redistribution permitted for any span of a beam forming part of a continuous frame should not exceed 30% of the maximum elastic moment derived for that span for any combination of design earthquake and gravity loading. The modified moments are used to calculate moments elsewhere in the span. This is, static equilibrium between the internal forces and the external loads must be maintained.

4.3.3 Plastic Hinge Regions

The plastic hinge regions are considered to extend over a length equal to twice the beam overall depth (2h) in the vicinity of the maximum moment sections, as illustrated in Fig. 11.

4.3.4 Longitudinal Reinforcement

The sections are designed for flexure by strength theory using a strength reduction factor $\phi = 0.9$.

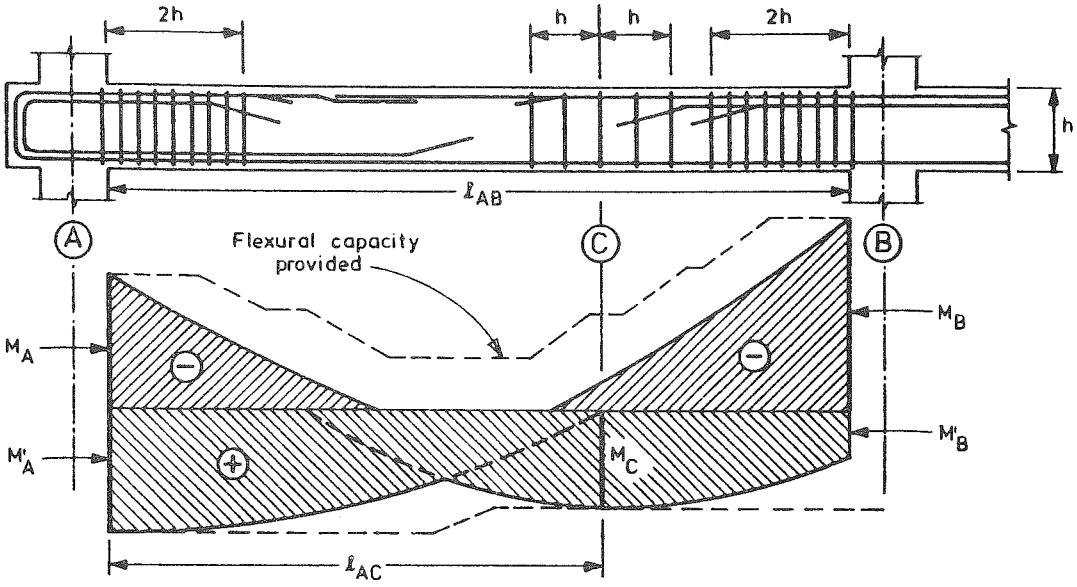

Figure 11 : Localities of Plastic Hinge Regions in Typical Beam and Bending Moment Envelope Due to Design Seismic Plus Gravity Loading [5].

In order to ensure ductile flexural behaviour during reversed loading at any section with a plastic hinge region:

(a) Tne tension steel ratio should not be greater than

$$\rho = \frac{1 + 0.17\left(\frac{f'_c}{7} - 3\right)}{100}\left(1 + \frac{\rho'}{\rho}\right) \qquad (4)$$

$$\text{or } \rho = 7/f_y \qquad (5)$$

whichever is smaller, where $\rho = A_s/b_w d$, $\rho' = A'_s/b_w d$, A_s = area of tension reinforcement, A'_s = area of compression reinforcement, b_w = width of beam web, d = effective depth of beam, f'_c = concrete compressive cylinder strength (MPa), and f_y = steel yield strength (MPa), where 1 MPa = 145 psi.

(b) The compression steel should be such that

$$A'_s \geq 0.5A_s \qquad (6)$$

The upper limit on ρ, as given by Eq. 5, is 2.55% for Grade 275 ($f_y \geq 40$ ksi) steel and 1.84% for Grade 380 ($f_y \geq 55$ ksi) steel. Generally the requirements of Eq. 4 will govern the maximum permitted ρ. For example if f'_c = 25 MPa (3,630 psi) and $\rho'/\rho = 0.5$, Eq. 4 gives $\rho = 1.65\%$ for both Grade 275 and Grade 380 steel. Eqs. 4 and 5 are plotted for Grades 275 and 380 steel in Fig. 12.

Note that these maximum permitted ρ values are more severe than currently allowed in the United States. For example, the seismic provisions of the ACI building code [9] permit $\rho = 2.5\%$ to be used.

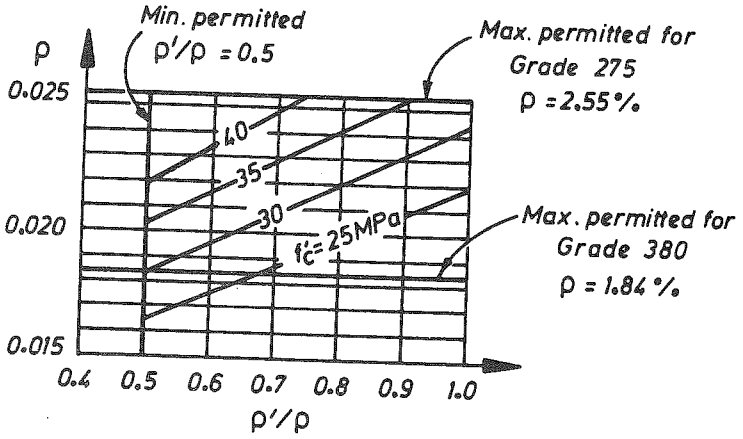

Figure 12 : Maximum Tension Steel Ratios for Beams (1 MPa = 145 psi) [5].

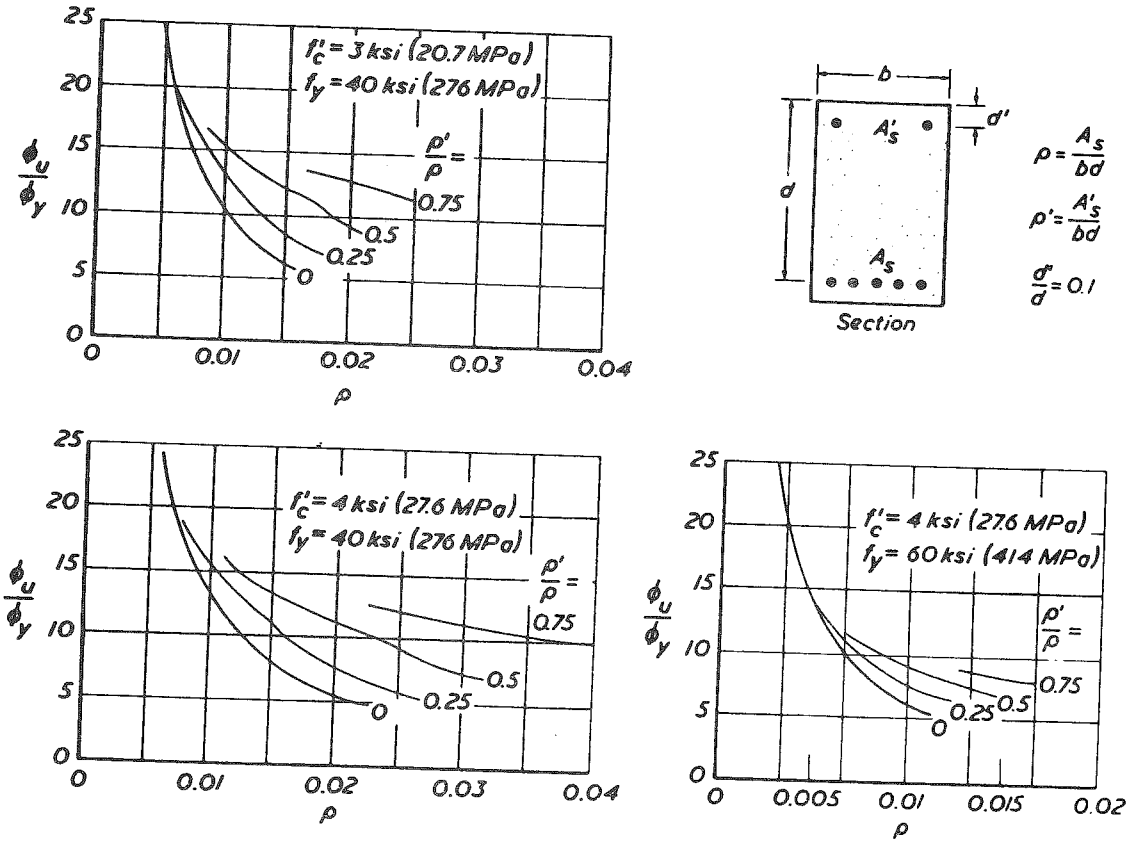

Figure 13 : Variation of Curvature Ductility Factor ϕ_u/ϕ_y for Doubly Reinforced Beam Section Assuming an Extreme Fibre Concrete Compressive Strain of 0.004 [3]

Fig. 13 shows the available curvature ductility ϕ_u/ϕ_y for a range of doubly reinforced rectangular concrete beam sections calculated assuming an extreme fibre concrete compressive stress of 0.004 [3]. The figure illustrates the increase in available ϕ_u/ϕ_y when ρ decreases and ρ'/ρ increases. The importance of the section containing a reasonable proportion of compression steel is evident from the figure and is recognised by the code requirement that $A'_s \geq 0.5A_s$.

From Fig. 13 it can be determined that the use of Eqs. 4 to 6 will result in a curvature ductility factor ϕ_u/ϕ_y of at least 12 being available for a rectangular section reinforced with Grade 275 ($f_y \geq 40$ ksi) steel when an extreme fibre concrete compressive strain of 0.004 is reached. It is to be noted that at that curvature there would be significant flexural cracking of concrete but no significant crushing of the compressed concrete. For sections with the same ρ, the available ϕ_u/ϕ_y when Grade 380 ($f_y \geq 55$ ksi) steel is used will be less than when Grade 275 steel is used.

Outside the plastic hinge regions at least two reasonable size longitudinal reinforcing bars should exist in both the top and bottom of the beam throughout its length. The top reinforcement should be not less than one quarter of the top reinforcement at either end and the bottom reinforcement should not be less than $\rho = 1.4/f_y$, where f_y = specified yield strength of the longitudinal reinforcement (MPa, where 1 MPa = 145 psi). This is to allow for unexpected deformations and moment distributions which may occur during major earthquakes.

In T and L beams built integrally with slabs the slab longitudinal reinforcement placed within the shaded areas shown in Fig. 14 should be considered to participate in resisting the negative moments at the supports of continuous beams. The widths of slab considered effective in Fig. 14 depend on whether the column is interior or exterior and whether transverse beams exist. The widths shown are conservative estimates of the effectiveness of force transfer from the slab bars to the joint core. During large inelastic displacement of the frame it is likely that there will be a contribution from slab bars at larger distances from the column than shown in Fig. 14.

Splices in longitudinal reinforcement in beams should not be located within beam-column joint cores or within twice the effective depth of the beam from the critical section of a plastic hinge in a beam. This is because of the possible degradation of anchorage during cycles of severe seismic loading.

4.3.5 Transverse Reinforcement to Prevent Premature Buckling of Longitudinal Reinforcement and to Confine Compressed Concrete

In potential plastic hinge regions where moment reversal may cause the longitudinal bars to yield both in compression and tension at each face of the beam (for example, the end regions of Fig. 11), the maximum permitted centre to centre spacing of stirrup ties is 150 mm (5.9 in) or d/4 or six longitudinal bar diameters, whichever is least, where d = effective depth of beam.

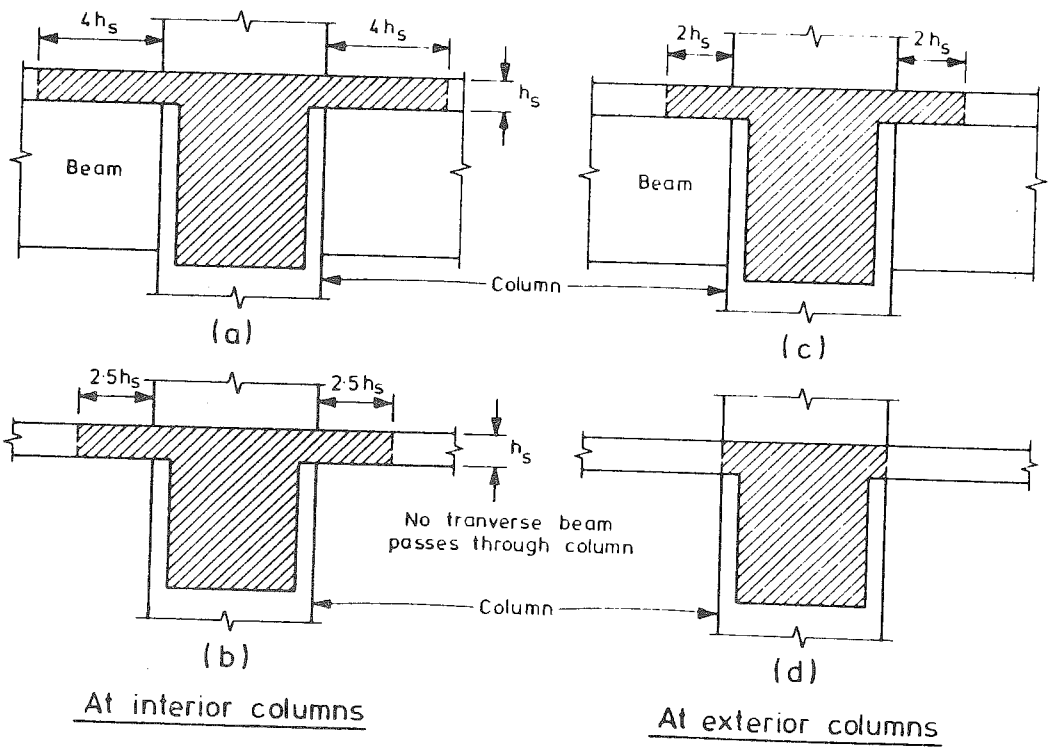

Figure 14 : Longitudinal Steel in Shaded Area to be Included in the Flexural Strength of the Beam at Column Face [5].

In potential plastic hinge regions of beams where yielding of longitudinal bars occurs only for one direction of moment (for example, the region C of Fig. 11) the maximum permitted centre to centre spacing of stirrup ties is 200 mm (7.9 in) or d/3 or twelve longitudinal bar diameters, whichever is least.

The above difference in the required spacing of transverse reinforcement is because premature buckling of longitudinal reinforcement can be prevented by wider spacing when yielding occurs only in compression. When yielding occurs in both tension and compression there is a reduction in the tangent modulus of the steel at low stress levels which makes the bars more prone to buckle (see Fig. 9). It is considered that the above recommended spacing of transverse reinforcement is also adequate to provide some confinement to the concrete in the compression zone. In beam the prevention of premature buckling of compression steel is a more important requirement than the confinement of concrete.

It is also necessary to ensure that an adequate quantity of stirrup ties are present in potential plastic hinge regions to provide the necessary lateral forces to the longitudinal steel to prevent premature buckling. It is recommended that the area of one leg of a stirrup tie should be not less than

$$A_{te} = \frac{1}{16} \frac{\Sigma A_b f_y}{f_{yh}} \frac{s}{100} \quad (mm^2) \qquad (7)$$

where ΣA_b = sum of areas of longitudinal bars reliant on the tie (mm^2), f_y = yield strength of longitudinal reinforcement (MPa), f_{yh} = yield strength of transverse reinforcement (MPa) and s = centre to centre spacing of ties (mm). (1 mm = 0.039 in, 1 MPa = 145 psi). This requirement is illustrated in Fig. 15 for the case where s = 100 mm (3.9 in).

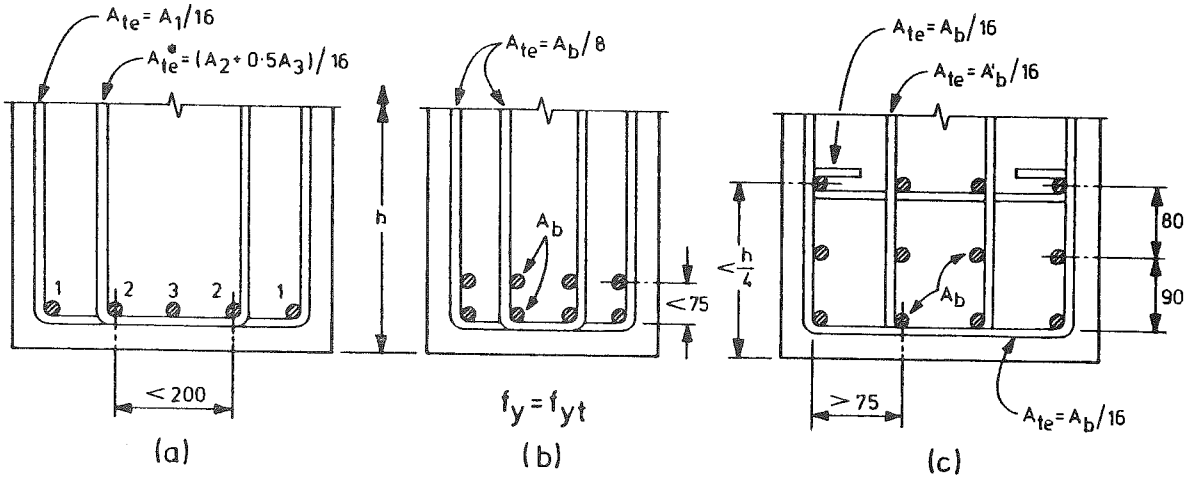

Figure 15 : Arrangement and Size of Stirrup Ties in Potential Plastic Hinge Regions of Beams [5] (Dimensions in mm, 1 mm = 0.039 in).

Note that the New Zealand requirements for the spacing of transverse reinforcement are more severe than currently recommended in the United States. The ACI code [9] in its seismic provisions requires that in potential plastic hinge regions the spacing of stirrup ties should not exceed d/4, eight longitudinal bar diameters, 24 transverse bar diameters and 12 in (305 mm), where d = effective depth of beam, whichever is least.

Outside the plastic hinge regions the detailing requirements are similar to those for gravity loading, but stirrup spacing should not exceed d/2, where d = effective depth of beam.

4.3.6 Transverse Reinforcement for Shear

The design shear force in beams should be determined by a capacity design procedure for when the flexural overstrength is reached at the most probable plastic hinge locations within the span and the factored gravity load is present. For example, for the beam in Fig. 11 the design shear force at B will be

$$V_{uB} = \frac{M'_{oA} + M_{oB}}{\ell_{AB}} + \frac{w\ell_{AB}}{2} \qquad (8)$$

where M'_{oA} and M_{oB} are the flexural overstrength capacities of the sections

for positive moment at A and negative moment at B, and w is the factored uniform dead and live load considered to be present per unit length. The flexural overstrength capacities are calculated using the overstrength factors for the reinforcing steel discussed in Section 4.2.1.

Since the design shear forces are found from the assumed flexural overstrengths, it is reasonable for the design of sections for shear to be carried out using a strength reduction factor ϕ for shear of 1.0. However it has been found from tests [3] that reversed flexure in plastic hinge regions causes a degradation of the shear carried by the concrete shear resisting mechanisms of aggregate interlock, dowel action and across the compression zone. Therefore it is required that shear reinforcement, normally in the form of vertical stirrups, should be provided to carry the total shear force in plastic hinge regions. Thus the area of vertical stirrup in plastic hinge regions is given by

$$A_v = \frac{V_u s}{d f_{yh}} \quad (mm^2) \tag{9}$$

where V_u = design shear force (N), s = centre to centre spacing of stirrups (mm), d = effective depth of beam (mm), and f_y = yield strength of stirrups (MPa) (where 1 N = 0.225 lb , 1 mm = 0.039 in, 1 MPa = 145 psi).

Also, tests [3] have demonstrated that full depth flexural cracks can exist in the plastic hinge regions, as well as inclined diagonal tension cracks, during much of the reversed loading range. This is because when longitudinal steel yields in tension for loading in one direction, open cracks will be present in the concrete "compression" zone when the load is applied in the opposite direction. These cracks will remain open until that steel yields in compression and allows the cracks to close and the concrete to carry some compression (see Fig. 16). Thus for parts of the loading cycles the bending moment will be carried by a steel couple alone. If the shear stress at the section is high a sliding shear deformation can occur along a full depth vertical crack (see Fig. 16) and the load-deflection hysteresis loop for the structure will become "pinched", resulting in reduced energy dissipation. To avoid a sliding shear failure and loss of energy dissipation, inclined shear reinforcement (for example, bent up bars), is required in plastic hinge regions when the shear stresses to be carried are high. Therefore it is recommended that the design shear forces are resisted only by vertical stirrups if

$$\frac{V_u}{b_w d} \leq 0.3\ (2 + r)\sqrt{f'_c} \quad (MPa) \tag{10}$$

where V_u = design shear force (N), b_w = web width of beam (mm), d = effective depth of beam (mm), f'_c = concrete compressive cylinder strength (MPa) and r = ratio at the plastic hinge section of the maximum shear force developed with positive moment hinging to the maximum shear force developed with negative moment hinging, always taken as negative (where 1 N = 0.225 lb, 1 mm = 0.039 in, 1 MPa = 145 psi). For higher values of $V_u/b_w d$ than permitted by Eq. 10, diagonal shear reinforcement should be

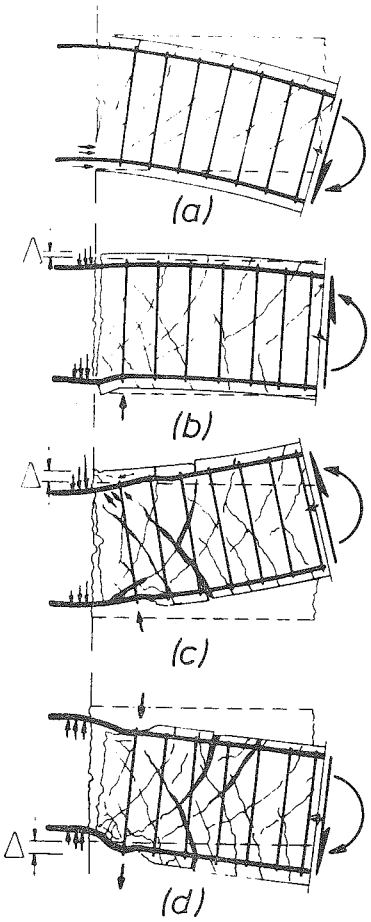

Figure 16 : Significant Stages of Development of Plastic Hinge During Cyclic Flexure With High Shear [10].

provided across the web in the plastic hinge region in one or both directions to resist a specified proportion of the shear force.

Outside the plastic hinge regions the shear may be considered to be carried by both transverse reinforcement and the concrete shear resisting mechanisms, and the shear reinforcement may be designed by the shear strength equations used for gravity load design.

4.4 Design of Columns

4.4.1 Design Moments and Axial Loads

A strong column-weak beam concept is adopted for frames with more than two storeys, in order to prevent as far as possible column sidesway mechanisms occurring during a major earthquake. To achieve this aim a capacity design approach is used to determine the design actions for the columns. In this approach the column bending moments found from elastic frame analysis for the code factored (ultimate) load combinations are amplified to take into account:

(1) The flexural overstrength at the beam plastic hinges, which results in higher moments being applied to the columns.

(2) The higher mode effects of dynamic loading, which can cause much higher column moments than calculated from the code static seismic loading which is based on mainly a first mode response. Nonlinear dynamic analyses have shown that in frames, due to higher modes of vibration, the points of contraflexure may occur well away from the mid-height of columns at various stages during an earthquake [3]. For example Fig. 17 shows a possible bending moment distribution in a column at an instant during an earthquake. It is evident that the total beam input moment $M_{b1} + M_{b2}$ may have to be resisted almost entirely by one column section, rather than be shared almost equally between the column sections above and below the joint as would be implied by the bending moment diagrams obtained using the code static seismic loading.

(3) The greater column moments in a two-way frame caused by the possible simultaneous yielding of beams in two directions due to seismic loading acting in a general (skew) direction and having components of load along both principal axes of the structure. For example, for the symmetrical building shown in Fig. 18, if a displacement ductility factor of 4 is reached in direction 2, it only requires $\Delta_1 = \Delta_2/4$ to cause yielding in direction 1 as well, and this occurs when θ is only 14°. Thus yielding

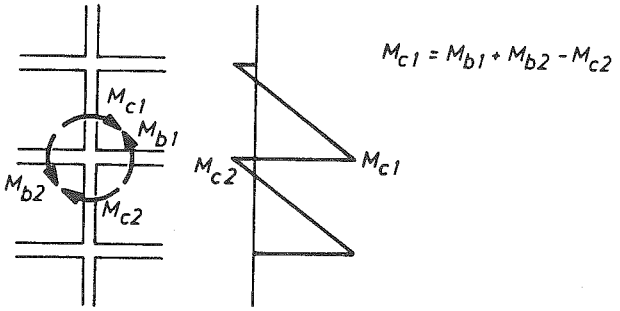

Figure 17 : Possible Column Moments During Dynamic Response.

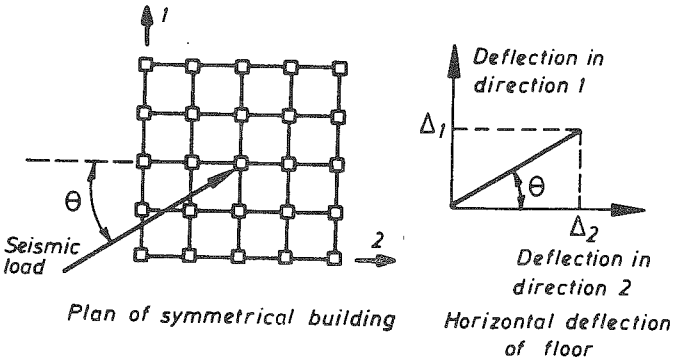

Figure 18 : General Direction of Earthquake Loading on Building.

in the beams in both directions may occur simultaneously for much of the seismic loading, and for a structure with beams of equal strength in each direction, the resultant beam moment input applied biaxially to the columns is $\sqrt{2}$ times the uniaxial beam moment input. Also biaxial bending will generally reduce the flexural strength of the column. Typically the flexural strength of a square column for bending about a diagonal may be 15% less than the flexural strength for uniaxial bending [3]. Therefore concurrent earthquake loading may cause the columns to yield before the beam unless columns are strengthened to take this effect into account.

It is evident that column flexural strengths much greater than the bending moments derived from the code static seismic loading are needed if plastic hinges in columns are to be avoided. The difficulty of preventing plastic hinges from forming in columns is such that some column yielding must be considered to be inevitable. The degree of protection of columns against plastic hinging is a debatable issue and needs to be approached on a probabilistic basis.

A method for the evaluation of column actions in ductile multistorey frames due to Paulay [6] has been placed in the Commentary of the code [5]. This procedure is aimed at giving reasonable protection against column yielding. In the procedure, the design uniaxial bending moment for the column, acting separately in each of the two principal directions of the structure, is given by

$$M_{col} = \phi_o \omega M_{code} \qquad (11)$$

where M_{code} = column moment at the beam centre line derived from the code static seismic loading and to be reduced as indicated by the moment gradient to give the column moment at the beam face,

ϕ_o = ratio of overstrength flexural capacity of the beams as detailed to the dependable moment capacity required by

the code ≧ 1.25/0.9 = 1.39 for Grade 275 (f_y ≧ 40 ksi) steel reinforcement,

ω = factor allowing for higher mode and concurrent load effects given for one-way frames as

$$\omega = 0.6T_1 + 0.85 \qquad (12)$$

but not less than 1.3 or more than 1.8, and for two-way frames as

$$\omega = 0.5T_1 + 1.0 \qquad (13)$$

but not less than 1.5 or more than 1.9, where T_1 = fundamental period of vibration of the structure.

Note that for two-way frames the columns are designed for uniaxial bending only, since ω includes some moment enhancement to make allowance for the effect of biaxial bending. The values of ω are based on dynamic analyses and judgement [6].

The design axial loads in columns P_{col} to be used with M_{col} for section design should be derived from the shear forces applied at the column faces by the gravity loads from the beams and the moment induced shears from the beam plastic hinge moments in both directions acting at flexural overstrength, except that a reduction in the moment induced shears is allowed to take into account the probability that not all beam plastic hinges have reached their overstrength up the height of the frame.

The maximum design axial load in columns is limited to $0.7f'_cA_g$ or $0.7P_o$, which ever is greater, where f'_c = concrete compressive cylinder strength, A_g = gross area of column section, and P_o = axial (concentric) load strength of column, since the ductility of very heavily loaded columns may be small even with extensive confining steel.

The column sections are designed for P_{col} and M_{col} by strength theory assuming a strength reduction factor ϕ = 1.0, since the design actions are maximum probable values.

It is evident that the multiplier $\phi_o\omega$ in Eq. 11 can vary from a minimum of 1.39 x 1.3 = 1.81 to much higher values. By comparison the approach of the seismic appendix of the ACI code [9] is to require the sum of the moments at the centre of the joint corresponding to the design flexural strength of the columns at the joint to be at least equal to 6/5 times the sum of the moments at the centre of the joint corresponding to the design flexural strength of the beams at the joint. If a strength reduction factor ϕ of 0.75 is assumed for the columns and 0.9 for the beams, this requirement involves a multiplier of 1.2 x 0.9/0.75 = 1.44. Note that in the New Zealand approach ϕ = 1.0 is assumed for the columns and the effect of ϕ = 0.9 for the beams is already included in $\phi_o\omega$, and hence the ACI multiplier of 1.44 can be compared directly with the New Zealand multiplier of 1.81 or greater.

4.4.2 Potential Plastic Hinge Regions

The length of the potential plastic hinge regions in the ends of columns to be confined is dependent on the magnitude of the ratio of $P_e/\phi f'_c A_g$, where P_e = column load in compression due to the design gravity and seismic loading, ϕ = strength reduction factor = 0.9 for confined members or 1 for confined members protected by capacity design, f'_c = concrete compressive cylinder strength, and A_g = gross area of column cross section. When $P_e \leq 0.3\phi f'_c A_g$, the potential plastic hinge region is taken as the longer column section dimension in the case of a rectangular section or the diameter in the case of a circular section, or where the moment exceeds 0.8 of the maximum moment at that end of the member, which ever is larger. When $P_e > 0.3\phi f'_c A_g$, the potential plastic hinge region is increased by 50%. This increase is because tests in New Zealand have shown that at high axial load levels the plastic hinge region tends to spread along the column because the flexural strength at the critical section is enhanced by the larger confining steel content. Thus flexural failure could occur in the less heavily confined adjacent regions of columns unless the heavy confining steel is spread over a longer length of the column.

4.4.3 Longitudinal Reinforcement

The area of longitudinal reinforcement should not be less than $0.008A_g$, nor greater than $0.06A_g$ for Grade 275 ($f_y \geq 40$ ksi) steel or $0.045A_g$ for Grade 380 ($f_y \geq 55$ ksi) steel, where A_g = gross area of column cross section. In potential plastic hinge zones the longitudinal bars should not be spaced further apart than 200 mm (7.9 in) between centres.

In a column the centre of a splice is required to be within the middle quarter of the column height, unless it can be shown that plastic hinging cannot develop at the column end.

Tests in New Zealand [11] have shown that lap splices should not be placed in plastic hinge regions of columns. To develop the lap in a plastic hinge region subjected to cyclic flexure requires a large amount of transverse reinforcement. If sufficient transverse reinforcement is available to transfer the longitudinal bar force satisfactorily, it was found that there is an undesirable concentration of curvature at the critical section which could lead to low cycle fatigue of the longitudinal steel there. The restricted length of plastic hinge occurs because yielding concentrates in only a small length of bar near the end of the lap at the end of the member. Therefore lap splices should be positioned away from the plastic hinge regions.

4.4.4 Transverse Reinforcement to Prevent Premature Buckling of Longitudinal Reinforcement and to Confine Compressed Concrete

(a) Spacing of Transverse Reinforcement in Potential Plastic Hinge Regions of Columns

For both circular and rectangular shaped transverse reinforcement, the centre to centre spacing in the longitudinal direction of the column in potential plastic hinge regions is required not to exceed the smaller of one-fifth of the least lateral dimension of the cross section, six

longitudinal bar diameters, or 200 mm (7.9 in).

For rectangular hoops the centre to centre spacing between hoop legs or supplementary cross ties across the section should not exceed 200 mm (7.9 in). Also, longitudinal bars should not be spaced further apart between centres than 200 mm (7.9 in).

For rectangular hoops, each longitudinal bar or bundle of bars should be laterally supported by a corner of a hoop having an included angle of not more than 135° or by a cross tie, except that longitudinal bars are exempted from this requirement if either:

(1) they lie between two bars supported by the same hoop where the distance between the laterally supported bars does not exceed 200 mm (7.9 in) between centres, or

(2) they lie within the concrete core of the section centred more than 75 mm (3.0 in) from the inner face of the hoop.

In addition, for rectangular hoops the yield force in the hoop bar or cross tie shall be at least one-sixteenth of the yield force of the longitudinal bar or bars it is to laterally restrain, including the contribution by any bar or bars excempted above from the direct support.

With regard to the limits on longitudinal spacing of transverse reinforcement, the one-fifth of the least column lateral dimension requirement is to ensure that the bars are close enough to effectively confine the compressed concrete and the six longitudinal bar diameter requirement is to ensure that premature buckling of compressed longitudinal reinforcing bars does not occur. The ACI code [9] requires the spacing of transverse reinforcement not to exceed one-quarter of the minimum member dimension or 4 in (102 mm).

Fig. 19, taken from the Commentary of the New Zealand code [5], illustrates typical arrangements of transverse reinforcement in potential plastic hinge regions of rectangular columns.

(b) Anchorage of Transverse Reinforcement in Potential Plastic Hinge Regions of Columns

It is required that transverse steel should be anchored by at least a 135° hook around a longitudinal bar plus an extension of at least eight transverse bar diameters at the free end of the bar into the core concrete of the member. Alternatively, the ends of the bars should be welded.

Note that the loss of concrete cover in the plastic hinge region, as a result of the cover concrete spalling during plastic hinge rotation, means that the transverse steel must be carefully detailed. It is inadequate to lap splice a spiral or a circular hoop in the cover concrete. If the cover concrete spalls the spiral or circular hoop will be able to unwind (as was observed in some bridge piers in the 1971 San Fernando earthquake [2]). Therefore if the transverse bars are lapped in the cover concrete full strength welds are required at the laps. Similarly, rectangular hoops and cross ties should be anchored either by bending the ends back into the core of the column or by welding.

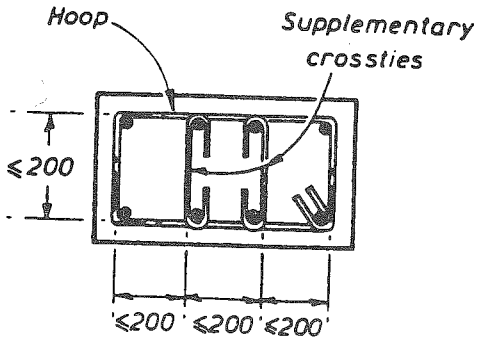

Single hoop plus two supplementary cross ties bent around longitudinal bars.

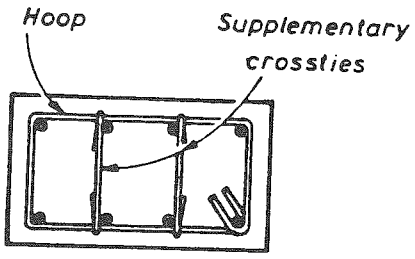

Single hoop plus two supplementary cross ties bent around hoop.

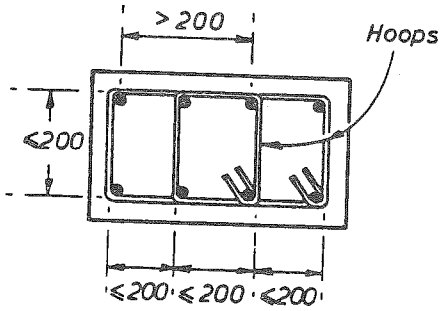

Two overlapping hoops - preferred detail

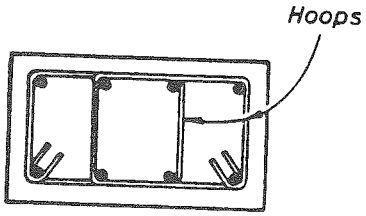

Two overlapping hoops - not preferred

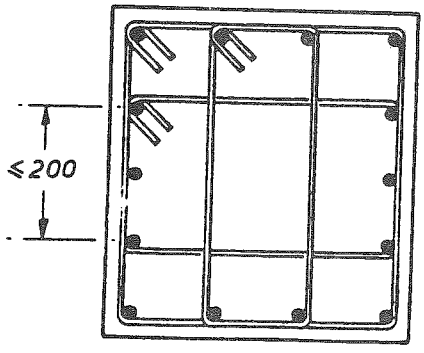

Three overlapping hoops

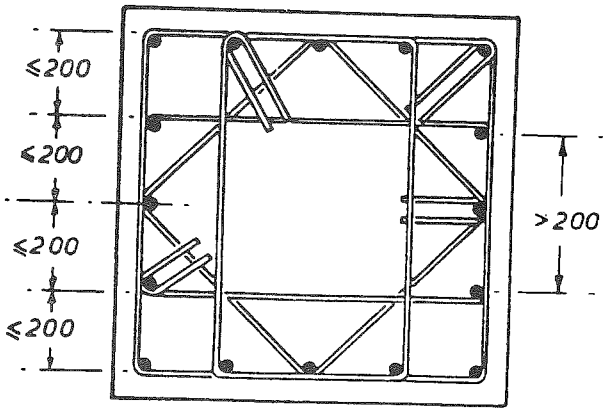

Four overlapping hoops

Figure 19 : Examples of Transverse Reinforcement in Columns According to Commentary of New Zealand Code [5]. (Dimensions in mm, 1 mm = 0.039 in).

Examples of anchorage details for cross ties taken from the Commentary of the ACI code [9] and the SEAOC recommendations [12] are shown in Figs. 20 and 21. A cross tie with a 90° bend at one end and a 135° bend at the other as shown in Fig. 20 has the construction advantage that it can be inserted into the reinforcing cage from the side when placing the steel. However it is considered in the New Zealand code that the 90° bend is undesirable since the extension of bar beyond the 90° bend is not embedded in the concrete core. Thus when the cover concrete spalls the 90° bend anchorage may become ineffective. One column recently tested in New Zealand [13] has shown that the 90° bend anchorage does eventually become ineffective at large column deformations, but that this detail may be satisfactory for limited ductility demands, for example for use in columns protected from plastic hinging by a capacity design procedure. Two columns recently tested in New Zealand [13] have indicated that the tension splice detail for cross ties shown in Fig. 21 can be satisfactory providing sufficient lap length is provided for adequate anchorage.

(c) Quantity of Transverse Reinforcement Required for Concrete Confinement in Potential Plastic Hinge Regions of Columns

The quantity of transverse reinforcement of circular shape for confinement is expressed in terms of ρ_s, which is the ratio of the volume of spiral or circular hoop reinforcement to the volume of the concrete core. Therefore

$$\rho_s = \frac{A_{sp}\,\pi d_s}{s\pi(d_s/2)^2} = \frac{4A_{sp}}{d_s s} \qquad (14)$$

where A_{sp} = area of spiral bar, d_s = diameter of spiral, and s = centre to centre spacing of spiral bar. For transverse reinforcement of rectangular shape for confinement with or without cross ties, the

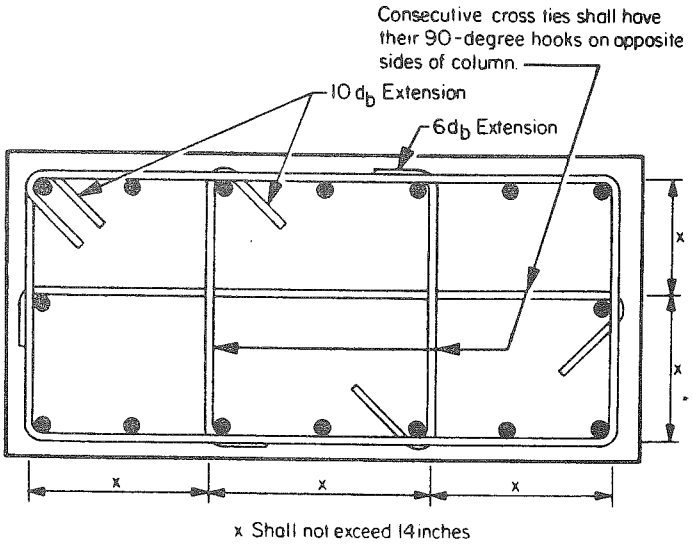

Figure 20 : Examples of Transverse Reinforcement in Columns According to the Commentary of the ACI Code [9].

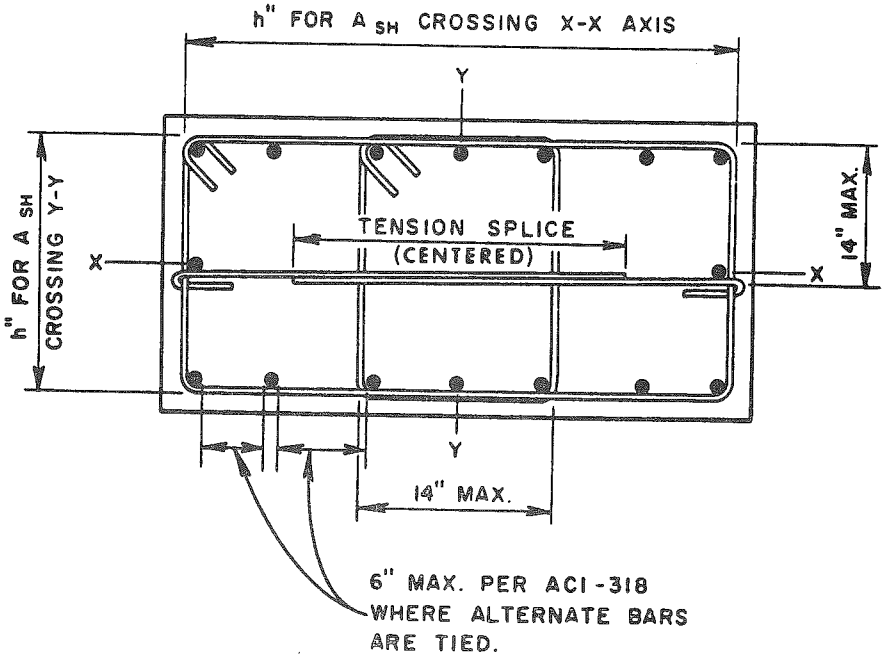

Figure 21 : Example of Transverse Reinforcement in Columns According to Commentary of SEAOC Recommendations [12].

quantity of transverse reinforcement is generally expressed in terms of A_{sh}, which is the total area of transverse reinforcement, including cross ties, in the direction under consideration within longitudinal spacing s_h.

The quantity of reinforcement specified is intended to ensure adequate ductility at the potential plastic hinge regions in the columns, in the event of plastic hinging occurring, for the level of seismic design force used. In potential plastic hinge regions when spirals or circular hoops are used the volumetric ratio ρ_s should not be less than

$$\rho_s = 0.45\left(\frac{A_g}{A_c} - 1\right)\frac{f'_c}{f_{yh}}\left(0.5 + 1.25\,\frac{P_e}{\phi f'_c A_g}\right) \qquad (15)$$

or

$$\rho_s = 0.12\,\frac{f'_c}{f_{yh}}\left(0.5 + 1.25\,\frac{P_e}{\phi f'_c A_g}\right) \qquad (16)$$

whichever is greater, where A_g = gross area of column cross section (mm^2), A_c = area of concrete core of section measured to outside of peripheral transverse steel (mm^2), f_{yh} = yield strength of transverse reinforcement (MPa), f'_c = concrete compressive cylinder strength (MPa), P_e = axial load on column (N), and ϕ = strength reduction factor = 0.9 if plastic hinging can occur or 1.0 if the column is protected from plastic hinging by a capacity design procedure. In potential plastic hinge regions when rectangular hoops with or without cross ties are used, the total area of transverse bars A_{sh} in each of the transverse directions within spacing

s_h should not be less than

$$A_{sh} = 0.3 s_h h'' \left(\frac{A_g}{A_c} - 1\right) \frac{f'_c}{f_{yh}} \left(0.5 + 1.25 \frac{P_e}{\phi f'_c A_g}\right) \quad (17)$$

or

$$A_{sh} = 0.12 s_h h'' \frac{f'_c}{f_{yh}} \left(0.5 + 1.25 \frac{P_e}{\phi f'_c A_g}\right) \quad (18)$$

whichever is greater, where h" = dimension of concrete core of the section measured perpendicular to the direction of the hoop bars to the outside of the perimeter hoop (mm), s_h = centre to centre spacing of hoop sets (mm), and the other notation is as for Eqs. 15 and 16 (where 1 N = 0.225 lb, 1 mm = 0.039 in and 1 MPa = 145 psi).

In frames where a capacity design procedure is used to provide protection from plastic hinging the required quantity of transverse reinforcement in the potential plastic hinge regions may be one-half of that required by Eqs. 15 to 18, but the previous spacing and anchorage requirements should be maintained. This reduction in the quantity of transverse reinforcement is not permitted at the base of columns of frames nor in columns forming part of frames designed using a weak column-strong beam concept.

(d) United States Provisions for Quantity of Transverse Reinforcement Required in Potential Plastic Hinge Regions of Columns

In the ACI code [9] and in the SEAOC recommendations [12] it is specified that in the potential plastic hinge regions when spiral reinforcement is used ρ_s should not be less than

$$\rho_s = 0.45 \left(\frac{A_g}{A_c} - 1\right) \frac{f'_c}{f_{yh}} \quad (19)$$

or

$$\rho_s = 0.12 \frac{f'_c}{f_{yh}} \quad (20)$$

whichever is greater. In the potential plastic hinge regions where rectangular hoops with or without cross ties are used A_{sh} should not be less than

$$A_{sh} = 0.3 s_h h'' \frac{f'_c}{f_{yh}} \left(\frac{A_g}{A_c} - 1\right) \quad (21)$$

or

$$A_{sh} = 0.12 s_h h'' \frac{f'_c}{f_{yh}} \quad (22)$$

whichever is greater. The notation used in Eqs. 19 to 22 is the same as for Eqs. 15 to 18, except that in the ACI code h" is the dimension of the concrete core measured to the centres of the perimeter hoop.

(e) Background of New Zealand and United States Provisions for Quantity of Transverse Reinforcement Required for Concrete Confinement in Potential Plastic Hinge Regions of Columns

It is evident that the New Zealand Eqs. 15 to 18 are similar to the United States Eqs. 19 to 22 except for the term $[0.5 + 1.25P_e/(\phi f'_c A_g)]$. The reason for this difference is that the US equations are based on a philosophy of preverving the axial load carrying capacity of the column after spalling of the cover concrete has occurred rather than aiming to achieve a particular curvature ductility factor for the section [3]. The philosophy of maintaining the axial load strength of the section after spalling of the cover concrete does not properly relate to the detailing requirements of adequate plastic rotation capacity of eccentrically loaded members. A more logical approach for the determination of the amount of transverse reinforcement necessary to achieve adequate curvature ductility would be based on ensuring a satisfactory moment-curvature relationship.

Theoretical moment-curvature analyses have been conducted in New Zealand by Park et al (3,14,15] to determine the influence of quantity of confining steel on the available curvature ductility. The idealised stress-strain curve for confined concrete used in these analyses were based on a limited number of tests on small concentrically loaded column specimens and the curves used are now known to be conservative. The complete stress-strain curve for confined concrete was used in the analyses. That is, the full extent of the "falling branch" of the stress-strain curve after the maximum stress was reached was utilised and hence no arbitrary value for the "ultimate" concrete compressive strain was assumed. Instead, the available curvature ductility factor of the section was judged by assessing the curvature after maximum moment was reached when the section was still carrying a reasonable proportion of the maximum moment. Fig. 22 shows diagramatically the form of the moment-curvature curves obtained for a particular column section with different transverse steel contents and a

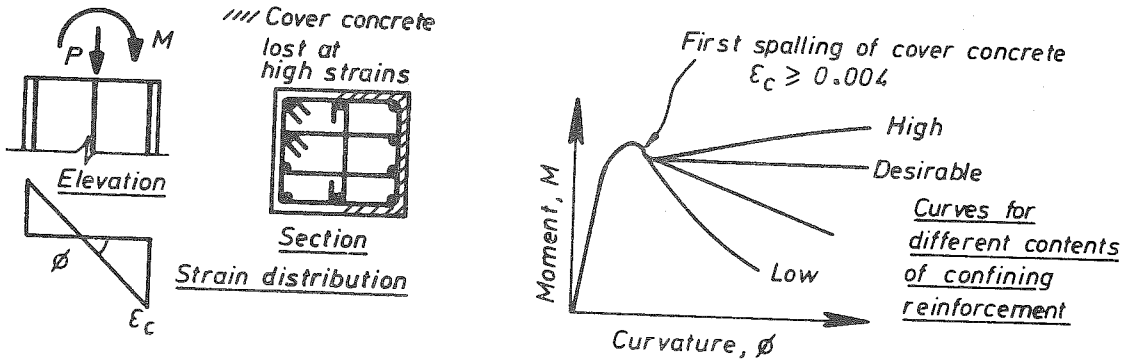

Figure 22 : Moment-Curvature Relations for a Reinforced Concrete Column Section With Constant Axial Load P and Different Contents of Confining Reinforcement.

constant axial load level. The theoretical moment-curvature relations for a range of transverse steel contents and axial load levels were computed. The analyses showed that the quantity of transverse steel specified by the ACI and SEAOC equations are conservative for low axial load levels but are unconservative for high axial load levels. Hence Eqs. 15 to 18 are based on the ACI and SEAOC equations but with a modification factor $[0.5 + 1.25P_e/(\phi f'_c A_g)]$ introduced to account for the effect of axial load level.

The amount of transverse reinforcement required by Eqs. 15 to 18 increases with the axial load level because a higher axial load means a larger neutral axis depth which in turn means that the flexural strength of the column is more dependent on the contribution of the concrete compressive stress block. Thus the higher the axial load the more important it becomes to maintain the strength and ductility of the concrete, thus leading to a greater quantity of transverse steel.

The behaviour of reinforced concrete columns subjected to simulated seismic loading has been studied extensively at the University of Canterbury in recent years. The test results from a wide range of columns have indicated that the New Zealand equations for the quantity of confining reinforcement results in columns with very satisfactory available ductility. A summary of the test results may be seen elsewhere [16].

(f) Examples of Comparisons of the Quantity of Confining Steel Required in Potential Plastic Hinge Regions of Columns by New Zealand and United States Codes

The difference between the provisions for transverse reinforcement of the New Zealand code [5] and the ACI and SEAOC codes [9,12] illustrated in Fig. 23 for a typical 1.5 m (59.1 in) diameter circular column confined by a spiral, and in Fig. 24 for a typical 700 mm (27.6 in) square column confined by an arrangement of square and octagonal hoops.

It is evident from Figs. 23 and 24 that the ACI and SEAOC provisions stipulate a constant quantity of transverse steel, regardless of the level of axial compressive load on the column. It should be noted however that for column compressive loads less than $0.1f'_c A_g$ the member could be defined as a beam according to the ACI code and then contain the reduced quantity of transverse steel specified for a beam. The New Zealand code quantity of transverse steel shows a linear increase with axial load from 50% of the ACI/SEAOC quantities at zero axial load, to 100% of the ACI/SEAOC amount at an axial load of $0.36f'_c A_g$, to 1.47 times the ACI/SEAOC amount at an axial load of $0.7f'_c A_g$, assuming $\phi = 0.9$ in the New Zealand code equations.

For the circular column of Fig. 23, the quantity of spiral steel required by the New Zealand code at an axial load level of $0.36f'_c A_g$, and by the ACI and SEAOC codes at all load levels, could be met using a spiral from 20 mm (0.79 in) diameter bar at 74 mm (2.9 in) centre to centre spacing. If a higher strength spiral steel was used the spiral bar diameter could be reduced or the spacing increased or both. For example, if f_{yh} = 60 ksi (414 MPa) spiral steel is used, a 3/4 in (19.1 mm)

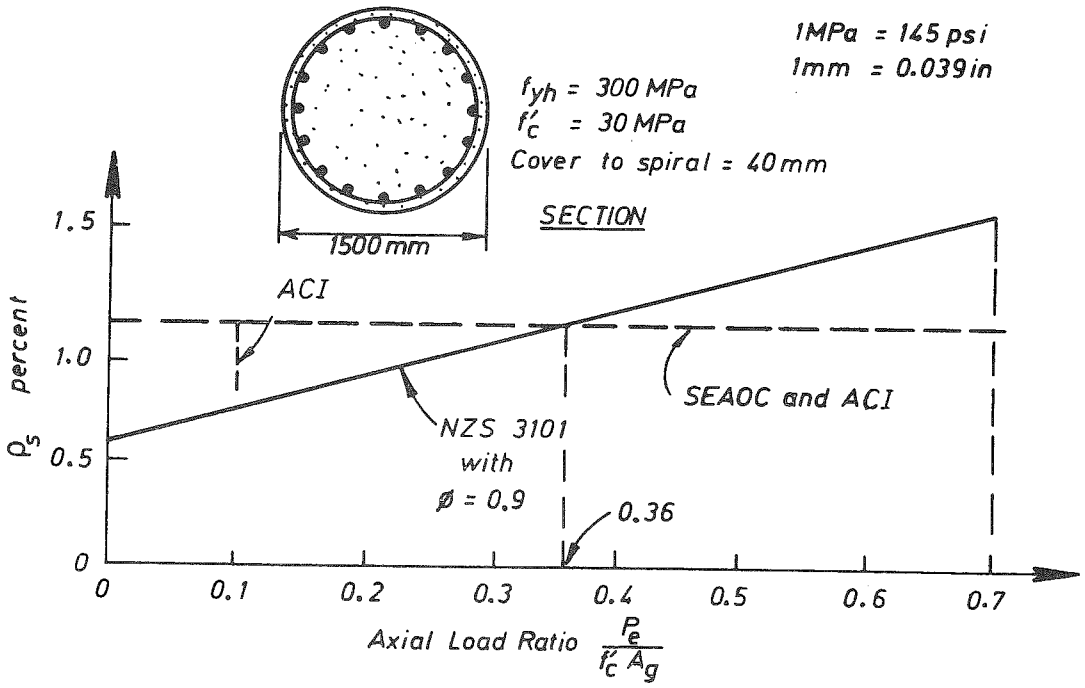

Figure 23 : Comparison of United States and New Zealand Code Spiral Steel Requirements for a Circular Column.

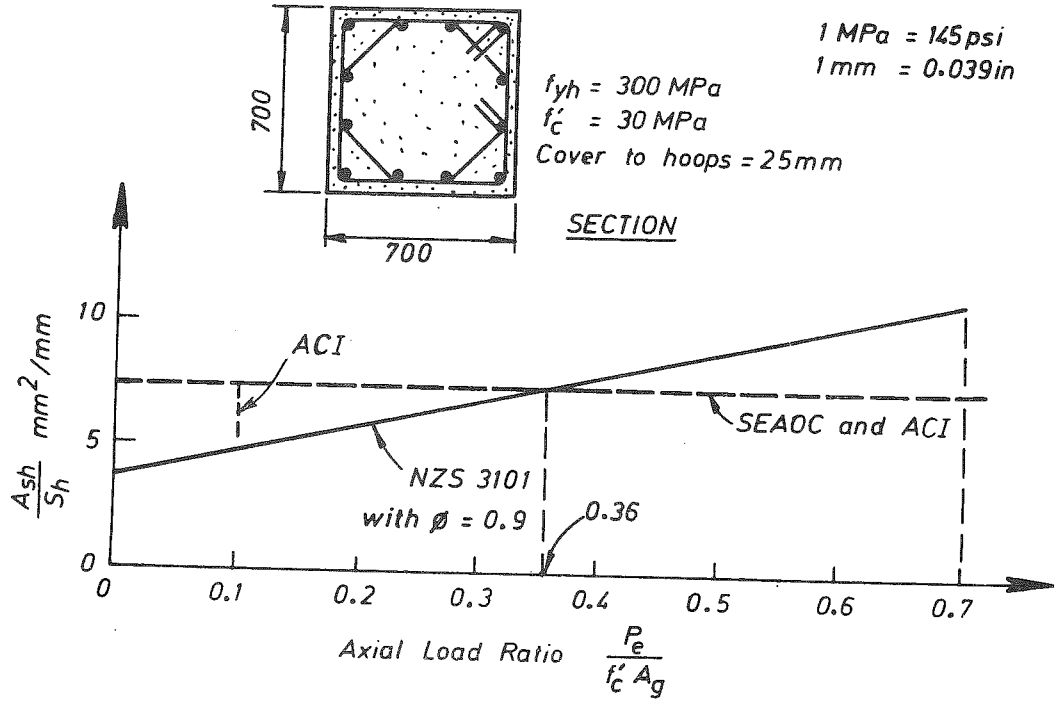

Figure 24 : Comparison of United States and New Zealand Code Hoop Steel Requirements for a Square Column.

diameter spiral bar at 3.7 in (93 mm) centre to centre spacing would be sufficient. It is obvious that large diameter columns require large diameter spiral steel bars at close centres for confinement.

For the square column of Fig. 24 the quantity of hoop steel required by the New Zealand code at an axial load level of $0.36f'_cA_g$, and by the ACI and SEAOC codes at all load levels, could be met using hoops from 16 mm (0.63 in) diameter bar with the hoop sets placed at 88 mm (3.5 in) centres. Again the quantity of transverse steel used could be reduced by using higher strength steel. For example, if f_{yh} = 60 ksi (414 MPa) hoop steel is used, a 5/8 in (15.9 mm) diameter hoop bar with hoop sets at 4.7 in (120 mm) centre to centre spacing would be sufficient.

Figs. 25 and 26 show theoretical moment-curvature relations derived for the columns of Figs. 23 and 24 for three different axial load levels, namely 0, $0.36f'_cA_g$ and $0.72f'_cA_g$. The stress-strain relation for the longitudinal steel used in the analysis included the effect of strain hardening. The stress-strain relation for confined concrete used was that due to Mander et al [17]. It is of interest that at the high axial load level of $0.72f'_cA_g$ the curve obtained for the ACI/SEAOC amount of confining steel shows a significant reduction in moment at curvatures beyond maximum moment (that is, relatively poor ductility), while the curve obtained for the New Zealand amount of confining steel shows more ductility. At zero axial load the curves obtained for the ACI/SEAOC and NZ amounts of confining steel are almost identical and show good ductility, indicating that the smaller NZ amount of confining steel is adequate.

(g) Examples of Comparisons of the Quantity of Confining Steel Required in Potential Plastic Hinge Regions of Circular and Square Column Sections

It is of interest to compare the volumes of transverse steel required for the three column sections shown in Fig. 27. Each section has twelve longitudinal bars. The circular column has spiral reinforcement. The square columns have two alternative arrangements of hoops. Case 1 has three overlapping hoops per set, made up of one square perimeter hoop surrounding all twelve bars and two interior rectangular hoops each surrounding four bars. Case 2 has two overlapping hoops per set, made up of one square perimeter hoop surrounding all twelve bars and one octagonal interior hoop surrounding eight bars.

The relative sizes of the circular and square cross sections are such that the nominal (ideal) flexural strengths of the three columns are approximately the same if the columns all have Grade 380 (f_y = 55 ksi) longitudinal reinforcement with $\rho_t = A_{st}/A_g = 0.02$, concrete with f'_c = 30 MPa (4,350 psi) and an axial load level of $0.3f'_cA_g$, where A_{st} = total area of longitudinal reinforcement, A_g = gross area of column section, and f'_c = concrete compressive cylinder strength. This equality of flexural strength may be demonstrated as follows. In both columns the distance between the bar centroids in extreme faces of the column is close to 0.8 of the overall column depth (within 2% of this proportion), and $\rho_t f_y/0.85f'_c = 0.02 \times 380/(0.85 \times 30) = 0.30$. If the strength reduction factor ϕ is 1.0, the nominal (ideal) flexural strength is 1690 kNm (1246 kip ft) for the circular column and 1730 kNm (1275 kip ft) for the

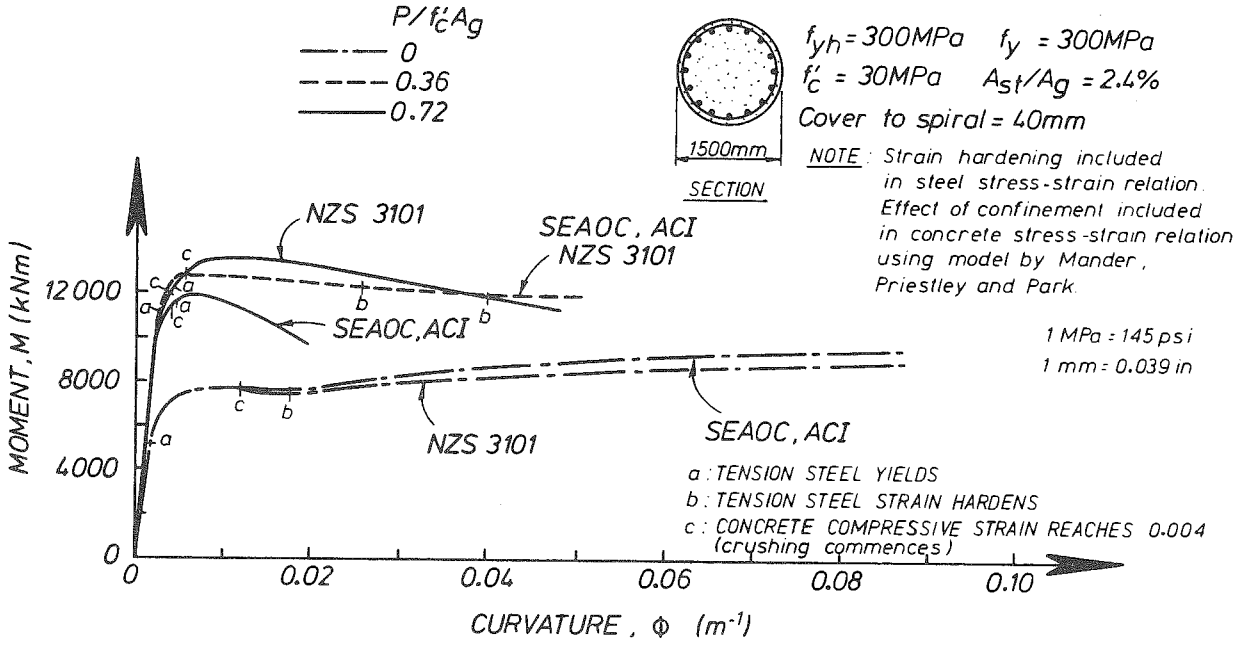

Figure 25 : Theoretical Moment-Curvature Relations for a Circular Column.

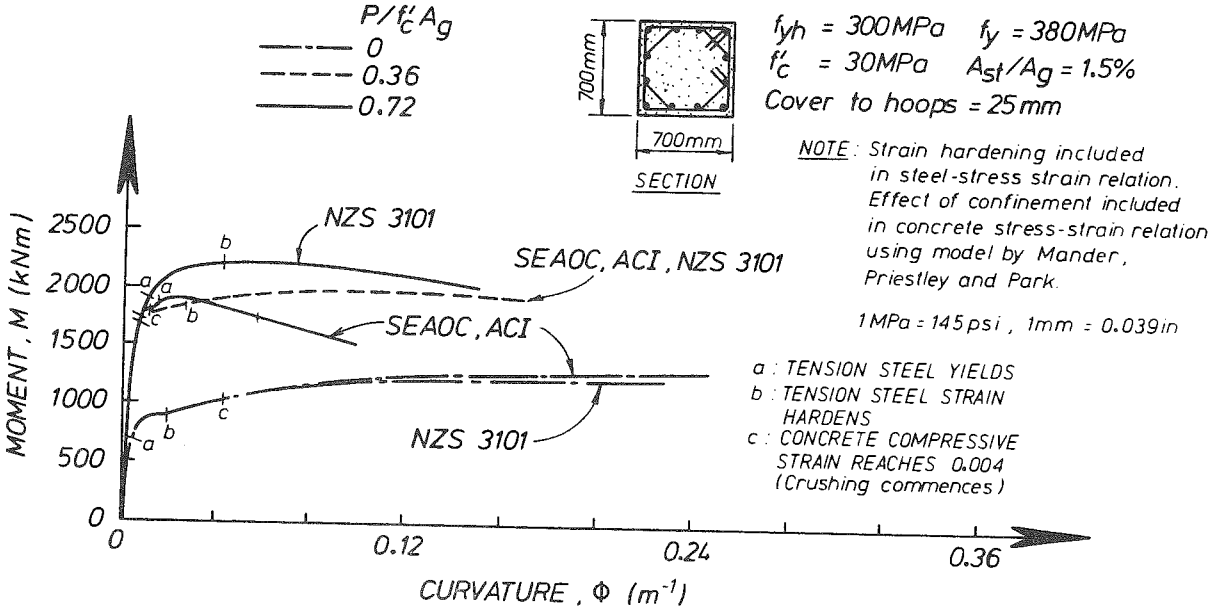

Figure 26 : Theoretical Moment-Curvature Relations for a Square Column.

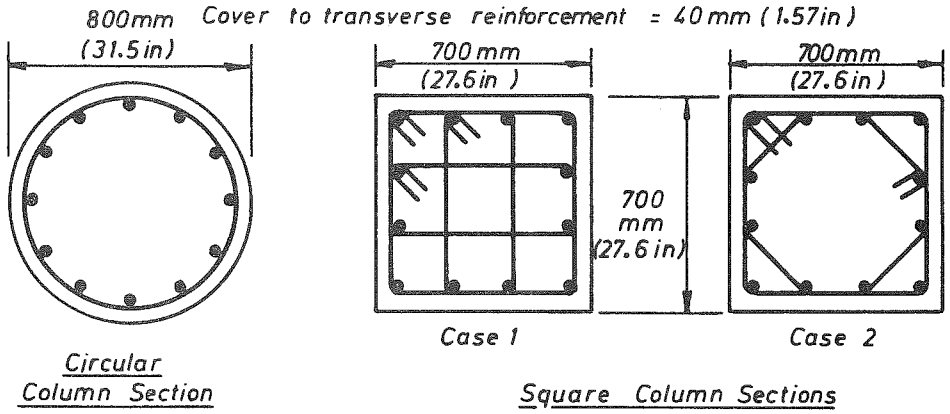

Figure 27 : Cross Sections of Example Column.

square column, as may be obtained from design charts, tables or by calculation from first principles.

For the same axial load level $P_e/\phi f'_c A_g$ on all three columns it can be shown using Eqs. 15 to 18 to calculate the quantities of transverse reinforcement that:

1. The volume of overlapping hoops in the square column is 2.0 to 2.2 times the volume of the spiral in the circular column.

2. The square column with sets of overlapping square and octagonal hoops (Case 2) requires 11% less transverse reinforcement volume than the square column with sets of overlapping square and rectangular hoops (Case 1).

3. For the same transverse bar diameter, the clear spacing between transverse bars is greatest in the circular column with the spiral. For example, if $P_e/\phi f'_c A_g = 0.4$ and if 16 mm (0.63 in) diameter bar from Grade 380 steel (f_{yh} = 55 ksi) is used for transverse reinforcement, the centre to centre spacing of the spirals or hoop sets is as follows from Eqs. 15 to 18.

   Circular Column:

   s = 118 mm (4.6 in)

   Clear spacing between spirals = 118 - 16 = 102 mm (4.0 in)

   Square Column, Case 1 (three overlapping hoops):

   s_h = 137 mm (5.4 in)

   Clear spacing between hoop sets = 137 - 48 = 89 mm (3.5 in)

   Square Column, Case 2 (two overlapping hoops):

s_h = 117 mm (4.6 in)

Clear spacing between hoop sets = 117 - 32 = 85 mm (3.3 in).

Note that this example points to the considerable reduction in the volume of transverse reinforcement possible according to the code if circular columns with spirals are used. The circular and the square columns had approximately the same concrete cross sectional area and for the same longitudinal steel content gave the same flexural strength at $P_e = 0.3f'_cA_g$.

4.4.5 Transverse Reinforcement for Shear

The design shear force is estimated from a probable critical moment gradient along the column. According to the method for the evaluation of column actions in ductile multistorey frames due to Paulay [6], placed in the Commentary of the code [5], the design shear force can be taken for columns of one-way frames as

$$V_{col} = 1.3\phi_o V_{code} \qquad (23)$$

and for columns of two-way frames as

$$V_{col} = 1.6\phi_o V_{code} \qquad (24)$$

where ϕ_o = beam overstrength factor defined as for Eq. 11, and V_{code} = column shear force derived for code static seismic loading. The larger value for two-way frames is to include the effect of concurrent seismic loading. That is, the design shear forces need only to be considered in each principal direction independently.

Since the design shear forces are found using flexural overstrengths, a strength reduction factor ϕ = 1 can be used in the design of shear reinforcement. In the potential plastic hinge regions at the ends of columns the shear stress carried by the concrete v_c is assumed to be zero unless the minimum design axial compression force produces an average stress in excess of $0.1f'_c$ over the gross concrete area. When the average compression stress exceeds $0.1f'_c$ the value of v_c is taken as follows:

$$v_c = 4v_b\sqrt{\frac{P_e}{f'_cA_g}} - 0.1 \quad \text{(MPa)} \qquad (25)$$

where v_b = shear stress carried by the concrete when P_e = 0 in gravity load design (MPa), P_e = minimum design compressive force (N), f'_c = concrete compressive cylinder strength (MPa), and A_g = gross area of column section (mm^2) (where 1 N = 0.225 lb, 1 mm = 0.039 in and 1 MPa = 145 psi). This equation gives a gradual transition from v_c = 0 to the full gravity load design value of v_c as P_e/f'_cA_g increases from 0.1.

The assumption of v_c = 0 for small axial load levels is to take into account the possible deterioration of the shear carried by the concrete during high intensity cyclic loading. Reversal of moment in plastic hinge

regions causes a reduction in the shear transferred by the concrete across the compression zone and in the shear force carried by aggregate interlock and dowel action [3].

The transverse reinforcement present should be capable of carrying by truss action that shear not carried by the concrete. The requirements of shear may govern the quantity of transverse reinforcement necessary in columns.

Away from the potential plastic hinge regions the shear may be considered to be carried by both the transverse reinforcement and the concrete, and the shear reinforcement may be designed by the shear strength equations used for gravity load design.

Column shear is an important design consideration since column shear failure can be extremely brittle. Note that the shear strength of a square column with load acting along a diagonal of the section and the shear strength of the same column with loading acting along a major axis of the section are almost identical. This is because for diagonal shear, although the component of transverse bar force in the direction of the shear force is smaller, the diagonal tension crack at 45° to the longitudinal axis of the member has a greater projected length and therefore intercepts more transverse bars.

4.5 Design of Beam-Column Joints

4.5.1 General

The strength of a beam-column joint core should be greater than the strength of the members it joins, since the joint core strength may degrade rapidly with cyclic loading, the joint core is difficult to repair, and failure of the joint core could lead to collapse of the column.

In past years designers have tended not to give much attention to the detailing of beam-column joints. However very few failures of beam-column joint cores have been observed during severe earthquakes. Collapses of frames during severe earthquakes have normally occurred as a result of inadequately detailed columns, particularly poor arrangements of transverse reinforcement. However beam-column joint cores can be subjected to extremely high shear and bond stresses when subjected to seismic loading. If the beams and columns are detailed for adequate ductility the joint cores could become the critical regions of the structure unless also carefully designed. The behaviour of beam-column joint cores has been studied extensively in New Zealand in recent years. A summary of the results of that work may be seen elsewhere [18].

4.5.2 Shear Resistance

Fig. 28 illustrates an interior beam-column joint core which forms part of a frame subjected to horizontal seismic loading. Consideration of the concrete and steel forces in the adjacent beams and columns acting at the boundaries of the joint core indicates that to satisfy the equilibrium requirements of the joint core there must be two mechanisms of joint core shear resistance [3], namely:

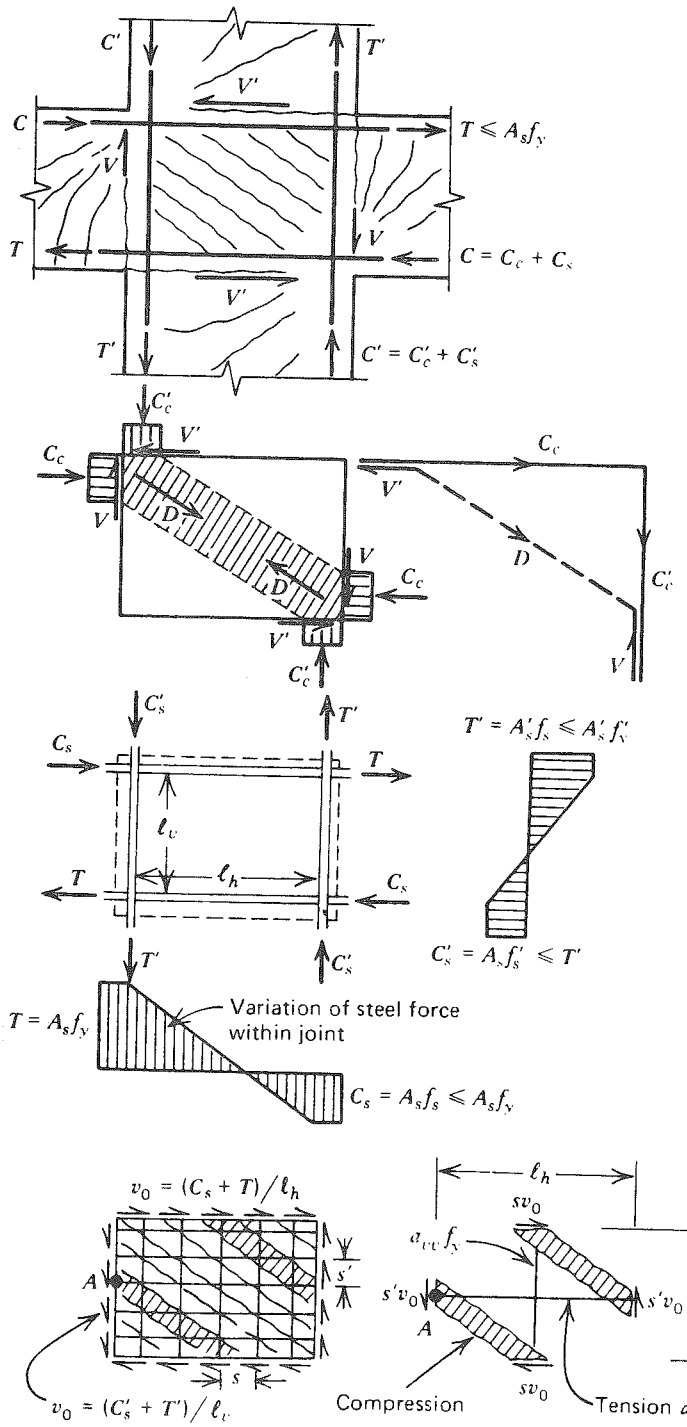

(a) Internal actions and crack patterns

(b) Shear transfer of concrete compression forces by diagonal compression strut mechanism

(c) Forces in the reinforcement only

(d) Shear transfer of reinforcement bond forces by truss mechanism

Figure 28 : Idealised Behaviour of Reinforced Concrete Beam-Column Joint of Frame Subjected to Horizontal Loading [3].

(1) a diagonal compression strut carrying the concrete compressive forces across the joint.
(2) a truss mechanism of joint core reinforcement carrying the longitudinal bar forces across the joint.

The diagonal compression strut mechanism transfers mainly the forces from the concrete compression zones of the adjacent beams and columns across the joint core. The truss mechanism is necessary to transfer the bond forces from the longitudinal beam and column reinforcement, which act along the boundaries of the joint core, across the joint core. The first mechanism is commonly referred to as the "shear carried by the concrete", and the second mechanism as the "shear carried by the shear reinforcement".

During reversed seismic loading full depth vertical cracks can occur in the beams at the column faces, as illustrated in Fig. 16. When full depth cracking occurs in the beams at the column faces the diagonal compression strut mechanism becomes much less effective, unless the axial compression on the column is large. Diagonal tension cracking in alternating directions in the joint core can also cause a degradation of the strength of the diagonal compression strut mechanism. Hence cyclic loading causes a transfer of the joint core shear resistance from the diagonal compression strut mechanism to the truss mechanism. The potential failure plane is a corner to corner crack in the joint core.

It is evident that the truss mechanism requires the presence of both horizontal and vertical shear reinforcement and a diagonal concrete compression field to satisfy the equilibrium requirements of the mechanism (see Fig. 28d). The horizontal and vertical reinforcement necessary for shear resistance can be provided by horizontal column hoops between the top and bottom longitudinal beam bars and longitudinal column bars between the corner longitudinal column bars.

4.5.3 Design Shear Forces

In order to ensure that energy dissipation occurs in the plastic hinge regions of the adjacent members and not in the joint core regions, the joint core should be designed to resist the forces arising when the overstrength of the framing members is developed (Section 4.2.1). That is, the stresses in the flexural steel at the plastic hinges are assumed to be 1.25 times the yield strength in the case of Grade 275 ($f_y \geq 40$ ksi) steel, or 1.4 times the yield strength in the case of Grade 380 ($f_y \geq 55$ ksi) steel. The design horizontal shear force V_{jh} and the design vertical shear force V_{jv} are found by taking into account the effect of the normal and shear forces acting on the joint core. When beams frame into the joint in two directions, these forces need only be considered in each principal direction independently.

The forces acting at the boundaries of joint cores of exterior and interior reinforced concrete beam-column joints are shown in Fig. 29. The horizontal shear force acting on the joint core is given by the resultant horizontal force acting above or below a horizontal plane at the mid-depth of the joint core. For the exterior joint the horizontal design shear force is

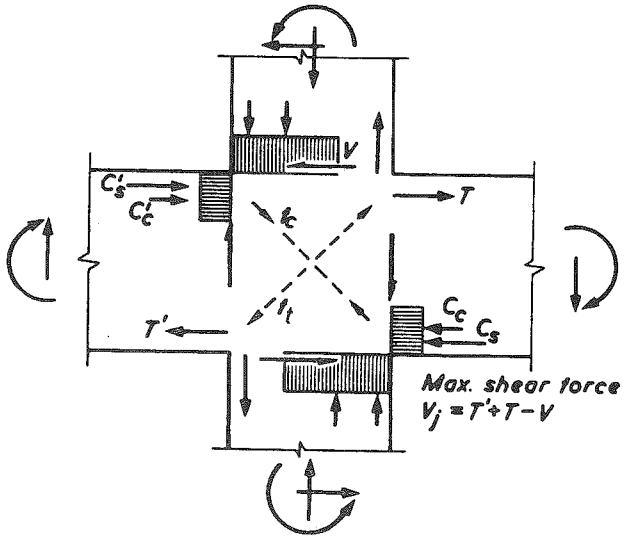

(a) Actions and stress resultants of interior joint

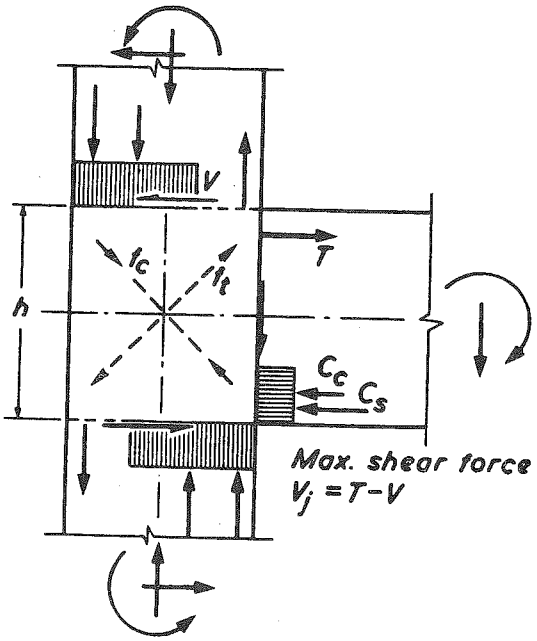

(b) Actions and stress resultants of exterior joint

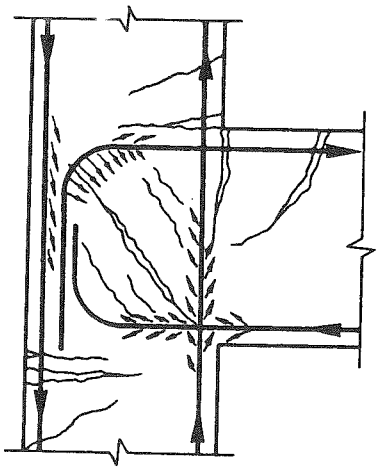

(c) Cracking and bond forces of exterior joint

Figure 29 : Reinforced Concrete Beam-Column Joints of Frame Subjected to Horizontal Loading.

$$V_{jh} = T - V \tag{26}$$

and for the interior joint the horizontal design shear force is

$$V_{jh} = C'_s + C'_c + T - V \qquad \text{where} \quad C'_s + C'_c = T'$$

$$= T' + T - V \tag{27}$$

where the notation is as shown in Fig. 29. The vertical design shear force may also be found from the forces acting on the boundaries of the joint core. As an approximation the vertical design shear force may be taken as

$$V_{jv} = V_{jh} \frac{h_b}{h_c} \tag{28}$$

where h_b = overall depth of beam and h_c = overall depth of column in the direction being considered.

In order to prevent the concrete diagonal compression strut from crushing, the nominal horizontal shear stress v_{jh} in either principal direction is limited to $1.5\sqrt{f'_c}$ MPa (or $18\sqrt{f'_c}$ psi) where

$$v_{jh} = \frac{V_{jh}}{b_j h_c} \tag{29}$$

and where f'_c = concrete compressive strength, h_c = overall depth of column in the direction being considered and b_j is the effective joint width defined as

When $b_c > b_w$

either $b_j = b_c$ or $b_j = b_w + 0.5h_c$, whichever is smaller.

When $b_c < b_w$

either $b_j = b_w$ or $b_j = b_c + 0.5h_c$, whichever is smaller.

where b_c = width of column and b_w = width of beam web.

4.5.4 Horizontal Joint Shear Reinforcement

The total area of horizontal shear reinforcement placed between the outermost layers of top and bottom beam reinforcement should not be less than

$$A_{jh} = \frac{V_{jh} - V_{ch}}{f_{yh}} \tag{30}$$

where V_{jh} = horizontal design shear force, f_{yh} = yield strength of horizontal shear reinforcement, and V_{ch} = shear carried by diagonal

compression strut mechanism should be taken as zero unless one of the following applies:

(1) When the minimum average compressive stress on the gross concrete area of the column above the joint exceeds $0.1f'_c/C_j$

$$V_{ch} = \frac{2}{3}\sqrt{\frac{C_j P_e}{A_g} - \frac{f'_c}{10}}\,(b_j h_c) \quad (N) \qquad (31)$$

where $C_j = V_{jh}/(V_{jx} + V_{jy})$ where V_{jx}, V_{jy} = horizontal design shear forces in joint core in the two principal directions (= 1 for one-way frame or 0.5 for symmetrical two-way frame), P_e = minimum axial compressive column load (N), A_g = gross area of column cross section (mm^2) and f'_c = concrete compressive cylinder strength (MPa) (where 1 N = 0.225 lb, 1 mm = 0.039 in and 1 MPa = 145 psi). The value for V_{ch} given by Eq. 31 recognises the degradation in the shear carried by the concrete diagonal compression strut during reversals of seismic loading, but acknowledges that an increase in the axial compressive load on the column results in an increase in V_{ch} due to the formation of a wider compression strut.

(2) The degradation of shear carried by the concrete diagonal compression strut during reversals of seismic loading can be greatly reduced if yielding of the longitudinal steel is forced to occur away from the faces of the joint core, since then full depth cracking will not occur at the faces of the joint core and the diagonal compression strut mechanism will be preserved. Thus an attractive design concept involves deliberately designing plastic hinges to form in the beams away from the columns. The code allows a reduction in the content of joint core shear reinforcement for this design situation. Plastic hinging can be forced away from the column faces by suitable reinforcing details or by haunching the beams, as shown in Fig. 30. For exterior joints the degradation in the shear carried by the diagonal compression strut mechanism during seismic load reversal is not so great as for interior joints. This is because it is possible for the diagonal compression strut to act between the

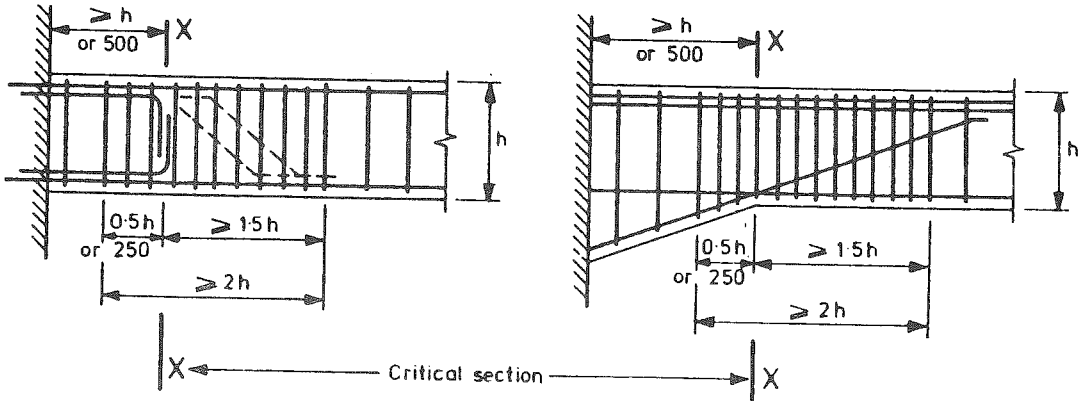

Figure 30 : Plastic Hinges Located in Beams Away from Column Faces [5].

the bend in the 90° hook of the flexural reinforcement and the hoops outside the joint core in the column placed near the beam bars (see Fig. 29). Hence even when full depth flexural cracks due to yielding beam steel exist in the beam at the column face V_{ch} has a significant value for exterior joints.

Hence when the design is such that plastic hinging occurs in the beam at a distance away from the column face not less than the beam depth nor 500 mm (19.7 in), or for exterior joints where the flexural steel is anchored outside the column core in a beam stub, the value of V_{ch} may be increased to

$$V_{ch} = 0.5 \frac{A'_s}{A_s} V_{jh} \left(1 + \frac{C_j P_e}{0.4 A_g f'_c}\right) \quad (N) \qquad (32)$$

where A'_s = area of compression reinforcement in beam (mm^2) and A_s = area of tension reinforcement in beam (mm^2) and other notation is as for Eq. 31. A'_s/A_s should not be taken larger than 1.0. When the axial column load results in tensile stresses over the gross concrete area exceeding $0.2f'_c$, $V_{ch} = 0$. For axial tension between these limits V_{ch} may be obtained by linear interpolation between zero and the value given by Eq. 32 when P_e is taken as zero.

(3) For exterior joints without beam stubs at the far face of column, Eq. 32 may be used when multiplied by the factor

$$\frac{3h_c (A_{jv} \text{ provided})}{4h_b (A_{jv} \text{ required})} \qquad (33)$$

which should not be taken as greater than 1.0. Use of this factor requires that the beam bars be anchored using a 90° standard hook in the joint core.

(4) When the ratio h_c/h_b is greater than or equal to 2.0, V_{ch} need not be taken as less than

$$V_{ch} = 0.2 b_j h_c \sqrt{f'_c} \quad (N) \qquad (34)$$

4.5.5 Vertical Joint Shear Reinforcement

The total area of vertical shear reinforcement, normally in the form of intermediate column bars at the side faces of the column, should not be less than

$$A_{jv} = \frac{V_{jv} - V_{cv}}{f_{yh}} \quad (mm^2) \qquad (35)$$

where V_{jv} = vertical design shear force (N), f_{yh} = yield strength of horizontal reinforcement (MPa), V_{vc} = shear carried by diagonal compression strut mechanism (N) (where 1 N = 0.225 lb, 1 mm = 0.039 in and 1 MPa = 145 psi). When plastic hinging is not expected to occur in the

column above or below the joint core

$$V_{cv} = \frac{A'_{sc}}{A_{sc}} V_{jv} \left(0.6 + \frac{C_j P_e}{A_g f'_c}\right) \quad (N) \qquad (36)$$

except where axial load results in tensile stresses over the column section, where A'_{sc} = area of compression reinforcement in one face of column (mm^2), A_{sc} = area of tension reinforcement in one face of column (mm^2), and other notation is as for Eq. 31. When P_e is tensile, the value of V_{cv} is interpolated linearly between the value given by Eq. 36 when P_e^{cv} is taken as zero and zero when the axial tensile stress over the gross concrete area is $0.2f'_c$. However, if plastic hinges are expected to form in the column above or below the joint core, but not when elastic behaviour is assured in the column or column stub on the opposite side of the joint, V_{cv} should be taken as zero for any axial load on the column.

The spacing of vertical shear reinforcement in each plane of any beam framing into the joint should not exceed 200 mm (7.9 in) and in no case should there be less than one intermediate bar in each side of the column in that plane.

4.5.6 Confinement of Joint Core

The horizontal transverse confinement reinforcement in the joint core should not be less than that required in the potential plastic hinge regions in the ends of the columns. In no case should the spacing of transverse reinforcement in the joint core exceed 10 times the diameter of the longitudinal column bar or 200 mm (7.9 in), whichever is less.

4.5.7 Anchorage of Longitudinal Reinforcement

It is clear from Figs. 28 and 29 that bond conditions for the longitudinal beam and column bars at the boundaries of the joint cores are unfavourable, because large steel forces need to be transferred to the concrete over relatively short lengths of bar, flexural and diagonal tension cracks are present which will alternate in direction during cyclic loading, and bond deterioration will occur during cyclic loading.

For interior joints, when plastic hinges form in the beams at the column faces, a beam bar will be yielding in tension on one side of the joint core and in compression on the other side of the core, and hence twice the yield force of the bar will need to be transferred by bond to the joint core, which may require extremely high bond stresses. Hence the bar diameters need to be limited to prevent excessive slip of bars through the joint core.

For exterior joints, degradation of bond strength will also cause yielding of longitudinal beam bars to penetrate into the joint core, thus reducing the effective anchorage length and possibly result in loss of anchorage. Therefore, it is recommended that at exterior beam-column joints in which plastic hinging occurs in the beam at the column face, the anchorage of beam steel should be considered to commence within the joint core. Also for exterior joints, the outer longitudinal column bars in Fig. 29 will be subjected to high bond stresses which can result in

vertical splitting of concrete along those bars.

Bond in the joint core is not so critical when plastic hinges form some distance away from the joint core, since then yield penetration into the joint core does not occur.

(1) Bar anchorage at exterior joints

The basic development length of a deformed bar in tension terminating with a standard 90° hook is

$$\ell_{dh} = \frac{66 d_b}{\sqrt{f'_c}} \frac{f_y}{275} \text{ (mm)} \qquad (37)$$

where d_b = diameter of longitudinal bar (mm), f_y = yield strength of longitudinal reinforcing steel (MPa), and f'_c = compressive cylinder strength of concrete (MPa) (where 1 mm = 0.039 in and 1 MPa = 145 psi). When the bar diameter is 32 mm (1.3 in) or smaller, with side cover not less than 60 mm (2.4 in) and cover on tail extension not less than 40 mm (1.6 in), the value may be reduced by multiplying by 0.7. Where the concrete is suitably confined the value may be reduced by multiplying by 0.8.

The basic development length for a deformed bar in compression is

$$\ell_{db} = 0.24 d_b f_y / \sqrt{f'_c} \text{ (mm)} \qquad (38)$$

but not less than $0.044 d_b f_y$. Where the concrete is suitably confined the value can be reduced to $0.75 \ell_{db}$.

The anchorage is considered to commence within the column at distance $0.5 h_c$ or $10 d_b$ from the column face whichever is less (see Fig. 31), except that when the plastic hinge is located sufficiently far away from the column face anchorage may be considered to commence at the column face (see Fig. 32), where h_c = column overall depth.

When the column depth is not great enough to accommodate the required development length for beam bars, a beam stub at the far face of the column, such as shown in Figs. 33 and 34, may be used to increase the available concrete length for anchorage. The presence of such a stub has been shown to result in considerable improvement in joint performance and are being used by some designers in New Zealand.

(2) Bar anchorage in interior joints

To keep bond stresses to an acceptable level, the diameters of longitudinal bars d_b passing through a joint core are limited as follows:

(i) Beam bars:
When plastic hinging can occur adjacent to the column face:
$d_b \leq h_c/25$ when f_y = 275 MPa, or
$d_b \leq h_c/35$ when f_y = 380 MPa.

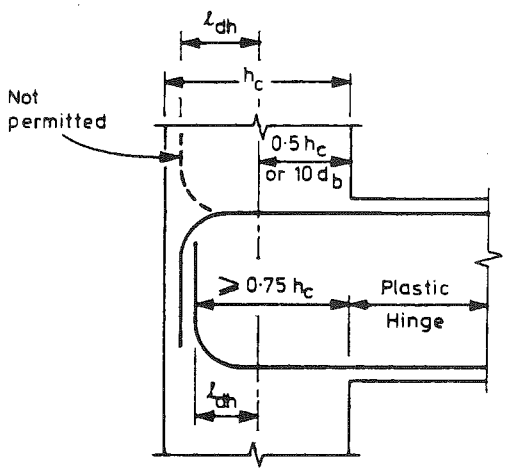

Figure 31 : Anchorage of Beam Bars When Critical Section of Plastic Hinge Forms at Column Face [5].

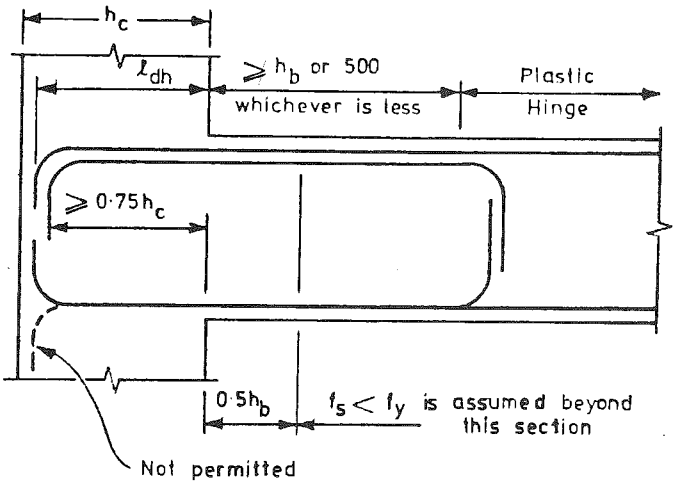

Figure 32 : Anchorage of Beam Bars When Critical Section of Plastic Hinge is Located at Sufficient Distance From Column Face [5].

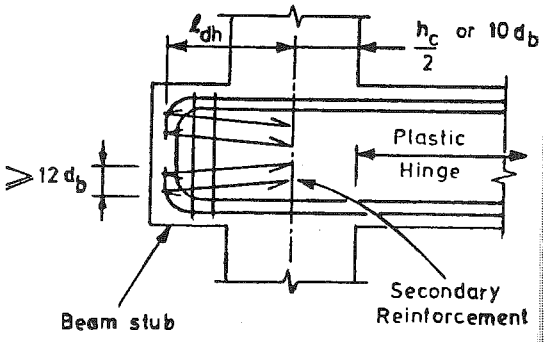

Figure 33 : Anchorage of Bars in Beam Stub [5].

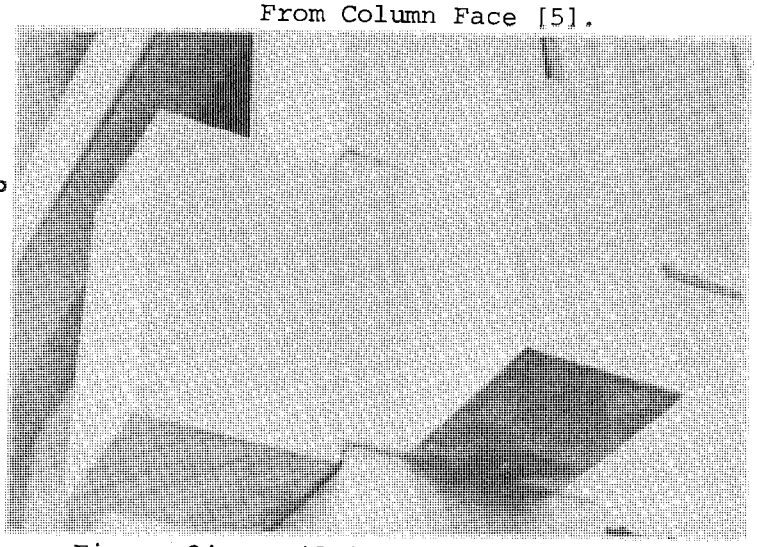

Figure 34 : Building with Beam Stubs.

When plastic hinging is located at a distance from the column face of at least the beam depth or 500 mm (19.7 in), whichever is less:

$d_b \leq h_c/20$ when f_y = 275 MPa, or

$d_b \leq h_c/25$ when f_y = 380 MPa.

where h_c = column overall depth and 1 MPa = 145 psi.

(ii) Column bars:

When columns are intended to develop plastic hinges:

$d_b \leq h_b/20$ when f_y = 275 MPa, or

$d_b \leq h_b/25$ when f_y = 380 MPa.

When columns are not intended to develop plastic hinges:

$d_b \leq h_b/15$ when f_y = 275 MPa, or
$d_b \leq h_b/20$ when f_y = 380 MPa.
where h_b = beam overall depth and 1 MPa = 145 psi.

4.5.8 American Concrete Institute Code Provisions for Beam-Column Joints

The 1983 ACI building code [9] in its seismic provisions has adopted a fundamentally different approach to the problem of beam-column joint shear. The design rules are based on the assumption that a joint can carry a design horizontal shear force if the concrete in the joint core is confined by the same quantity of transverse reinforcement as used to confine the ends of the column.

The design horizontal shear force in the joint core V_u is calculated in the same manner as for the New Zealand code. The stresses in the steel are assumed to be 25% greater than the yield strength regardless of the grade of steel. The calculated value of V_u should satisfy

$$V_u \leq \gamma \sqrt{f'_c} A_j \quad (N) \qquad (39)$$

where γ = 1.67 for a confined joint and 1.25 for other joints, f'_c = concrete compressive cylinder strength (MPa) and A_j = effective joint area (mm^2) (where 1 MPa = 145 psi and 1 mm = 0.039 in). A joint is considered to be confined if members frame in on all vertical faces and if at least 75% of each face of the joint is covered by the framing member. The effective joint area is the area of the column but if the column has a larger width than the beam the effective joint width should not be taken to exceed the width of the beam plus the overall depth of the column.

Transverse reinforcement as specified by Eqs. 19 and 20 or 21 and 22 should be provided within the joint core, except that if the joint is a confined joint as defined above it is permitted to reduce the transverse reinforcement in the joint to one-half of that specified by those equations.

Hence there is no specific calculation for the horizontal joint core shear reinforcement required for the horizontal shear force V_u. Also there is no calculation procedure or specific requirement for vertical column reinforcement crossing the joint core. The spacing between longitudinal bars is governed indirectly by the maximum permitted horizontal spacing of the tie legs across the section which is 335 mm (14 in). This means that no intermediate column bars between corner bars need be used when the column size is less than about 450 mm (18 in).

No special requirements exist for the anchorage of beam bars at interior joints and there are no limitations on usable bar diameters. At exterior joints the development length for hooked bars anchored in the joint core is taken from the face of the column.

It is evident that the ACI code approach [9] is not based on a rational model for joint core shear behaviour. The design of joint core hoop reinforcement on the basis of the quantity of transverse steel

required to confine the ends of columns is illogical and cannot produce any degree of accuracy because it does not take into account the possible varying conditions for shear in the joint cores. This is especially the case when the wide range of joint types and column axial loads used in design in practice is considered. Also, the ACI approach does not give any attention to the requirements of vertical shear reinforcement, or to the anchorage of beam bars passing through interior joints.

4.5.8 Congestion of Reinforcement

A serious problem in the construction of ductile reinforced concrete frames is the congestion of steel reinforcement in the critical regions adjacent to and in the beam-column joints, which makes the fabrication of the reinforcement cages and the placing the concrete difficult. Fig. 35 shows some reinforcement arrangements in the potential plastic hinge regions of beams and columns and beam-column joint cores of ductile frames. The congestion in those regions arises mainly from the close spacing and the multi-leg arrangements of the transverse reinforcement.

The fabrication of reinforcement cages is best carried out as far as possible under factory conditions where good workmanship is more readily achieved than on the building site. Construction problems can be eased by giving careful attention to the manner in which the reinforcement will be placed on the site in the frames. For work to proceed rapidly and efficiently, standardization of detailing of the reinforcement should be sought.

Congestion can be made a less serious problem by using larger cross sectional dimensions for the concrete members so that relatively low reinforcement ratios are adequate to achieve the required flexural strength. For example, a tension steel ratio in beams of approximately 1% is considered a practical maximum in New Zealand since the design shear forces in beam-column joint cores are then moderate and the required quantity of horizontal joint core hoops for shear is reduced and can be placed with less difficulty. Similarly, the use of larger column sections results in lower average compressive stresses on the gross area of the column and then the required quantity of horizontal confining steel in the column ends is not large.

The placement of concrete in congested reinforced concrete cages is difficult. However, proper compaction of concrete is obviously essential if the structure is to perform adequately under service load conditions and when subjected to large deformations during major earthquakes.

5. CONCLUSIONS

The emphasis in the seismic design of reinforced concrete frames should be on good structural concepts and detailing. It is recognised that uncertainty exists regarding the selection of the mathematical model representing the behaviour of the structure and the form of the imposed ground shaking. Major damage observed in earthquakes has been shown to be due mainly to poor structural concepts (for example: column sidesway mechanisms and/or considerable twisting, due to soft storey, or lack of symmetry and uniformity), and poor ductile detailing (for example:

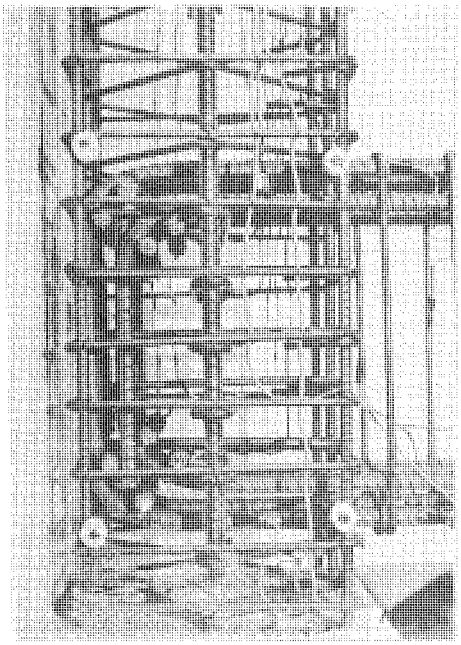

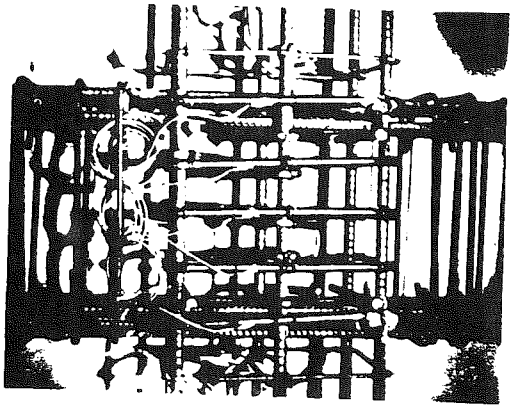

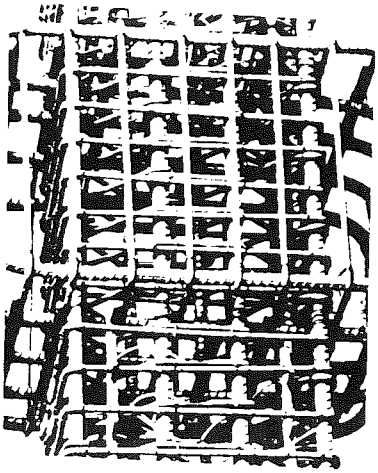

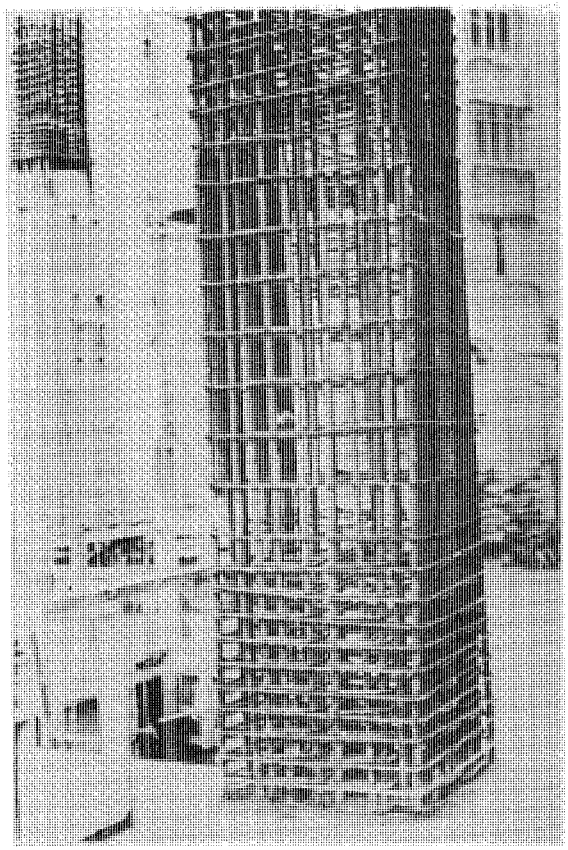

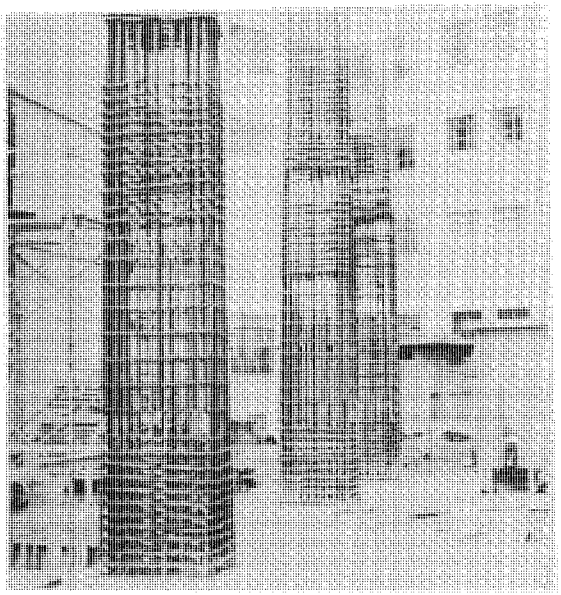

Figure 35 : Some Reinforcement **Arrangements** for Ductile Reinforced Concrete Frames.

brittle connections, inadequate anchorage of reinforcement or insufficient transverse reinforcement to prevent shear failure, premature buckling of compressed bars and crushing of concrete).

The aim in seismic design should be to impart to the structure features which will result in the most desirable behaviour which implies establishing a desirable hierarchy in the possible failure modes for the structure. In the New Zealand concrete design code this philosophy is incorporated in a rational capacity design procedure which considers the required levels of flexural and shear strength of the members and joints. A proper assessment of the strength and ductility of a structure cannot be made using the working stress design method and hence strength design is used.

In the ductile design approach for reinforced concrete frames specified in the New Zealand concrete design code special consideration is given to the ratio of column to beam flexural strength necessary to reduce the likelihood of plastic hinges forming simultaneously in the top and bottom of columns, the detailing of beams and columns for adequate ductility, and the mechanisms of shear resistance and bar anchorage in members and in beam-column joints.

ACKNOWLEDGEMENTS

The author acknowledges many informative discussions with professional engineers in New Zealand, particularly with his university colleagues Professor T. Paulay and Dr. M.J.N. Priestley.

REFERENCES

1. Hanson, R.D. and Degenkolb, H.J., "The Venezuela Earthquake July 29, 1967", American Iron and Steel Institute, New York, 1969, p.176.

2. Jennings, P.C., editor, "Engineering Features of the San Fernando Earthquake February 9, 1971", Earthquake Engineering Research Laboratory, California Institute of Technology, Pasadena, June 1971, p.512.

3. Park, R. and Paulay, T., "Reinforced Concrete Structures", John Wiley and Sons, New York, 1975, p.769.

4. "Code of Practice for General Structural Design and Design Loadings for Buildings, NZS 4203:1984", Standards Association of New Zealand, Wellington, 1984, p.100.

5. "Code of Practice for the Design of Concrete Structures, NZS 3101 Part 1:1982", and "Commentary on the Design of Concrete Structures, NZS 3101 Part 2:1982", Standards Association of New Zealand, Wellington, 1982, p.127 and 156.

6. "Papers Resulting from Deliberations of the Society's Discussion Group on Seismic Design of Ductile Moment Resisting Reinforced Concrete Frames", Bulletin of the New Zealand National Society for Earthquake Engineering, Vol. 2, No. 2, June 1977, pp.69-105; Vol. 10, No. 4,

December 1977, pp.219-237; and Vol. 11, No. 2, June 1978, pp.121-128.

7. "Papers Resulting from Deliberations of the Society's Discussion Group on Seismic Design of Reinforced Concrete Walls and Diaphragms", Bulletin of the New Zealand National Society for Earthquake Engineering, Vol. 13, No. 2, June 1980, pp.103-193.

8. "Papers Resulting from Deliberations of the Society's Discussion Group on the Seismic Design of Bridges", Bulletin of the New Zealand National Society for Earthquake Engineering, Vol. 13, No. 3, September 1980, pp.226-309.

9. "Building Code Requirements for Reinforced Concrete (ACI 318-83)", and "Commentary on Building Code Requirements for Reinforced Concrete (ACI 318-83)", American Concrete Institute, Detroit, 1983, p.111 and 155.

10. Paulay, T., "Developments in Seismic Design of Reinforced Concrete Frames in New Zealand", Canadian Journal of Civil Engineering, Vol. 8, No. 2, June 1981, pp.91-113.

11. Paulay, T., "Lap Splices in Earthquake-Resisting Columns", Journal of American Concrete Institute, Vol. 79, No. 6, November-December 1982, pp.458-469.

12. "Recommended Lateral Force Requirements and Commentary", Structural Engineers' Association of California, San Francisco, 1975.

13. Tanaka, H., Park, R. and MacNamee, B., "Anchorage of Transverse Reinforcement in Rectangular Reinforced Concrete Columns in Seismic Design", Bulletin of the New Zealand National Society for Earthquake Engineering, Vol. 18, No. 2, June 1985, pp.165-190.

14. Park, R. and Sampson, R.A., "Ductility of Reinforced Concrete Column Sections in Seismic Design", Journal of the American Concrete Institute, Vol. 69, No. 9, September 1972, pp.543-551.

15. Park, R. and Leslie, P.D., "Curvature Ductility of Circular Reinforced Concrete Columns Confined by the ACI Spiral", 6th Australasian Conference on the Mechanics of Structures and Materials, Vol. 1, Christchurch, August 1977, pp.342-349.

16. Priestley, M.J.N. and Park, R., "Strength and Ductility of Bridge Substructures", Research Report 84-20, Department of Civil Engineering, University of Canterbury, December 1984, p.120.

17. Mander, J.B., Priestley, M.J.N. and Park, R., "Seismic Design of Bridge Piers", Research Report 84-2, Department of Civil Engineering, University of Canterbury, February 1984, p.442 plus appendices.

18. Paulay, T. and Park, R., "Joints in Reinforced Concrete Frames Designed for Earthquake Resistance", Research Report 84-9, Department of Civil Engineering, University of Canterbury, June 1984, p.71.

NOTATION

A_b = area of a longitudinal bar

A_c = area of concrete core of column measured to outside of the peripheral transverse reinforcement

A_g = gross area of column cross section

A_j = effective joint area

A_{jh} = total area of horizontal shear reinforcement placed between top and bottom beam reinforcement in a beam-column joint

A_{jv} = total area of vertical shear reinforcement, at the side faces of the column, placed between the corner bars of a beam-column joint

A_s = area of longitudinal tension reinforcement in a beam

A'_s = area of longitudinal compression reinforcement in a beam

A_{sc} = area of longitudinal tension reinforcement in one face of column

A'_{sc} = area of longitudinal compression reinforcement in one face of column

A_{sh} = total area of transverse reinforcement, including cross ties, in direction under consideration within longitudinal spacing s_h

A_{sp} = area of spiral bar

A_{te} = area of one leg of a stirrup-tie

A_v = area of vertical shear reinforcement in beam within longitudinal spacing s

b = width of compression face of member

b_c = width of column

b_j = effective width of joint

b_w = width of beam web

$C_j = V_{jh}/(V_{jx} + V_{jy})$

C'_c = compression force in concrete of beam during positive moment

C'_s = compression force in longitudinal beam reinforcement during positive moment

d = distance from extreme compression fibre of concrete to centroid of tension steel

d_b = diameter of longitudinal reinforcing bar

d_s = diameter of spiral

f'_c = concrete compressive strength

f_y = yield strength of longitudinal reinforcement

f_{yh} = yield strength of transverse reinforcement

h'' = dimension of concrete core of section, perpendicular to the direction of hoop bars, measured to the outside of the perimeter hoop in the New Zealand code or to the centres of the perimeter hoop in the ACI code

h_b = overall depth of beam

h_c = overall depth of column

ℓ_{db} = basic development length of a deformed bar in compression

ℓ_{dh} = basic development length of a deformed bar in tension terminating with a standard 90° hook

M_{code} = column moment derived from the code static seismic loading

M_{col} = design uniaxial bending moment for column

P_e = column load in compression due to the design gravity and seismic loading

P_{col} = design axial load for column

P_o = axial (concentric) load strength of column

r = see Eq. 10

s = centre to centre spacing of stirrups or ties or spirals or circular hoops

s_h = centre to centre spacing of hoop sets

T = tensile force in longitudinal beam reinforcement during negative moment

T' = tensile force in longitudinal beam reinforcement during positive moment

T_1 = fundamental period of vibration of the structure

v_b = shear stress carried by the concrete when $P_e = 0$ in gravity load design

v_c = shear stress carried by concrete of a column

v_{jh} = nominal horizontal shear stress in a beam-column joint

V = column shear

V_{ch} = horizontal shear carried by diagonal compression strut mechanism in a beam-column joint

V_{code} = column shear force derived from the code static seismic loading

V_{col} = design shear force for column

V_{cv} = vertical shear carried by diagonal compression strut mechanism in a beam-column joint

V_{jh} = horizontal design shear force in a beam-column joint

V_{jv} = vertical design shear force in a beam-column joint

V_{jx} = horizontal design shear force in x direction in a beam-column joint

V_{jy} = horizontal design shear force in y direction in a beam-column joint

V_u = design shear force

γ = see Eq. 39

Δ_u = maximum displacement

Δ_y = displacement at first yield

μ = Δ_u/Δ_y

ρ = $A_s/b_w d$

ρ' = $A'_s/b_w d$

ρ_s = ratio of total volume of spiral or circular hoop reinforcement to total volume of concrete core measured to the outside of the spirals or hoops

ϕ = strength reduction factor

ϕ_o = ratio of overstrength flexural capacity of beam to the dependable moment capacity of beam required by the code

ϕ_u = maximum curvature

ϕ_y = curvature at first yield

ω = factor allowing for higher mode and concurrent loading effects on the bending moments in columns

MOMENT RESISTING REINFORCED CONCRETE FRAMES OF LIMITED DUCTILITY

R. Park

MOMENT RESISTING REINFORCED CONCRETE FRAMES OF LIMITED DUCTILITY

by R. Park
University of Canterbury

Summary

A brief summary of New Zealand code provisions for the seismic design of moment resisting reinforced concrete frames of limited ductility is outlined.

(a) Existing New Zealand Design Codes for Moment Resisting Frames of Limited Ductility for Buildings

NZS 4203:1984 "Code of Practice for General Structural Design and Design Loadings for Buildings" [1] states that "Structures of limited ductility, not specifically designed to ensure ductile flexural yielding through the application of the principles of capacity design, shall be suitably designed and detailed in accordance with the appropriate materials code". Moment resisting frames of limited ductility having a maximum height of 4 storeys or 18 m, or if the roof and wall mass are less than 150 kg/m^2 a maximum height of 5 storeys or 22.5 m, are assigned a structural type factor of S = 2.0. This structural type factor may be compared with the value of S = 0.8 assigned to "ductile frames". That is, moment resisting frames of limited ductility are designed for seismic forces which are 2.0/0.8 = 2.5 times the seismic force used for the design of ductile moment resisting frames.

NZS 3101:1982 "Code of Practice for the Design of Concrete Structures" [2] has a Section 14 "Seismic Requirements for Structures of Limited Ductility" which is intended to be used with the "General Principles and Requirements" and the "Additional Principles and Requirements for Members Not Designed for Seismic Loading" specified in other sections of the code. The main features of Section 14 for moment resisting reinforced concrete frames of limited ductility are:

- Capacity design is not required.
- Design for concurrent earthquake effects from loadings in two principal directions is not required.
- Shear strengths provided are to have a suitable margin over the required flexural strengths.
- Flexural strengths outside the designated end regions are to have a suitable margin over the design moments.
- Lengths of designated end regions of beams and columns are equal to the member depth, or whole member length if the flexural strengths outside the designated end regions do not satisfy the code requirements.
- Transverse reinforcement in designated end regions should have spacing not exceeding 10 longitudinal bar diameters and an equation is given for the area of hoop steel required for concrete confinement. Transverse reinforcement for confinement may not be required, particularly when significant compression steel is present.
- In the designated end regions the "shear carried by the concrete" may be assumed to be one-half of that for gravity load design, and spacing of shear reinforcement should not exceed one-quarter of the effective depth of the member.

(b) Comparison of New Zealand Design Codes for Ductile Frames and Frames of Limited Ductility for Buildings

A comparison of the main design provisions of New Zealand codes for reinforced concrete ductile moment resisting frames and moment resisting frames of limited ductility are given in Table 1.

Table 1 : Seismic Design Provisions for Reinforced Concrete Moment Resisting Frames

Clause	Ductile Frames	Clause	Frames of Limited Ductility
NZS 4203 3.3.3.1	1. Definition Ductile frames shall be capable of dissipating seismic energy in a flexural mode at a significant number of plastic hinges in beams except that dissipation of seismic energy at plastic hinges in columns is permitted for buildings which comply with Clause 3.3.3.5	NZS 4203 3.4.2 Table 5	1. Definition Frames of limited ductility have a maximum height of four storeys or 18 m, or if roof and wall mass are less than 150 kg/m^2 a maximum height of five storeys or 22.5 m
NZS 4203 3.4.2 Table 5 NSZ 3101 3.5.1.1 and 6.5.1.4	2. Design Actions The structural type factor used for determining seismic design forces is S = 0.8 Capacity design is used and the effects of concurrent seismic forces are included	NZS 4203 3.4.2 Table 5 NZS 3101 14.4.3	2. Design Actions The structural type factor used for determining seismic design forces is S = 2.0 Capacity design and design for concurrent seismic forces are not required
NZS 3101 4.3.1 C3.A and 6.5.1.4	3. Required Flexural Strengths Flexural strengths: Beams $\phi M_i \geq M_u$ Columns $M_i \geq M_u^o$	NZS 3101 14.4.2.2	3. Required Flexural Strengths In end regions: Beams $\phi M_i \geq M_u$ Columns $\phi M_i \geq M_u$ Outside end regions: Beams $\phi M_i \geq M_g + 1.5M_{eq}$ Columns $\phi M_i \geq M_g + 1.5M_{eq}$
NZS 3101 7.5.1.1 7.5.1.2 9.5.2	4. Required Shear Strengths Beams $V_i \geq V_u^o$ Columns $V_i \geq V_u^o$ Joints $V_i \geq V_u^o$	NZS 3101 14.4.2.1	4. Required Shear Strengths Beams $\phi V_i \geq V_g + 2V_{eq}$ Columns $\phi V_i \geq V_g + 2V_{eq}$ Joints $\phi V_i \geq V_g + 2V_{eq}$

Table 1 Continued

Clause	Ductile Frames	Clause	Frames of Limited Ductility
NZS 3101 6.5.3.1	5. Length of Potential Plastic Hinge Regions Beams: Over lengths equal to twice the beam depth at the ends of the beam and within the span where plastic hinges can form.	NZS 3101 14.5.2	5. Length of End Regions Beams and columns: Over lengths equal to the depth of the member at the ends of the member, except that if Clause 14.4.2.2 is not complied with it is considered to be the whole length of the member.
6.5.4.1	Columns: Over end regions equal to the larger of the largest cross section dimension or where the moment exceeds 0.8 of the moment at that end of the member. This length is increased by 50% if $P_e \geq 0.3f'_c A_g \phi$.		
NZS 3101	6. Transverse Reinforcement Within the Potential Plastic Hinge Regions	NZS 3101	6. Transverse Reinforcement Within the End Regions
6.5.3.3	Beams: If yielding of flexural steel can occur on both faces of member, the centre to centre spacing of stirrup-ties s is not to exceed the smaller of d/4 or six longitudinal bar diameters, or 150 mm.	14.6.2	Beams and Columns: The centre to centre spacing of stirrup-ties, or rectangular hoops or cross ties, is not to exceed ten longitudinal bar diameters. The area of transverse reinforcement for confinement is given by $A_{sh} = R_c(0.02 s_h h \frac{f'_c}{f_{yh}})$ if $\gamma > 1.0$ where $\gamma = \frac{M^*_e + 0.3P_e h}{0.6\phi f'_c A_g h} \leq 3.0$ and $0 \leq R_c = \left[\frac{\gamma}{1+\rho^* m} - 1\right] \leq 1.0$
6.5.3.3	The yield force of the stirrup-tie must at least equal one-sixteenth of the yield force of the longitudinal bar or bars it is to restrain multiplied by s/100.		
7.5.2.2	The stirrups must also satisfy shear strength requirements computed assuming $v_c = 0$.		
6.5.4.3	Columns: The centre to centre spacing of transverse confining steel is not to exceed the smaller of one-fifth of the least lateral dimension of the cross section or six longitudinal bar diameters or 200 mm. The yield force of the transverse bar in rectangular arrangements of hoop steel must at least equal one-sixteenth of the yield force of the longitudinal bar or bars it is to restrain. The transverse reinforcement	14.7.2	The transverse reinforcement provided must also satisfy the shear strength requirements computed assuming v_c is one-half of that for gravity load design.
		14.7.5	Maximum spacing of shear reinforcement is not to exceed d/4.

Table 1 Continued

Clause	Ductile Frames	Clause	Frames of Limited Ductility
7.5.2.2	must satisfy the code equations 6-22 and 6-23 for spirals or circular hoops or equations 6-24 and 6-25 for rectangular hoops. The transverse reinforcement must also satisfy shear strength requirements computed assuming $v_c = 0$ if $P_e/f'_c A_g \leq 0.1$ or v_c as given by equation 7-41 if $P_e/f'_c A_g > 0.1$.		
NZS 3101 9.3 and 9.5	7. Beam-Column Joints Shear: Transverse and vertical reinforcement must satisfy the shear strength requirements for horizontal and vertical shear using equations 9-1 to 9-15.	NZS 3101	7. Beam-Column Joints No specific design rules stated. Use design rules for non-seismic joints with full value of v_c
5.5.2.1 -5.5.2.2	Anchorage: Longitudinal reinforcement passing through interior joint cores should have diameters not exceeding that permitted by the code. Longitudinal beam reinforcement anchored in column cores or beam strips shall have anchorage commencing either at mid-depth of the column or at $10d_b$ from the column face, unless plastic hinging is located away from the column face in which case anchorage can be considered to commence at the column face.		

(c) Possible Future Developments in the Concrete Design Code

The aim for future developments should be to produce more complete yet simple provisions for the design of moment resisting reinforced concrete frames for buildings of limited ductility, maintaining the policy of not requiring capacity design or design for concurrent loading.

Research is also needed to provide further information on the following aspects:

- Design actions for moment, axial load and shear in beams, columns and joints.
- Beam design-end regions, distribution of longitudinal and transverse reinforcement, shear capacity.
- Column design-end regions, distribution of longitudinal and transverse reinforcement, shear capacity.
- Beam-column joint design - development of beam and column longitudinal bars, shear capacity.

The equations for the area of transverse reinforcement for confinement for flexural members with or without axial load at present specified in Section 14 of NZS 3101 are difficult to use. It may be more appropriate to revert to separate requirements for transverse steel for confinement for beams and columns. For example, for columns in designated end regions the spacing of hoops and spirals could be required not to exceed one-quarter of the least lateral dimension of the member or six longitudinal bar diameters, whichever is smaller, and the specified quantity of transverse confining reinforcement could be required to be at least one-half of that required for columns of ductile frames not protected against plastic hinging. Note that the columns are not protected by capacity design from the possible formation of column sidesway mechanisms forming in one storey, but it could be considered that for frames up to the permitted height the above recommended quantity of confining reinforcement and the limited maximum spacing of it would ensure adequate ductility.

For the beam-column joints significant shear could be considered to be carried by the concrete mechanisms (that is, $v_c > 0$) even for low axial loads on columns. It is likely that the joint shear could be catered for by carrying the transverse reinforcement in the column ends through the joint core and ensuring that at least one intermediate longitudinal column bar is present at each face of the joint core. No special design rules for development of beam and column longitudinal bars may need to be recommended. That is, for exterior joints beam bar anchorage could be considered to commence at the column face, and for interior joints no restriction on bar diameter may need to be recommended. Note that the shear resisted by the concrete diagonal compression strut mechanism, and the bond strength, in the joint core degrade progressively during loading cycles when significant inelastic deformations occur in the adjacent plastic hinge regions. This degradation during "limited ductility" deformations will be less than during "full ductility" deformations and hence shear and bond are not so critical in design for limited ductility. Further research is needed to clarify the above suggested design provisions.

(d) References

1. "Code of Practice for General Structural Design and Design Loadings for Buildings, NZS 4203:1984", Standards Association of New Zealand, Wellington, 1984, p.100.

2. "Code of Practice for the Design of Concrete Structures, NZS 3101 Part 1: 1982", and "Commentary on the Design of Concrete Structures, NZS 3101 Part 2:1982", Standards Association of New Zealand, Wellington, 1982, p.127 and 156.

(e) Notation

A_g = gross area of section of member

A_g^* = gross area of concrete located between the compressive edge of the section and a line 0.2h therefrom

A_{sh} = total effective area of hoop bars and supplementary cross-ties in the direction under consideration within centre to centre spacing s_h

d = distance from the extreme compression fibre of the concrete to the centroid of the tension reinforcement

d_b = diameter of longitudinal bar

f'_c = compressive cylinder strength of concrete

f_y = yield strength of longitudinal reinforcement

f_{yh} = yield strength of transverse reinforcement

h = overall depth of member

h_c = overall depth of column

M_e^* = moment resulting from loading combination U involving factored gravity and earthquake loads referred to mid-depth of section

M_{eq} = moment associated with earthquake load E

M_g = moment associated with factored gravity loads

M_i = ideal flexural strength

M_u = design moment due to factored load combinations U

M_u^o = design column moment found from capacity design taking into account overstrength beam moments, concurrent seismic loading and magnification of column moments due to dynamic effects

m = $f_y/0.85f'_c$

P_e = design axial load on column due to loading combination U involving factored gravity and earthquake loads

R_c = reduction factor for confinement

S = structural type factor

s = centre to centre spacing of sets of stirrup-ties

s_h = centre to centre spacing of sets of hoops or supplementary cross-ties

V_{eq} = shear force associated with earthquake load E

V_g = shear force associated with factored gravity loads

V_i = ideal shear strength

V_u^o = shear force found using capacity design taking into account overstrength beam moments, concurrent seismic loading and magnification of column moments due to dynamic effects, where appropriate

v_c = ideal shear stress provided by the concrete shear resisting mechanisms

γ = strength parameter used for confinement criteria

ϕ = strength reduction factor

COMPARISON OF RECENT NEW ZEALAND AND UNITED STATES SEISMIC DESIGN PROVISIONS FOR REINFORCED CONCRETE BEAM-COLUMN JOINTS

AND

TEST RESULTS FROM FOUR UNITS DESIGNED ACCORDING TO THE NEW ZEALAND CODE

R. Park and J.R. Milburn

COMPARISON OF RECENT NEW ZEALAND AND UNITED STATES SEISMIC DESIGN PROVISIONS FOR REINFORCED CONCRETE BEAM-COLUMN JOINTS AND TEST RESULTS FROM FOUR UNITS DESIGNED ACCORDING TO THE NEW ZEALAND CODE

R. Park* and J.R. Milburn**

This paper will be presented at the Third South Pacific Regional Conference on Earthquake Engineering, Wellington, May 1983.

SYNOPSIS

A comparison is made of the seismic design provisions for reinforced concrete beam-column joints required by the new New Zealand concrete design code NZS 3101 and recently proposed United States procedures. Large differences are shown to exist between these new provisions of the two countries. Results are reported of cyclic load tests which were conducted according to the requirements of the new NZS 3101. The test results showed that location of plastic hinges in beams away from the column faces may be of considerable advantage in the design of joints, when member sizes are small and joint shears are high, due to less congestion of reinforcement and better anchorage conditions.

INTRODUCTION:

The procedures for the seismic design of reinforced concrete beam-column joints given in the new New Zealand concrete design code NZS 3101 (1) are based on a considerable amount of test evidence accumulated through the years and on behavioural models for joint core shear resistance based on those test results. A summary of tests conducted in New Zealand on reinforced concrete beam-column joints is given elsewhere(2). The mechanisms of joint core shear resistance on which the code equations are based are also described elsewhere(1,2,3,4). It is of interest that current proposals for the revision of codes in the United States show that a greatly different approach to the seismic design of beam-column joints is being adopted in that country. The United States approach leads to less transverse reinforcement in the joint core in some cases and to more in other cases. The differences between the New Zealand and United States approaches are of interest, particularly since difficulties are often experienced in placing the amount of shear reinforcement required by codes in joint cores.

This paper first sets out a comparison between the New Zealand and the recently proposed United States approaches for the design of reinforced concrete beam-column joints. The results of some recent tests conducted at the University of Canterbury on four reinforced concrete beam-column joints are then described. The four test specimens were designed to illustrate various design approaches permitted by NZS 3101, including the concept of locating the plastic hinge away from the joint core, and to examine possible conservatism in the New Zealand approach.

* Department of Civil Engineering, University of Canterbury, Christchurch
** Holmes, Wood, Poole & Johnstone, Consulting Engineers, Christchurch

COMPARISON OF RECENT NEW ZEALAND AND UNITED STATES SEISMIC DESIGN PROVISIONS FOR REINFORCED CONCRETE BEAM-COLUMN JOINTS:

The new New Zealand code NZS 3101 (1) contains detailed provisions for the seismic design of reinforced concrete beam-column joints. Currently in the United States drafts are available of proposed revisions to the existing Appendix A of ACI 318-77(5) which give special provisions for seismic design. Also, ASCE-ACI Committee 352 on Joints and Connections in Monolithic Concrete Structures, which published its last report in 1976(6), is currently revising its recommendations(7). These two proposed United States procedures are similar in approach and the proposed ASCE-ACI Committee 352 approach is compared in detail with the New Zealand approach below.

Approach of New Zealand Code NZS 3101(1)

(i) Design Assumptions

The NZS 3101 code provisions are intended to ensure that joints are designed in such a way that when inelastic lateral displacements occur in ductile frames the required energy dissipation occurs in the potential plastic hinge regions of the adjacent members and not in the joint core regions. Accordingly, the joint core should be designed to resist the forces arising when the overstrength of the framing members is developed. That is, the stresses in the flexural steel at the plastic hinges are assumed to be 1.25 times the specified yield strength in the case of Grade 275 steel, or 1.4 times the specified yield strength in the case of Grade 380 steel. The design horizontal shear force V_{jh} and the design vertical shear force V_{jv} are found by rational analysis taking into account the effect of all the forces acting on the joint. When beams frame into the joint in two directions, these forces need only be considered in

each principal direction independently.

In determining the shear strength of the joint core the strength reduction factor ϕ is taken as unity. The shear applied to the joint core is assumed to be carried by a mechanism consisting of a concrete diagonal compression strut and a mechanism consisting of truss action from a concrete diagonal compression field and the shear reinforcement. The first mechanism is commonly referred to as the "shear carried by the concrete" and the second as the "shear carried by the shear reinforcement". Shear reinforcement is detailed to carry the design shear forces in excess of those carried by the concrete.

In order to prevent the concrete diagonal compression strut from crushing, the nominal horizontal shear stress v_{jh} in either principal direction is limited to $1.5\sqrt{f'_c}$ MPa, where

$$v_{jh} = \frac{V_{jh}}{b_j h_c} \qquad (1)$$

The effective joint width, b_j, is defined as

a) when $b_c > b_w$

either $b_j = b_c$ or $b_j = b_w + 0.5h_c$,

whichever is smaller.

b) when $b_c < b_w$

either $b_j = b_w$ or $b_j = b_c + 0.5h_c$,

whichever is the smaller.

(ii) Horizontal Joint Shear

The total area of horizontal shear reinforcement placed between the outermost layers of top and bottom beam reinforcement is required to be not less than

$$A_{jh} = V_{sh}/f_{yh} \qquad (2)$$

where the horizontal design shear force to be resisted by this shear reinforcement is given by

$$V_{sh} = V_{jh} - V_{ch} \qquad (3)$$

In Eq. 3, V_{ch} should be taken as zero unless one of the following situations applies:

(a) When the minimum average compressive stress on the gross concrete area of the column above the joint exceeds $0.1\, f'_c/C_j$

$$V_{ch} = \frac{2}{3}\sqrt{\frac{C_j P_e}{A_g} - \frac{f'_c}{10}}\,(b_j h_c) \qquad (4)$$

(b) When the design is such that plastic hinging occurs in the beam at a distance away from the column face not less than the beam depth nor 500 mm, or for external joints where the flexural steel is anchored outside the column core in a beam stub, the value of V_{ch} may be increased to

$$V_{ch} = 0.5\,\frac{A'_s}{A_s}\,V_{jh}\left(1 + \frac{C_j P_e}{0.4 A_g f'_c}\right) \qquad (5)$$

where A'_s/A_s should not be taken larger than 1.0. When the axial column load results in tensile stresses over the gross concrete area exceeding $0.2f'_c$, $V_{ch} = 0$. For axial tension between these limits V_{ch} may be obtained by linear interpolation between zero and the value given by Eq. 5 when P_e is taken as zero.

(c) For external joints without beam stubs at the far face of column, Eq. 5 may be used when multiplied by the factor

$$\frac{3h_c(A_{jv}\text{ provided})}{4h_b(A_{jv}\text{ required})} \qquad (5a)$$

which should not be taken as greater than 1.0. Use of this factor requires that the beam bars be anchored using a 90° standard hook in the joint core in accordance with the relevant code section.

(d) When the ratio h_c/h_b is greater than or equal to 2.0, V_{ch} need not be taken as less than

$$V_{ch} = 0.2 b_j h_c \sqrt{f'_c} \qquad (6)$$

(iii) Vertical Joint Shear

The total area of vertical shear reinforcement, normally in the form of intermediate column bars on the side faces of the column crossing the critical corner to corner diagonal tension crack, should not be less than

$$A_{jv} = V_{sv}/f_y \qquad (7)$$

where the vertical design shear force to be resisted by this shear reinforcement is

$$V_{sv} = V_{jv} - V_{cv} \qquad (8)$$

In Eq. 8, V_{cv} is given by

$$V_{cv} = \frac{A'_{sc}}{A_{sc}}\,V_{jv}\left(0.6 + \frac{C_j P_e}{A_g f'_c}\right) \qquad (9)$$

except where axial load results in tensile stresses over the column section. When P_e is tensile, value of V_{cv} is interpolated linearly between the value given by Eq. 9 when P_e is taken as zero and zero when the axial tensile stress over the gross concret area is $0.2f'_c$.

However, if plastic hinges are expected to form in the column above or below the joint core, but not when elastic behaviour is assured in the column or

column stub on the opposite side of the joint, V_{cv} should be taken as zero for any axial load on the column.

The spacing of vertical shear reinforcement in each plane of any beam framing into the joint should not exceed 200 mm and in no case should there be less than one intermediate bar in each side of the column in that plane.

(iv) Confinement

The horizontal transverse confinement reinforcement in the joint core should not be less than that required in the potential plastic hinge regions in the adjacent columns. Thus for columns with hoops and supplementary cross ties the total area of transverse steel in each of the principal directions of the cross section should be at least equal to

$$A_{sh} = 0.3 s_h h'' \left(\frac{A_g}{A_c} - 1\right)\frac{f'_c}{f_{yh}} \left(0.5 + 1.25\frac{P_e}{\phi f'_c A_g}\right) \qquad (10)$$

but not less than

$$A_{sh} = 0.12 s_h h'' \frac{f'_c}{f_{yh}} \left(0.5 + 1.25\frac{P_e}{\phi f'_c A_g}\right) \qquad (11)$$

However if the joint has beams framing into all four column faces and is designed using the conditions applicable for Eq. 5, the transverse reinforcement in the joint core may be reduced to one-half of that required by Eqs. 10 and 11.

In no case shall the spacing of transverse reinforcement in the joint core exceed 10 times the diameter of the longitudinal column bar or 200 mm, whichever is less.

(v) Bar Anchorage in Interior Joints

To keep bond stresses to an acceptable level, the diameters of longitudinal bars d_b passing through a joint core are limited as follows:

Beam bars:

When plastic hinging can occur adjacent to the column face:

$d_b \leq h_c/25$ when $f_y = 275$ MPa, or

$d_b \leq h_c/35$ when $f_y = 380$ MPa.

When plastic hinging is located at a distance from the column face of at least the beam depth or 500 mm, whichever is less:

$d_b \leq h_c/20$ when $f_y = 275$ MPa, or

$d_b \leq h_c/25$ when $f_y = 380$ MPa.

Column bars:

When columns are intended to develop plastic hinges:

$d_b \leq h_b/20$ when $f_y = 275$ MPa, or

$d_b \leq h_b/25$ when $f_y = 380$ MPa.

When columns are not intended to develop plastic hinges:

$d_b \leq h_b/15$ when $f_y = 275$ MPa, or

$d_b \leq h_b/20$ when $f_y = 380$ MPa.

(vi) Bar Anchorage at Exterior Joints

The basic development length of a deformed bar in tension terminating with a standard 90^o hook is

$$\ell_{hb} = \frac{66 d_b}{\sqrt{f'_c}} \frac{f_y}{275} \qquad (14)$$

Where the bar diameter is 32 mm or smaller with side cover not less than 60 mm and cover on tail extension not less than 40 mm, the value may be reduced to $0.7\ell_{hb}$, or where the concrete is suitably confined the value may be reduced to $0.8\ell_{hb}$.

The basic development length for a deformed bar in compression is

$$\ell_{db} = 0.24 d_b f_y/\sqrt{f'_c} \qquad (15)$$

but not less than $0.044 d_b f_y$. (15a)

Where the concrete is suitably confined the value may be reduced to $0.75\ell_{db}$.

The anchorage is considered to commence within the column at distance $0.5h_c$ or $10d_b$ from the column face, whichever is less, except that when the plastic hinge is located away from the column face anchorage may be considered to commence at the column face.

Draft Approach of ASCE-ACI Committee 352 (7)

(i) Design Assumptions

The draft revisions of ASCE-ACI Committee 352(7) have adopted a fundamentally different approach to the whole problem of joint shear, which is also similar in principle to that proposed in the draft Appendix A of the 1983 revision of the building code of the American Concrete Institute, ACI 318. In the existing ACI and ASCE recommendations (5,6) the approach was similar, although more simplistic, to that used in New Zealand. The draft ASCE-ACI Committee 352 proposals are reviewed below.

Provisions are given for two types of joints, essentially differentiating between joints expected to be subjected to cyclic inelastic deformations (Type 2) and those not (Type 1). The requirements for Type 2 joints only will be reviewed. Only horizontal joint shear is considered in the approach.

(ii) Horizontal Joint Shear

The forces in the reinforcing bars of the beams acting at the joint core boundaries are determined assuming that the steel stress is 25% greater than the specified yield strength, regardless of the grade of steel. For joints with beams framing in from two perpendicular directions the horizontal shear in the joint is checked independently in each direction. The design horizontal shear force, V_u, is computed for the horizontal plane at midheight of the joint by considering the shear forces on the boundaries of the free body of the joint and the normal tension and compression forces in the members framing into the joint.

The calculated value of V_u should satisfy

$$V_u \leq \phi\gamma \sqrt{f'_c} b_c h_c \qquad (16)$$

where ϕ is the strength reduction factor for shear taken as 0.85, and b_c and h_c are the gross width and thickness of the column, respectively. However, the value for b_c in Eq. 16 should not be taken as greater than twice the width of the beam framing into the joint. The value for f'_c used in Eq. 16 should not be taken as larger than 34 MPa. The value of γ depends on the joint configuration and is 1.33 for an interior joint, 1.00 for an exterior joint, and 0.67 for other joints. To be classified as an interior joint, members must frame into all four sides of the joint and cover at least three-quarters of the width and depth of the joint face. To be classified as an exterior joint, members must frame into three sides of the joint and the width and total depth of the beams on opposite faces of the joint must not vary by more than 25%.

(iii) Vertical Joint Shear

No calculation procedure is recommended to check resistance for vertical joint shear forces.

(iv) Confinement

Where rectangular hoop and cross tie transverse reinforcement is used, the total area of a single or overlapping hoops, or hoops with cross ties of the same size, in each direction should be at least equal to

$$A_{sh} = 0.3 \frac{s_h h'' f'_c}{f_{yh}} \left(\frac{A_g}{A_c} - 1 \right) \qquad (17)$$

but not less than

$$A_{sh} = 0.09 \frac{s_h h'' f'_c}{f_{yh}} \qquad (18)$$

For interior joints, the required transverse steel can be one-half of that required by Eqs. 17 and 18. The hoop spacing s_h should not exceed one quarter of the minimum column dimension, 6 times the diameter of the longitudinal bar or 200 mm, but need not be less than 150 mm.

The centre-to-centre spacing between adjacent longitudinal column bars should not exceed the larger of 200 mm or one-third of the column cross section dimension in that direction.

(v) Bar Anchorage

The diameter of all straight bars passing through joints should be selected such that for beam bars $d_b \leq h_c/24$, and for column bars $d_b \leq h_b/24$.

The development length of a bar terminating with a standard 90° hook is given by

$$\ell_{dh} = 0.21 f_y d_b / \sqrt{f'_c} \qquad (19)$$

but not less than $8d_b$ or 150 mm, whichever is greater. Bar diameters should not exceed 35 mm and hooks should be situated in the column core located as far from the critical section as possible. If the confinement steel spacing does not exceed $3d_b$, ℓ_{dh} may be reduced by 20%. The anchorage is considered to commence at the edge of the concrete core.

Comparison of the NZS 3101 and the Draft ASCE-ACI Committee 352 Approaches

The main differences:

There are large differences in the approaches to joint core shear design adopted in NZS 3101 and in the draft ASCE-ACI Committee 352 procedures.

The NZS 3101 requirements are based on a rational model for the mechanisms of shear resistance of the joint core, namely a mechanism consisting of a concrete diagonal strut and a mechanism consisting of truss action of a concrete diagonal compression field and shear reinforcement. Account is taken of the reduced capacity of the diagonal compression strut mechanism, particularly in interior joints, when plastic hinging forms adjacent to the core faces and results in full depth flexural cracking there during reversed loading. Increased concrete shear capacity and less severe bond and anchorage criteria are permitted if plastic hinging is forced to occur away from the joint core faces. Both horizontal and vertical shear reinforcement are designed to carry that shear in excess of the concrete capacity.

The draft ASCE-ACI Committee 352 approach assumes that providing the design horizontal shear force on the joint core does not exceed a quantity $\phi\gamma\sqrt{f'_c} b_c h_c$, the amount of transverse reinforcement required for column confinement, reduced by one half in those cases where the joint is adequately confined by structural members on all four faces, will also be adequate for

shear resistance in the joint core. That is, once the size and spacing of transverse reinforcement in the potential plastic hinge regions in the ends of the column have been established, that quantity or one half is continued through the joint core. This approach has been adopted evidently because Meinheit and Jirsa (8) have concluded that shear strength of joint cores was not as sensitive to joint core shear reinforcement as is implied in the earlier report by ASCE-ACI Committee 352(6).

In the view of the authors, this ASCE-ACI Committee 352 approach is largely empirical and is too simplistic. It does not apply to the design of joints with unusual configurations, it makes little distinction between interior and exterior joints, and it does not allow for the difference in performance of joints with plastic hinges adjacent to or removed from the joint core. When compared with the NZS3101 approach it is conservative in some cases and unconservative in others.

The lack of a calculation procedure for vertical joint steel in the draft ASCE-ACI Committee 352 approach may well be offset by the requirement that at least an eight bar column be used. However, the amount of vertical shear reinforcing required may be greater than that provided to satisfy column flexural demand.

The anchorage requirements of the draft ASCE-ACI Committee 352 approach are considerably less severe for bars passing through joints than those of NZS 3101. For the case of exterior joints, anchorage is considered to commence at the surface of the concrete core. That is, loss of bond in the cover concrete only is assumed.

Examples of Comparisons of Joint Shear Reinforcement

(1) Comparison of an interior joint with beams on all four faces.

Draft ASCE-ACI Approach

For a large column, if $h'' = 0.9b_c$, from Eq. 18

$$A_{sh} = 0.5 \times 0.09 \frac{s_h 0.9 b_c f'_c}{f_{yh}}$$

$$\therefore A_{sh} f_{yh}/s_h = 0.0405 b_c f'_c \qquad (i)$$

Also from Eq. 16, the shear strength of the joint core is

$$V_u = 0.85 \times 1.33\sqrt{f'_c} b_c h_c$$

$$= 1.13\sqrt{f'_c} b_c h_c \qquad (ii)$$

That is, the amount of joint shear reinforcement given by Eq. i should satisfy the horizontal joint shear force imposed in Eq. ii.

NZS 3101 Approach

(a) For plastic hinge forming adjacent to joint core:

If $P_e/f'_c A_g = 0.1$, from Eq. 4 $V_{ch} = 0$

Design joint horizontal shear force, from Eqs. 2, 3 and 4 and assuming that

$A_{jh} = A_{sh} h_b/s_h$, is

$$V_{jh} = V_{sh} = A_{jh} f_{yh} = A_{sh} f_{yh} h_b/s_h$$

If $A_{sh} f_{yh}/s_h$ from Eq. i is substituted

$$V_{jh} = (0.0405 b_c f'_c) h_b$$

$$= (0.0405\sqrt{f'_c} \frac{h_b}{h_c})\sqrt{f'_c} b_c h_c$$

Say $f'_c = 25$ MPa and $h_b/h_c = 1$, then $V_{jh} = 0.203\sqrt{f'_c} b_c h_c$

But from Eq. ii, draft ASCE-ACI approach would allow

$V_{jh} = 1.13\sqrt{f'_c} b_c h_c$, which is 5.6 times the V_{jh} allowed by NZS 3101.

(b) For plastic hinge forming away from the joint core:

If $P_e/f'_c A_g = 0.1$, $A'_s = A_s$ and

$C_j = 0.5$, from Eq. 5

$$V_{ch} = 0.5 V_{jh}(1 + \frac{0.5 \times 0.1}{0.4}) = 0.536 V_{jh}$$

$\therefore$ Design horizontal shear force, from Eqs. 2, 3 and 5 and assuming that

$A_{jh} = A_{sh} h_b/s_h$

$V_{jh} = 0.563 V_{jh} + V_{sh}$

$\therefore V_{jh} = 2.29 V_{sh} = 2.29 A_{sh} f_{yh} h_b/s_h$

If $A_{sh} f_{yh}/s_h$ from Eq. i is substituted

$$V_{jh} = 2.29 \times 0.0405 f'_c h_b b_c$$

$$= (0.0927\sqrt{f'_c} \frac{h_b}{h_c})\sqrt{f'_c} b_c h_c$$

Say $f'_c = 25$ MPa and $h_b/h_c = 1$, then $V_{jh} = 0.463\sqrt{f'_c} b_c h_c$

But from Eq. ii, draft ASCE-ACI approach would allow $V_{jh} = 1.13\sqrt{f'_c} b_c h_c$ which is 2.4 times the V_{jh} allowed by NZS 3101.

Note: For higher axial load levels than $0.1 f'_c A_g$, more shear will be carried by the concrete in the NZS 3101 approach than in the above example and the difference between the two approaches would be reduced.

(2) Comparison of a corner joint.

Draft ASCE-ACI Approach

$A_{sh}f_{yh}/s_h = 0.08 1 b_c f'_c$ (i.e. twice that for the interior joint)

$V_u = 0.85 \times 0.67\sqrt{f'_c}b_c h_c = 0.57\sqrt{f'_c}b_c h_c$

NZS 3101 Approach

(a) For plastic hinges forming adjacent to joint core without a beam stub.

If $P_e/f'_c A_g = 0.1$, $A'_s = A_s$,

$C_j = 0.5$, $h_c = h_b$,

and A_{jv} provided = A_{jv} required, from Eqs. 5 and 5a,

$$V_{ch} = \left[0.5 V_{jh} \left(1 + \frac{0.5 \times 0.1}{0.4} \right) \right] \times \frac{3}{4} = 0.422 V_{jh}$$

$\therefore V_{sh} = V_{jh} - V_{ch} = 0.578 V_{jh}$

$\therefore V_{jh} = 1.73 V_{sh} = 1.73(0.08 1 b_c f'_c) h_b$

$$= (0.140\sqrt{f'_c}\,\frac{h_b}{h_c}\,\sqrt{f'_c}b_c h_c$$

Say f'_c = 25 MPa and $h_b/h_c = 1$,

then $V_{jh} = 0.70\sqrt{f'_c}b_c h_c$

But draft ASCE-ACI approach would allow $V_{jh} = 0.57\sqrt{f'_c}b_c h_c$,

which is 0.81 times the V_{jh} allowed by NZS 3101.

(b) For plastic hinges forming away from the joint core.

If $P_e/f'_c A_g = 0.1$, $A'_s = A_s$, $C_j = 0.5$,

and $h_c = h_b$, from Eq. 5

$$V_{ch} = 0.5 V_{jh}(1 + \frac{0.5 \times 0.1}{0.4}) = 0.563 V_{jh}$$

$$\therefore V_{jh} = 2.29 V_{sh} = (0.185\sqrt{f'_c}\,\frac{h_b}{b_c}\,)\sqrt{f'_c}b_c h_c$$

Say f'_c = 25 MPa and $h_b/h_c = 1.0$,

then $V_{jh} = 0.927\sqrt{f'_c}b_c h_c$

But draft ASCE-ACI approach would allow $V_{jh} = 0.57\sqrt{f'_c}b_c h_c$,

which is 0.62 of the V_{jh} allowed by NZS 3101.

Note: Again for higher axial load levels than $0.1 f'_c A_g$, more shear would be carried by the concrete in the NZS 3101 approach.

TEST PROGRAMME:

Details of the Beam-Column Joint Units

Four reinforced concrete beam-column joint units were tested. Two were interior joints (Units 1 and 2) and two were exterior joints (Units 3 and 4). The units were designed according to the seismic provisions of NZS 3101 (1) to illustrate possible approaches permitted by that code. The units were tested under simulated seismic loading to compare the performance resulting from the different design approaches.

The overall dimensions of the units are shown in Fig. 1. The size of the cross sections may be taken as being representative of about ½ to ¾ of that of full scale members of a multistorey building frame. The units can be regarded as being that part of the joint regions of a plane frame between the midspan of the beams and the midheight of the columns. The columns of the units were designed to be stronger than the beams so that during severe seismic type loading the plastic hinges occurred in the beams. The plastic hinges in the beams were designed to occur either at the column faces (conventional design) or away from the column faces (relocated plastic hinge design), as illustrated in Fig. 2.

The units were loaded as shown in Fig. 2 by axial loads P at the ends of the columns and by vertical loads V at the ends of the beams while the ends of the columns were held in a vertical line by the loads V on the beams the effects of earthquake loading was simulated. The load reversals were applied slowly. The axial column load was held constant at $0.1 f'_c A_g$ during the tests.

Material Properties

The concrete was from Ordinary Portland cement and graded aggregate with a maximum aggregate size of 20 mm. The concrete properties are shown in Table 1. The test units were cast in the horizontal plane and damp cured for a week after casting. The steel reinforcement had the measured yield and ultimate strengths shown in Table 2 and the stress-strain curves shown in Fig. 3 measured over a 51 mm gauge length. All reinforcing steel was of Grade 275, except for the longitudinal column steel which was of Grade 380.

Table 1 : Properties of Concrete

Unit	1	2	3	4
Slump, mm	100	80	90	90
Age at Test, days	69	49	42	38
f'_c at Test, MPa	41.3	46.9	38.2	38.9

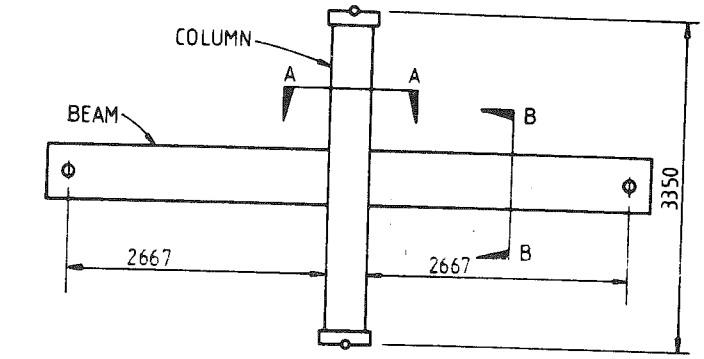

UNITS 1&2

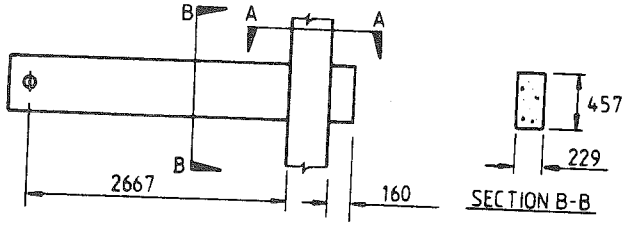

UNIT 3

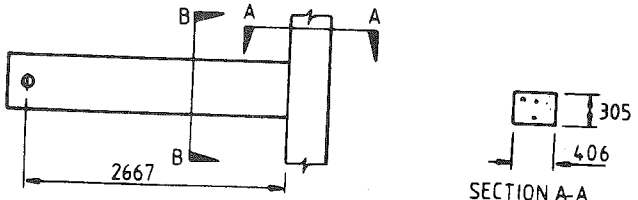

UNIT 4

All dimensions in millimetres.

Fig. 1 Dimensions of the Test Units

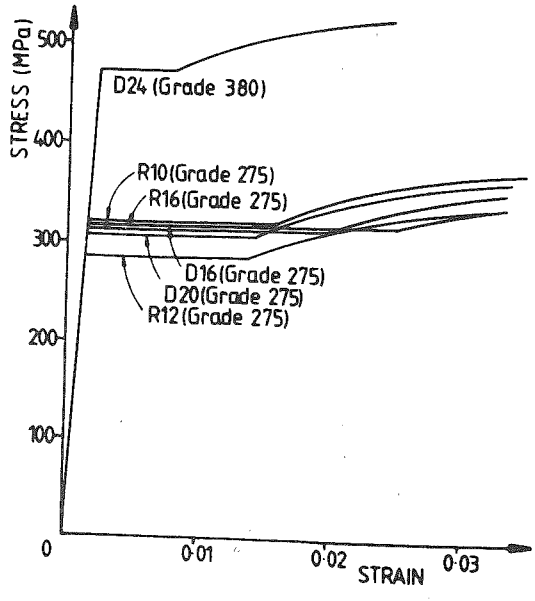

Fig. 3 Reinforcing Steel Measured Stress-Strain Curves

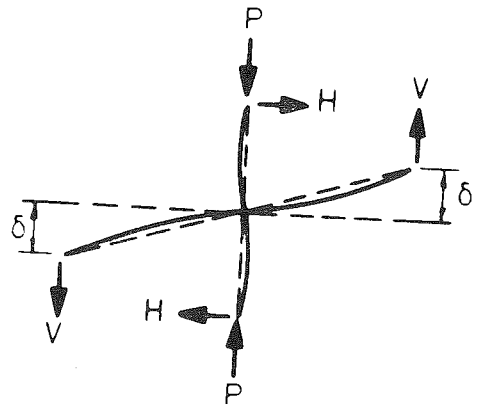

Loading of Units 1 and 2

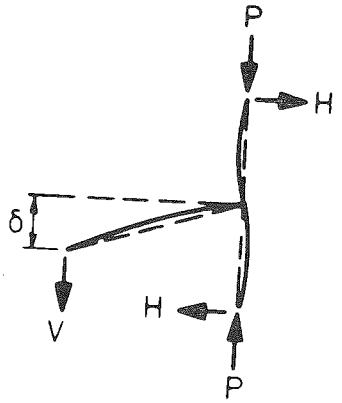

Loading of Units 3 and 4

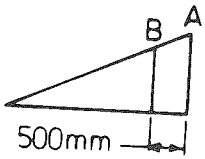

Bending Moment Diagram for Beam

Conventional Design:

Reinforcement is provided so that required M_u is achieved with critical plastic hinge section at A.

Relocated Plastic Hinge Design:

Reinforcement is provided so that required M_u is achieved with critical plastic hinge section at B and so that yielding at A cannot occur unless the moment at B reaches its overstrength value.

Fig. 2 Loading of Test Units and Concepts for the Location of Plastic Hinges in Beams

Table 2 : Properties of Steel Reinforcement

Grade of Bar	Grade 275						Grade 380	
Bar designation	R10	R12	R16	D16	D20	D24	D20	D24
Measured f_y (or f_{yh}) MPa	321	286	320	315	307	303	485	473
Measured f_u, MPa	437	414	468	463	458	453	784	767

Design Features of the Test Units

The design features of the four beam-column joints are summarized below.

Unit 1 was an interior beam-column joint with the plastic hinge regions in the beams designed to be located adjacent to the column faces (conventional design). The ratios of longitudinal steel for the beams were $\rho = \rho' = 1.75\%$, and this relatively high steel content led to considerable congestion of shear reinforcement in the joint core, as shown in Fig. 4.

Unit 2 was an interior beam-column joint with the plastic hinge regions in the beams designed to be located away from the column faces (relocated plastic hinge design). This was achieved by the beam reinforcing details shown in Fig. 5, which has two main advantages: less shear reinforcement is required in the joint core, and larger diameter beam bars are allowed. This improved design situation is because the joint core and nearby beam regions are considered to remain in the elastic range during loading. Therefore, the joint shear carried by the concrete diagonal compression strut is not considered to degrade during cyclic loading, and a longer length of beam bar is present between the positive and negative moment plastic hinge regions so that bond in the joint is not so critical. The beams of Unit 2 had approximately the same strength for end load as those of unit 1, and hence the design joint core shear forces were similar for the two units. The ratios of longitudinal steel for the beams at the critical sections 500 mm from the column faces were $\rho = \rho' = 1.32\%$ and at the column face were $\rho = \rho' = 2.04\%$. The design was such that yielding of the beam flexural reinforcement at the column faces was not expected unless a moment of 1.16 times the theoretical flexural strength, based on the measured f_y and f'_c values, was reached at the critical sections 500 mm from the column face. Units 1 and 2 can be regarded as alternative solutions to the same design problem.

Unit 3 was an exterior beam-column joint with the plastic hinge region in the beam designed to be located adjacent to the column face (conventional design) and with the beam bars anchored in a beam stub at the far face of the column. The ratios of longitudinal steel for the beam were $\rho = \rho' = 1.90\%$. The beam stub was necessary because bar anchorage was considered to commence at the mid-depth of the column and the column section was not large enough to allow anchorage within the column. The reinforcing details are shown in Fig. 6.

Unit 4 was an exterior beam-column joint with the plastic hinge region in the beam designed to be located away from the column face (relocated plastic hinge design). This was achieved using the reinforcing details shown in Fig. 7. The ratios of longitudinal steel for the beams at the critical section 500 mm from the column face were $\rho = \rho' = 2.68\%$. The design was such that yielding of the beam flexural reinforcement at the column face was not expected unless a moment of 1.20 times the theoretical flexural strength based on the measured f_y and f'_c values was reached at the critical section 500 mm from the column face. Units 3 and 4 can be regarded as alternative solutions to the same design problem. However unit 4 was stronger due to the greater areas of longitudinal steel provided.

Theoretical Strengths of Units

In all strength calculations the strength reduction factor ϕ was taken as unity.

At the applied axial load of $0.1f'_cA_g$, the ratio of the theoretical flexural strength of the columns to that of the beams calculated using the measured material strengths were 1.55 and 1.64 for units 1 and 2, respectively. For units 3 and 4 at an axial load of $0.1f'_cA_g$ the ratio of the sum of the column theoretical flexural strengths above and below the joint to the beam theoretical flexural strength calculated using the measured material strengths were 1.78 and 1.75, respectively. The relatively high flexural strengths of the columns was partly due to the high measured yield strength of the Grade 380 steel in the columns.

The required shear strength of the joint cores, V_{jh} and V_{jv} required, calculated from the forces acting on the joint, are shown in Table 3 for units 1, 2, 3 and 4 and also for a unit S1 of a previous test (9). The ratios of $v_{jh}/\sqrt{f'_c}$ are also shown in the table, and these values do not exceed 1.5, as is required by the code. The table also shows the components of shear carried by the concrete, V_{ch} and V_{cv} provided, and hence the shear required to be carried by the shear reinforcement V_{sh} and V_{jv} required. That component can be compared with the shear strength provided by the shear reinforcement actually present, V_{sh}, and V_{sv} provided. It is evident that in all cases, except in the previous unit S1,

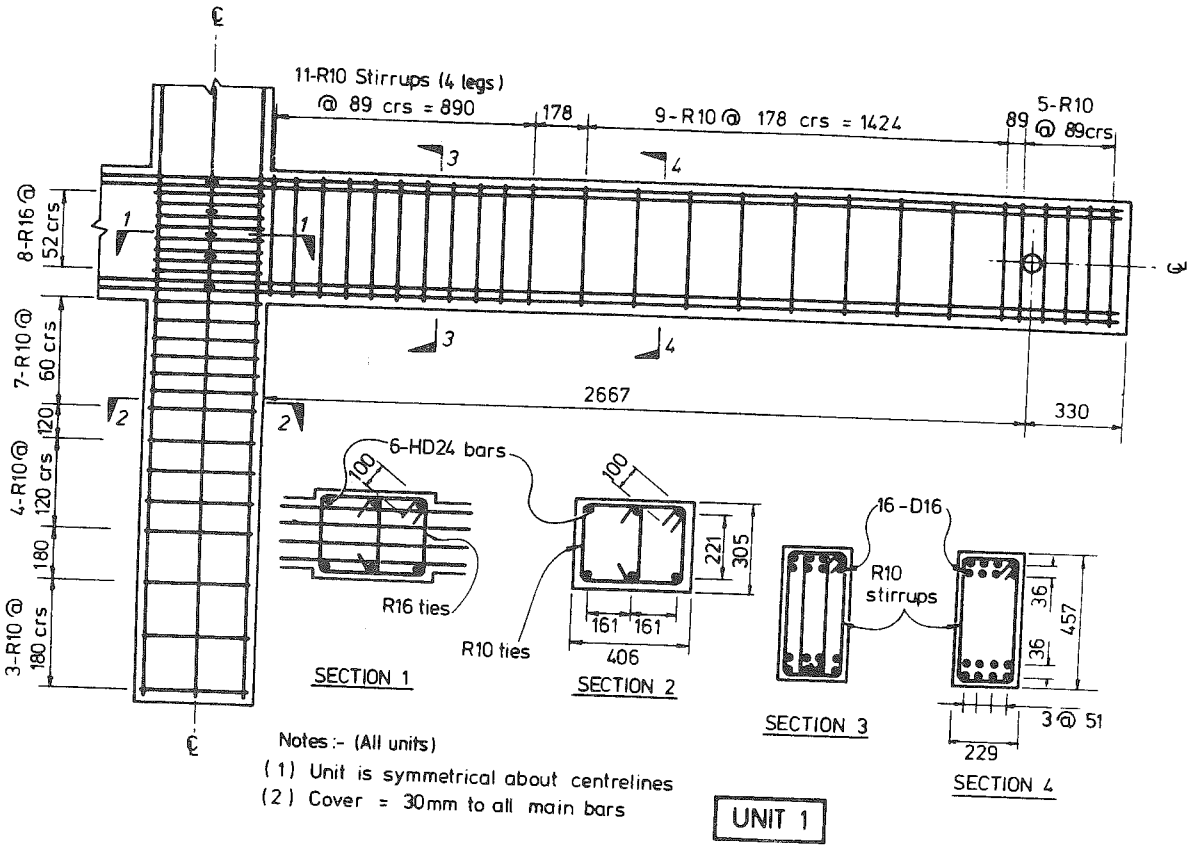

Fig. 4 Reinforcing Details for Unit 1

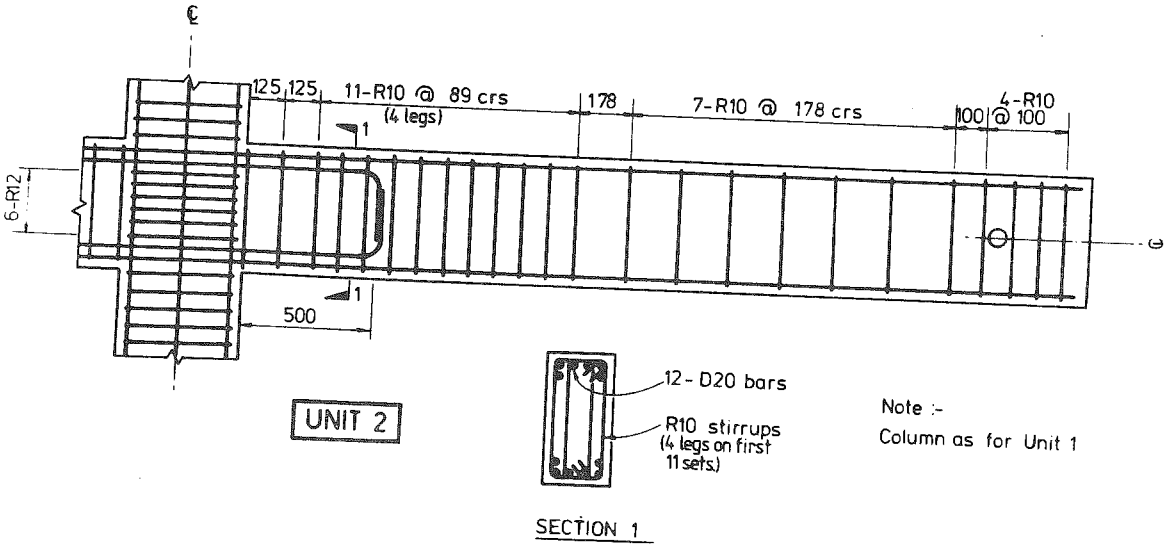

Fig. 5 Reinforcing Details for Unit 2

the joint core shear code requirements were satisfied.

The ratio of beam bar diameter to column depth was 1/25.4 for unit 1 and 1/20.3 for unit 2, both of which were very close to the maximum values permitted by the code. Anchorage of other bars met the code requirements.

Table 3 : Components of Joint Core Shear Resistance According to NZS 3101, kN

UNIT	For Horizontal Shear Forces					For Vertical Shear Forces			
	V_{jh} req'd	$\frac{v_{jh}}{\sqrt{f'c}}$	V_{ch} prov'd	V_{sh} req'd	V_{sh} prov'd	V_{jv} req'd	V_{cv} prov'd	V_{sv} req'd	V_{sv} prov'd
1	980	1.23	0	980	1030	1103	772	331	428
2	974	1.15	609	365	388	1096	767	329	428
3	545	0.64	341	204	202	614	430	184	304
4	597	0.77	373	224	252	672	470	202	304
S1	966	1.34	178	788	614	1088	910	178	259

Notes: i) V_{jh} req'd is calculated using a longitudinal beam bar stress of 1.25 times the specified yield stress.

ii) $V_{jv} = V_{jh}.h_b/h_c$

iii) $v_{jh} = V_{jh}/b_j h_c$

iv) V_{sh} and V_{sv} prov'd are calculated using the measured f_{yh}

Test Procedure

The beam-column units were subjected to several slow load reversals simulating very severe earthquake loading. The first loading cycle was in the elastic range, and this was followed by a series of deflection controlled cycles in the inelastic range comprising two full cycles to each of the displacement ductility factors of 2, 4, 6 and sometimes higher, as illustrated in Fig. 8. The "first yield" displacement at the end of the beam was found by loading to 3/4 of the flexural strength of the beam, as calculated on the basis of the measured material strengths, and multiplying that deflection by 4/3. That deflection can be considered as the deflection at ultimate load taking into account cracking and only elastic behaviour.

Longitudinal strains in the beam steel were measured using a Demec (demountable mechanical) strain gauge with a 102 mm gauge length. The Demec points were attached to the ends of steel studs which had been welded to the longitudinal steel and which projected sideways through holes in the cover concrete. Strains on the transverse steel hoops in the joint core were measured using electrical resistance strain gauges which were positioned on the steel in the direction of the horizontal shear so that any bending of the hoop bar due to the tendency of the concrete to bulge outwards would not alter the strain reading. Curvatures of the beam in the potential plastic hinge regions were measured using dial gauges attached to steel holding frames which in turn were attached to horizontal steel bars which passed through the concrete core just inside the longitudinal steel. The shear distortion of the joint core was found from dial gauge readings made in the direction of the joint core diagonals. The dial gauges for the shear distortion readings were attached to the ends of horizontal steel bars which passed through the joint core just inside the intersecting beam and column longitudinal bars. Deflections of the units were measured using dial gauges.

The column ends were grouted into steel caps and the column loads were applied through steel pins which allowed free rotation during the testing. The beam loads were also applied through steel pins which allowed free rotation at the load points.

General Behaviour of Test Units and Definition of "Adequate Ductility"

Figs. 9, 10, 11, 12 and 13 show for the four test units the measured beam end load versus beam end deflection curves, the measured strains in the bottom bars of the beams, the measured strains in the joint core hoops, and photographs illustrating damage during testing. The percentage of the measured overall deflection caused

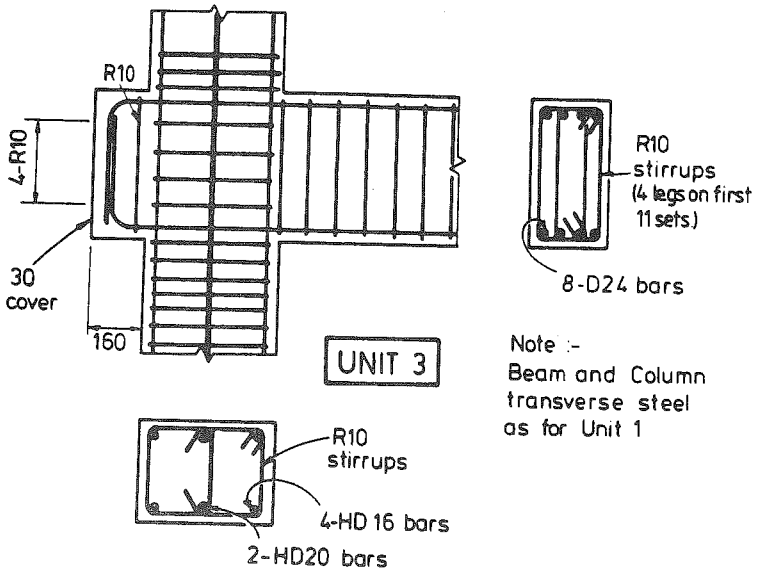

Fig. 6 Reinforcing Details for Unit 3

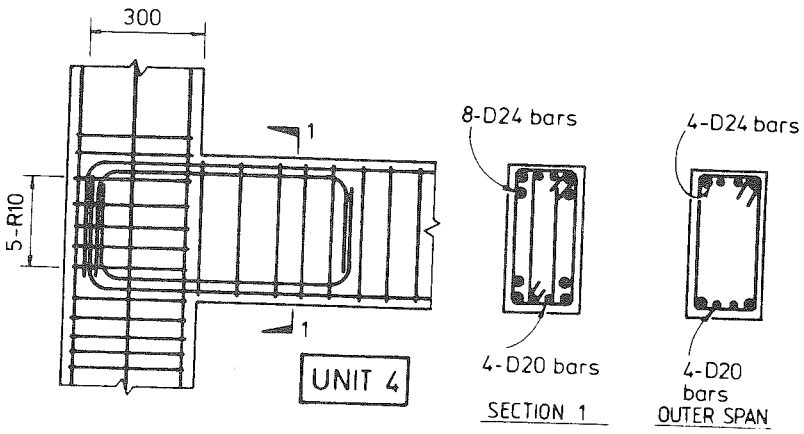

Note - Column as for Unit 3
Beam transverse steel as for Unit 2

Fig. 7 Reinforcing Details for Unit 4

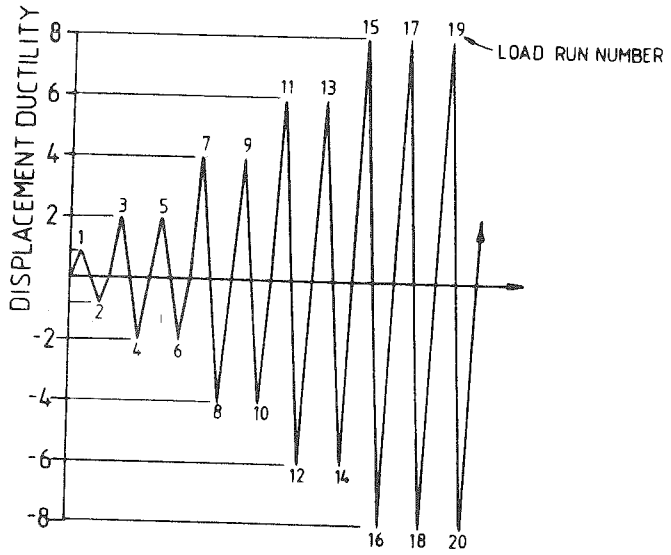

Fig. 8 Imposed Displacement Ductility Factors During Loading Runs

by shear deformation of the joint core, and the percentage of the horizontal shear in the joint core resisted by the hoops, are shown in Table 4. The contribution to the overall deflection from joint core deformation was calculated from the diagonal displacements measured on the joint core. The horizontal shear carried by the joint core hoops was calculated from the strains measured on those hoops, and the imposed horizontal joint core shear was calculated from the internal forces required to achieve the measured beam end loads.

It should be noted that the commentary on the New Zealand loadings code (10) gives an approximate criterion for "adequate ductility" to be met in the case of reasonably regular symmetrical frames without sudden changes in storey stiffness. The approximate criterion is that the building as a whole should be capable of deflecting laterally through at least eight load reversals so that the total horizontal deflection at the top can reach at least four times that at first yield without the horizontal load carrying capacity being reduced by more than 20%. The horizontal deflection at the top at first yield can be taken as that at the design seismic load calculated on the assumption of elastic behaviour. The detailing procedures of the concrete design code (1) are meant to assure that ductile structures are capable of meeting this criterion.

It is evident that the eight load reversals (that is, four load cycles) to a displacement ductility factor μ of 4 amounts to a cummulative μ of $4 \times 2 \times 4 = 32$. For the purpose of assessing the results of the tests the criterion will be taken as requiring that the strength of the units should not decrease to less than 80% of the theoretical strength of the units during the two load cycles to $\mu = 2$, the two load cycles to $\mu = 4$ and the one load cycle to $\mu = 6$, which is a cummulative μ of 36. The theoretical strength of the units will be defined as that strength calculated using the measured (actual) f_y and f'_c values and a strength reduction factor ϕ of unity. The strength of units was governed by the flexural strength of the beams and the theoretical strengths so defined are shown as dashed lines in Figs. 9a, 10a, 11a and 12a.

Unit 1 Results

Fig. 9a shows that the theoretical strength of the unit was approached but not exceeded during the test. Nevertheless, at the maximum deflection during the first cycle to $\mu = 6$, the load carried was 88% of the theoretical strength and hence the unit satisfied the NZS 4203 criterion for adequate ductility. The pinching of the load-deflection response was due to the change in stiffness caused by the closure during the loading runs of open cracks in the concrete "compression" zone and in the joint core. The rounding of the load-deflection response near peak load was due to the Bauschinger effect on the stress-strain curve of the longitudinal steel. Strain hardening of the longitudinal steel did occur, as is shown in Fig. 9b, and resulted in steel stresses which would have been at least 1.25 times the specified yield strength.

It was apparent that the shear strength of the joint core degraded during the loading cycles and eventually the joint core strength governed the strength of the unit. Table 4 summarizes the behaviour of the joint core in terms of components of deformation and shear resistance. The increase in the deflection component from joint core deformation, and the reduction in the joint core shear carried by the concrete diagonal strut mechanism, as the loading progressed, are both evident. Despite the provision of sufficient hoops in the joint core to resist the entire horizontal shear force, yielding eventually occurred in that transverse steel in the first load cycle to $\mu = 6$ (see Fig. 9c) and at the end of the test the whole of the joint shear was carried by the hoops as assumed in the design (see Table 4). Visible damage to the joint during testing is shown in Fig. 13.

It is of interest to note that although the horizontal shear stress in the joint core was comfortably within the maximum allowed by NZS 3101 ($v_{jh}/\sqrt{f'_c} = 1.23 < 1.5$) there was extreme congestion of joint core shear reinforcement. Hence it is obviously better to use larger size member sections to ease congestion of reinforcement in the joint core for this type of design with beam plastic hinging adjacent to the column faces.

Table 4 : Behaviour of Joint Cores of Test Units

Load Run No.[a]		1	2	3	4	5	6	7	8	9	10	11	12	13	14	15	16	17	18	19	20	NZS 3101 V_{sh}/V_{jh} req'd, percentage
Displacement Ductility Factor, μ		¾	-¾	2	-2	2	-2	4	-4	4	-4	6	-6	6	-6	8	-8	8	-8	8	-8	
Measured Percentage of Total Deflection of Beam Ends due to Joint Core Shear Deformation	Unit 1	9	1	2	7	10	9	6	11	5	8	10	35	32	36							
	Unit 2	18	21	15	15	18	16	12	12	17	20	32	66	59	73	64						
	Unit 3	11	18	8	15	16	23	8	13	8	14	5	8	10	16	12	18	23	30	35	43	
	Unit 4	9	6	9	6	10	8	7	7	10	10	11	21	35	51	70						
Measured Percentage of Horizontal Joint Core Shear Resisted by the Hoops, V_{sh}/V_{jh}%	Unit 1	17	38	35	58	57	65	67	75	80	76	93	73	100	100							100
	Unit 2	27	21	28	22	26	21	27	27	32	32	34	37	40	41	44	70					37
	Unit 3	1	3	10	17	22	21	25	31	29	36	31	33	33	29	31	35	34	35	35	37	37
	Unit 4	19	26	26	30	26	34	27	36	31	37	35	38	39	45	48	60					38

[a] As shown on the beam end load-deflection curves in Figs. 9a, 10a, 11a and 12a.

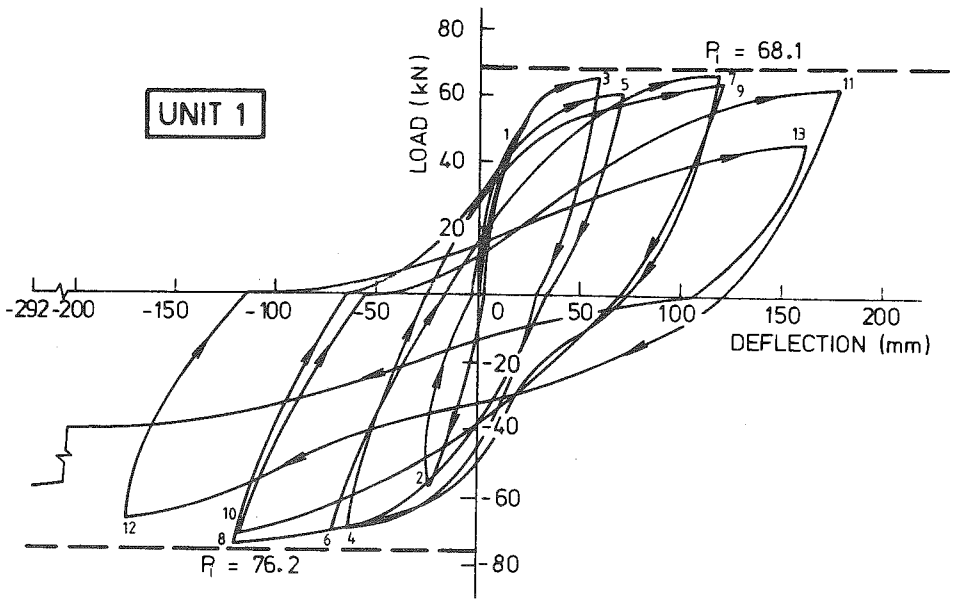

(a) Vertical Beam End Load Versus Beam End Displacement

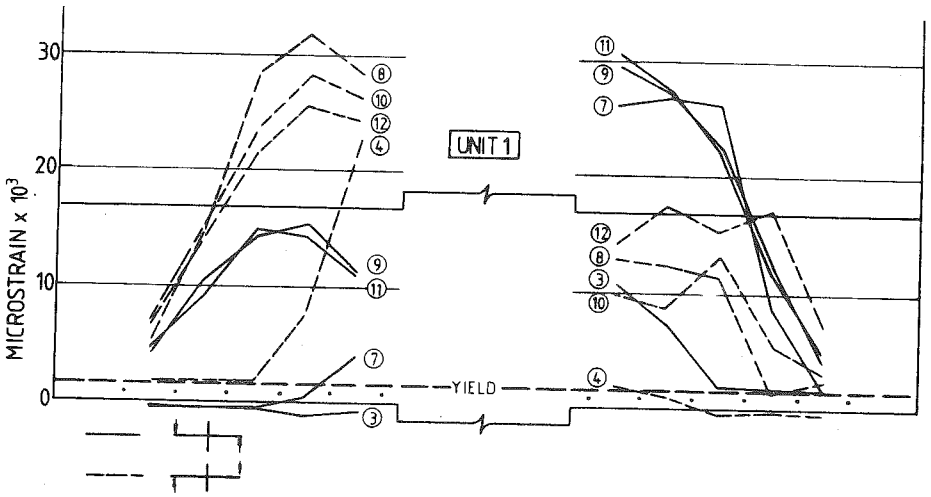

(b) Strains in Beam Longitudinal Bottom Bars

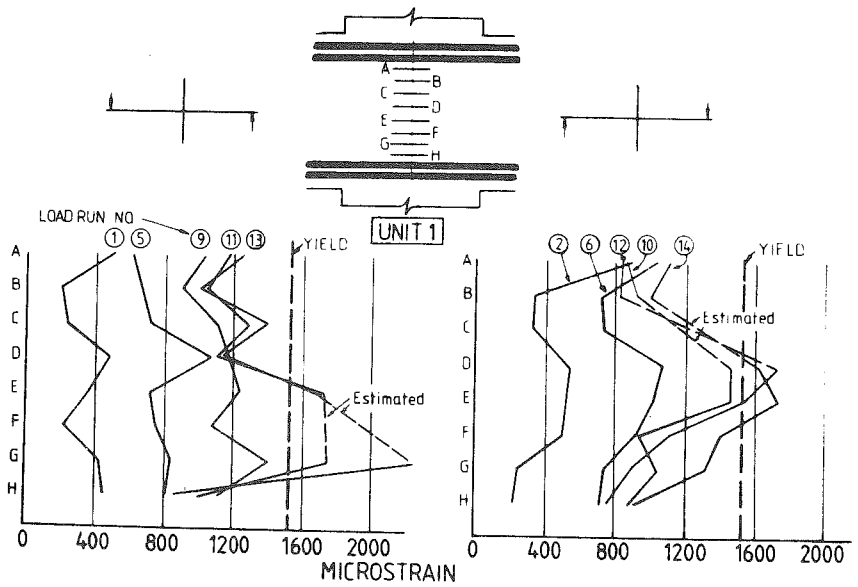

(c) Strains in Joint Core Hoops

Fig. 9 Test Results from Unit 1

Unit 2 Results

Fig. 10a shows that the theoretical strength of the unit was exceeded during the test. In the first cycle to $\mu = 6$, the beam loads attained peaks which were about 10% greater than the theoretical strengths, due to strain hardening of the steel raising the stress above the measured yield stress (see Fig. 10b). Hence the NZS 4203 criteria for adequate ductility was satisfied. Less pinching of the load-deflection response occurred in this unit, mainly because of the better control of shear cracking in the joint core.

The joint core retained its shear strength well, as is shown in Table 4. The shear resistance assigned to the concrete diagonal compression strut mechanism in the design, $0.63V_{jh}$, was indeed being carried during the first load cycle to $\mu = 6$. Yielding of the joint hoops occurred during that load cycle (see Fig. 10c).

The strain distributions along the longitudinal bars adjacent to the joint core shown in Fig. 10b are of interest. Initially yielding of these beam bars occurred only in the vicinity of the designed plastic hinge regions away from the column face. During the loading cycles to $\mu = 2$ strain hardening of steel commenced in those plastic hinge regions. This strain hardening increased with further load cycles and eventually the beam flexural capacity at the critical section 500 mm from the column face was greater than 1.16 times the value based on the measured yield strength and yield penetration had progressed along the beam to the column face, accompanied by a corresponding increase in beam curvature at the column face (see Fig. 10b). At the peak of the second cycle to $\mu = 4$ it was considered that the joint core was no longer in the elastic range. During the first cycle to $\mu = 6$ the beam bars at the column faces reached strains close to that associated with strain hardening. During the second cycle to $\mu = 6$ the joint core deformation had increased to the point where the plastic rotations in the beams were decreasing significantly, and the joint core strength was degrading and governing the strength of the unit. In the latter stages of testing some evidence of sliding shear deformation was noticed at the designed critical section in the beams, but this was not serious since at the theoretical strength of the unit the nominal shear stress at the beam section was only $0.12\sqrt{f'_c}$ MPa. Visible damage to the joint core during testing is shown in Fig. 13.

Unit 3 Results

Fig. 11a shows that the theoretical strength of the unit was exceeded during the test. In the loading cycles to $\mu = 6$ the beam loads attained peaks which were 15 to 20% greater than the theoretical strengths, because of strain hardening of the steel. Hence the performance of the unit was significantly better than required by the NZS 4203 criterion for adequate ductility. (From this observation it could be considered that a reduction in the quantities of joint core reinforcing could be made, but it should be noted that the joint core hoops were already less than the code minimum necessary for confining steel). The pinching of the load-deflection loops was only noticeable in the loading cycles to high ductility values.

There was not a significant loss of shear stiffness or strength of the joint core during testing, despite the yielding of the joint core hoops (see Fig. 11c) which commenced in the first cycle to $\mu = 4$ and the large inelastic joint core hoop strains that occurred in the subsequent load cycles. Table 4 shows that the deformation of the joint core accounted for not more than 16% of the unit deflection in the two load cycles to $\mu = 6$ and the percentage of joint core shear carried by hoops did not increase markedly during the cyclic loading. The shear resistance assigned to the concrete diagonal compression strut mechanism in the design, $0.63V_{jh}$, can be compared with measured value of $0.67V_{jh}$ carried by that mechanism during the first load cycle to $\mu = 6$. Thus yielding of hoops and full depth flexural cracking in the beams at the face of the column did not significantly reduce the diagonal compression strut mechanism for this exterior joint, whereas it caused a significant reduction in the case of the interior joint of unit 1 (see Table 4). The better performance of exterior joints compared with interior joints is recognised by NZS 3101 (1). It is considered to be due to the diagonal compression strut being able to form between the anchorage bend in the beam tension bars and the column ties placed close to but just outside the joint core, even when full depth cracking occurs in the beam, as postulated by Paulay and Scarpas (11).

The strain distributions measured along the beam longitudinal bars shown in Fig. 11b indicate that yield of beam steel penetrated well into the joint core. The code requirement that the anchorage of those bars be considered to commence at the mid-depth of the column was reasonable for this unit. No significant slip of beam bars was observed to occur. Damage to the unit visible during testing is illustrated in Fig. 13.

Unit 4 Results

Fig. 11a shows that the theoretical strength of the unit was exceeded during the test. During the first cycle to $\mu = 6$ the beam ends sustained peak loads which were about 18% greater than the theoretical strengths based on the measured yield strengths, because of strain hardening of the steel. Hence the performance of the unit was again significantly better than required by the NZS 4203 criterion for adequate ductility. The pinching of the load-deflection loops was limited.

The joint core retained its shear strength well, as is indicated in Table 4. The shear resistance assigned to the concrete diagonal compression strut mechanism in the design, $0.62V_{jh}$, was

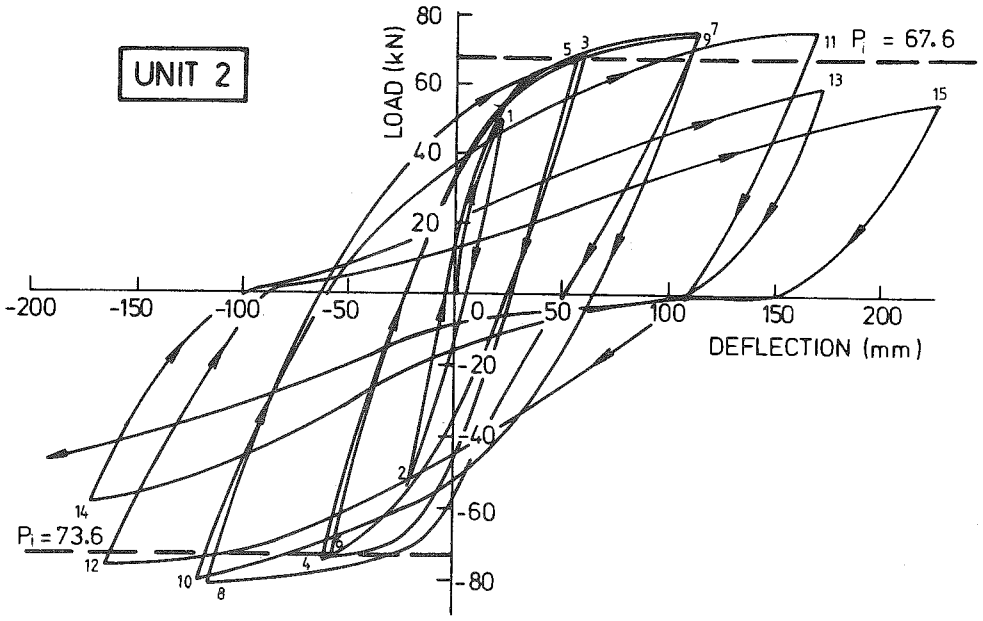

(a) Vertical Beam End Load Versus Beam End Displacement

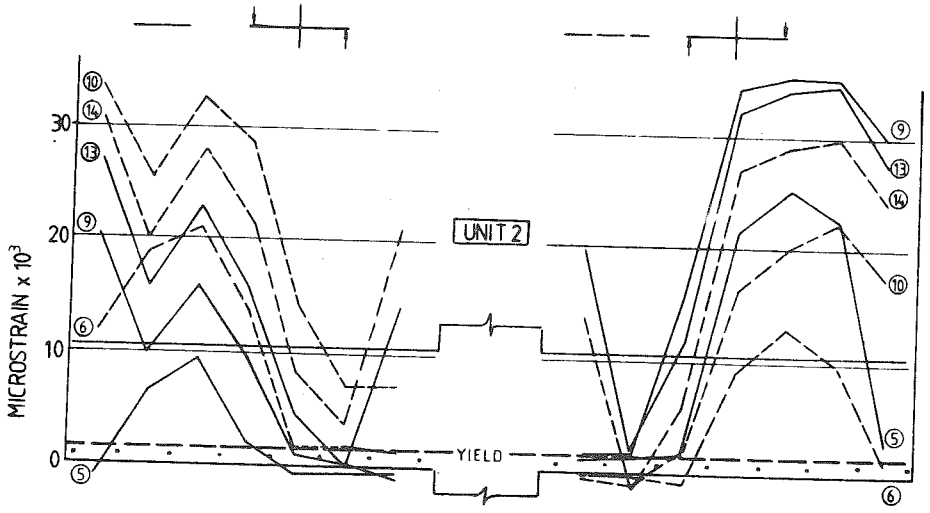

(b) Strains in Beam Longitudinal Bottom Bars

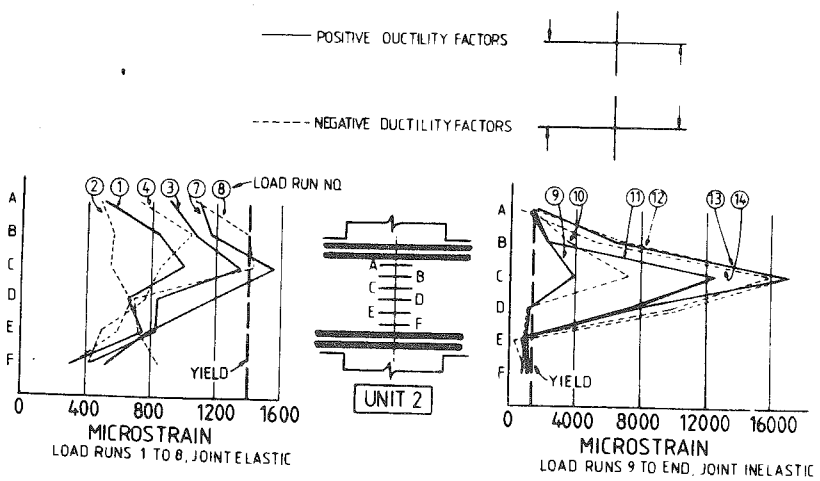

(c) Strains in Joint Core Hoops

Fig. 10 Test Results from Unit 2

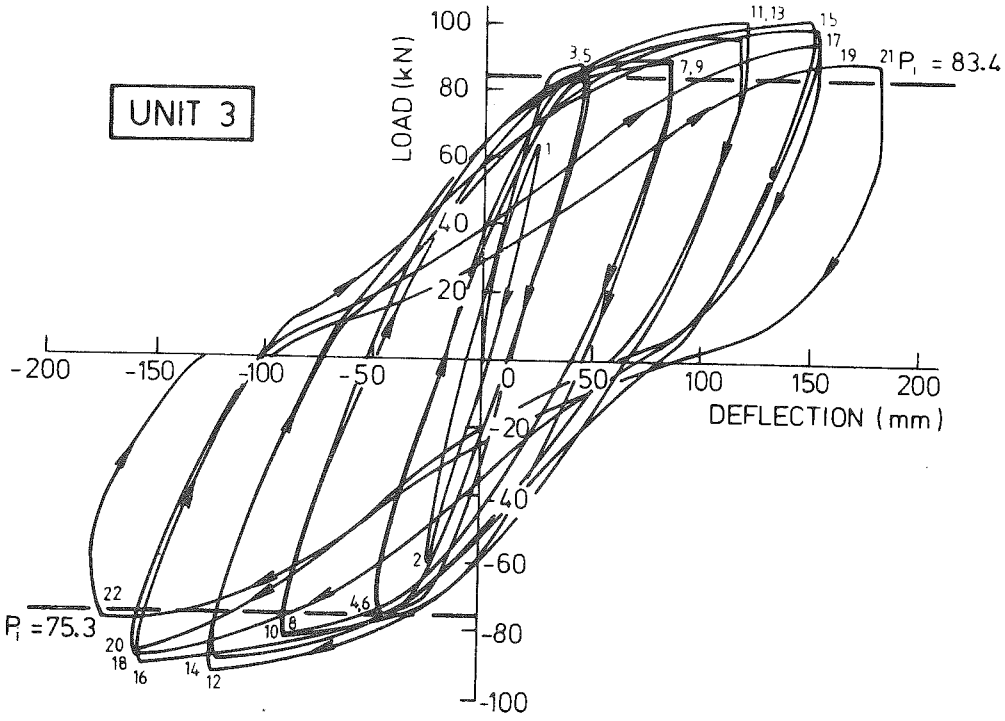

(a) Vertical Beam End Load Versus Beam End Deflection

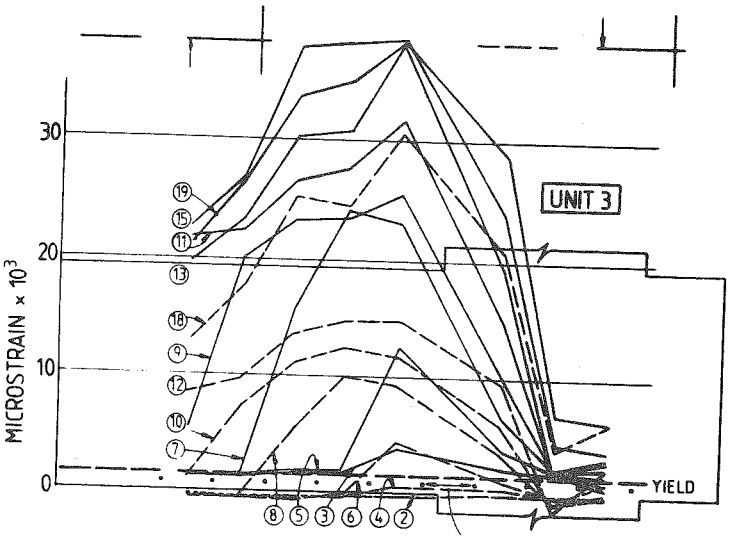

(b) Strains in Beam Longitudinal Bottom Bars

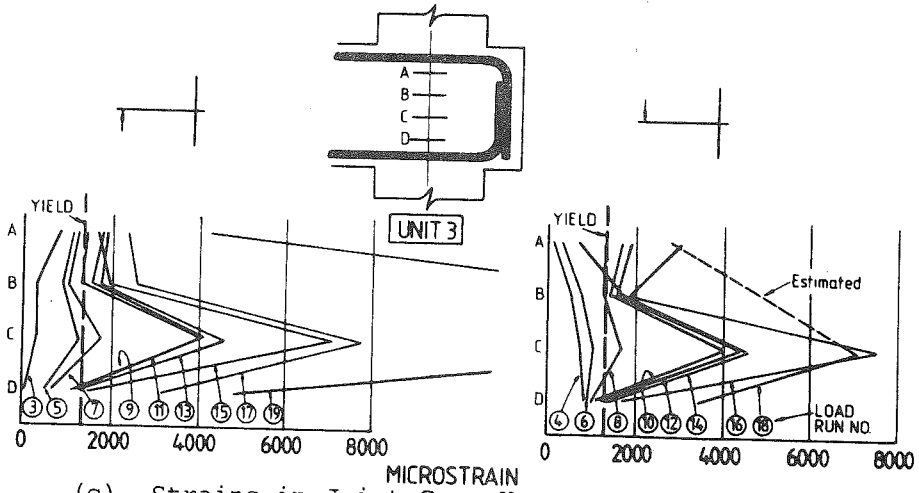

(c) Strains in Joint Core Hoops

Fig. 11 Test Results from Unit 3

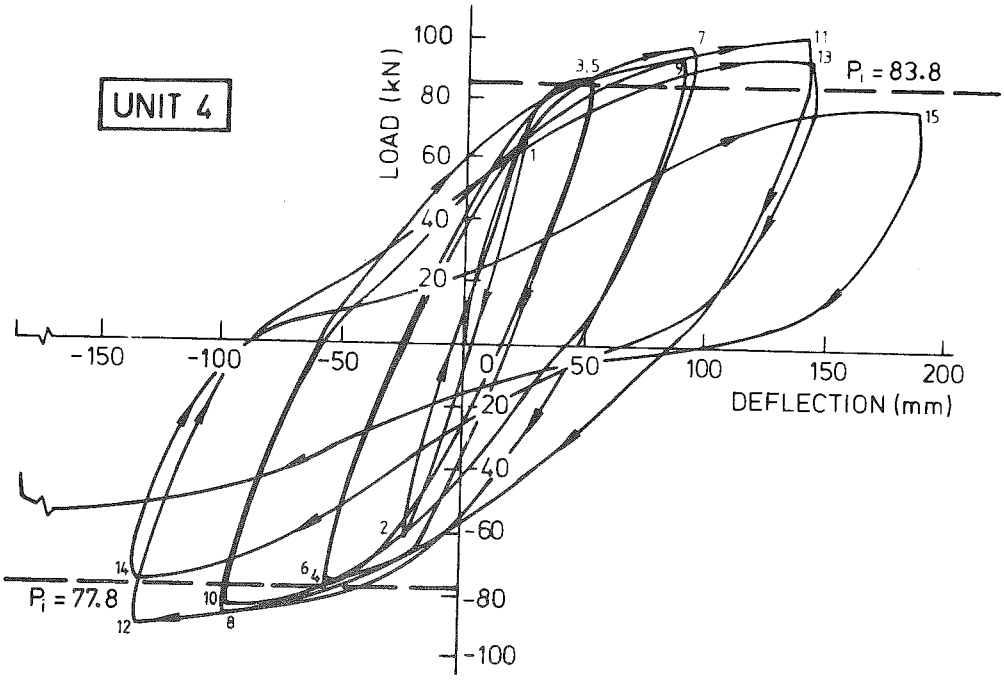

(a) Vertical Beam End Load Versus Beam End Deflection

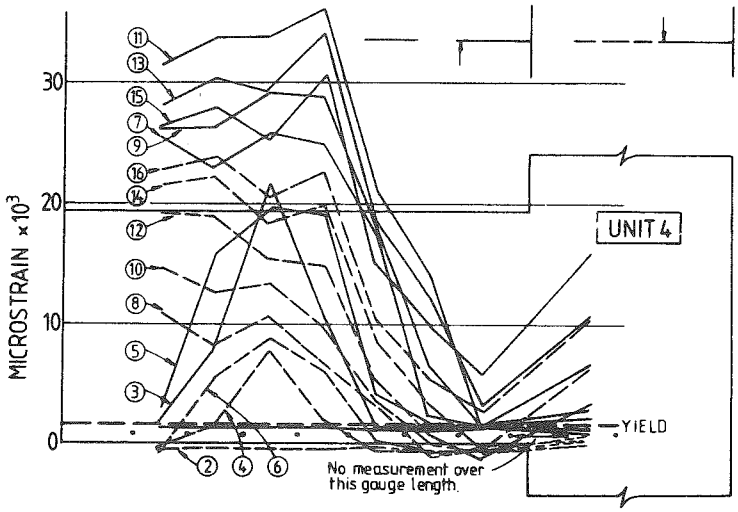

(b) Strains in Beam Longitudinal Bottom Bars

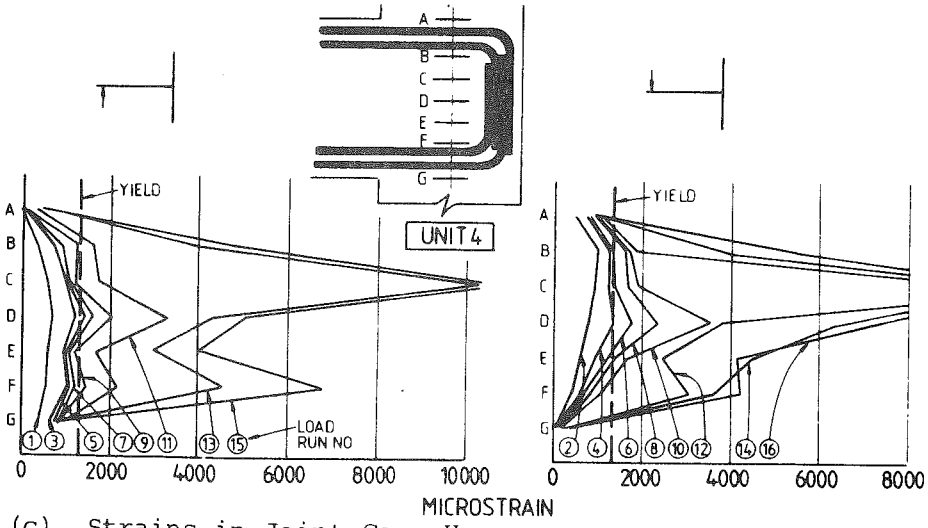

(c) Strains in Joint Core Hoops

Fig. 12 Test Results from Unit 4

indeed carried during the first load cycle to $\mu = 6$. Yielding of joint core hoops had commenced in the first cycle to $\mu = 4$ (see Fig. 12c) but this did not cause a marked decrease in the shear strength or stiffness of the joint core, as is shown in Table 4.

The strains measured along the longitudinal bars shown in Fig. 12b indicated that initially the beam underwent plastic rotations in the designed plastic hinge region, but in the later stages of the test yielding of longitudinal steel penetrated along the beam to the column face and into the joint core resulting in plastic rotation occurring over a greater region. No slip of beam bars was noticeable. This yield penetration occurred because strain hardening of the beam reinforcing at the design plastic hinge region 500 mm from the face raised the flexural capacity there sufficiently to cause yielding in the beam at the column face as well. Sliding shear deformation was noticeable at the designed critical section in the later stages of testing, but this was not serious since at the theoretical strength of the unit the nominal shear stress in the beam was only $0.15\sqrt{f'_c}$ MPa. Damage to the unit visible during testing is illustrated in Fig. 13.

Comparison of NZS 3101 and the Draft ASCE-ACI Committee 352 Design Recommendations for the Joint Cores of the Units

The measured percentage of the horizontal shear force in the joint core carried by the joint core hoops (V_{sh}/V_{jh}) in the first loading cycle to $\mu = 6$ shown in Table 1 compared very well with the values of 100, 37, 37 and 38% recommended by NZS 3101 for units 1, 2, 3 and 4, respectively, for the column axial load level of $0.1f'_cA_g$ applied in these tests. It is of interest also to recall the result from the previously tested unit S1 (9), which was an interior beam-column joint with a column axial load level of $0.24f'_cA_g$ and with plastic hinging occurring in the beams at the column faces. As Table 3 shows, unit S1 had only 68% of the horizontal joint core shear reinforcement required by NZS 3101. In that test the beams did not reach their theoretical flexural strength and shear failure occurred in the joint core which resulted in the strength of the unit falling to 61% of the theoretical strength based on beam moment capacity after two load cycles to $\mu = 2$, two load cycles to $\mu = 4$, and one load cycle to $\mu = 6$. Hence the NZS 4203 criterion for adequate ductility was not met by unit S1.

As discussed previously, the joint core shear requirements of NZS 3101 (1) differ markedly from the recommendations of the draft ASCE-ACI Committee 352 report (7). According to the draft ASCE-ACI approach the quantity of hoop steel required in the joint core for both confinement and shear is given by the confinement equations (Eqs. 17 and 18) and the horizontal shear should not exceed a limiting value (Eq. 16). According to the NZS 3101 approach, the quantity of joint core hoop steel required is that necessary to carry the shear actually present (Eqs. 2 to 5) but should not be less than that required for confinement (Eqs. 10 and 11). The A_{sh}/s_h values calculated for the four units using these two approaches are shown in Table 5; also tabulated is the A_{sh}/s_h actually provided for each unit. Note that the quantity actually provided in unit 3 satisfied the NZS 3101 requirement for shear but was 76% of the NZS 3101 requirement for confinement. In all other cases NZS 3101 was satisfied.

It is of interest to note that according to the draft ASCE-ACI approach the horizontal shear force on the joint cores should not exceed the value given by Eq. 16, namely $V = 1.0 \times 0.67\sqrt{34} \times 305 \times 406N = 484$ kN for all units, whereas according to NZS 3101 the horizontal shear strength of the joint cores as reinforced was 1030, 997, 543 and 625 kN for units 1, 2, 3 and 4, respectively, assuming a strength reduction factor of unity for both approaches. Thus the four test units reinforced according to NZS 3101 were able to sustain much greater horizontal joint core shears than permitted by the draft ASCE-ACI recommendations. Note also that units 1 and 2 contained more hoops that required by the ASCE-ACI approach but units 3 and 4 contained less hoops than required by the ASCE-ACI approach.

These considerable differences between the two design approaches arise because in the draft ASCE-ACI method no consideration is given to the mechanisms of shear resistance in the joint core. Thus the draft ASCE-ACI approach may be conservative in some cases and unconservative in others, depending on the particular joint conditions.

Table 5 : Comparison of Quantity of Joint Core Hoops Required for Shear and Confinement by NZS 3101 and Draft ASCE-ACI Committee 352 Recommendations, and Quantity Actually Provided, A_{sh}/s_h mm^2/mm.

Unit	1	2	3	4
Draft ASCE-ACI Requirements for Confinement and Shear	3.22	3.97	2.84	2.89
NZS 3101 Requirements: For Confinement	2.68	3.31	2.37	2.41
For Shear	10.5	4.48	1.83	2.48
Actually Provided	11.0	4.76	1.80	2.79

Notes: (i) All required A_{sh}/s_h values are calculated using the measured f_y and f'_c values.

(ii) Horizontal shear strength of the joints according to the draft ASCE-ACI requirement (Eq. 16) was 484 kN for all units. Taking ϕ=1 and γ=0.67

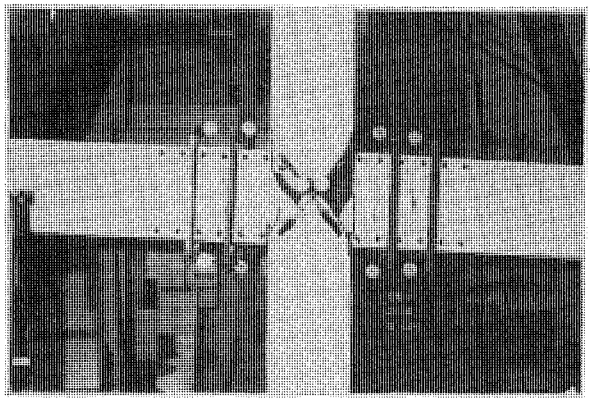

Unit 1 After Second Load Cycle to μ = 4

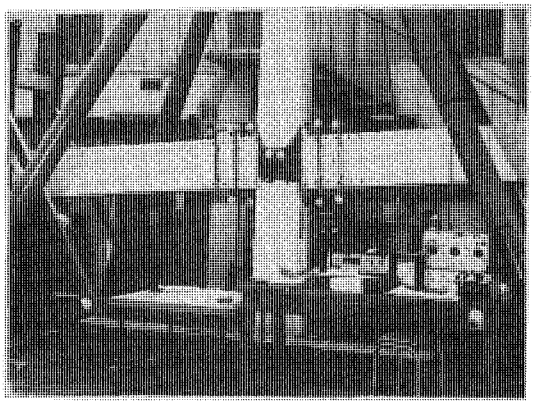

Unit 1 After Second Load Cycle to μ = 6

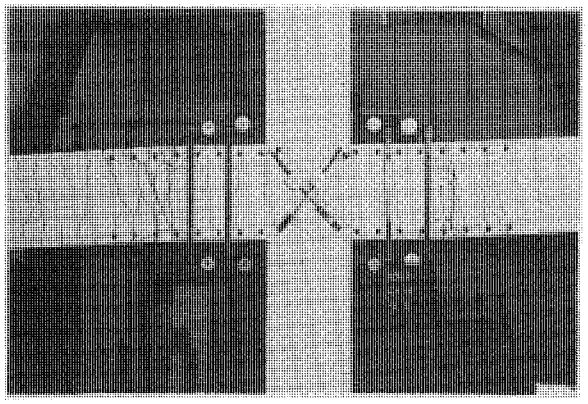

Unit 2 After First Load Cycle to μ = 4

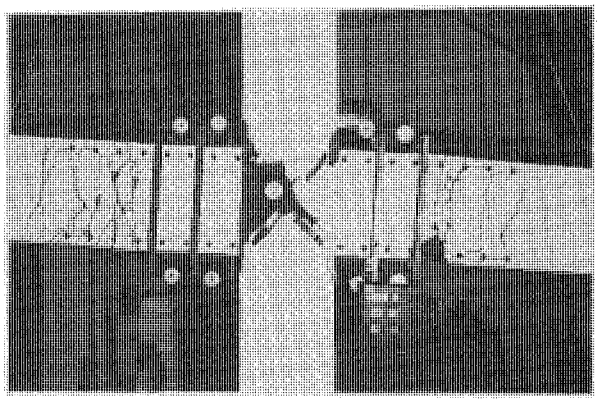

Unit 2 After First Load Cycle to μ = 6

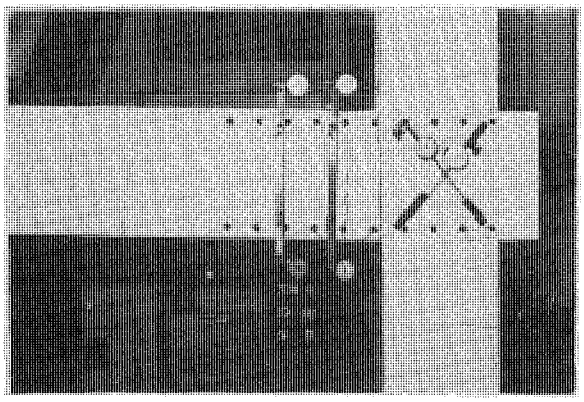

Unit 3 After First Load Cycle to μ = 4

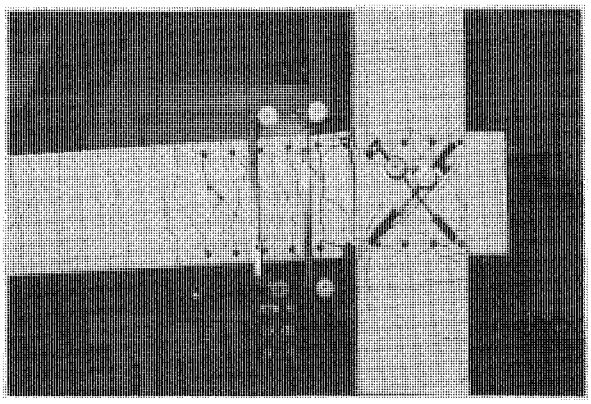

Unit 3 After First Load Cycle to μ = 8

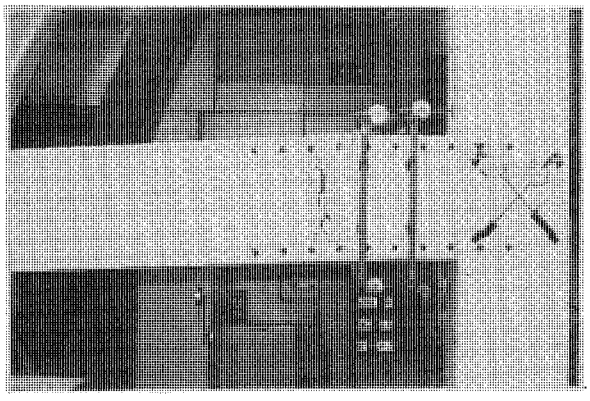

Unit 4 After Second Load Cycle to μ = 4

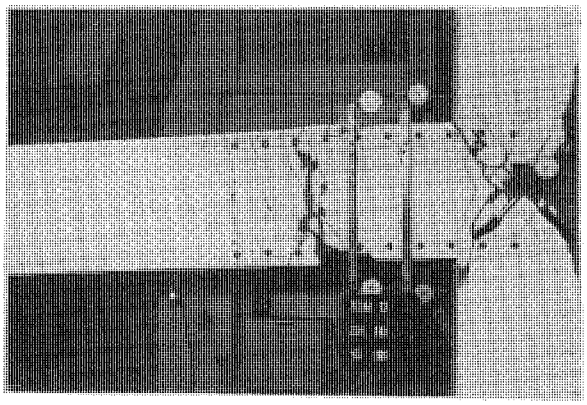

Unit 4 After Second Load Cycle to μ = 6

Fig. 13 Damage Visible During Testing of Units

Notes cont'd...

(iii) Horizontal shear strength according to the NZS 3101 requirements (Eqs. 2 to 5) for the joints as actually reinforced were 1030, 997, 543 and 625 kN for units 1, 2, 3 and 4, respectively.

CONCLUSIONS:

1. The recent draft recommendations for the design of reinforced concrete beam-column joints of ASCE-ACI Committee 352 show large differences from the approach used in NZS 3101. The NZS 3101 approach for joint core shear strength is based on a rational model which sums the shear carried by the concrete diagonal compression strut and the shear carried by truss action of the shear reinforcement. The draft ASCE-ACI approach assumes that providing the horizontal shear stress in the joint core does not exceed a limiting value the amount of transverse steel required for column confinement is satisfactory, and vertical shear is considered by the requirement of at least an eight bar column. In the opinion of the authors, the design of joint core hoop reinforcement on the basis of the quantity of transverse steel required to confine the ends of columns is illogical and cannot produce any degree of accuracy because it does not take into account the possible varying conditions for shear in joint cores. This is especially the case when the wide range of joint types and column axial loads used in design in practice is considered. Recognition of the different concrete diagonal compression strut mechanisms existing in interior and exterior joints also appears necessary.

2. The four reinforced concrete beam-column joint units 1, 2, 3 and 4 which had been designed according to the requirements of NZS 3101 were shown by tests under simulated seismic loading to satisfy the approximate criterion for adequate ductility of NZS 4203. It was apparent that the detailing requirements of NZS 3101 for joint core design were not overly conservative for these designs.

3. Unit 1 was a conventional interior beam-column joint with the critical plastic hinge sections in the beams designed to be located at the column faces. There was considerable congestion of hoop reinforcement in the joint core due to the large shear stresses in the joint core resulting from the high ratios of longitudinal reinforcement in the beams ($\rho = \rho' = 1.75\%$). This congestion could have been eased by using larger member cross sections. The relatively low axial column load of $0.1 f'_c A_g$ meant that all the horizontal shear in the joint core needed to be allocated to the hoops.

4. Unit 2 was an interior beam-column joint with the critical plastic hinge sections in the beams designed to be located 500 mm away from the column faces. The beam sizes and strengths were the same as for unit 1. However, because the beam longitudinal steel was designed so as not to yield at the column faces, the improved bond conditions meant that the diameter of longitudinal beam bars could be 25% greater than in unit 6. Also, because the joint core was considered to remain in the elastic range the concrete diagonal compression strut mechanism could be considered to carry significant shear and only 37% of the horizontal shear in the joint core needed to be allocated to the hoops.

5. Unit 3 was an exterior beam-column joint with the critical plastic hinge section in the beam designed to be located at the column face and with the beam bars anchored in a beam stub at the far face of the column. In exterior joints, even when plastic hinging occurs in the beam at the column face, the concrete diagonal compression strut mechanism can be preserved quite well during cyclic loading, evidently because a steeper diagonal strut can form between the bend in the beam tension steel at the far face of the column and the column ties at the near face just outside the joint core. As a result, only 37% of the joint core horizontal shear needed to be allocated to the hoops. The penetration of steel yield along the beam bars into the joint core demonstrated that requiring the anchorage to commence within the joint core as specified by NZS 3101 was reasonable. This anchorage requirement had meant that to provide sufficient anchorage length for the beam bars a stub was required at the far face of the column because of the relatively small column depth.

6. Unit 4 was an exterior beam-column joint with the critical plastic hinge section in the beam designed to be located 500 mm away from the column face. This design permitted anchorage of the beam bars within the column core, because the beam steel was designed not to yield at the column face, and therefore anchorage could be considered to commence at the column face of entry. Hence an anchorage stub was not needed. Because the joint core was designed to remain in the elastic range only 38% of the joint core shear needed to be allocated to the hoops.

7. In the case of interior beam-column joints the design of plastic hinge regions in beams to be located away from the column faces (that is, "relocated plastic hinges"), so that the joint core remains in the elastic range as in unit 2, was shown to allow much easier detailing of steel when member sizes are small and joint shear are high.

8. In the case of exterior beam-column joints the design of relocated plastic hinges appears to be only of advantage when beam bars cannot otherwise be anchored within in the column core because of small column size, and when beam stubs at the outside face of the column are not present because of architectural or space restrictions.

9. The use of an overstrength factor of 1.25 for Grade 275 reinforcement at relocated plastic hinges, when determining the longitudinal steel areas required in the beams at the column faces to suppress

yield there, should lead to satisfactory design. The overstrength factor used in the design of the interior beam-column joint unit 2 was 1.16 and for the exterior beam-column joint unit 4 was 1.20. In both of these units during the tests, strain hardening of the longitudinal reinforcing at the relocated plastic hinge raised the flexural capacity there sufficiently to cause yield of longitudinal steel to spread along the beam to the column face and to penetrate into the joint core, leading eventually to yield of the joint core hoops. Hence use of an overstrength factor of less than 1.25 for Grade 275 reinforcement would be inadvisable.

10. In general, the use of relocated plastic hinges, as employed in units 2 and 4 seems to be a practical design alternative to conventional design. Note however that if the ratio of gravity load to seismic load induced moment is high the moment gradient may not allow the use of such a design because only a short length of beam will have negative moment. Also, the use of relocated plastic hinges will impose a higher curvature ductility demand on those plastic hinge sections, because the smaller length of beam between the critical positive and negative moment sections will mean that greater plastic hinge rotations are required at these sections to achieve the required displacement ductility factor. This increased curvature ductility demand should not be of concern except for beams with short spans.

ACKNOWLEDGEMENTS

The tests were conducted by J.R. Milburn during Master of Engineering studies under the supervision of R. Park. The experimental work was made possible by financial assistance provided by the Ministry of Works and Development which is gratefully acknowledge. Mr G.H.F. McKenzie, Chief Structural Engineer, MWD, is thanked for his interest and support.

REFERENCES

1. New Zealand Standard Code of Practice for the Design of Concrete Structures, NZS 3101 Parts 1 & 2 : 1982, Standards Association of New Zealand, Wellington, 1982.

2. Milburn, J.R. and Park, R., "Behaviour of Reinforced Concrete Beam-Column Joints Designed to NZS 3101", Research Report 82-7, Department of Civil Engineering, University of Canterbury, New Zealand, February 1982, 107p.

3. Park, R. and Paulay, T., "Reinforced Concrete Structures", John Wiley and Sons, New York, 1975, 769p.

4. Paulay, T., Park, R. and Priestley, M.J.N., "Reinforced Concrete Beam-Column Joints Under Seismic Actions", Journal of American Concrete Institute, Proceedings Vol. 75, No. 11, November 1978, pp. 585-593.

5. ACI Committee 318, "Building Code Requirements for Reinforced Concrete (ACI 318-77)", American Concrete Institute, Detroit, 1977, 102p.

6. ASCE-ACI Committee 352, "Recommendations for Design of Beam-Column Joints in Monolithic Reinforced Concrete Structures", Journal of American Concrete Institute, Proceedings Vol. 73, No. 7, July 1976, pp. 375-393.

7. ASCE-ACI Committee 352, Revised Recommendations with Commentary, June 1982. (In draft form and unpublished).

8. Meinheit, D.F. and Jirsa, J.O., "The Shear Strength of Reinforced Concrete Beam-Column Joints", CESRL Report No. 77.1, University of Texas, Austin, January 1977. (See also Journal of the Structural Division, ASCE, Vol. 107, No. ST11, November 1982, pp. 2227-2244).

9. Park, R., Gaerty, L. and Stevenson, E.C., "Tests on an Interior Reinforced Concrete Beam-Column Joint", Bulletin of New Zealand National Society for Earthquake Engineering, Vol. 14, No. 2 June 1981, pp. 81-92.

10. New Zealand Standard Code of Practice for General Structural Design and Design Loadings for Buildings, NZS 4203:1976, Standards Association of New Zealand, Wellington, 1976.

11. Paulay, T. and Scarpas, A., "The Behaviour of Exterior Beam-Column Joints", Bulletin of the New Zealand National Society for Earthquake Engineering, Vol. 14, No. 3, September 1981, pp. 131-144.

NOTATION

(All units are mm and N)

A_c = area of concrete core section measured to outside of peripheral hoop.

A_g = gross area of section

A_{jh} = total area of effective horizontal joint shear reinforcement

A_{jv} = total area of effective vertical joint shear reinforcement

A_s = total area of tension beam reinforcement

A'_s = total area of compression beam reinforcement

A_{sc} = area of tension reinforcement in one face of the column section

A'_{sc} = area of compression reinforcement in one face of the column section

A_{sh} = total effective area of hoop bars and supplementary cross ties in direction under consideration within spacing s_h

b_c = overall width of column

b_j = effective width of joint

b_w = web width of column

C_j = participation factor = $V_{jh}/(V_{jx} + V_{jz})$

d_b = bar diameter

f'_c = compressive cylinder strength of concrete

f_y = yield strength of longitudinal reinforcement

f_{yh} = yield strength of transverse reinforcement

f_u = ultimate strength of reinforcement

h" = dimension of concrete core of section measured perpendicular to the direction of the hoop bars to outside of peripheral hoop

h_b = overall depth of beam

h_c = overall depth of column in the direction of the horizontal shear to be considered

M_u = design moment due to factored gravity and earthquake loads

P_e = design axial load due to factored gravity and earthquake loads

ℓ_{db} = basic development length for deformed bar in compression

ℓ_{dh} = development length for a deformed bar in tension terminating with standard 90^o hook according to ASCE-ACI Committee 352

ℓ_{hb} = basic development length for deformed bar in tension terminating with standard 90^o hook

s_h = centre to centre spacing of hoop sets

v_{jh} = $V_{jh}/b_j h_c$

V_{ch} = horizontal joint shear strength provided by diagonal concrete strut

V_{cv} = vertical joint shear strength provided by diagonal concrete strut

V_{jh} = total horizontal shear force across the joint

V_{jv} = total vertical shear force across the joint

V_{jx} = total horizontal joint shear force in the x-direction

V_{jz} = total horizontal joint shear force in the z-direction

V_{sh} = horizontal joint shear strength provided by horizontal joint shear reinforcement

V_{sv} = vertical shear strength provided by vertical joint shear reinforcement

V_u = total horizontal shear force across joint

γ = joint shear strength factor

ρ = ratio of longitudinal tension reinforcement = A_s/bd where b and d are beam width and effective depth, respectively

ρ' = ratio of longitudinal compression reinforcement = A'_s/bd where b and d are beam width and effective depth, respectively

ϕ = strength reduction factor

μ = displacement ductility factor = ratio of maximum displacement to displacement at first yield

THE DESIGN OF DUCTILE REINFORCED CONCRETE STRUCTURAL WALLS FOR EARTHQUAKE RESISTANCE

T. Paulay

THE DESIGN OF DUCTILE REINFORCED CONCRETE STRUCTURAL WALLS FOR EARTHQUAKE RESISTANCE

Thomas Paulay, M.EERI

In the design of reinforced concrete multistorey buildings, in which lateral load resistance has been assigned to structural walls, the emphasis should be on a rational strategy in the positioning of walls and the establishment of a hierarchy in the development of strengths to ensure that in the event of a very large earthquake brittle failure will not occur. The preferred mode of energy dissipation should be flexure in a predictable region. Therefore failures due to diagonal tension or compression, crushing of concrete in compression, sliding along construction joints, instability of wall elements or reinforcing bars and breakdown of anchorages should be suppressed. These aims may be achieved with the application of a deterministic design philosophy and they necessitate special detailing and dimensioning of potentially plastic regions of walls. In several areas differences exist between code provisions and practices in the United States and New Zealand.

1. INTRODUCTION

The usefulness of structural walls in the framing of buildings has long been recognized. When walls are situated in advantageous positions in a building, they can form an efficient lateral load-resisting system, while also simultaneously fulfilling other functional requirements. Because a large fraction of, if not the entire lateral load on the building and the horizontal shear force resulting from it, is often assigned to such structural elements, they have been called shear walls. The name is unfortunate for it implies that shear might control their behaviour. This need not be so. An attempt should be made to inhibit shear failures in reinforced concrete structures subjected to seismic loading. It is shown in subsequent sections how this can be readily achieved also in walled structures. To avoid this unjustified connotation of shear, the term structural walls will be used.

The primary purpose of structural walls in a seismic environment is to provide significant stiffness. Thereby greatly increased, if not complete,

Department of Civil Engineering
University of Canterbury
Christchurch, New Zealand.

protection against all forms of damage during small earthquakes can be achieved. Interstorey deflections in multistorey buildings can be kept to acceptable limits. In many situations the often difficult and costly separation of nonstructural components from the primary earthquake resisting structure can be avoided. To minimize structural damage during less frequent but more intense ground shaking, an attempt must be made to ensure basically elastic structural response. To satisfy this second criterion, structural walls must possess adequate strength. Cracking in walls per se, should not be considered as damage. Even some local yielding of the reinforcement, restricted by adjacent regions which remain elastic, need not be classified as objectionable damage. When resistance close to their ideal strength is required to be developed, most structural walls will be stiff enough, even after extensive flexural and shear cracking, to provide full protection against damage to nonstructural contents of the building.

Requirements for ductility and ability to dissipate energy during inelastic seismic response to very large earthquakes also need to be met. The view that structural walls are inherently brittle, perhaps because so often they have been observed to have developed shear failure mechanisms, is still widely held. For this reason some codes require buildings with structural walls to be designed for significantly increased seismic forces. The principles of the inelastic seismic behaviour of reinforced concrete components are generally applicable also to structural walls. With good detailing it is relatively easy to dissipate seismic energy in a stable manner [1,2,3]. The means of achieving ductile response in walls is the major topic of this review.

In studying various features of inelastic response of structural walls and subsequently in developing a rational procedure for their design, a number of fundamental assumptions are made:

(i) In the cases studied here, structural walls are assumed to possess adequate foundations which can transmit actions from the superstructure into the ground without allowing the walls to rock. Inelastic deformations which may occur in the foundation structure or the supporting ground are not considered.

(ii) Inertia forces at each floor are introduced to structural walls by rigid diaphragm action of the floor system and by adequate connections to the diaphragm. In terms of in-plane loading, floor systems (diaphragms) are assumed to remain elastic at all times.

(iii) Walls, principally acting as cantilevers, will be considered either in isolation or within a group of interacting structural walls. The structural contribution of other elements during seismic response is not examined in this study.

Fundamental principles relevant to the design philosophy used in New Zealand, particularly those relating to desired strength, expected ductility demands and the role and quality of detailing, as applied to ductile reinforced concrete frames, have been described by Park [4]. With few exceptions those precepts also apply to ductile structural walls.

2. STRUCTURAL WALL SYSTEMS

To facilitate the separation of various problems which arise with the design of structural walls, it is convenient to establish a classification in terms of geometric configurations or roles in structural contributions.

2.1 Strategies in the Location of Structural Walls

Individual walls, generally acting as cantilevers, in a group of structural walls within one building may be subjected to axial, translational and torsional displacements. Depending on its geometric configuration, orientation and location within the plan of the building, a wall will contribute to the resistance of overturning moments, storey shear forces and storey torsion. The positions of the structural walls within a building are usually dictated by functional requirements. These may or may not suit structural planning.

In this context it should be appreciated that, while it is relatively easy to accommodate any kind of wall arrangement to resist wind load, it is much more difficult to ensure satisfactory overall building response to large earthquakes when wall locations deviate considerably from those dictated by seismic considerations. The difference in concern arises from the fact that in the case of wind a fully elastic response is expected, while during large earthquake demands inelastic deformations will arise. The key in the strategy of planning for structural walls is the desire that inelastic deformations, when required for significant energy dissipation, be distributed reasonably uniformly over the whole plan of the building, rather than allowed to concentrate only in a few walls only. The latter case leads to the underutilization of some walls while others might be subjected to excessive ductility demands which might result in excessive loss of resistance.

Most structural walls are open thin-walled sections with small torsional rigidities. Hence in seismic design it is customary to neglect the torsional resistance of individual walls. Tubular sections are exceptions. The torsional stability of a wall system can be examined with the aid of Fig. 1. It is seen that torsional resistance of the wall arrangements of Fig. 1(a), (b) and (c) could only be achieved if the lateral load resistance of each wall with respect to its weak axis was significant. As this is not the case, these examples represent torsionally unstable systems. The circles marked CR refer to the centre of rigidity of the wall system. In the case of the arrangement in (a) or (c), computations may show no eccentricity of horizontal inertia forces. However, these systems will not accommodate torsion due to other causes, for which, justifiably, building codes make provisions, for example by specifying minimum eccentricities.

Figure 1(d), (e) and (f) show cases of apparent torsional stability. Even in the case of the arrangement in (d), where significant eccentricity is present when lateral load in the east-west direction is applied, torsional resistance can be efficiently provided by the forces induced in the plane of the short walls. Some of these examples, often quoted in connection with design for wind load, are not necessarily suitable when ductile seismic response is to be expected. Figure 1(d) and (f) are particular examples which should not be favoured in earthquake resisting buildings unless

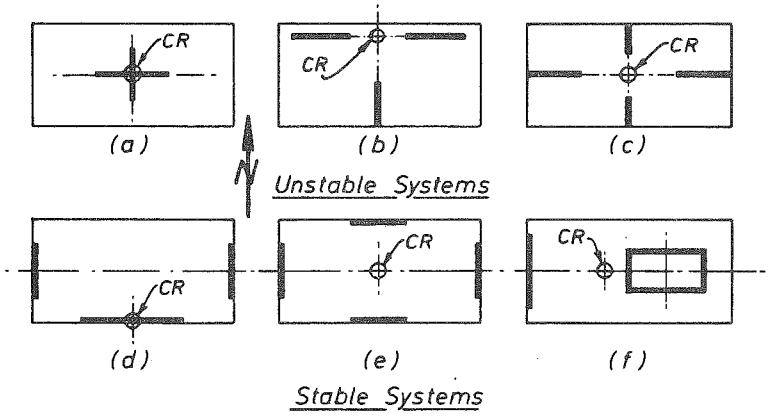

Figure 1 : Examples for the Torsional Stability of Wall Systems

additional lateral load resisting systems, such as ductile frames, are also present.

To illustrate the torsional stability of inelastic wall systems, the arrangements shown in Fig. 2 may be examined. The horizontal force, H, in the east-west direction, acting through the centre of gravity [CG], can be efficiently resisted in both systems. In the case of Fig. 2(a) the the eccentricity, if any, will be small, and the elements in the north-south direction could provide the torsional resistance even though the flange of the T-section may well be subject to inelastic strains due to the seismic shear H.

When an earthquake attack, E, in the north-south direction is considered, it would be easy to satisfy equilibrium requirements in the two end walls which are affected. However, in the case of the arrangement in Fig. 2(a), it would not be possible to ensure that both walls would commence to yield at the same instant. One of the walls, i.e. that at A, might remain elastic, while the wall at the other end (at B) could be subjected to excessive inelastic deformations leading to the twisting of the floor about a vertical axis as shown. Only the wall at B would contribute to energy dissipation. In Fig. 2(b) under the same circumstances, the three other walls of the building would be expected to remain elastic. Thereby approximately uniform floor translations would occur, ensuring that both walls in the north-south direction would participate in the dissipation of the required energy.

In choosing suitable locations for lateral load resisting structural walls, three additional aspects should be considered:

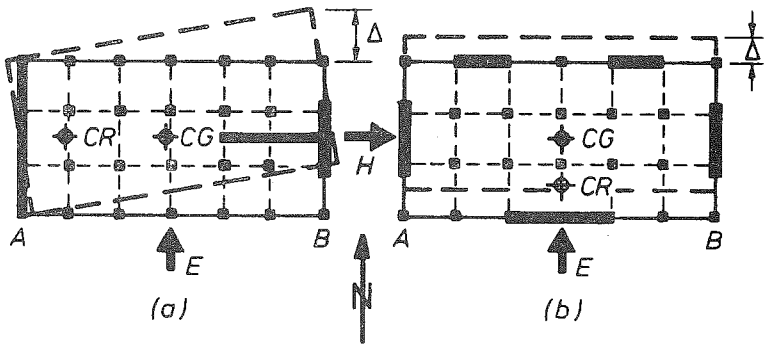

Figure 2 : Torsional Stability of Inelastic Wall Sections.

(i) For the best torsional resistance, as many of the walls as possible should be located at the periphery of the building. The walls on each side may be individual cantilevers or they may be coupled to each other.

(ii) The more gravity load can be routed to the foundations via a structural wall, the less will be the demand for flexural reinforcement in

that wall and the more readily can foundations be provided to absorb the overturning moments generated in that wall.

(iii) A concentration of the total lateral load resistance in one or two structural walls only may introduce very large forces to the foundation structure, so that conventional foundations may not be adequate.

2.2 Sectional Shapes

Individual structural walls of a group may have different sections. Some typical shapes are shown in Fig. 3. The thickness of such walls is often determined by code requirements for minima to ensure workability of fresh concrete or to satisfy fire ratings. When the earthquake loading is significant, shear strength and stability requirements, to be examined subsequently in detail, may necessitate an increase in thickness.

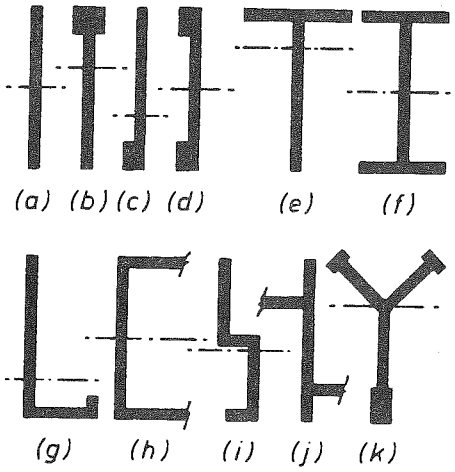

Figure 3 : Common Sections of Structural Walls

Boundary elements, such as shown in Fig. 3(b) (c) and (d), are often present to allow beams at right angles to the walls to be effectively anchored. Even without beams, such elements (bar bells) are often used to accommodate the principal flexural reinforcement, to provide stability against out of plane buckling of a thin-walled section, and, if necessary, to enable more effective confinement of the compressed concrete in potential plastic hinges.

Walls meeting each other at right angles will give rise to flanged sections. Such walls are normally required to resist earthquake loads in both principal directions of the building. They often possess great potential strength.

Some flanges consist of long transverse walls, such as shown in Fig. 3(h) and (j). The designer must then decide how much of the width of such wide flanges should be considered to be effective. Code provisions [5] for the effective width of compression flanges of T and L beams may be considered to be relevant, with the span of the equivalent beam being taken as twice the height of the cantilever wall. Such rules are generally conservative and therefore quite acceptable when designing for wind load.

As in the case of beams of ductile multistorey frames [4], it will also be necessary to determine the flexural overstrength of the critical section of structural walls. This overstrength* will be governed primarily by the amount of tension reinforcement which will be mobilized during a large inelastic seismic pulse. Thus some judgement is required in evaluating the effective width of a tension flange. Generally the width assumed for the

---

* The flexural overstrength of the critical section within a potential plastic hinge of a member is based on the probable strength of the materials with allowance for strain hardening and participation of all reinforcement present at the section, as built, in the presence of a probable axial load during the largest expected seismic event.

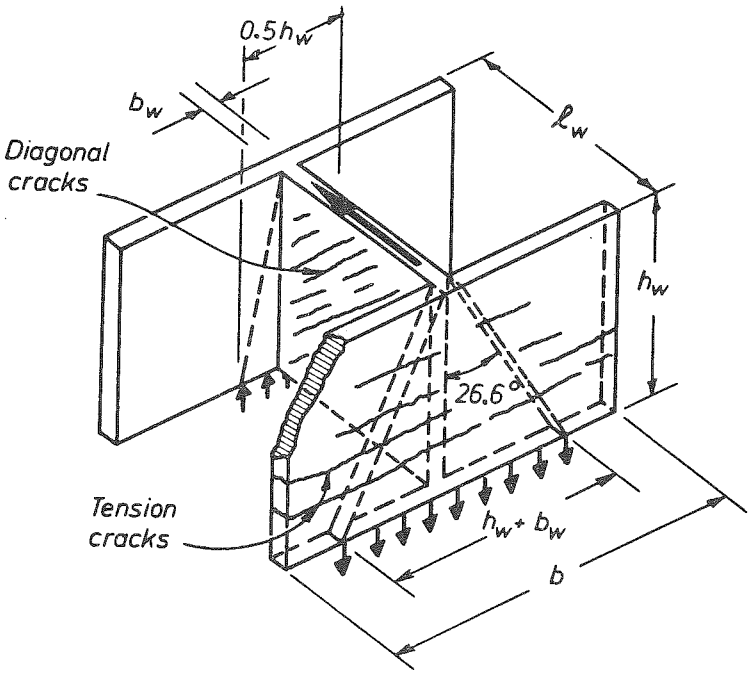

Figure 4 : Estimation of Effective Flange Widths in Structural Walls

compression flange will have negligible effect on the estimate of flexural overstrength.

One suggested approximation for the effective width flanged structural walls is shown in Fig. 4. This is based on the assumption that shear stresses introduced by the web of the wall into the tension flange spread out at a slope of 1 in 2 (i.e. 26.6 degrees). Accordingly it may be assumed that with the notation of Fig. 4, the effective width of the tension flange of a wall is

$$b_{eff} = h_w + b_w \leq b \qquad (1a)$$

and that of the compression flange is

$$b_{eff} = 0.5\ h_w \leq b \qquad (1b)$$

The above approximations represent a compromise, for it is not possible to determine uniquely the effective width of wide flanges in the inelastic state. The larger the rotations in the plastic hinge region of the flanged wall, the larger the width which will be mobilized to develop tension.

The foundation system must be examined to ensure that the flange forces, as assumed, can in fact be transmitted at the wall base.

2.3 Variations in Wall Geometry

Often walls will have openings either in the web or the flange part of the section. Some judgement is required to assess whether such openings are small, so that they can be neglected in design computations, or large enough to affect either shear or flexural strength. In that case due allowance need be made in both strength evaluation and detailing of the reinforcement. It is convenient to examine separately solid cantilever structural walls and those which are pierced with openings in some pattern.

2.3.1 Cantilever walls without openings

Most cantilever walls, such as shown in Fig. 5(a), can be treated as ordinary reinforced concrete beam-columns. The lateral load is introduced by means of a series of point loads through the floors acting as diaphragms. Because the floor slab stabilizes the wall against lateral buckling, relatively thin wall sections, such as shown in Fig. 3, may be used. In such walls it is relatively easy to ensure that, when required, a plastic hinge at the base will develop with adequate plastic rotational capacity [6].

In low-rise buildings or in the lower storeys of medium to high-rise buildings, walls of the type shown in Fig. 5(b), may be used. These are characterized by a small height to length ratio, h_w/ℓ_w. The potential flexural strength of such walls may be very large, even when a minimum amount of vertical reinforcement is used. Because of the small height, relatively large shearing forces must be generated to develop the flexural strength at the base. The inelastic behaviour of such walls is often strongly affected by effects of shear. However, it is possible to ensure inelastic flexural response [7], even though energy dissipation will be diminished by effects of shear. It is advisable to design such walls for larger lateral load resistance in order to reduce ductility demands [4].

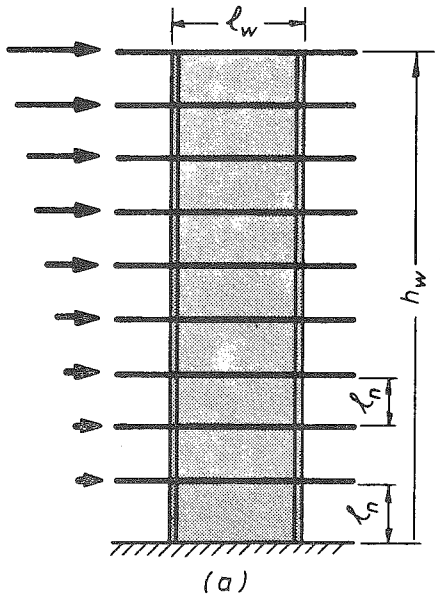

Figure 5 : Cantilever Structural Walls

To allow for the effects of squatness, it is recommended [8] that the design base shear specified for ordinary structural walls be increased by the factor Z where

$$1.0 < Z = 2.5 - 0.5\, h_w/\ell_w < 2.0 \qquad (2)$$

It is seen that this is applicable when the ratio $h_w/\ell_w < 3$. In most situations it is found that this requirement does not represent a penalty because of the great inherent flexural strength of such walls.

2.3.2 Structural walls with openings

In many structural walls a regular pattern of openings will be required to accommodate windows or doors or both. When arranging openings, it is essential to ensure that a rational structure results, the behaviour of which can be predicted by bare inspection [1]. The designer must ensure that the integrity of the structure, in terms of flexural strength, is not jeopardized by gross reduction of wall area near the extreme fibres of the section. Similarly the shear strength of the wall, in both the horizontal and vertical directions, should remain viable and adequate to ensure that its flexural strength can be fully developed.

Windows in stair wells are sometimes arranged in such a way that an extremely weak shear fibre results where inner edges of the openings line up, as shown in Fig. 6(a). It is difficult to make such connections sufficiently ductile and hence it is preferable to avoid this arrangement. Larger spaces between staggered openings would, however, allow an effective diagonal compression and tension field to develop after the formation of diagonal cracks (Fig. 6(b)). When suitably reinforced, overloading by shear of regions between openings can be prevented, and a ductile cantilever response due to flexural yielding at the base only can be enforced.

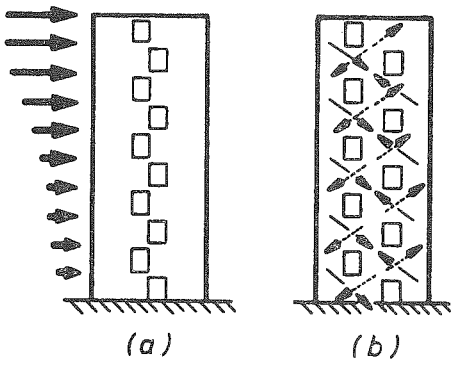

Figure 6 : Shear Strength of Walls as Affected by Openings

Extremely efficient structural systems, particularly suited for ductile response with very good energy dissipation characteristics, can be conceived when openings are arranged in a regular pattern. Examples are shown in Fig. 7. It is seen that a number of walls are interconnected or coupled to each other by beams. For this reason they are generally referred to as coupled structural walls. The implication of this terminology is that the connecting beams, which may be relatively short and deep, are substantially weaker than the walls. The walls, which behave predominantly as cantilevers, can then impose sufficient rotations on these connecting beams, when necessary, to make them yield. When suitably detailed, such beams can dissipate energy over the entire height of the structure. Two identical walls (Fig. 7(a)) or two walls of differing stiffnesses (Fig. 7(b)) may be coupled by a single row of beams. In other cases a series of walls may be interconnected by rows to beams between them, as seen in Fig. 7(c). The coupling beams may be identical at all floors or they may have different depths or widths. In service cores coupled walls may extend above the roof level where elevator machine rooms or space for other services are to be provided. In such cases walls may be considered to be interconnected by an infinitely rigid diaphragm at the top, as shown in Fig. 7(d). Because of their importance in earthquake resistance, a more detailed examination of the design of coupled structural walls is given in section 5.

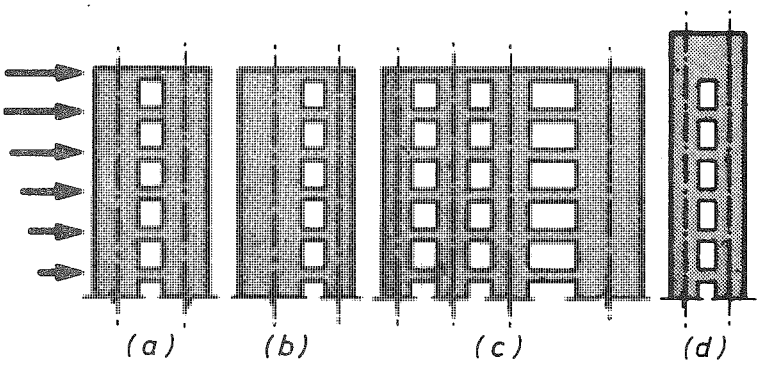

Figure 7 : Types of Coupled Structural Walls

From the point of view of seismic resistance, an undesirable structural system may result in medium to high-rise buildings, when openings are arranged in such a way that the connecting beams are stronger than the walls. As shown in Fig. 8, a storey mechanism is likely to develop in such a system because a series of piers in a particular storey may be overloaded, while none of the deep beams would become inelastic. Because of the squatness of such conventionally reinforced piers, shear failure with limited ductility and poor energy dissipation will characterize the response to large earthquakes. Such a wall system should be avoided, or if it is to be used, much larger lateral design load should be used to ensure that only limited ductility demand, if any, will arise.

Designers sometimes face the dilemma, particularly when considering shear strength, whether coupled walls, such as shown in Fig. 7(a) or (d), should be treated as two walls interconnected or as one wall with a series of openings. The issue may be resolved if one considers the behaviour and

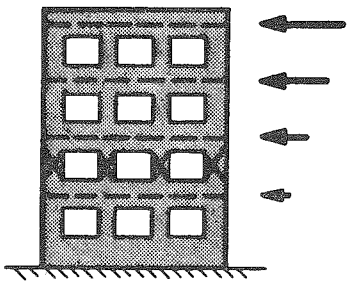

Fig. 8 : Pierced Walls Undesirable for Earthquake Resistance

mechanisms of resistance of a cantilever wall and compares these with those of coupled walls. These aspects are qualitatively shown in Fig. 9.

It is seen that the total overturning moment, M_o, is resisted at the base of the cantilever (Fig. 9(a)) in the traditional form by flexural stresses, while in the coupled walls moments as well as axial forces need to be resisted. These satisfy the following simple equilibrium statement

$$M_o = M_1 + M_2 + \ell T \qquad (3)$$

The magnitude of the axial force, being the sum of the shear forces of all the coupling beams at upper floors, will depend on the relative stiffness and strength of those beams. For example in a structure with strong coupling beams, shown in Fig. 9(b), the contribution of the axial force to the total flexural resistance, as expressed by the parameter

$$A = \frac{T\ell}{M_o} \qquad (4)$$

will be significant. Hence this structure will behave in much the same way as the cantilever of Fig. 9(a) would. Therefore one could treat the whole structure as one wall.

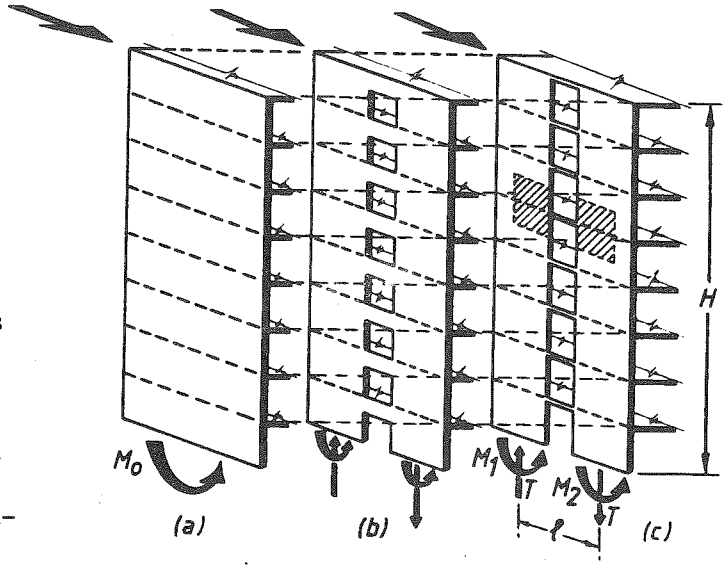

Figure 9 : A Comparison of Flexural Resisting Mechanisms in Structural Walls

When the coupling is relatively weak, as is often the case in apartment buildings, where, because of headroom limitation, coupling by slabs only is possible, as shown in Fig. 9(c), the major portion of the moment resistance is by moment components M_1 and M_2. In this case the value of A (Eq. 4) is small. One should then consider each wall in isolation with a relatively small axial load induced by earthquake actions.

In recognition of the significant contribution of appropriately detailed beams to energy dissipation at each floor in walls with strong coupling (Fig. 9(b)), it is recommended in New Zealand [9] that somewhat reduced lateral load intensity may be used in the design. The reduction factor R_v, with respect to base shear intensity applicable to two cantilever walls, is then such that

$$1.0 \geq R_v = 1.2 - 0.6A \geq 0.8 \qquad (5)$$

when

$$1/3 \leq A = \frac{T\ell}{M_o} \leq 2/3 \qquad (6)$$

In terms of lateral design load intensity, coupled walls with $A \geq 2/3$, may then be treated the same way as ductile frames, for which $R_v = 0.8$ is applicable [9].

3. ANALYSIS PROCEDURES

3.1 Modelling Assumptions

3.1.1 Modelling of member properties

When, for the purpose of either a static or dynamic elastic analysis, stiffness properties of various elements of reinforced concrete wall structures need be evaluated, some approximate allowance for the effects of cracking should be made. In this, it is convenient to assume that reinforced concrete components exhibit properties which are similar to those of elements with identical geometric configurations but made of perfectly elastic, homogeneous and isotropic materials. An approximate allowance for shear and anchorage deformations may also be made.

It should be appreciated that the stiffness of reinforced concrete components depends on the level of loading or amplitude of displacement and hence on the extent of cracking previously imposed. Therefore any assumption made is necessarily a compromise. Within the limits of conventional assumptions, the stiffness of walls may vary by a factor of four [10]. Whatever assumption is made, it should be used consistently in estimating both, periods of vibration and drifts due to lateral loading [11].

Depending on the importance of accuracy in arriving at the equivalent stiffness of a wall section, flexural deformations of the cracked wall, anchorage deformations at the wall base and shear deformations after the onset of diagonal cracking may be considered. Deformations of the foundation structure and the supporting ground, such as tilting or sliding, are not considered in this study, as these produce only rigid body displacement for the wall superstructure. Such deformations should, however, be taken into account when the period of the structure is being evaluated or when the deformations of a structural wall are related to those of adjacent frames or walls which are supported on independent foundations. Elastic structural walls are sensitive to foundation deformations [12].

Accordingly, for cantilever walls subjected predominantly to flexural deformations, the equivalent second moment of area I_e may be taken as 60% of the value based on the uncracked gross concrete area of the cross section, I_g, with the contribution of reinforcement being ignored i.e.

$$I_e = 0.60\ I_g \qquad (7)$$

When elastic coupled walls are considered, where, in addition to flexural deformation, extensional distortions due to axial loads are also being considered, the equivalent moment of inertia, I_e, and area, A_e, may be estimated as follows:

For a wall subjected to axial tension

$$I_e = 0.5\ I_g \qquad (8a) \qquad A_e = 0.5\ A_g \qquad (8b)$$

For a wall subjected to compression

$$I_e = 0.8\ I_g \qquad (9a) \qquad A_e = A_g \qquad (9b)$$

If a more refined analysis is preferred, axial load effects may be allowed for thus

$$I_e = (0.6 + \frac{P_e}{A_g f'_c})\ I_g \leq I_g \qquad (10)$$

where P_e is the axial load considered to act on the wall during an earthquake, taken negative when causing tension.

For diagonally reinforced coupling beams [13], to be examined in section 5.2.1, with depth h and clear span ℓ_n

$$I_e = 0.4\ I_g/(1 + 3(\frac{h}{\ell_n})^2) \qquad (11a)$$

For conventionally reinforced coupling beams [14]

$$I_e = 0.2\ I_g/(1 + 3(\frac{h}{\ell_n})^2) \qquad (11b)$$

In the above expressions the subscripts "e" and "g" refer to the "equivalent" and "gross" sectional properties respectively.

For cantilever walls with aspect ratios, h_w/ℓ_w, larger than 4, the effect of shear deformations upon stiffness may be neglected. When a combination of "slender" and "squat" structural walls provide the seismic resistance, the latter may be allocated an excessive proportion of the total load if shear distortions are not accounted for. For such cases, i.e. when $h_w/\ell_w < 4$, it may be assumed that

$$I_w = \frac{I_e}{1.2 + F} \qquad (12a)$$

where

$$F = \frac{30\ I_e}{h_w^2\ b_w \ell_w} \qquad (12b)$$

where b_w = web thickness of wall section, ℓ_w = horizontal length of wall, h_w = height of wall.

In Eq. (12a) some allowance has also been made for deflections due to anchorage (pull-out) deformations at the base of a wall, and therefore these

deformations do not need to be calculated separately. Deflections due to code-specified lateral static loading may be determined with the use of the above equivalent sectional properties.

3.1.2 Geometric modelling

The accuracy of geometric stiffness modelling may vary considerably. This is particularly true for deep membered structures, such as shown in Fig. 10. In coupled walls, for example, axial deformations may be significant, and these affect the efficiency of shear transfer across the coupling system. It is difficult to model accurately axial deformations in deep members after the onset of flexural cracking. Figure 11 illustrates the difficulties which arise. Structural properties are conventionally concentrated at the reference axis of the wall, and hence, under the action of flexure only, rotation about the centroid of the gross concrete section is predicted as shown in Fig. 11, by line (1). After flexural cracking, the same rotation will occur about the neutral axis of the cracked section, as shown by line (2), and this will result in elongation Δ, measured at the reference axis. This deformation may affect accuracy, particularly when the dynamic response of the structure is evaluated. Its significance in terms of inelastic response is, however, likely to be small.

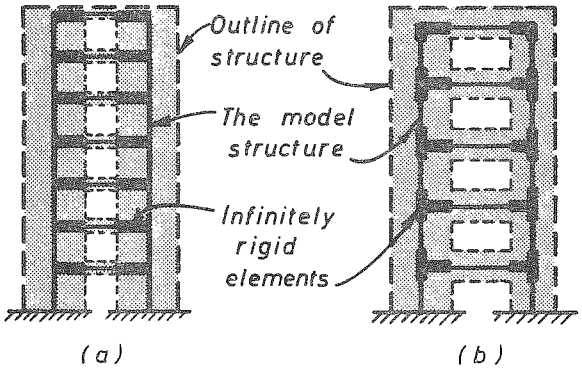

Figure 10 : Modelling of Deep Membered Wall-Frames

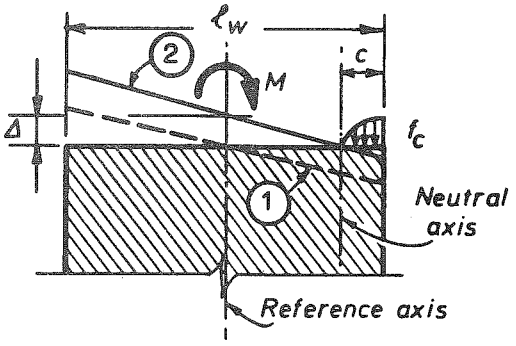

Figure 11 : The Effect of Curvature on Uncracked and Cracked Wall sections

3.2 The Analysis of Wall Sections

The computation of deformations, stresses in or strength of a wall section is based on the traditional concepts of equilibrium and strain compatibility consistent with the plane section hypothesis. Because of the variability of wall section shapes, design aids, such as axial load-moment interaction charts for rectangular column sections, cannot often be used. Frequently the designer will have to resort to the working out of the required flexural reinforcement from first principles [1]. Programs to carry out the section analysis can readily be developed for calculators. The manual section design usually consists of a number of successive approximation analyses of trial sections. However, with a little experience, convergence can be fast.

A simple example of a wall section is shown in Fig. 12. It represents one wall of a typical coupled wall structure, such as shown in Fig. 7. The

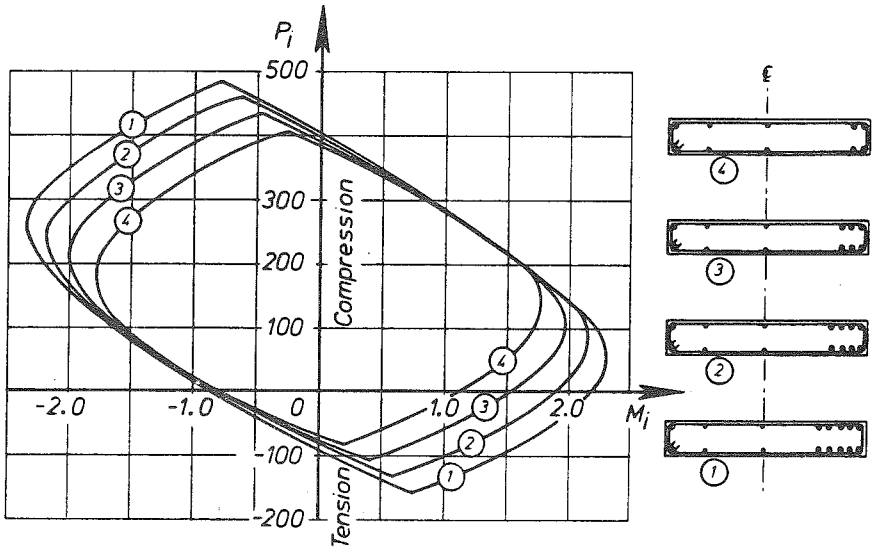

Figure 12 : Axial Load-Moment Interaction Curves for Unsymmetrical Wall Section

four sections are intended to resist the design actions at four different levels of the structure. When the bending moment (assumed to be positive) causes tension at the more heavily reinforced right hand edge of the section, net axial tension is expected on the wall. On the other hand, when flexural tension is induced at the left hand edge of the section by (negative) moments, axial compression is induced in that wall. The moments are expressed as the product of the axial load and the eccentricity, measured from the reference axis of the section, which is conveniently taken through the centroid of the gross concrete area. It is expedient to use the same reference axis also for the analysis of the cross section. It is evident that the plastic centroids in tension or compression do not coincide with this reference axis of the wall section. Consequently the maximum tension or compression strength of the section, involving uniform strain across the entire wall section, will result in axial forces which act eccentrically with respect to the reference axis of the wall. The axial load-moment interaction relationships of Fig. 12 and particularly the associated neutral axis depth positions, give a much more reliable prediction of flexural behaviour than simplistic elastic stress calculations [5] which are based on gross concrete sections.

3.3 Analyses for Wall Actions

Analysis techniques used to derive actions, such as moments, shear and axial forces, due to specified equivalent lateral static loads or dynamic response, are well known. Therefore only the use of results are commented on here. It is common practice to use elastic analyses separately for factored gravity and lateral loading and subsequently to superimpose the result to identify locations and magnitudes of critical actions. However, with the recognition of the inelastic behaviour of walls, when full strength is being developed, some redistribution of design actions may be utilized.

3.3.1 Interacting cantilever walls

Often the entire lateral load resistance is assigned to a number of strategically positioned full height cantilever walls. Assuming, as is generally done, that floor slabs act as infinitely rigid diaphragms, lateral load is readily allocated to each wall [1]. In this allowance for various effects on wall stiffness, as outlined in section 3.1, should be made.

In recognition of the fact that during a severe earthquake, all walls of such a system will need to develop plastic hinges with significant rotational ductility, some redistribution of resistance between walls should be considered. In this the designer will, among other aspects, need to consider the potential flexural strength of a wall and the resistance of foundations with respect to plastic hinge development at the wall base. For example Wall 3 in Fig. 13 may carry significantly larger gravity loads than the other two walls. Thereby its potential for flexural and hence lateral load resistance is enhanced. Hence the designer may decide to reduce the initial load demands on Walls 1 and 2 and correspondingly assign more resistance to Wall 3. This may be seen in Fig. 13 when the moments for elastic analysis, shown by full lines, are compared with those after load redistribution, shown by the dashed line curves. To ensure that no reduction in the total resistance occurs, the condition

$$\Delta M_1 + \Delta M_2 \leq \Delta M_3$$

must be satisfied. Such load redistribution has negligible effect on the ductility potential of a well detailed wall, if the reduction of flexural resistance does not exceed 30% of the initial value [8].

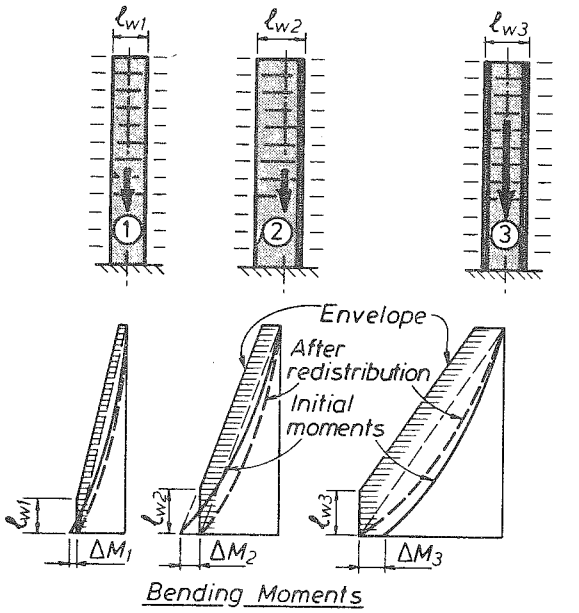

Figure 13 : Load Distribution Between Interconnected Cantilever Walls and Design Moment Envelopes

3.3.2 Coupled walls

Some of the advantages which coupled walls, such as shown in Fig. 7, can offer in seismic design, were discussed in section 2.3.2, together with the basic modes of lateral load resistance. These were shown in Fig. 9. While elastic analyses techniques [15,16,17] form the basis of design, recognition of inelastic response may offer very significant advantages.

The desired full energy dissipating mechanism in coupled walls is similar to that in multistorey frames with strong columns and weak beams [4]. This involves the plastification of all the coupling beams and the development of a plastic hinge at the base of each of the walls, with no inelastic deformation anywhere else along the height of the walls. This is readily achieved because the walls are usually very much stronger than the connecting beams. Such a mechanism is shown in Fig. 14(d). Hence, as in the case of beams and columns of ductile frame [4], inelastic redistribution of

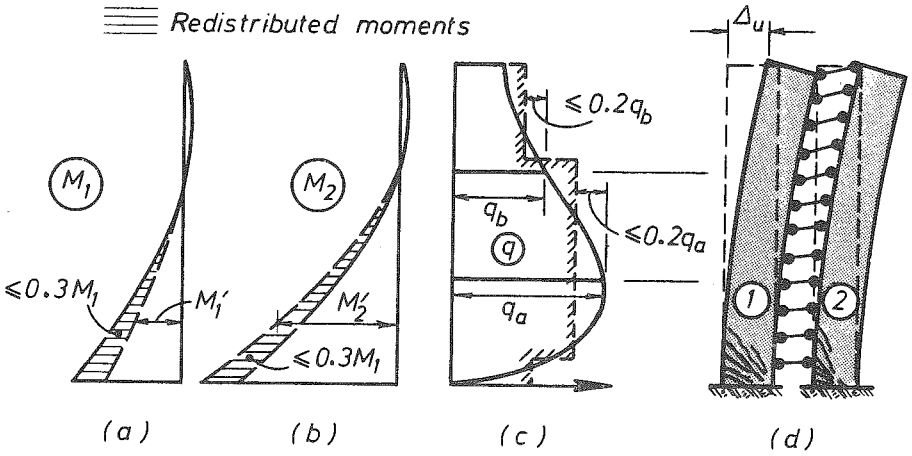

Figure 14 : Load Redistribution Between Components of Coupled Walls

actions, while approaching the development of the full strength of the coupled wall structure, should be considered. This will allow a more practical and economical distribution of the reinforcement to be made.

The elastic analysis for such a symmetrical structure may have resulted in bending moments M_1 and M_2 for the tension and compression walls respectively, as shown by full lines in Fig. 14(a) and (b). In this analysis the elastic redistribution of moments from the tension to the compression wall, due to the effects of cracking, as outlined in section 3.1 has already been considered. In spite of M_1 being smaller than M_2, more tension reinforcement is likely to be required in Wall 1 because it may be subjected to large lateral load induced axial tension. The moment of resistance of Wall 2 on the other hand will normally be enhanced by the increased axial compression. It is therefore suggested that, if desirable and practical, the moments in the tension wall be reduced by up to 30% and that these moments be redistributed to the compression wall. This range of maximum redistributable moments is shown in Figs. 14(a) and (b). Ductile walls would be quite capable of much larger inelastic moment redistribution. The limit of 30% is considered to be a prudent measure to protect walls against excessive cracking during moderate earthquakes. Moment redistribution from one wall to another also implies redistribution of wall shear forces of approximately the same order.

Similar considerations lead to the intentional redistribution of vertical shear forces in the coupling system. It has been shown [1] that considerable ductility demands may be imposed on the coupling beams [18]. Hence they will need to be designed and detailed, to be shown in section 5.2.1, for very large plastic deformations. Typical elastic distribution of shear forces in coupling beams, q, is shown in Fig. 14(c). For practical reasons, as many identically reinforced coupling beams would be provided as possible. Shear and hence moment redistribution vertically among coupling beams can be utilized, and the application of this is shown by the stepped shaded lines in Fig. 14(c). It is suggested that the reduction of design shear in any coupling beam should not exceed 20% of the shear predicted for this beam by the elastic analysis. It is seen that with this technique a large number of beams can be made identical over the height of the building.

When shear is redistributed in the coupling system, it is important to ensure that no shear is "lost". That is, the total axial load introduced to the walls, supplying the $T\ell$ component of the moment resistance, as seen in Fig. 9(c), should not be reduced. Therefore the area under the stepped and

shaded lines of Fig. 14(c) must not be allowed to be less than the area under the curve giving the theoretical elastic beam shear, q.

4. DESIGN OF WALL ELEMENTS FOR STRENGTH AND DUCTILITY

4.1 Failure Modes in Structural Walls

A prerequisite in the design of ductile structural walls is that flexural yielding in clearly defined plastic hinge zones should control the strength, inelastic deformation and, hence, energy dissipation in the entire structural system. As a corollary to this fundamental requirement, brittle failure mechanisms or even those with limited ductility, should not be permitted to occur. This is achieved by either designing for fully elastic response or, when relying on inelastic behaviour, by establishing a desirable hierarchy in the failure mechanics.

The principal source of energy dissipation in a laterally loaded cantilever wall (Fig. 15) should be the yielding of the flexural reinforcement in the plastic hinge regions, normally at the base of the wall, as shown in Fig. 15(b) and (e)

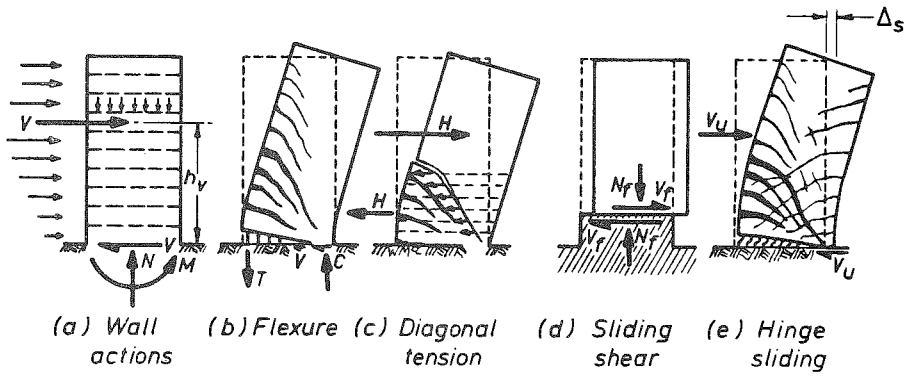

Figure 15 : Failure Modes in Cantilever Walls

Failure modes to be prevented are those due to diagonal tension (Fig. 15(c)) or diagonal compression caused by shear, instability of thin walled sections or of the principal compression reinforcement, sliding shear along construction joints, shown in Fig. 15(d), and shear or bond failure along lapped splices or anchorages. Attempts must be made to control effects, particularly those due to shear, which lead to both premature stiffness and strength degradation and consequently to reduced ability for energy dissipation.

An example of the undesirable response of a structural wall to reversed cyclic loading is shown in Fig. 16. Particularly severe is the steady reduction of strength and ability to dissipate energy. Fig. 17 shows the response of a conventionally designed [5] test wall in which no special efforts were made to improve energy dissipation [19]. Even though its response is superior when compared with that shown in Fig. 16, a steady reduction of

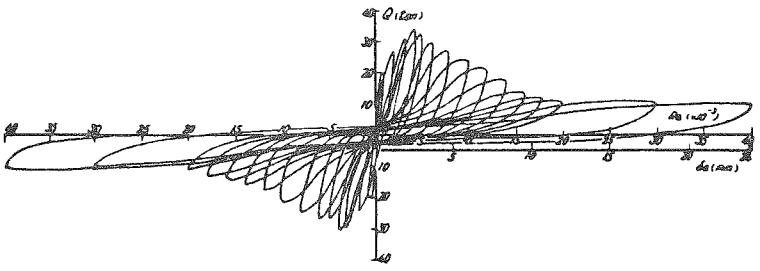

Figure 16 : Hysteretic Response of A Structural Wall Controlled by Shear Mechanisms

stiffness with increased displacement ductility is evident. It is also seen that after a larger inelastic excursion full strength at lower displacement amplitudes is no longer attained. Even though the strength attained at the end of each displacement cycle, as shown by the envelope curve in Fig. 17, is close to the load-displacement curve which was obtained from monotonic loading of a companion specimen, the energy dissipating capacities of the two walls are significantly different.

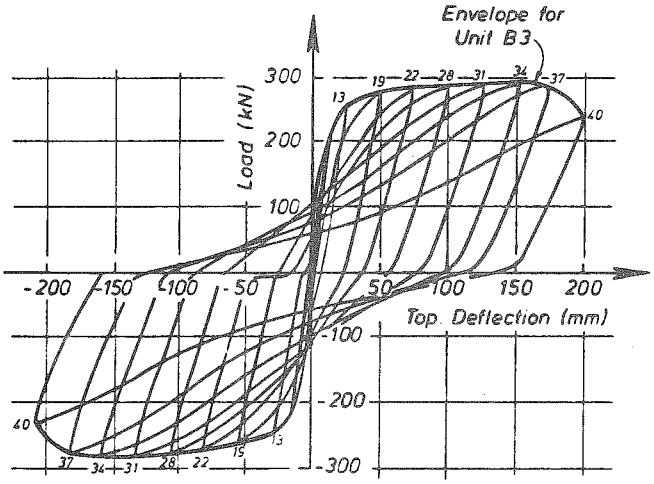

Figure 17 : Hysteretic Response of a Cantilever Wall with Significant Shear Deformations [19]

Numerous theoretical studies have been conducted recently, particularly in the United States and Japan, to establish suitable mathematical models for such degrading hysteresis relationships in order to predict more realistically nonlinear structural response to various earthquake records. These studies sometimes imply that responses, such as shown in Figs. 16 and 17, are inevitable, being in the nature of reinforced concrete. However, this need not be the case. With foresight and judicious detailing of the reinforcement in critical areas of structural walls, greatly improved and sometimes optimal response can be readily achieved. Figure 18 shows such a response, obtained from the test of a 1/3 full size cantilever structural wall with rectangular cross section. It is seen that a displacement ductility of approximately 4 has been attained in a very stable manner [20]. Failure due to inelastic instability, to be examined subsequently, occurred only after 2 cycles to a displacement ductility of 6, when the lateral deflection was 3.5% of the height of the wall.

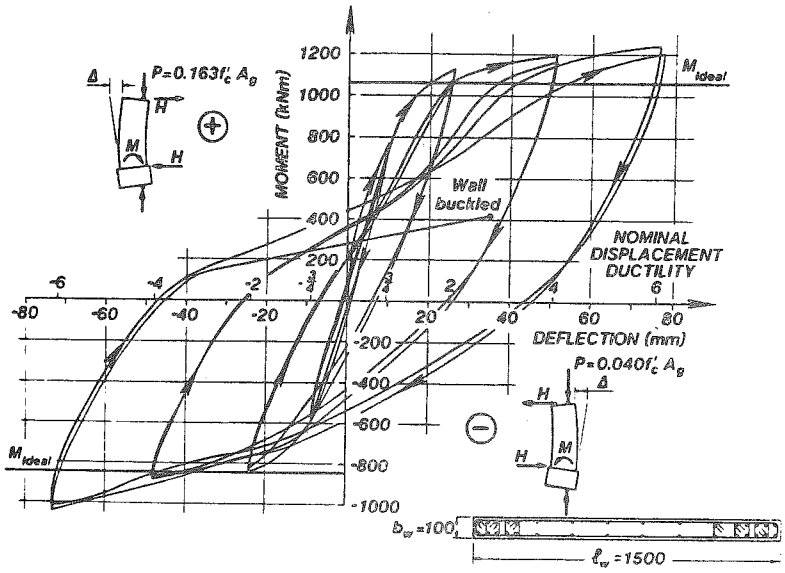

Figure 18 : The Stable Hysteretic Response of a Ductile Wall Structure [20]

4.2 Flexural Strength and Ductility

4.2.1 Flexural response

The evaluation of flexural strength is based on well established principles, and this was briefly reviewed in section 3.2 and illustrated with the M-P relationship in Fig. 12. The ability of a particular section to sustain plastic rotations, as measured by the curvature ductility, follows from the same simple principles.

The development of the ideal flexural strength of a section, such as shown in

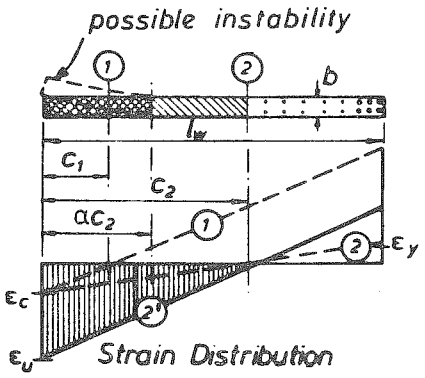

Figure 19 : Strain Patterns for Rectangular Wall Sections

Fig. 18, is associated with a particular strain pattern. This is defined by the failure strain, ε_c, of the concrete and the neutral axis depth, c. With moment only or moment with small axial compression and, even more, with axial tension, the neutral axis depth, c_1 of the rectangular section in Fig. 19 will be small relative to the length of the wall, ℓ_w. Consequently the curvature ductility will be large and usually adequate to accommodate the plastic hinge rotations imposed on the structure during a large earthquake. However, when the wall is simultaneously subjected to moment and large axial compression, a large flexural compression zone will be required, resulting in a relatively large neutral axis depths, such as c_2 in Fig. 19. The resulting strain profile, shown with the line (2), indicates clearly very small curvature ductility. If these two walls are part of an interconnected wall system, similar curvatures will be required to develop in all walls. This means that the wall with large compression load will have to develop the strain profile shown by line (2') in Fig. 19. This would imply concrete compression strains in the extreme fibre, ε_u, considerably in excess of the critical value, ε_c. Clearly such curvature could not be sustained unless the concrete subjected to excessive compressive strains is confined. This is examined in section 4.2.5.

The effect of sectional configuration on the ductility potential of a wall section can be studied with the example of a channel shaped wall in Fig. 20. In the case of Wall (A), subjected to earthquake loading in the direction shown, all the internal tension forces resulting from the yielding of the bars in the flanges of the channel and also some considerable axial compression load on the wall could be equilibriated by the long but narrow compression zone in the web part of the section. The associated theoretical neutral axis, c_1, is very small and hence the ensuing curvature, shown by the dashed line, is extremely large. This large curvature is not likely to be required and possibly the one shown by the full line would be adequate. Thus concrete compression strains might remain subcritical at all times. In cases such as this, even at moderate ductility demands, moments in excess of the ideal flexural strength may be developed because of strain hardening of the steel located in the regions of large tensile strains.

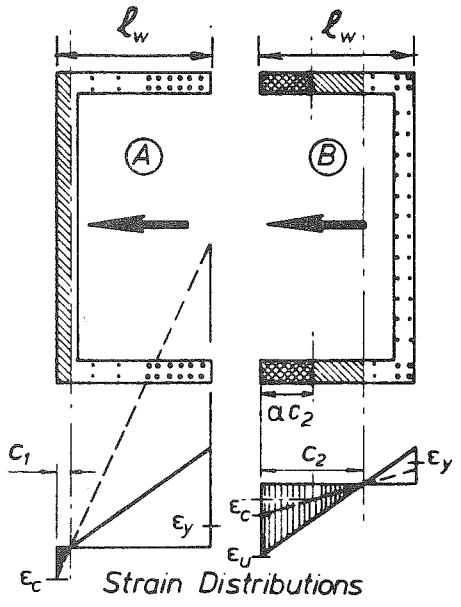

Figure 20 : Strain Profiles Showing Ductility Potential in Channel Shaped Walls

Wall B of Fig. 20, on the other hand, requires a large neutral axis depth, c_2, to develop a compression zone large enough to balance the tension forces generated in the web part of the section. Even specified minimum wall reinforcement placed in a long wall, as in Fig. 20, can develop a

significant tension force when yielding. As the dashed line strain profile indicates, the curvature developed with the ideal strength will not be sufficient if the same ductility demand as in Wall (A), shown by the full line strain profiles, is imposed. The excessive concrete compression strain in the vicinity of the tip of the flanges of Wall (B), will require confinement to be provided if a brittle failure is to be avoided.

It is thus seen that the depth of the neutral axis, c, relative to the length of the wall, ℓ_w, is a critical quantity. If a certain curvature ductility is to be attained, the ratio c/ℓ_w will need to be limited, and thus is examined in section 4.2.4.

As in the case of beams and columns [4], the ideal flexural strength of wall sections is based on specified material properties f'_c and f_y. During large inelastic displacement pulses, particularly when large curvature ductility demands arise, such as shown for Wall (A) in Fig. 20, much larger moments may be developed at the critical wall section. This strength enhancement needs to be taken into account. This can be quantified with the flexural overstrength factor $\phi_{o,w}$ which in the case of cantilever walls is the ratio of the overstrength moment of resistance to the moment resulting from the code specified lateral loading, where both moments refer to the base section of the wall. This is defined in Eq. (20).

4.2.2 Ductility relationships in walls

Whether a structural wall is capable of sustaining plastic deformations consistent with an expected displacement ductility ratio, will depend on the ability of its plastic hinge, normally at the base of the wall, to sustain corresponding plastic rotations. These hinge rotations will in turn depend on the available curvature ductility and the expected length of the plastic hinge [1]. It is important to appreciate that curvature ductility and displacement ductility ratios are not equal. Plastic hinge length, ℓ_p, is primarily a function of the wall length, ℓ_w. Typical values are such that $0.5 < \ell_p/\ell_w < 1.0$. The yield deflection, normally measured at the top of the wall and used in defining the displacement ductility ratio, rapidly increases with the height of the wall, h_w. Hence the curvature ductility demand, $\mu_\phi = \phi_u/\phi_y$, corresponding with an imposed displacement ductility ratio, $\mu_\Delta = \Delta_u/\Delta_y$, is also influenced by the aspect ratio of the wall h_w/ℓ_w. These relationships are shown graphically [21] in Fig. 21. The shaded bands result from two different suggestions for estimating the length of the plastic hinge, ℓ_p. It is seen that for a rather slender wall with an aspect ratio of 10, a curvature ductility of approximately 12 is required to sustain a top deflection which is four times that at yield, i.e. $\mu_\Delta = 4$. With this knowledge, recommendations may be made with respect to the c/ℓ_w ratio to ensure adequate curvature ductility in any wall section. It is evident that rather large curvature ductility demands would arise in slender walls when $\mu_\Delta > 5$.

4.2.3 Wall stability

When part of a thin wall section is subjected to large compression strains, the danger of premature failure by instability arises. This is the case when a large neutral axis depth is required in the plastic hinge zone of the wall, as shown in Fig. 19, while the length of the plastic hinge, ℓ_p, is large, i.e. one storey high or more. The problem is compounded when

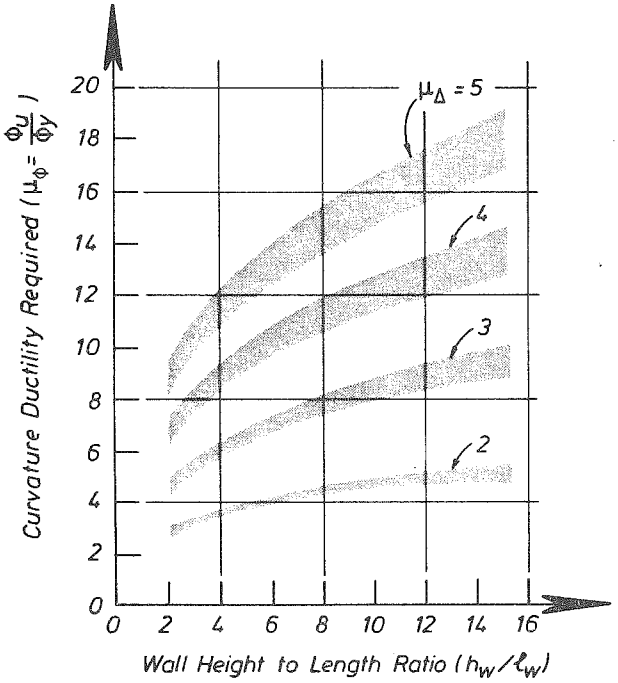

Figure 21 : The Variation of the Curvature Ductility Ratio at the Base of Cantilever Walls with the Aspect Ratio and the Imposed Displacement Ductility Demand [21]

cyclic inelastic deformations occur. Instability should not govern the seismic response of ductile walls.

The problem of the inelastic out-of-plane buckling of thin walled reinforced concrete sections does not lend itself to meaningful analytical assessment. However, an appreciation of the mechanisms involved should assist the designer in inhibiting the influence of instability on overall ductile wall response. For this reason the perceived major factors of out-of-plane buckling, as well as its consequencies, are briefly described in the following paragraphs.

At large curvature ductilities large tensile strains will be imposed on vertical bars placed at the extreme tension edge of a section, such as shown in Fig. 18. At this stage uniformly spaced approximately horizontal cracks of considerable width develop over the plastic hinge length. In a somewhat idealized form, these are shown in Fig. 22(a).

During the subsequent reversal of wall displacements, and hence unloading, the tensile stresses in these bars reduce to zero. Further reduction of lateral load, and in the case of coupled walls an increase of axial compression on the wall, will eventually produce compression stresses in all these bars. Unless the cracks, seen in Fig. 22(a), close, the entire internal compression within the section must

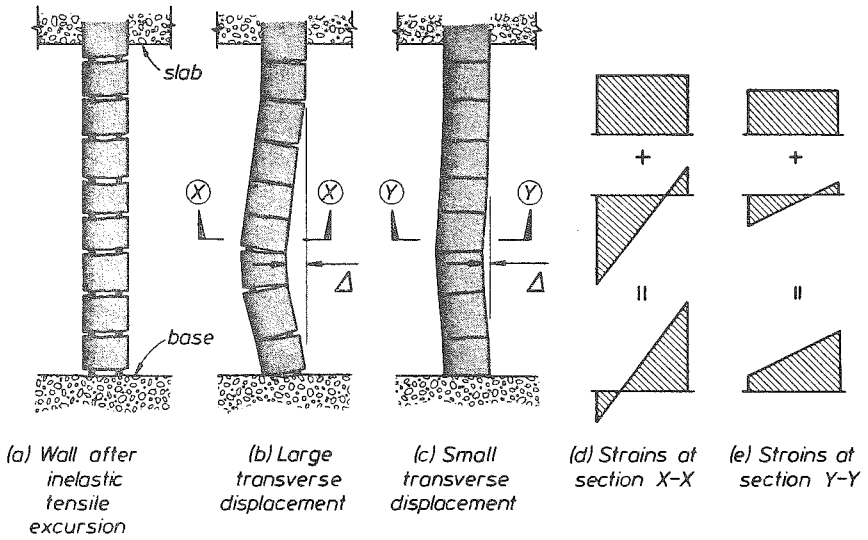

Figure 22 : Deformations and Strain Patterns in a Buckled Zone of a Wall Section

be resisted by the vertical reinforcement. Due to Bauschinger effect, the modulus of elasticity for steel is reduced at this stage. Out-of-plane buckling, shown in Fig. 22(b) may commence when the tangent modulus of steel reaches a critically small value, while residual cracks in the concrete are still open.

If horizontal cracks across the thickness of the wall (Fig. 22(c)) close before such a critical stage is reached, concrete compression stresses will again develop. The crack closure may gradually stiffen the section and transverse instability at that level of loading may be arrested. If buckling does occur, transverse displacements can be restricted only if and when the affected part of the section can develop an adequate redistributed stress state. This stress state must permit the resistance of internal forces from both lateral and axial loading on the wall and also transverse moment due to out-of-plane eccentricity (Fig. 22(d) and (e)).

If crack widths are still wide at the onset of instability, out-of-plane displacements may increase rapidly, even if internal vertical compression forces are small. This means that after large inelastic displacements, failure by buckling can occur at relatively small lateral load on the wall. The response of a test wall [20] which failed in this manner, is shown in Fig. 18.

When only a small part of the wall section tends to buckle because of lateral support afforded by other parts which are in tension, increase of axial compression and lateral load on the wall is possible without significant changes in transverse displacements. However, as ductility demands and consequent strains in the compression zone increase, the depth of the compression zone c (Fig. 19) in the section may also increase. This may be due to the combination of loss of cover, the decline in the resistance of the compressed concrete subjected to these higher strains, especially during repeated cycles with large ductility, and mainly the non-uniform strain distribution across the wall thickness due to out-of-plane displacements, as shown in Figs. 22(d) and (e). This increase of the neutral axis depth, c, may then lead to excessive compression strains in the unconfined part of the section with consequent crushing of the concrete. Concrete compression stress distributions in the absence and presence of out-of-plane displacements are compared in Fig. 23. The skewing of stress distribution and the consequent increase of the average neutral axis depth c_{av}, is seen in Fig. 23(b).

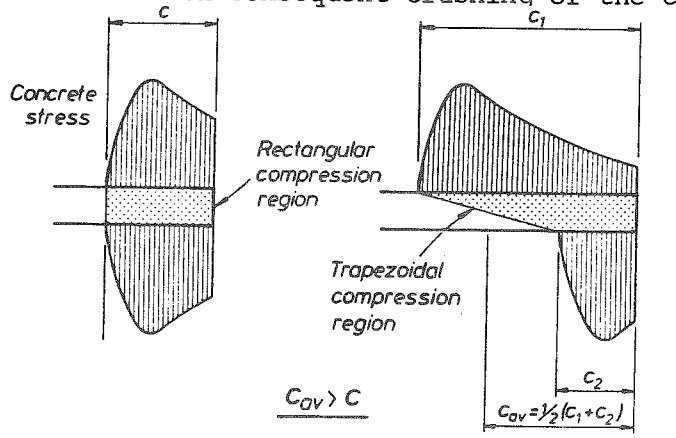

(a) No out of plane bending (b) Significant out of plane bending

Figure 23 : Skewing of Wall Stress Distribution Due to Out-of-Plane Bending

There are several other factors which may influence out-of-plane buckling of thin walls [20]. Most of these factors are beyond the control of the designer. The two features, discussed above and considered to be most important, which affect the ductile response of walls, are:

(a) Instability at relatively low loads may occur when bars, previously subjected to large inelastic tensile strains, are subjected to compression before previously formed large flexural cracks can close.

(b) Relatively small out-of- plane displacements during reversed cyclic loading, cause a skewing of compression strains (Fig. 23(b)) and this loads to the migration of flexural compression stresses away from extreme fibres of the wall section, causing premature crushing of unconfined regions of the plastic hinge zone.

In the absence of more accurate information on the "compactness" of reinforced concrete wall sections, existing code rules [5], relevant to short columns are best considered as guides. For such columns, the effective height to width ratio, ℓ_n/b, should not exceed 10. In walls, ℓ_n is the clear height of the wall in the critical storey. Therefore intuitive judgement was used [8] to recommend that, with the exceptions to be set out subsequently, in the outer half of the conventionally computed compression zone, the wall thickness, b, should not be less than one tenth of the clear vertical distance between floors or other effective lines of lateral support, ℓ_n.

When the computed netural axis depth is small, as shown by the strain distribution (1) in Fig. 19, the compressed area may be so small that adjacent vertical strips of the wall will stabilize it. Accordingly, when the fibre at 0.5c is within a distance of the lesser of 2b or 0.15 ℓ_w from the compressed edge, the $b > \ell_n/10$ limit should not need to be complied with [8]. In terms of neutral axis depth, these criteria are met when $c < 4b$ or $c < 0.3\ \ell_w$, whichever is less. The strain profile (1) in Fig. 19, which occurs commonly in lightly reinforced walls with small gravity load, clearly satisfies this condition.

These recommendations are intended for structural walls in which displacement ductilities of the order of 4 are expected. It has been suggested [22,23] that the expected ductility demand should also be considered in slenderness limitation. The smaller the inelastic excursion the less critical will instability be. Hence it is suggested that for walls with a wide range of lateral load resistance, the thickness limit, discussed above, may be controlled by*

$$b \geq \frac{\ell_n}{10\sqrt{\phi_{o,w}K - 0.2}} \qquad (13a)$$

or

$$b \geq \frac{\ell_n}{22\sqrt{\phi_{o,w}/R - 0.05}} \qquad (13b)$$

where, K is the horizontal force factor defined in the Uniform Building Code [24], and R is the response modification coefficient in the tentative provisions of ATC [25]. It was assumed that K = 0.8 and R = 5.5 approximate an expected displacement ductility demand of the order of 4.

It may be assumed that only in buildings 3 storeys or higher would the plastic hinge length at the base, extending toward the first floor, be large enough to warrant an examination of instability criteria.

---

*Using S defined by NZS 4203:1984

$$b \geq \frac{0.09\ell_n}{\sqrt{0.7\phi_{o,w}S - 0.2}}$$

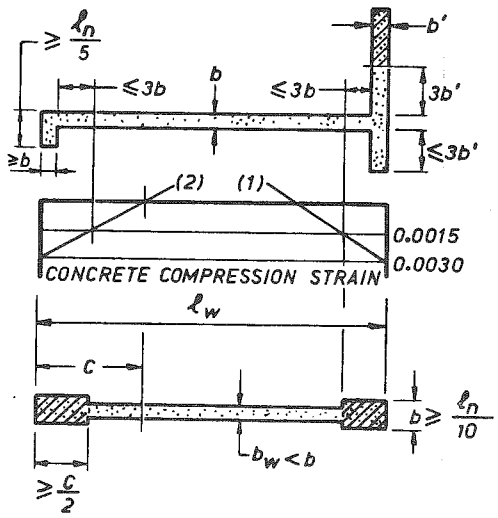

Figure 24 : Dimensional Limitations on Wall Sections to Prevent Premature Instability

Certain components of walls, such as shown in Fig. 24, provide continuous lateral support to adjacent compressed elements. Therefore it is considered that parts of a wall along its length ℓ_w, within c/2 from the compression edge, which is within a distance of 3b of such a line of lateral support, should be exempted from slenderness limitations [8]. Figure 24 shows a number of such locations. The shaded part of the thin flange is considered to be too remote to be effectively restrained by the web portion of the wall, and hence it should comply with the requirement of Eq. (13). In the absence of a flange, the width of which is at least $\ell_n/5$, a boundary element may be formed which satisfies the slenderness limit. This latter case is shown at the bottom of Fig. 24. Similar recommendations have been adopted in Canada [33].

It is preferable to use walls with boundary elements, such as shown in Fig. 3(d) and (f). Substantial boundary elements provide protection against instability of the flexural compression region [23]. Also such elements are easier to confine (Fig. 26).

4.2.4 Limitations on curvature ductility

Because of the variety of cross sectional shapes and arrangements of reinforcement which can be used, and the presence of some axial load, the availability of ductility in walls cannot be checked by the simple rules suggested by codes [5,8]. In the analysis of wall sections for flexure and axial load, as shown in Fig. 19, the neutral axis depth, c, is always determined. Hence the ratio c/ℓ_w, an indicator of the curvature ductility required at the development of the ideal strength, can be readily found.

The curvature ductility demand in the plastic hinge zone of cantilever walls was related to the displacement ductility in section 4.2.2. Typical relationships are shown in Fig. 21, where it is seen that in a relatively slender wall with $h_w/\ell_w = 8$ for example, a curvature ductility of approximately 11 is required if the displacement ductility is to be 4. It may be shown from first principles that the yield curvature in a wall with length ℓ_w, is approximately $\phi_y = 0.0025/\ell_w$. Hence the expected ultimate curvature for this example wall would need to be of the order $\phi_u = 0.0275/\ell_w$, a value also observed in tests [22]. By assuming that the maximum compression strain attained in the unconfined concrete during an earthquake may reach the value of 0.004, it is found that the neutral axis depth at the development of $\phi_u = 11\ \phi_y$ needs to be be $c \simeq \ell_w/7$.

The above approach was based on cantilever walls in which the flexural overstrength at the base, corresponding with an overstrength factor of $\phi_{o,w} = 1.4$, is associated with a displacement ductility demand of 4. When the flexural overstrength is larger, or when larger K and lower R factors are used in the design, curvature ductility demand is expected to reduce and hence the acceptable neutral axis depth may be increased. Consequently this critical

depth can be conservatively estimated [8] from*

$$c_c = \phi_{o,w} K \ell_w/8 \quad \text{or} \quad c_c = 0.55 \phi_{o,w} \ell_w/R \qquad (14)$$

In view of the approximations involved in seismic design load assessments, a more elaborate curvature estimate is hardly warranted. If desired the effect of aspect ratio h_w/ℓ_w, shown in Fig. 21, may be taken into account [8] thus*

$$c_c = \frac{10.8 \phi_{o,w} K}{(4 - 0.88 K)(17 + h_w/\ell_w)} \ell_w \quad \text{or} \quad c_c = \frac{11.8 \phi_{o,w}}{(R - 1)(17 + h_w/\ell_w)} \ell_w \qquad (15)$$

Whenever the computed neutral axis depth for the design load exceeds the critical value, c_c, given by Eq. (14) or Eq. (15), it is necessary to assume that the required ductility can be attained only at the expense of concrete compression strains in excess of 0.004.

4.2.5 Confinement of structural walls

From the examination of curvature relationships in the simple terms of c/ℓ_w ratio, it is found that when the neutral axis depth is larger than the critical value c_c, at least a portion of the compression region of the wall section over the height of the plastic hinge needs to be confined. In this context three aspects need to be addressed:

(a) The area of wall section within which compressed concrete is to be confined - The strain gradient associated with previous assumptions and the critical neutral axis depth is shown by the shaded line (1) in Fig. 25. When the neutral axis depth becomes larger, as shown by line (2), a length $\alpha' c$ will be subjected to strains larger than 0.004, if the same curvature is to be attained. Hence it is suggested that by taking previously mentioned factors, particularly those relevant to effects of out-of-plane displacements, into account, the length of wall section to be confined should be αc where

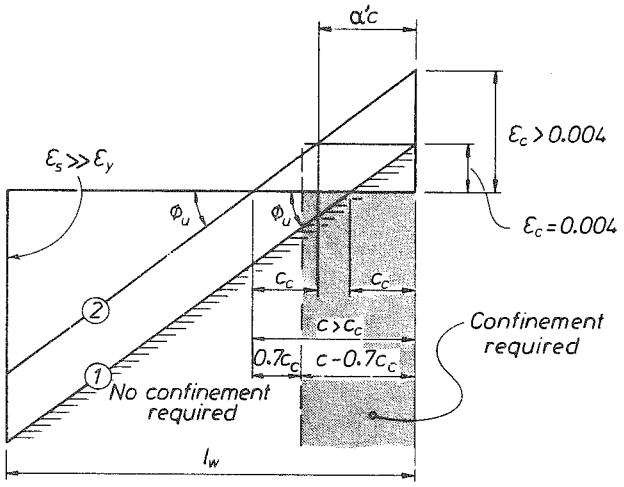

Figure 25 : Strain Patterns for Wall Sections

$$\alpha = (1 - 0.7\, c_c/c) \geq 0.5 \qquad (16)$$

whenever $c/c_c > 1$. When c is only a little larger than c_c, a very small and impractical value of α is obtained. In such cases at least one half of the theoretical compression zone [8] should be confined. The length of the confined region is independent of the configuration of a possible boundary element which may be present.

---

*Using S defined by NZS 4203:1984

$$c_c = 0.10 \phi_{o,w} S \ell_w \qquad (14) \quad \text{or} \quad c_c = \frac{8.6 \phi_{o,w} S \ell_w}{(4 - 0.7 S)(17 + h_w/\ell_w)} \qquad (15)$$

(b) The quantity of confining reinforcement - The principles of concrete confinement [1,4] to be used are those relevant to columns, with the exception that very rarely will the need arise to confine the entire wall section. The governing principle is that as the compressed area in a wall section increases, concrete strains associated with the necessary ductility also increase proportionally and hence the amount of confining reinforcement must also increase. Accordingly it is recommended [8] that rectangular or polygonal hoops and supplementary ties surrounding the longitudinal bars in the region to be confined should be used so that

$$A_{sh} = 0.3\, s_h h'' \left[\frac{A_g^*}{A_c^*} - 1\right] \frac{f'_c}{f_{yh}} \left(0.5 + 0.9\, \frac{c}{\ell_w}\right) \qquad (17a)$$

or

$$A_{sh} = 0.12\, s_h h'' \frac{f'_c}{f_{yh}} \left(0.5 + 0.9\, \frac{c}{\ell_w}\right) \qquad (17b)$$

whichever is greater. In practice the ratio c/ℓ_w will seldom exceed 0.3. In the above equations: A_{sh} = total effective area of hoops and supplementary cross ties in direction under consideration within spacing s_h, mm^2, s_h = vertical centre to centre spacing of hoop sets, mm, A_g^* = gross area of the wall section which is to be confined in accordance with Eq. (16), mm^2, A_c^* = area of concrete core within area A_g^*, measured to outside of peripheral hoop legs, mm^2, f'_c = specified compression strength of concrete, MPa, f_{yh} = specified yield strength of hoop or supplementary cross tie reinforcement, MPa, h" = dimension of concrete core of section measured perpendicular to the direction of the hoop bars, mm.

These equations are similar to and are based on those developed for columns [26]. The area to be confined is thus extending to αc_2 from the compressed edge as shown by cross hatching in the examples of Figs. 19 and 20.

For the confinement to be effective, the vertical spacing of hoops or supplementary ties, s_h, should not exceed 6 times the diameter of vertical bars in the confined part of the wall section, one half of the thickness of the confined part of the wall or 150 mm, whichever is least [8]. When confinement is required, walls with a single layer of reinforcement should not be used for obvious reasons. This confining transverse reinforcement should extend vertically over the probable plastic hinge length of the wall, which for this purpose should be assumed to be equal to ℓ_w or $h_w/6$, whichever is greater, but need not exceed 2 ℓ_w.

(c) Confinement of longitudinal bars - A secondary purpose of confinement is to prevent the buckling of the principal vertical wall reinforcement where this may be subjected to yielding in compression. It is therefore recommended [8] that in the regions of potential yielding of the longitudinal reinforcement within a wall with two layers of reinforcement, where the longitudinal reinforcement ratio, ρ_ℓ, computed

from Eq. (19), exceeds $2/f_y$ (f_y in MPa), transverse tie reinforcement, satisfying the following requirements, should be provided:

(i) Ties suitably shaped should be so arranged that each longitudinal bar or bundle of bars placed close to the wall surface is restrained against buckling by a 90 degree bend or at least a 135 degree standard hood of a tie. When two or more bars, at not more than 200 mm centres apart, are so restrained, any bars between them may be exempted from this requirement.

(ii) The area of one leg of a tie, A_{te}, in the direction of potential buckling of the longitudinal bar, should be computed from Eq. (18) where ΣA_b is the sum of the areas of the longitudinal bars reliant on the leg of a tie, including the tributary area of any bars exempted from being tied in accordance with (i) above.

$$A_{te} = \frac{\Sigma A_b f_y}{16 f_{yh}} \frac{s_h}{100} \qquad (18)$$

Longitudinal bars centred more than 75 mm from the inner face of stirrup ties need not be considered in determining the value of ΣA_b.

(iii) The centre to centre spacing of ties along the longitudinal bars should not exceed six times the diameter of the longitudinal bar to be restrained.

(iv) Where applicable, ties may be assumed to contribute to both the shear strength of a wall and the confinement of the concrete core.

(v) The vertical reinforcement ratio which determines the need for transverse ties should be computed from

$$\rho_\ell = \frac{\Sigma A_b}{b s_v} \qquad (19)$$

where the terms of the equation, together with the interpretation of the above requirements are shown in Fig. 26. The interpretation of Eq. (19) with reference to the wall return at

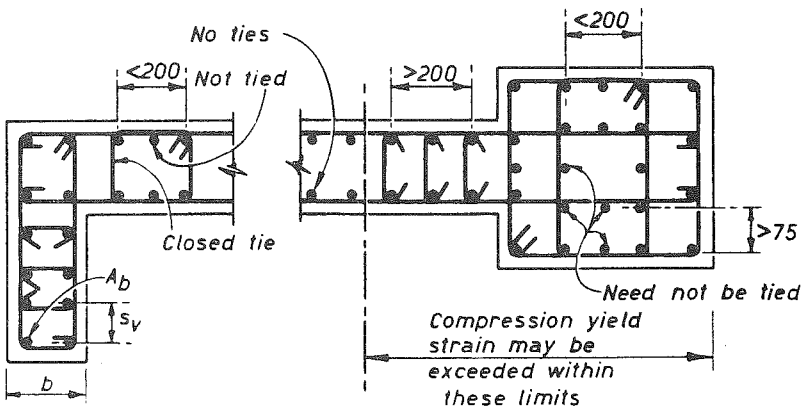

Figure 26 : Transverse Reinforcement in Potential Yield Zones of Wall Section

the left hand end of Fig. 26 is as follows: $\rho_\ell = 2A_b/bs_v$. When low local reinforcement content, typically $\rho_\ell \leq 0.005$, is used in a part of the wall, the contribution of the bars to compression strength of the area is negligible, and hence the loss of this contribution due to possible buckling of the bars is of no consequence in terms of overall strength.

4.2.6 Curtailment of flexural reinforcement

With the use of code specified lateral loads, bending moment diagrams of the types shown in Figs. 13, 14(a) and (b) are obtained. If the flexural reinforcement were to be curtailed exactly in accordance with the moment so indicated, instantaneous plastic hinges could form anywhere along the height of such walls during a strong earthquake. This would be undesirable from a design point of view because potential plastic hinges require special and necessarily more expensive detailing. Some of these special requirements were examined in the previous sections. Moreover, as in the case of beams [4], the shear strength of reinforced concrete walls will diminish in regions where yielding of the flexural reinforcement occurs. This would then necessitate additional horizontal shear reinforcement at all levels. It is preferable to ensure that plastic hinges can develop only in predetermined locations, logically at the base of walls, by providing flexural strength over the remainder of the wall which is in excess of the likely maximum demands.

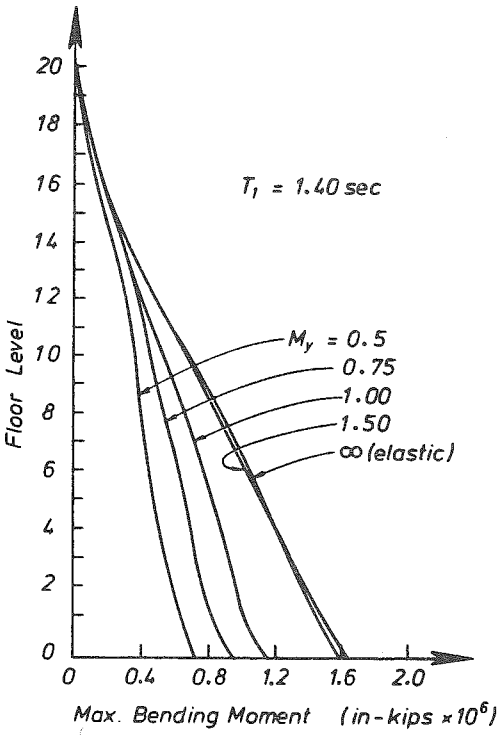

Figure 27 : Dynamic Moment Envelopes for a 20 Storey Cantilever Wall with Different Base Yield Moment Strengths

Bending moment envelopes, covering moment demands which arise during the dynamic response, are different from bending moment diagrams resulting from static loading. This may be readily shown with modal superposition techniques or from time history analyses of wall structures using a variety of earthquake records [27, 28,29]. Typical bending moment envelopes obtained analytically for 20 storey cantilever walls with different base yield moment strengths and subjected to particular ground excitations, are shown in Fig. 27 [28]. It is seen that there is an approximate linear variation of maximum moment demands during the inelastic as well as elastic dynamic response of the walls to ground shaking.

For the reasons enumerated above the flexural reinforcement in cantilever walls in New Zealand is required [8] to be curtailed so as to give a linear variation of moment of resistance with height, as shown in Fig. 13. Once the critical wall section at the base has been designed and the exact size and number as well as the positions of flexural bars have been established, the ideal flexural strengths of this section, to be developed in the presence of realistic axial loads on the

wall, can be evaluated. It is this ideal (nominal) flexural strength rather than the maximum moment derived from the specified lateral load, which is to be used at the bases when constructing the linear moment envelope.

4.3 The Control of Shear

4.3.1 Determination of shear load

To ensure that shear forces will not interfere with the ductile behaviour of wall systems and that shear effects will not significantly reduce energy dissipation during hysteretic response, they must not be allowed to control strength. Therefore an estimate must be made for the maximum shear intensity which may be encountered by a structural wall during a very large earthquake. Thereby, as in beams of ductile frames [4], energy dissipation will be largely confined to flexural yielding.

Clearly the design shear must not be less than that associated with the development of the flexural overstrength, M^o. For a wall which has been designed, this can be readily evaluated by means of the "overstrength factor" $\phi_{o,w}$, which is defined as

$$\phi_{o,w} = \frac{\text{Flexural overstrength}}{\text{Moment resulting from code loading}} = \frac{M^o}{M_{o,code}} \qquad (20)$$

where both moments refer to the base section of the wall. Thus the corresponding shear force would be $\phi_{o,w}\ V_{code}$.

Optimum values of $\phi_{o,w}$ are affected by the grade of steel used and the relevant strength reduction factor ϕ. The actual value of the overstrength factor encountered during the design will be modified by the excess or deficiency of strength provided by the designer and the changes in M_{code} resulting from moment redistribution which may have been carried out within a wall system.

Further increase of shear demand may result from dynamic effects. During a predominantly first mode response of the structure, the distribution of inertial storey forces will be as shown in Fig. 28(a). This force pattern is similar to that used in standard code specified static loadings. The centre of inertial forces is typically located at approximately 0.7 h_w above the base. When the response is strongly influenced by the 2nd and 3rd mode of vibration, the storey forces may be distributed as seen in Fig. 28(b) with the resultant force being located much lower than in the previous case. If a plastic hinge at overstrength M^o develops at the base in both of these cases, then the induced shear in the second case is obviously much larger. The contribution of the higher modes to shear will increase as the fundamental period of the structure increases. From a specific study of this problem [27] the following recommendation [8] has been deduced in New Zealand for the estimation of the total design shear.

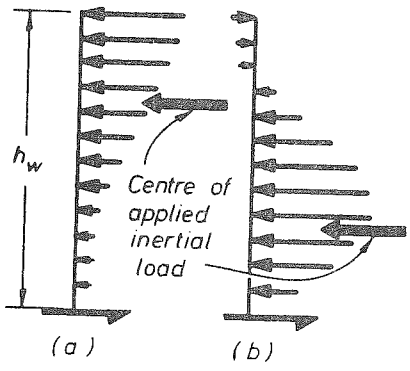

Figure 28 : Modal Storey Forces

$$V_{wall} = \omega_v \phi_{o,w} V_{code} \tag{21}$$

where V_{code} is the horizontal shear demand derived from code specified lateral static loads, $\phi_{o,w}$ is as defined by Eq. (20) and ω_v is the dynamic shear magnification factor, to be taken as

$$\omega_v = 0.9 + n/10 \tag{22a}$$

for buildings up to six storeys, and

$$\omega_v = 1.3 + n/30 \tag{22b}$$

for buildings over six storeys, where n is the number of storeys, which in Eq. (22b) need not be taken larger than 15.

An application of this approach will show that the design shear force at the base of a structural wall can become a critical quantity. When the potential flexural strength of the wall at its base is very large and much in excess of that required, the value of $\phi_{o,w}$, and hence V_{wall}, may also become excessively large. Obviously a wall need not be designed for shear forces larger than those corresponding with the elastic response of the building. As the shear given by Eq. (22) is considered to be an upper bound estimate, the strength reduction factor associated with this capacity design procedure is $\phi = 1.0$ [8], rather than 0.85 [5].

4.3.2 The control of shear failure mechanisms

(a) Inelastic regions - The approach to the design for shear resistance may be based on established practice [5], whereby it is assumed that some of the shear in a wall is resisted by only concrete mechanisms and the remainder is assigned to shear reinforcement. In recognition of the inevitable deterioration of the concrete in the potential plastic hinge regions, the contribution of the concrete may be conservatively estimated [8] with

$$v_c = 0.6 \sqrt{P_e/A_g} \quad \text{(MPa)} \tag{23}$$

where P_e is the design axial compression force on the wall derived from appropriately factored loads or capacity design considerations, and A_g is the gross concrete sectional wall area, including flanges or boundary elements.

To simplify computations, the total shear stress, serving as an index, is estimated [5,8] with

$$v_i = \frac{V_{wall}}{0.8\, b_w \ell_w} \quad \text{(MPa)} \tag{24}$$

The web reinforcement, consisting of reasonably closely spaced and adequately anchored horizontal bars, is then readily determined from

$$A_v = \frac{(v_i - v_c)\, b_w s}{f_y} \qquad (25)$$

and thereby diagonal tension failure can be precluded. It should be recognized, however, that after reversed cycles of large displacements, wide flexural cracks interconnect with shear cracks. These in turn may develop at angles larger than 45° to the axis of a member. Thus eventually some yielding of the web reinforcement will also occur.

To prevent the web from prematurely crushing because of large diagonal compression forces, it is recommended [8] that in the plastic hinge regions the total shear stress be limited to

$$v_{i,max} \leq 0.9 \sqrt{f'_c} \quad \text{(MPa)} \qquad (26)$$

Tests have shown, however, that when imposed displacement ductilities are in excess of approximately 4, such high shear stresses may lead to web crushing [19,22,30]. When boundary elements with a well confined group of vertical bars were provided, significant shear could be carried after the failure of the web panel, because the boundary elements acted as short columns [22,30]. It is considered, however, that it is more efficient to rely on the shear strength of the web, by preventing diagonal compression failure, rather than on the second line of defence offered by the boundary elements. To ensure this, either the ductility demand on a wall with large shear stresses must be reduced, or if this is not done, the shear stress, used as a measure of diagonal compression, should be limited [8] to*

$$v_{i,max} \leq (0.37\phi_{o,w}K + 0.16) \sqrt{f'_c} < 0.9 \sqrt{f'_c} \quad \text{(MPa)} \qquad (27a)$$

or

$$v_{i,max} \leq (1.65\phi_{o,w}/R + 0.16) \sqrt{f'_c} \quad \text{(MPa)} \qquad (27b)$$

These equations recognise that the use of larger K or smaller R factors and excess flexural strength provided in the wall as built (when $\phi_{o,w} > 1.4$) will reduce ductility demands and hence allow larger maximum shear stresses to be used in the design. Equation (27) often controls the wall thickness at the base.

(b) Elastic regions - The strategy adopted in section 4.2.6, whereby flexural yielding outside the potential plastic hinge region is inhibited (Fig. 13), will enable the design for shear in these regions to be based on the same principles which are routinely used for gravity loaded structures [5]. As a consequence wall thicknesses and shear reinforcement contents can be significantly reduced in upper storeys of ductile walls.

(c) Sliding shear - Excessive sliding displacements along construction joints [1] or near horizontal flexural cracks, which, after inelastic load reversals, may form a plane of potential weakness in the plastic region, may diminish energy dissipation in structural walls. In walls with aspect ratio h_w/ℓ_w larger than 3, sliding displacements can be readily controlled by adequate quantity, A_{vf}, of distributed vertical

---

*Using S defined by NZS 4203:1984

$$v_{i,max} = (0.3\phi_{o,w} S + 0.16) \sqrt{f'_c} \quad \text{(MPa)}$$

reinforcement. This provides the necessary clamping force for the shear friction mechanism. This is

$$A_{vf} = \frac{V_{wall} - \mu P_e}{\mu f_y} \qquad (28)$$

where V_{wall} = the maximum shear force given by Eq. (21) (N), μ = coefficient of friction, the value of which may be between 1.0 and 1.4, depending on the surface roughness which is provided [8], P_e = maximum axial compression which can be relied on during an earthquake (N) and f_y = yield strength of the steel (MPa). Commonly the designer simply checks that the total vertical reinforcement provided in the shear area (web) satisfies Eq. (28).

Sliding shear is more critical in squat walls, which are not examined here. Depending on the shear stress intensity and the likely demand for ductility, expressed by the K or R factors, it may be necessary to provide diagonal reinforcement to resist a significant fraction of the shear force across a potential sliding plane [31].

5. CAPACITY DESIGN PRINCIPLES AS APPLIED TO COUPLED WALLS

Having examined several features of the behaviour, analysis and detailing of structural walls for seismic regions, in the following sections the main conclusions are summarized. For this purpose the specific example of a coupled wall structure, such as shown in Fig. 7(a)(b) and (d), is used. The highlights of modelling and response to lateral static load, both in the elastic and inelastic domain, were reviewed in sections 2.3.2, 3.1.1 and 3.3.2. Because of their large stiffness, coupled structural walls provide protection against all forms of damage in moderate earthquakes, while, when carefully detailed, they also possess excellent energy dissipating properties, to be utilized in large earthquakes [1].

5.1 Preliminary Studies

Before any analysis is undertaken, the geometry of the structure must be reviewed to ensure that in critical regions compact cross sections (4), suitable for energy dissipation, will be used (section 4.2.3). From the relative stiffness of coupling beams, their contribution of overturning moments (Eq. (4)) must be established to determine the appropriate value of as structural response factor, such as K or R, (Eqs. (5) and (6)). Having established the value of the overturning moment, M_o, at the base of the coupled wall (Eq. (3)), the foundation structure must be examined to ensure that it will be capable of absorbing moments developed with the overstrength of the superstructure, $M^o = \phi_{o,w} M_o$. Otherwise the intended energy dissipation in the ductile superstructure may not be mobilized.

5.2 The Design of Components

5.2.1 Coupling beams

Allowing for some moment redistribution between coupling beams, as shown in section 3.3.2 and Fig. 14(c), design shear forces for groups of beams are established. When coupling beams* are short and relatively deep,

* These are also referred to as wall segments [5].

conventional design procedures and detailing [5] will almost certainly lead to a diagonal tension failure, shown in Fig. 29(a). Such a beam is seen in Fig. 30. When excess stirrup reinforcement is provided, so that diagonal tension failure cannot occur, sliding shear, shown in Fig. 29(b), will inhibit the development of satisfactory hysteretic response [1]. Therefore, whenever the ideal (nominal) shear stress exceeds

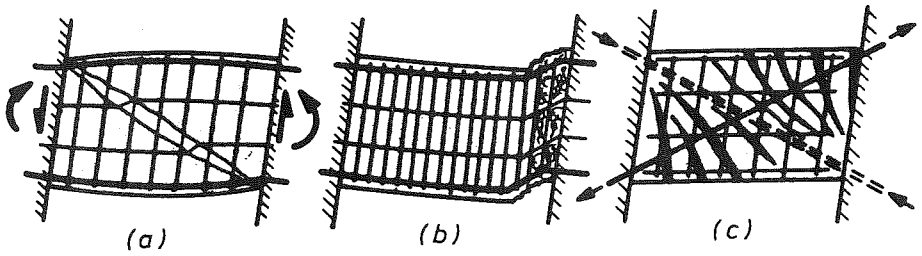

Figure 29 : The Mechanisms of Shear Resistance in Coupling Beams

$$v_i = 0.1(\ell_n/h)\sqrt{f'_c} \quad \text{(MPa)} \qquad (29)$$

diagonal reinforcement, to resist both shear and moments, as shown in Figs. 29(c), and 31 should be used [8]. In Eq. (29) ℓ_n and h are the clear span and overall depth of the beam respectively. In determining the diagonal forces T_b and C_B in Fig. 31, only first principles are used [1].

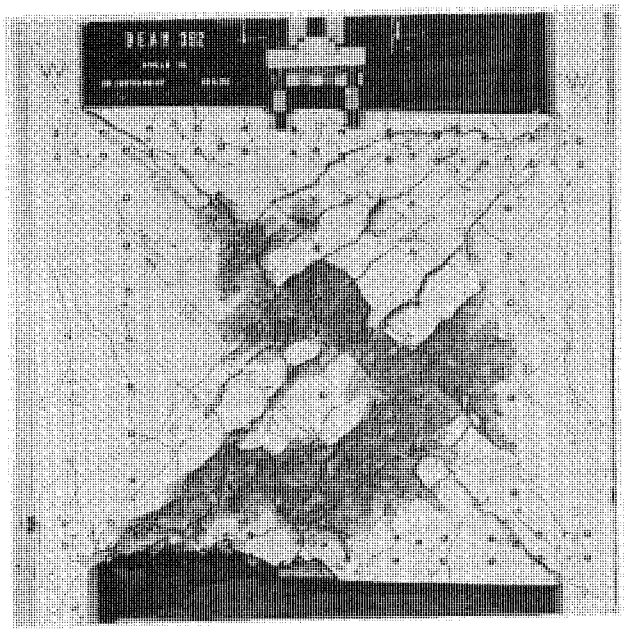

Figure 30 : A Conventional Reinforced Deep Coupling Beam which has been Subjected to Seismic Type of Loading [1]

Specific requirements [8] for the detailing of the reinforcement for coupling beams, such as shown in Fig. 31, include provisions of:

(i) transverse ties, around the cage of diagonal bars, in accordance with Eq. (18), spaced no further than 100 mm,

(ii) increase of development length specified for individual bars, by 50%, extending into the adjacent walls,

(iii) "basketing" nominal mesh reinforcement in the remainder of the beam.

5.2.2 Coupled wall

As the moments at the base have been established from the code specified factored lateral loading, they may now be considered, together with the appropriate combination of axial load due to factored gravity and lateral loads. It will often be found that considerably more flexural reinforcement is required in the tension than in the compression wall. For this or other reasons, moment redistribution from the tension to the compression wall, as

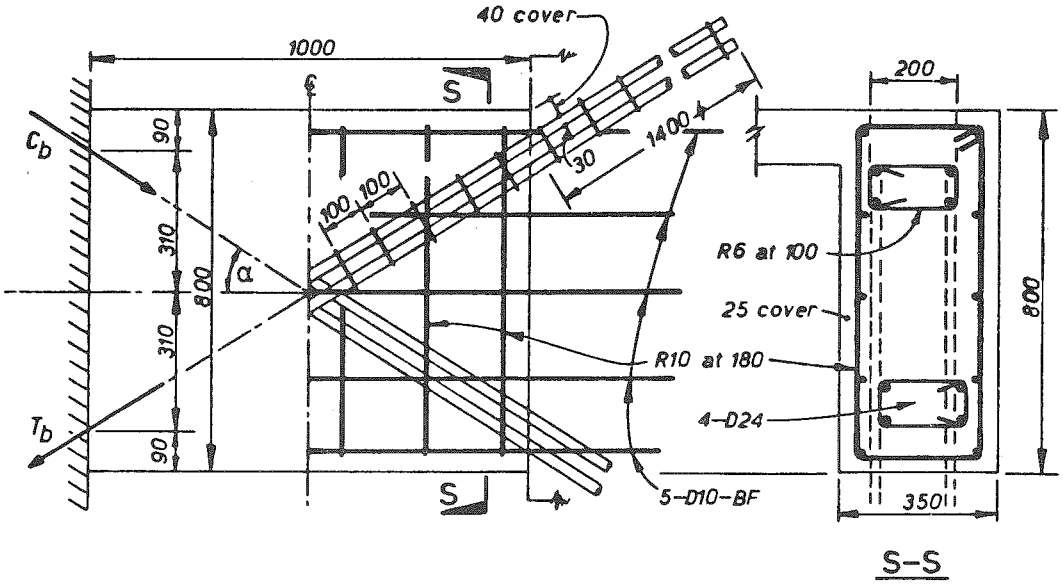

Figure 31 : Details of a Typical Ductile Coupling Beam

outlined in section 3.3.2, should be undertaken. In determining the amount of flexural reinforcement for both directions of lateral loading, a strength reduction factor [8] $\phi = 0.9$ may be used. The recommendations for minima and maxima for reinforcement contents should also be considered.

5.2.3 Considerations for shear design

In accordance with the principles of capacity design, the design shear forces across the walls should be those developed with the flexural overstrength of the coupled wall structure rather than those derived from the specified and factored lateral loading. Therefore the following sources to flexural overstrength need be studied.

(a) Overstrength of coupling beams - As the design of the beams has been finalized, their overstrength in terms of shear force Q_i^o, based on λf_y, can be readily evaluated. Typically the value of λ is 1.25 and 1.4 when the specified yield strength of the steel is f_y = 275 and 380 MPa respectively [8]. The value of λ should be evaluated for the type of steel used in the structure.

(b) Earthquake induced axial force - The maximum feasible axial load on a wall would occur when all coupling beams above the level considered would develop their overstrength, Q_i^o. For multistorey coupled walls it is recommended that the earthquake induced axial force at overstrength be estimated as

$$P^o_{eq,i} = (1 - \frac{n}{80}) \sum_i^n Q^o_i \qquad (30)$$

where n = number of floors above level i, the value of which should not be taken larger than 20.

(c) The flexural overstrength of the walls - As every detail of the wall base sections is known at this stage of the design, the flexural overstrengths, based on λf_y, may be readily estimated. For this purpose a rational estimate for the concurrent axial load on each wall need also be made. For this extreme event, effects of live load may be neglected, so that the axial load becomes for the

(i) tension wall $P_1^o = P_{eq}^o - P_D$

(ii) compression wall $P_2^o = P_{eq}^o + P_D$

With these axial forces the flexural overstrength for the two walls become M_1^o and M_2^o respectively, from which the overstrength factor for the system is simply

$$\phi_{o,w} = \frac{M_1^o + M_2^o + P_{eq}^o \, \ell}{M_{o,code}} \qquad (31)$$

where $M_{o,code}$ is the total overturning moment at the base due to code specified lateral load as given by Eq. (3).

To sustain the energy dissipating mechanisms of coupled wall structures, the foundation system must be capable of absorbing an overturning moment $\phi_{o,w} \, M_{o,code}$.

(d) Estimation of wall shear forces - Using the concepts of load redistribution among interacting inelastic walls, outlined in section 3.3.2, the maximum shear force for each wall can be estimated, as for cantilever walls (section 4.3.1 and Eq. (21)), from

$$V_{i,wall} = \omega_v \phi_{o,w} \left(\frac{M_i^o}{M_1^o + M_2^o}\right) V_{code} \; ; \; i = 1,2 \qquad (32)$$

where ω_v = dynamic shear magnification factor given by Eq. (22).

5.3 Detailing of Coupled Walls

As outlined for cantilever walls in section 4, the requirements for detailing are significantly different in the elastic and potential plastic regions of the walls. These were defined with the use of linear moment envelopes shown in Fig. 13. In every respect the detailing of one of the coupled walls rests on the principles applicable to cantilever walls (section 4).

6. CONCLUSIONS

Design procedures were outlined for reinforced concrete buildings in which earthquake resistance is provided entirely by ductile structural walls. Emphasis was placed on those design features which were developed in New Zealand [8] and in parts adopted elsewhere (32,33). The design strategy described evolved from the following precepts:

(i) Current predictions of the characteristics of large earthquakes are crude. Therefore an aim to achieve a high degree of precision in analytical techniques, to predict both earthquake induced actions and deformations within the structure, is not justified.

(ii) Provided that a reasonable level of resistance to lateral forces, such as prescribed for seismic zones by relevant national building codes, is chosen, than errors arising from inability to provide good predictions for the effects of future earthquakes, will manifest themselves only in erronous predictions of structural displacements, i.e. ductility demands.

(iii) Types and localities of energy dissipating mechanisms, chosen as part of the "capacity design procedure", in which a unique hierarchy of strengths has been established, are not affected by erronous structural displacements. Ductility demands during an earthquake may, however, differ significantly from values anticipated by building codes.

(iv) With few exceptions, rationally detailed inelastic regions of structural walls can be made very ductile with relative ease and at little additional cost. Hence walls, designed in accordance with described deterministic principles, are made very tolerant to earthquakes in terms of inelastic displacements. This tolerance compensates for an ability to estimate the desired level of earthquake resistance only crudely.

Various steps in the description of the design procedure were intended to emphasize the designer's determination to "tell the structure what to do". This simple approach should ensure excellent inelastic response provided that, as a complementary task, all critical regions are judiciously detailed. The numerous detailed recommendations presented [8], manifest attempts in New Zealand to quantify unambiguously the goodness of detailing. Thereby walls are enabled to perform "as they were told to do".

ACKNOWLEDGEMENTS

The author acknowledges the stimulus gained from many informative discussions with professional engineers and particularly with his university colleagues Professor R. Park and Dr. M.J.N. Priestley, and also the steady support of the New Zealand National Society for Earthquake Engineering.

REFERENCES

1. Park, R. and Paulay, T., "Reinforced Concrete Structures", John Wiley and Sons, New York, 1975, p.769.

2. Paulay, T. and Williams, R.L., "The Analysis and Design of and the Evaluation of Design Actions for Reinforced Concrete Ductile Shear Walls", Bulletin of the New Zealand National Society for Earthquake Engineering, Vol. 13, No. 2, June 1980, pp.108-143.

3. Paulay, T., "Earthquake Resisting Shear Walls - New Zealand Design Trends", Proceedings, Journal of the American Concrete Institute, Vol. 77, No. 3, May-June 1980, pp.144-152.

4. Park. R., "Ductile Design Approach for Reinforced Concrete Frames", Earthquake Spectra, Earthquake Engineering Research Institute, Vol. 2, No. 2, May 1980, pp.

5. "Building Code Requirements for Reinforced Concrete", (ACI 318-83), American Concrete Institute, Detroit, 1983, p.111.

6. Oesterle, R.G., Fiorato, A.E., Aristazabal-Ochoa, J.D. and Corley, W.G., "Hysteretic Response of Reinforced Concrete Structural Walls", Publication SP-63, Reinforced Concrete Structures Subjected to Wind and Earthquake Forces, American Concrete Institute, 1980, pp.243-273.

7. Paulay, T., Priestley, M.J.N. and Synge, A.J., "Ductility in Earthquake Resisting Squat Shearwalls", ACI Journal, Proceedings, V. 79, No. 4, July-August 1982, pp.257-269.

8. "New Zealand Standard Code of Practice for the Design of Concrete Structures", NZS 3101:Part 1, p.127, Commentary NZS 3101:Part 2, p.156, Standard Association of New Zealand, Wellington, New Zealand, 1982.

9. "New Zealand Standard Code of Practice for General Structural Design and Design Loadings for Buildings", NZS 4203:1984, Standards Association of New Zealand, Wellington, New Zealand, 1984.

10. Freeman, S.A., Czarwecki, R.M. and Honda, K.K., "Significance of Stiffness Assumptions on Lateral Force Criteria", Publication SP-63, Reinforced Concrete Structures Subjected to Wind and Earthquake Forces, American Concrete Institute, 1980, pp.437-457.

11. Gates, W.E., "The Art of Modeling Buildings for Dynamic Seismic Analysis", Earthquake-Resistant Reinforced Concrete Building Construction. Proceedings of a Workshop Held at the University of California, Berkeley, Vol. II, 1977, pp.857-886.

12. Poland, C.D., "Practical Application of Computer Analysis to the Design of Reinforced concrete Structures for Earthquake Forces", Publication SP-63, Reinforced Concrete Structures Subjected to Wind and Earthquake Forces, American Concrete Institute, 1980, pp.409-436.

13. Paulay, T. and Binney, J.R., "Diagonally Reinforced Coupling Beams of Shear Walls", Shear in Reinforced Concrete, ACI Special Publication SP42, Detroit, 1974, Vol. I, pp.579-598.

14. Paulay, T., "Seismic Seismic Loading of Spandrel Beams", Journal of the Structural Division, American Society of Civil Engineers, Vol. 97, No. ST9, Sept. 1971, pp.2407-2419.

15. Beck, H., "Contribution to the Analysis of Coupled Shear Walls", Proceedings of the Journal of the American Concrete Institute, Vol. 59, Aug. 1962, pp.1055-1070.

16. Rosman, R., "Approximate Analysis of Shear Walls Subjected to Lateral Loads", Proceedings, Journal of the American Concrete Institute, Vol. 61, June 1964, pp.717-733.

17. Coull, A. and Choudhury, J.R., "Analysis of Coupled Shear Walls", Proceedings, Journal of the American Concrete Institute, Vol. 64, Sept. 1976, pp.587-593.

18. Paulay, T. and Santhakumar, A.R., "Ductile Behaviour of Coupled Shear Walls", Journal of the Structural Division, American Society of Civil Engineers, Vol. 102, No. ST1, Jan. 1976, pp.93-108.

19. Oesterle, R.G., Fiorato, A.E. and Corley, W.G., "Reinforcement Details for Earthquake-Resistant Structural Walls', Concrete International Design and Construction, Vol. 2, No. 12, 1980, pp.55-66.

20. Goodsir, W.J., "The Design of Coupled Frame-Wall Structures for Seismic Actions", Research Report No. 85-8, Department of Civil Engineering, University of Canterbury, Christchurch, New Zealand, 1985, p.383.

21. Paulay, T. and Uzumeri. S.M., "A Critical Review of the Seismic Design Provisions for Ductile Shear Walls of the Canadian Code and Commentary", Canadian Journal of Civil Engineering, Vol. 2, No. 4, 1975, pp.592-601.

22. Vallenas, J.M., Bertero, V.V. and Popov, E.P., "Hysteretic Behaviour of Reinforced Concrete Structural Walls", Earthquake Engineering Research Center, College of Engineering, University of California, Berkeley, Report No. UCB/EERC-79/20, Aug. 1979, p.234.

23. Bertero, V.V., "Seismic Behaviour of Reinforced Concrete Wall Structural Systems", Proceedings of 7WCEE, Vol. 6, Istanbul, Turkey 1980, pp.323-330.

24. "Uniform Building Code", (Chapter 23, Section 2312:Earthquake Regulations), International Conference of Building Officials, U.S.A., 1982.

25. Applied Technical Council, "Tentative Provisions for the Development of Seismic Regulations for Buildings", Publication ACT 3-06, June 1978, p.505.

26. Park, R., "Columns Subjected to Flexure and Axial Load", Bulletin of the New Zealand National Society for Earthquake Engineering, Vol. 10, No. 2, June 1977, pp.95-105.

27. Blakeley, R.W.G., Cooney, R.C. and Megget, L.M., Seismic Shear Loading at Flexural Capacity in Cantilever Wall Structures", Bulletin of the New Zealand National Society for Earthquake Engineering, Vol. 8, No. 4, Dec. 1975, pp.278-290.

28. Fintel, M., Derecho. A.T., Freskasis, G.N., Fugelso, L.E. and Gosh, S.K., "Structural Walls in Earthquake Resistant Structures", Progress Report to the National Science Foundation, (RANN) Portland Cement Association, Skokie, Aug. 1975, p.261.

29. Iqbal, M. and Derecho, A.T., "Inertial Forces over Height of Reinforced Concrete Structural Walls During Earthquakes", Publication SP-63, Reinforced Concrete Structures Subjected to Wind and Earthquake Forces, American Concrete Institute, 1980, pp.173-196.

30. Bertero, V.V., Popov, E.P., Wang, T.Y. and Vallenas, J., "Seismic Design Implications of Hysteretic Behaviour of Reinforced Concrete Structural Walls", 6th World Conference on Earthquake Engineering, New Delhi, Vol. 5, 1977, pp.159-165.

31. Paulay, T., Priestley, M.J.N. and Synge, A.J., "Ductility in Earthquake Resisting Squat Shearwalls", Proceedings, Journal of the American Concrete Institute, Vol. 79, No. 4, July-Aug. 1982, pp.257-269.

32. Comite Euro-International du Beton, "Model Code for Seismic Design of Concrete Structures", Bulletin D'Information No. 160, (1-Final Draft Oct. 1983)), p.117.

33. "Design of Concrete Structures for Buildings", A National Standard of Canada, CAN-A23.3-M84, Canadian Standards Association, 1984, p.281.

NOTATION

A = a factor defined by Eq. (4)

A_b = area of individual bar, mm^2

A_c^* = area of concrete core within area A_g^*, measured to outside of peripheral hoop legs, mm^2

A_e = effective area of section, mm^2

A_g = gross area of a section, mm^2

A_g^* = gross area of the wall section which is to be confined in accordance with Eq. (16), mm^2

A_{sh} = total effective area of hoops and supplementary cross ties in direction under consideration within spacing s_h, mm^2

A_{te} = area of one leg of a stirrup-tie or hoop, mm^2

A_v = area of shear reinforcement within distance s, mm^2

A_{vf} = area of shear friction reinforcement, mm^2

b = width of compression face of member or width of a flange, or thickness of wall element, mm

b_{eff} = effective width of a flange, mm

b_w = width of web or wall thickness, mm

c, c_1, c_2 = neutral axis depth measured from extreme compression fibre of section

c_{av} = average neutral axis depth

c_c = critical neutral axis depth

f'_c = specified compressive strength of concrete, MPa

f_y = specified yield strength of steel, MPa

f_{yh} = specified yield strength of hoop or supplementary cross tie reinforcement, MPa

F = a factor defined by Eq. (12b)

h = overall thickness (depth) of member

h'' = dimension of concrete core of section measured perpendicular to the direction of hoop bars, mm

h_w = total height of wall from base to top

I_e = equivalent second moment of area of section

I_g = second moment of area of the gross concrete section

I_w = equivalent second moment of wall area allowing for shear deformations

K = horizontal force factor [24]

ℓ = span of beam measured between centre lines of supporting columns or walls

ℓ_n = clear length of member measured from face of supports

ℓ_p = plastic hinge length

ℓ_w = horizontal length of wall

M = bending moment

M_1, M_2 = design moment assigned to Wall 1 and 2

M'_1, M'_2 = design moments assigned to Wall 1 and 2 after load redistribution

M^o = flexural overstrength of wall section as built taking into account strain hardening of steel

M^o_1, M^o_2 = flexural overstrength of the base section of Wall 1 and 2 respectively

M_{code} = bending moment derived from code specified lateral loading

M_o = total overturning moment at the base of a cantilever wall or coupled walls

$M_{o,code}$ = total overturning moment at the base of the structure derived from code specified lateral loading

n = number of storeys

P_D = axial load due to dead load

P_e = design axial load with given eccentricity due to factored gravity loading acting on a member during an earthquake, N

P_{eq} = axial load induced by lateral earthquake load only

P^o_{eq} = axial load induced by earthquake at the development of the over-strength of the structure

P^o_1, P^o_2 = total axial load on Wall 1 and 2 respectively at the development of the overstrength of the structure

R = response modification coefficient [25]

R_v = lateral load reduction factor applicable to coupled walls

q, q_a, q_b = theoretical shear forces in coupling beams

Q^o_i = shear force developed in a coupling beam at overstrength

s = spacing of sets of stirrups for shear resistance, mm

s_h = vertical centre to centre spacing of horizontal hoop sets, mm

s_v = horizontal centre to centre spacing of vertical bars, mm

T = tension force, or axial force induced in coupled walls by lateral load

v_c = ideal shear stress provided by concrete, MPa

v_i = total shear stress, MPa

$v_{i,max}$ = maximum total shear stress, MPa

V_{code} = shear force derived from code specified lateral loading

z = factor allowing for squatness of walls

α = factor relevant to neutral axis depth c

Δ = displacement

Δ_u = maximum displacement

Δ_y = displacement at first yield

ε_c = concrete compression strain in the extreme fibre

ε_u = concrete compression strain at the ultimate state

ε_y = yield strain of steel

λ = strength enhancement factor for steel

μ = coefficient of friction

μ_Δ = displacement ductility ratio

μ_ϕ = curvature ductility ratio

ρ_ℓ = the ratio of vertical wall reinforcement area to unit area of horizontal gross concrete section, Eq. (19)

ϕ = strength reduction factor

ϕ_o = flexural overstrength factor

$\phi_{o,w}$ = overstrength factor for a wall

ϕ_u = maximum curvature

ϕ_y = yield curvature

ω_v = dynamic shear magnification factor

THE CAPACITY DESIGN OF REINFORCED CONCRETE HYBRID STRUCTURES FOR MULTISTOREY BUILDINGS

T. Paulay and W.J. Goodsir

THE CAPACITY DESIGN OF REINFORCED CONCRETE HYBRID STRUCTURES FOR MULTISTOREY BUILDINGS

T. Paulay[1] and W. J. Goodsir[2]

SYNOPSIS

To complement existing capacity design procedures used in New Zealand for reinforced concrete buildings in which earthquake resistance is provided by ductile frames or ductile structural walls, an analogous methodology is presented for the design of ductile hybrid structures. Modelling and types of structures in which the mode of wall contribution is different are briefly described. A step by step description of a capacity design procedure for a structural system in which fixed base ductile frames and walls, both of identical height, interact, is presented. The rationale for each step is outlined and, where necessary, evidence is offered for the selection of particular design parameters and their magnitudes. A number of issues which require further study are briefly outlined. These relate to irregularity in layout, torsional effects, diaphragm flexibility, shortcomings in the predictions for dynamic shear demands in walls, and to limitations of the proposed design procedure. It is believed that the methodology is logical, relatively simple and that it should ensure, when combined with appropriate detailing, excellent seismic structural response.

INTRODUCTION

When lateral load resistance is provided by the combined contributions of ductile multi-storey frames and structural walls, the system is often referred to as a "hybrid structure". In North America, the term "dual system" is used. These structures combine the advantages of their constituent components. Because of the large stiffness of walls which are provided with adequate restraints at the foundations, excellent storey drift control may be obtained. Moreover, suitably designed walls can ensure that storey mechanisms (soft storeys) will not develop in any event. Interacting ductile frames on the other hand, while carrying the major part of the gravity load, can provide, when required, significant energy dissipation, particularly in the upper storeys.

Despite the attractiveness and indeed existence of many such structures in New Zealand, comparatively little research effort has been directed to them. The New Zealand Code of Practice for Design of Concrete Structures[1] draws designers' attention to the need for "special studies" when designing "ductile hybrid structures". No specific guidance is, however, provided. Known studies refer primarily to elastic response, despite the obvious importance of the features of inelastic behaviour.

A study was initiated with the aim of ultimately formulating a design procedure for hybrid structures which would be analogous to those developed in New Zealand for ductile frames and ductile structural walls[1]. It was hoped that a scheme could be formulated which would provide a smooth transition between design approaches for space frames*[1] and those for buildings in which seismic resistance is provided by structural walls only*[1,2]. To this end numerous analytical studies of prototype building structures were conducted[3,4] to provide appropriate calibration of the principal design parameters. This paper reports on the findings and conclusions as they relate to design procedures rather than on details of features of structural behaviour.

The traditional procedure of designing for earthquake resistance, utilizing elastic analysis techniques and equivalent lateral static loads, is well established. The resulting distribution of lateral load resistance over the height of buildings with ductile frames, or structural walls, is generally accepted as meeting satisfactorily actual earthquake load demands. There was little evidence to indicate that this would be the case also with hybrid structures. One source of concern for possibly drastic differences between "elastic static" and "elasto-plastic dynamic" responses of hybrid structures stems from the recognition of fundamental differences in the behaviour of

* Details of the "capacity design" of reinforced concrete structures are given in NZS 3101:1982 and the background to this design philosophy is outlined in some detail in the commentary of the code of practice.

1 Professor of Civil Engineering, University of Canterbury, New Zealand.
2 Engineer, Ove Arup Partnership, London, England.

beam-column frames and structural walls. These differences stem from dissimilar deformation patterns when subjected to the same lateral load, as shown in Fig. 1. Frames and walls, while sharing in the resistance of shear forces in the lower storeys, oppose each other in the storeys near the top of the building. It was of major interest to examine the load sharing between these two types of interacting elements during inelastic dynamic response to a major seismic event.

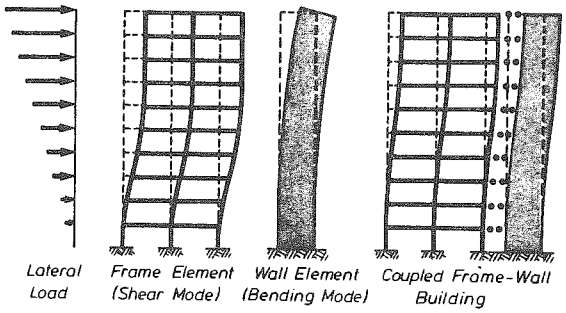

Fig. 1 Deformation Patterns of Laterally Loaded Frame, Walls and Coupled Wall-Frame Elements.

A step by step design methodology is proposed to meet the intent of the "capacity design" philosophy. The presentation concentrates solely on issues relevant to the largest expected seismic event envisaged by the code[5]. The emphasis is therefore on issues of ductility and the prevention of collapse. Existing procedures, to satisfy design criteria for stiffness and minimum strength, both relevant primarily to damage control, and considered to be equally applicable to hybrid structures, are not referred to in this paper.

The dominant feature of the capacity design strategy is the a priori establishment of a rational hierarchy in strength between the components of the entire structural system. Accordingly, the approach to the design of each primary lateral load resisting component which is to be protected against yielding or brittle failure, such as due to shear, can be described by the simple general expression for the ideal strength S_i, thus

$$S_i \geq \omega \phi_o S_{code} \qquad (1)$$

where S_{code} is the required dependable strength of the member selected for energy dissipation, as determined by elastic analysis techniques for a code[5] specified lateral static load on the structure; ϕ_o is the ratio of the maximum strength, S_o, which can be developed in the selected inelastic component (as built) by large displacements during a severe seismic event, to the strength required, S_{code}, for the same member by the code specified lateral loading; and ω is a dynamic magnification factor which quantifies deviations in strength demands on the member to be protected, from demands indicated by elastic analysis. Extreme demands are expected to occur during the inelastic dynamic response of the structure.

For the sake of completeness, certain aspects of the "capacity design" of ductile frames are restated.

2. TYPES OF HYBRID STRUCTURES AND THEIR MODELLING

In the following, some distinct and common types of hybrid structures, in which walls and frames interact in a particular manner, are described. No attempt is made, however, to categorize all possible combinations in which these two systems may be utilized. Conventional modelling techniques, to be used for the purposes of analysis, are briefly reviewed and suggestions made for choices of suitable energy dissipating systems in hybrid structures.

2.1 Interacting Ductile Frames and Ductile Cantilever Walls

In the majority of reinforced concrete multistorey buildings, lateral load resistance is assigned to both ductile space frames and cantilever structural walls. Figure 2(a) shows in plan the somewhat idealized symmetrical disposition of frames and walls in a 12 storey example building. The properties of these two distinct structural elements may be conveniently lumped into a single frame and a single cantilever wall, as shown in Fig. 2(b). Instead of individual walls, shown in Fig. 2(a), tubular cores, or coupled structural walls, are also used frequently.

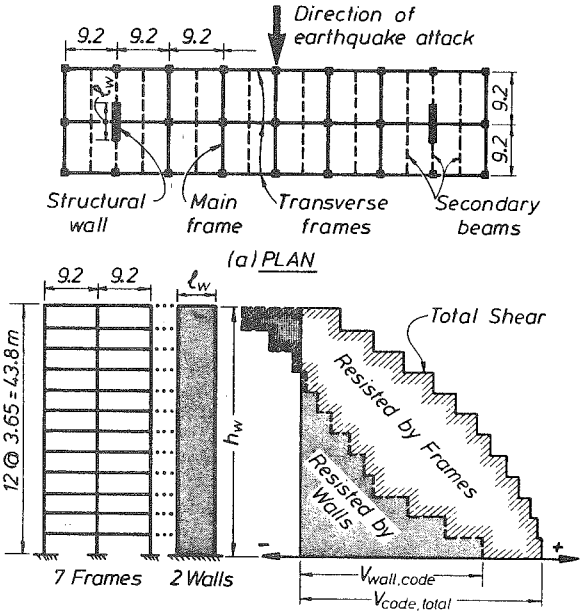

Fig. 2 Modelling of and Lateral Load Sharing in a Typical Wall-Frame System.

It is customary to assume that floor slabs at all levels have infinite inplane rigidity. Such diaphragms will then ensure that storey displacements for frames and walls are the same or that in the case of storey torsion, a simple linear relationship exists between the storey displacements of vertical elements. When diaphragms are relatively slender and when large concentrated lateral storey forces need to be introduced to

relatively stiff walls, particularly when these are spaced far apart, the flexibility of floor diaphragms may need to be taken into account. This issue is briefly reviewed in Section 4.3.

The extensionally infinitely rigid horizontal connection between lumped frames and walls at each floor, shown in Fig. 2(b), enables the analysis of such laterally loaded elastic structures to be carried out speedily. Typical results are shown in Fig. 2(c). Here the sharing between walls and frames of the total storey shear forces is illustrated. The relative participations which reflect the behaviour of the two different systems, as shown in Fig. 1, indicate a rapid decline with height of the contribution of the walls to shear resistance. Figure 2(c) also shows how the two systems oppose each other in the top storeys. The distribution of magnitudes of shear forces with height for each system will depend primarily on the relative stiffnesses of the walls and frames. This example structure, shown in Fig. 2, will be subsequently used to illustrate typical distributions of forces and moments for both walls and frames, as a consequence of inelastic dynamic response to seismic excitations.

As the flexural response of walls is intended to control deflections in hybrid structures, the danger of developing "soft storeys" should not arise. The designer may therefore freely choose those members or localities in frames where energy dissipation should take place when required. A preferable and practical mechanism for the frame of Fig. 2 is shown in Fig. 4(a). In this frame, plastic hinges, when required during a large expected seismic event, are made to develop in all the beams and at the base of all vertical elements. At roof level, plastic hinges may form in either the beams or the columns. The main advantage of this system is in the detailing of the potential plastic hinges. Generally it is easier to detail beam rather than column ends for plastic rotation. Moreover, the avoidance of plastic hinges in columns allows lapped splices to be constructed at the bottom end rather than at midheight of columns in each upper storey.

The design procedure described in considerable detail in Section 3, is relevant to this type of structural system and its preferred energy dissipating mechanisms.

When long span beams are used, and in particular when gravity rather than earthquake loading governs the strength of beams, it may be preferable to admit the development of plastic hinges at both ends of all columns over the full height of the structure, as shown in Fig. 4(c).

2.2 Ductile Frames and Walls Coupled by Beams.

Structural walls, instead of being isolated as free standing cantilevers, may be connected by continuous beams in their plane to adjacent frames. The model of such a system is shown in Fig. 3(a). Beams with span lengths ℓ_1 and ℓ_2 are rigidly connected to the walls. A possible mechanism that can be utilized in this type of system is shown in Fig. 4(b). Beam hinges at or close to the wall edges must develop. However, at columns, the designer may decide to allow plastic hinges to form in either the beams or the columns, above and below each floor, as shown in Fig. 4(c)

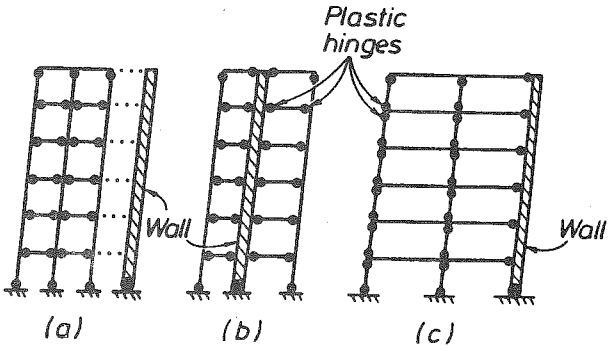

Fig. 4 Complete Energy Dissipating Mechanisms Associated with Different Hybrid Structural Systems.

This type of system could be utilized also in the building of Fig. 2(a) if the walls were to be connected to the adjacent columns by primary lateral load resisting beams. In that case the entire structural system would consist of 7 ductile frames, shown in Fig. 2(b) and two coupled frame-walls of the type given in Fig. 4(b).

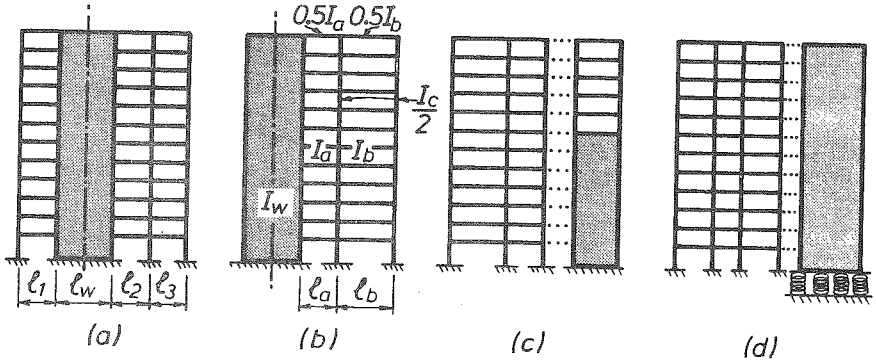

Fig. 3 Modelling of Different Types of Hybrid Systems.

Simplified analysis techniques, useful at least for preliminary design, have been developed for such a mixture of interacting frames and walls[6]. The structural idealization used in shown in Fig. 3(b). The stiffness of all walls, as quantified by the second moment of area, are lumped into a stiffness, I_w, of a single wall. Where appropriate allowance for shear distortions in the walls should also be made[2]. The beams framing directly into wall edges, i.e. those with span lengths ℓ_1 and ℓ_2 in Fig. 3(a), are lumped at each floor into a single beam having a mean second moment of area, I_a, and span ℓ_a, as shown in Fig. 3(b). All other beams, such as span ℓ_3 in Fig. 3(a) and the beams of the frames in Fig. 2(a), are also lumped and replaced at each floor with beams having the mean properties of I_b and ℓ_b shown in Fig. 3(b). The aim is to obtain representative mean I/ℓ ratios for the beams. Finally all the columns of the buildings are lumped into two identical columns, each having one half of the moment inertia, $0.5I_c$, of the sum of the moment of inertia of all columns of the real structure. Standard solutions for a range of relative stiffnesses have been presented for this type (Fig. 3(b)) of structure[6].

Another useful technique replaces all frames with a single equivalent "shear" cantilever and connects this continuously over the height of the building to a single equivalent "bending" cantilever wall[7]. The method is similar to that used in the "laminar analysis" of coupled structural walls. It is limited to regular structures with vertically constant geometric properties.

Before the design of individual members can be finalised, it is necessary to identify clearly the locations in beams and columns at which plastic hinges are intended in order to enable the capacity design procedure to be applied.

2.3 Frames Interacting with Walls of Partial Height

Although in most buildings structural walls extend over the full height, there are cases when for architectural or other reasons, walls are terminated below the level of the top floor. A model of such a structure is shown in Fig. 3(c).

Because of the abrupt discontinuity in total stiffnesses at the level where walls terminate, the seismic response of these structures is viewed with some concern. Gross discontinuities are expected to result in possibly critical features of dynamic response which are difficult to predict. It is suspected that the regions of discontinuity may suffer premature damage and that local ductility demands during the largest expected seismic events might exceed the ability of affected components to deform in the plastic range without significant loss of resistance.

On the other hand, elastic analyses for lateral static loads show that structural walls in the upper storeys may serve no useful structural purpose. Figure 2 suggests that the termination of walls below the top floor may beneficially affect overall behaviour.

The response of such structures has also been studied recently[11]. A limited number of case studies, using the 1940 El Centro earthquake record, suggested no features that could not be readily accommodated in currently used design procedures. The findings of this study, together with the appropriate application of the capacity design approach, will be reported separately.

2.4 Hybrid Structures with Walls on Deformable Foundations

It is customary to assume that cantilever walls are fully restrained against rotations at the base. It is recognised, however, that full base fixity for such large structural elements is very difficult, if not impossible, to achieve. Foundation compliance may result from soil deformations below footings and/or from deformations occurring within the foundation structure, such as piles. Base rotation is a vital component of wall deformations. Therefore it may significantly affect the stiffness of cantilever walls and hence possibly their share in the lateral load resistance within elastic hybrid structures. The reluctance to address the problem may be attributed to our limitations in being able to estimate reliably stiffness properties of soils. Moreover, soil stiffness is generally very different for static and dynamic loading. For the latter, frequency and amplitude are also parameters which affect soil response.

To gauge the sensitivity of hybrid structures of the type shown in Fig. 2(b) with respect to foundation compliance of the wall elements only, parametric studies were conducted[11]. The major variables in the structures chosen for analyses were:

(1) Variation of wall restraint between the extreme limits of full rotational fixity and a hinge at the base.

(2) Variation in the number of storeys in a building. Predominantly 6 and 12 storey structures were studied.

(3) The relative contribution of walls to total lateral load resistance within the structure were varied. This was achieved with appropriate variation of wall lengths, ℓ_w, shown in Fig. 2(a).

(4) Elastic response to code specified lateral static load was compared with the elasto-plastic dynamic response of the structure to the 1940 El Centro earthquake record.

Details of this study are to be reported. Those aspects of the conclusions which are particularly relevant to the issues examined in this paper are as follows:

(a) Above the first floor, the static response of the structure with walls with moderate stiffness is not significantly affected by the degree of base restraint. As a corollary, the stiffer a wall the more profound is the influence of foundation compliance.

(b) In pinned base walls, as expected, very large and reversed base shear forces are predicted by elastic analyses for static lateral load. This points to the need for studying the transfer of these large forces to the diaphragm at

first floor level. The wall shear reversals in the first storey necessitated dramatic increases in column shear forces in that storey. In the first storey the sum of the column shear forces exceed therefore the total static base shear for the entire structure.

(c) The single most important parameter affecting the seismic dynamic response of such hybrid structures was found to be the period shift brought about by the reduction of wall stiffnesses when complete loss of rotational restraint at the base was assumed.

(d) Extreme levels of shear forces, predicted by elastic analyses for columns and walls, did not eventuate during the time history analysis for the El Centro event.

(e) In the upper storeys important design quantities for the example hybrid structures, such as drifts, column and wall moments, and rotational ductility demands in plastic hinges of beams, were only insigniciantly affected when walls were modelled with pinned bases.

(f) Full wall base fixity is normally assumed in design, although it is known to be generally unavailable. These parametric studies indicated, however, that errors due to quite significant relaxation in base restraint, are not likely to seriously affect elasto-plastic dynamic response.

Brief comparisons of a few features of the analytically predicted response of prototype hybrid structures with fixed or pinned based walls, are made in Section 3.

3. DETAILS OF A CAPACITY DESIGN PROCEDURE

In the following sections a capacity design approach for hybrid structures is described in a step-by-step manner. The presentation follows the pattern of, and is similar to, the design procedure suggested for reinforced concrete ductile frames in the Commentary of NZS 3101[1]. Where necessary, the presentation of a design step is followed by comments, sometimes extensive. These are relevant to the purpose of and intend to explain the justification for that particular step. Frequent reference is made to Fig. 2, which shows a prototype frame-wall structure.

The procedure outlined in the following 19 steps is relevant to the types of structures shown in Figs. 4(a) and (b). In these columns in upper storeys are intended to be protected against significant plastic deformations. Thereby various concessions with respect to their detailing for ductility[1] may be utilised.

Step 1 - Derive the bending moments and shear forces for all members of the frame-shear wall system subjected to the code specified equivalent lateral static earthquake load only. These actions are subscripted "code".

In the analysis for the elastically responding structure, due allowance should be made for the effects of cracking on the stiffness of both frame members and walls. Both frames and walls may generally be assumed to be fully restrained at their base. Load effects are referred to as E.

Step 2 - Superimpose the beam bending moments obtained in Step 1 upon corresponding beam moments which are derived for appropriately factored gravity loading on the structure.

This superposition corresponds with the combinations of factored loads $U = D + 1.3L_R \pm E$, where D is the dead load and L_R is the live load reduced as the tributary area increases[5].

Step 3 - If advantageous, redistribute design moments obtained in Step 2 horizontally at a floor between any or all beams in each bent, and vertically between beams of the same span at different floors.

In the process of moment redistribution, the peak values of beam moments, resulting from the load combinations $U = D + 1.3L_R \pm E$, may be reduced by up to 30%[1]. However, the curtailment of the beam flexural reinforcement along a beam must be such that at least 70% of the moment obtained from elastic analyses in Step 2 can be resisted[1]. Final moments obtained after redistribution should be checked to ensure that no loss in the total lateral load resistance of the structure results[8]. Also combinations for gravity load alone, $U = 1.4D + 1.7L_R$, must be examined before the proportioning of beams commences.

The principles of redistribution of moments at a level among different spans of beams within frames are well established[1,8]. One of the advantages which may result is the reduction of the peak beam negative moment at an exterior column which is associated with the load combination $U = D + 1.3L_R + E$. The reduction is achieved at the expense of increasing the (usually non-critical) positive moment at the same section associated with the combination $U = D + 1.3L_R + E$. In the latter case the

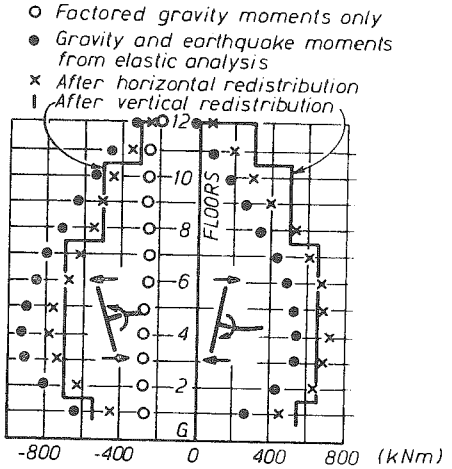

Fig. 5 The Redistribution of Design Moments Among Beams of a Hybrid Structure.

gravity and earthquake moments, superimposed in Step 2, oppose each other. An example in Fig. 5 shows magnitudes of beam design moments at each floor at an exterior column at various stages of the analysis. The gravity moments (always negative), shown by circles, are changed by the addition of earthquake moments $\dot{E}$ or $\dot{E}$, to values shown by solid circles.

Because near their base, walls make very significant contributions to the resistance of both horizontal shear (Fig. 2) and overturning moment, the flexural demands on the beams of hybrid structures are relatively small in the lower storeys. The distribution of beam and wall moment demands with the height of the elastic structure depends on the relative stiffness of walls and frames[3]. In the example frames, the beam moments at the exterior column could be redistributed so as to result in magnitudes shown by crosses in Fig. 5. It is seen that the negative and positive moment demands are now comparable in magnitudes.

To optimize the practicality of beam design, whereby beams of identical strength are preferred over the largest possible number of adjacent floors, some vertical redistribution of beam design moments should also be considered. In the example of Fig. 5, the design moments shown by crosses may be redistributed up and down the frames so as to result in magnitudes shown by the continuous stepped lines. It is seen that beams of the same flexural strength could be used over 6 floors. The stepped line has been chosen in such a way that the area enclosed by it is approximately the same as that within the curve formed by the crosses. This choice means that the contribution of the frames to the resistance of overturning moments is only insignificantly altered by vertical moment redistribution.

It may be noted that horizontal redistribution of beam moments at a particular level will change the moment input to individual columns. Hence the shear demand across individual columns will also change with respect to that indicated by the elastic analysis used in Step 1. However, the total shear demand on columns of a bent must not change. This is referred to as redistribution of design shear forces between columns.

When vertical redistribution of beam moments is carried out, the total moment input to some or all columns at a floor will also change. Hence the total shear demand on columns of a particular storey may decrease (the 5th storey in Fig. 5), while in other storey (the 2nd storey in Fig. 5) it will increase. To ensure that there is no decrease in the total storey shear resistance intended by the code specified lateral loading, there must be a horizontal redistribution of shear forces between the vertical elements of the structure, i.e. columns and walls. It will be shown subsequently that the upper regions of walls will be provided with sufficient shear and flexural strength to accommodate additional shear forces shed by upper storey columns. The principles involved in vertical load redistribution discussed here are similar to those used in the design of coupling beams of coupled structural walls[2].

To safeguard against premature yielding in beams during small earthquakes, the reduction of beam moments resulting from combined horizontal and vertical moment redistribution should not exceed 30%.

Step 4 - Design all critical beam sections so as to provide the required dependable flexural strengths, and detail the reinforcement for all beams in all frames.

These routine steps require the determination of the size and number of reinforcing bars to be used to resist moments along all beams in accordance with the demands of moment envelopes obtained after moment redistribution. It is important at this stage to locate the two potential plastic hinges in each span (Fig. 4(a)) for each direction of earthquake attack. In locating plastic hinges which require the bottom (positive) flexural reinforcement to yield in tension, both load combinations $U = D + 1.3L_R + \dot{E}$ and $U = 0.9D + \dot{E}$,[5] should be considered, as each combination may indicate a different hinge position. Detailing of the beams should then be carried out in conformity with the relevant code[1] provisions.

Step 5 - In each beam determine the flexural overstrength of each of the two potential plastic hinges corresponding with each of the two directions of earthquake attack.

The procedure, incorporating allowances for strain hardening of the steel and the possible participation in flexural resistance of all reinforcement present in the structure as built, is the same as that used in the design of beams of ductile frames[1]. The primary aim is to estimate the maximum moment input from beams to adjacent columns associated with the largest seismic event.

Step 6 - Determine the lateral displacement induced shear force, V_{oe}, associated with the development of flexural overstrength at the two plastic hinges in each beam span for each direction of earthquake attack.

These shear forces are readily obtained from the flexural overstrengths of potential plastic hinges, determined in Step 5, which were located in Step 4. When combined with gravity induced shear forces, the design shear envelope for each beam span is obtained, and the required shear reinforcement can then be determined[1]. The displacement induced maximum beam shear forces, V_{oe}, are used subsequently to determine the maximum lateral displacement induced axial column load input at each floor.

Step 7 - Determine the beam flexural overstrength factor, ϕ_o, at the centre line of each column at each floor for both directions of earthquake attack. Fixed values of ϕ_o are:

(a) At ground level $\phi_o = 1.4$

(b) At roof level $\phi_o = 1.1$.

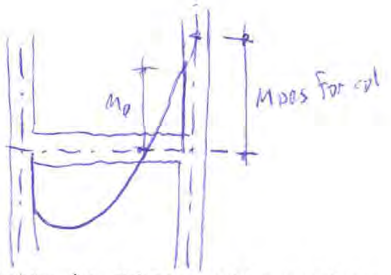

This factor is subsequently used to estimate the maximum moment which could be introduced to columns by fully plastified beams. The beam overstrength factor, ϕ_o, at a column, is the ratio of the sum of the flexural overstrengths developed by adjacent beams, as detailed, to the sum of the flexural strengths required in the given direction by the code specified lateral earthquake loading alone, both sets of values being taken at the centre line of the relevant column[1].

The beam moments at column centre lines can be readily obtained graphically from the design bending moment envelopes, after the flexural overstrength moments at the exact locations of the two plastic hinges along the beam have been plotted.

Step 8 - Evaluate the column design shear forces in each storey from

$$V_{col} = \omega_c \phi_o V_{code} \qquad (2)$$

where column dynamic shear magnification factor, ω_c, is 2.5, 1.3 and 2.0 for the bottom, intermediate and top storeys respectively. The design shear force in the bottom storey columns should not be less than

$$V_{col} = \frac{(M^o_{col} + 1.3\phi_o M_{code})}{(\ell_n + 0.5h_b)} \qquad (3)$$

where M^o_{col} = the flexural overstrength of the column base section consistent with the axial load and shear which are associated with the direction direction of earthquake attack.

$M_{code,top}$ = the value of M_{code} for the column at the centre line of the first floor beams.

ℓ_n = the clear height of the column

h_b = the depth of the first floor beam

The procedure for the evaluation of column design shear forces is very similar to that used in the capacity design of ductile frames[1]. It reflects a higher degree of conservation because of the intent to avoid a column shear failure in any event. Case studies show that in spite of the apparent severity of Eqs. (2) and (3), shear requirements very seldom govern the amount of transverse reinforcement to be used in columns.

Dynamic analyses of example hybrid structures[11] indicated that shear forces induced in the bottom and top storey columns may exceed by a large margin the magnitudes predicted by elastic (Step 1) analyses, V_{code}[3,4]. It may be noted, however, that in hybrid structures, as Fig. 2 suggests, the computed static column shear forces, V_{code}, are often very small in these two specific storeys.

Step 9 - Estimate in each storey the maximum likely lateral displacement induced axial load on each column from

$$P_{eq} = R_v \Sigma V_{oe} \qquad (4)$$

where $R_v = (1 - n/67) \geq 0.7$ (5)

is a reduction factor which takes the number of floors, n, above the storey under consideration, into account.

The magnitudes of the maximum lateral displacement induced beam shear forces, V_{oe}, at each floor, were obtained in Step 6. The probability of all beams above a particular level developing simultaneously plastic hinges at flexural overstrength diminishes with the number of floors above that level. The reduction factor, R_v, makes an approximate allowance for this.

Step 10 - Determine the total design axial load on each column for each of the two directions of earthquake attack from

$$P_{e,max} = P_D + P_{LR} + P_{eq} \qquad (6)$$

and $$P_{e,min} = 0.9P_D - P_{eq} \qquad (7)$$

where P_D and P_{LR} are axial forces due to dead and reduced live loads respectively.

Step 11 - Obtain the design moments for columns above and below each floor from

$$M_{col} = R_m (\omega \phi_o M_{code} - 0.3 h_b V_{col}) \qquad (8)$$

where ω = the dynamic moment magnification factor, the value of which is given in Fig. 6.

ϕ_o = the beam overstrength factor applicable to the floor and the direction of lateral loading under consideration

h_b = the depth of the beam which frames into the column

and $$R_m = 1 + 0.55(\omega - 1)(10 \frac{P_e}{f'_c A_g} - 1) \leq 1 \qquad (9)$$

is a design moment reduction factor applicable when

$$-0.15 \leq \frac{P_e}{f'_c A_g} \leq 0.10$$

where P_e is to be taken negative when causing axial tension.

These requirements are very similar to those recommended for columns of ductile frames[1].

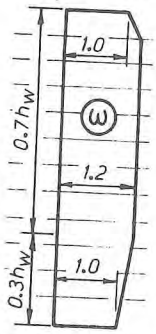

Fig. 6 Dynamic Moment Magnification Factor for Columns in Hybrid Structures.

The steps in the derivation of the column design moment, M_{col}, are given in Fig. 7 as follows. The variation of column moments due to code loading (Step 1), M_{code}, above and below a floor is shown with shaded lines. These moments are magnified throughout the height of the column to $\phi_o M_{code}$, when beams adjacent to the column develop flexural overstrengths at their plastic hinges. It is assumed that the maximum moment input from the two beams, ΣM^o_{beam}, as shown in Fig. 7, cannot be exceeded during an earthquake. However, the distribution of this total moment imput between the columns above and below the floor, during the dynamic response, is uncertain. Allowance for disproportionate distribution is made by the dynamic magnification factor $\omega \leq 1.2$. For example the estimated maximum moment for the upper column in Fig. 7, measured at the beam centre line, is thus $\omega \phi_o M_{code}$. At the top of the beam, at the critical section of this column, the moment is less. The reduction depends on the magnitude of the column shear force generated simultaneously. For this purpose a conservative assumption is made, whereby $V_{min} = 0.6 V_{max} = 0.6 V_{col}$ (Step 8). Hence the moment reduction at the top of the beam becomes $0.5 h_b V_{min} = 0.3 h_b V_{col}$ as shown in Fig. 7.

When the axial load on the column produces small compression, i.e. $P_e \leq 0.1 f'_c A_g$, or results in net axial tension, some yielding of the column is not unacceptable. Such columns should exhibit sufficient ductility even without special confining reinforcement in the end regions. Hence for this situation the design moments are reduced by the factor R_m given in Eq. (9). This expression will give the same values that have been recommended[1] for columns of ductile frames, provided that the value of ω is not taken larger than 1.2. The minimum value of R_m is 0.72. This will enable the amount of required tension reinforcement in exterior columns, where this situation arises, to be reduced.

Because the value of the dynamic moment magnification factor for columns in hybrid structures is relatively small, i.e. $\omega \leq 1.2$, the above reduction of column design moments will seldom exceed 20%. To simplify computations, the designer may prefer to use $R_m = 1.0$.

When the reduction factor, R_m, is used in determining the amount of column reinforcement, the design shear V_{col}, obtained in Step 8, may also be reduced proportionally.

Having obtained the critical design quantities for each column, i.e. M_{col} from Step 11 and V_{col} from Step 8, the required flexural and shear reinforcement at each critical section can be found. Because the design quantities have been derived from beam overstrengths imput, the appropriate strength reduction factor for these columns is $\phi = 1.0$[1]. End regions of columns need further be checked to ensure that the transverse reinforcement provided satisfies the code[1] requirements for confinement, stability of vertical reinforcing bars and lapped splices.

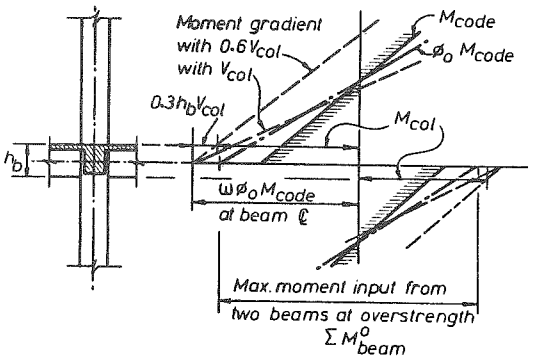

Fig. 7 The Derivation of Design Moments for Columns.

The design of columns at the base, where the development of a plastic hinge in each column must be expected, is the same as for columns of ductile frames[1].

Step 12 - Determine the appropriate gravity and earthquake induced axial forces on walls.

In the example structure (Fig. 2), it was implicitly assumed that lateral load on the building does not introduce axial forces to the cantilever walls. For this situation the design axial forces on the walls are $P_e = P_D + 1.3 P_{LR}$ or $P_e = 0.9 P_D$. Generally the latter, when considered together with lateral load induced moments, governs the amount of vertical wall reinforcement to be used.

If walls are connected to columns via rigidly connected beams, as shown for example in Fig. 3(a), the lateral load induced axial forces on the walls are obtained from the initial elastic analysis of the structure (Step 1). Similarly this applies when, instead of cantilever walls, coupled structural walls[2] share with frames in lateral load resistance.

Step 13 - Determine the maximum bending moment at the base of each wall and design the necessary flexural reinforcement, taking into account the most adverse combination with axial forces on the wall.

This simply implies that the requirements of strength design be satisfied. The appropriate combination of actions is $M_u = M_{code}$ and $P_u = P_e$. Because the wall should meet the additional seismic requirements specified by the code[1], the appropriate strength reduction factor to be used is $\phi = 0.9$[1], irrespective of the level of axial compression. The exact arrangement of bars within the wall section at the base, as built, is to be determined to allow the flexural overstrength of the section to be estimated.

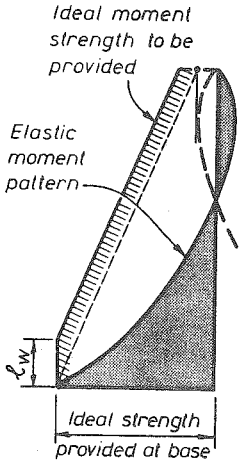

Fig. 8 Design Moment Envelope for Walls of Hybrid Structures.

Step 14 - When curtailing the vertical reinforcement in the upper storeys of walls, provide flexural resistance not less than given by the moment envelope in Fig. 8.

The envelope shown is similar to but not the same as that recommended for cantilever walls[1]. It specifies slightly larger flexural resistance in the top storeys. Its construction from the initial moment diagram, obtained from the elastic analysis in Step 1, may be readily followed in Fig. 8. It is important to note that the envelope is related to the ideal flexural strength of a wall at its base, as built, rather than the moment required at that section by the analysis for lateral load. The envelope refers to effective ideal flexural strength. Hence vertical bars in the wall must extend by at least full development length beyond levels indicated by the envelope.

The aim of this apparently conservative approach is to ensure that significant yielding will not occur beyond the assumed height, ℓ_w, of the plastic hinge at the base. Thereby the shear strength of the wall in the upper storeys is also increased[1], and hence reduced amounts of horizontal shear reinforcement may be used.

Figure 9 compares wall moment demands, encountered during the analysis for the 1940 El Centro and the 1971 Pacoima Dam earthquake records, with the moment envelopes given in Fig. 8. Three 12 storey buildings, in plan as shown in Fig. 2, with walls of 3.0, 3.6 and 7.0 metres length, were studied. All buildings were designed in accordance with this capacity design procedure. While the envelopes appear to provide considerable reserve flexural strength in the upper storeys during the El Centro record, at various instants of the extreme (and unrealistic) Pacoima Dam event the analysis predicted the attainment of the ideal flexural strength in most storeys. Analyses showed, however, that curvature ductility demands, even during this extreme event, were very small in the upper storeys. As part of the study of the effects of foundation compliance, discussed in Section 2.4, these structures, with pinned base walls, but otherwise identical with the prototype structures, were also analysed for the El Centro record. It is seen in Fig. 9, that wall moment demands for the El Centro event in the upper storeys are very similar to those experienced with fixed base walls.

Step 15 - Determine the magnitude of the flexural overstrength factor $\phi_{o,w}$, for each wall. This is the ratio of the flexural overstrength of the wall, M^o, as detailed, to the moment required to resist the code specified lateral loading, M_{code}; both moments taken at the base section of a wall.

The meaning and purpose of this factor, $\phi_{o,w} = (M^o/M_{code,base})$, is the same as that evaluated for beams in Step 7. Strictly, for walls there are two limiting values of overstrength, M^o, which could be considered. These are the moments developed in the presence of two different axial load intensities, i.e. $P_{e,max}$ and $P_{e,min}$. However, it is considered to be sufficient for the intended purpose to evaluate flexural overstrength developed with axial compression on cantilever walls due to dead load alone[2].

Step 16 - Compute the wall shear ratio, ψ. This is the ratio of the sum of the shear forces at the base of all walls, $\Sigma V_{wall,code}$, predicted by the analysis for design load, to the total design base shear for the entire structure, $V_{code,total}$.

The relative contribution of all walls to the required total lateral load resistance is expressed as a matter of convenience by

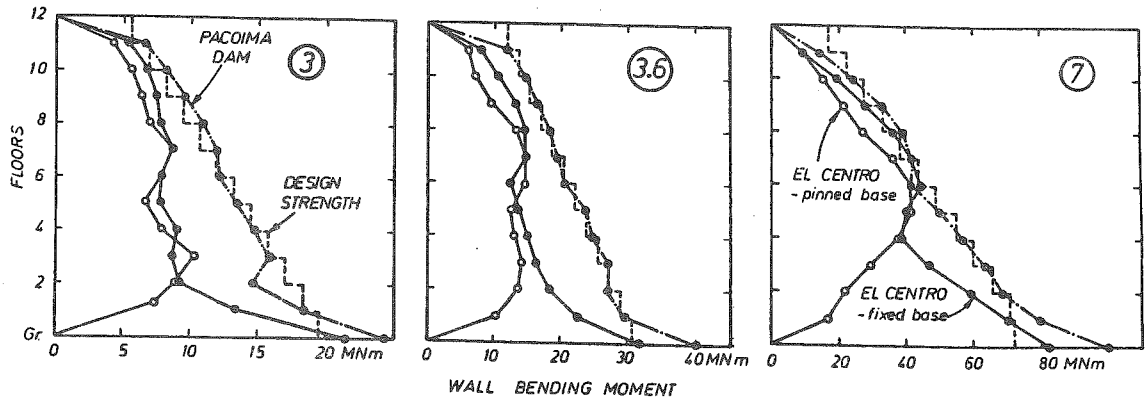

Fig. 9 Wall Moment Demands Encountered During Earthquake Records.

the shear ratio

$$\psi = \left(\sum_{i=1}^{n} V_{i,wall,code} / V_{code,total}\right)_{base} \quad (10)$$

It applies strictly to the base of the structure. As Fig. 2(c) shows, such a shear ratio would rapidly reduce with height, and near the top it could become negative. This indicates that the parameter ψ is a convenient but not unique measure to quantify the share of walls in the total lateral load resistance.

Step 17 - Evaluate for each wall the design shear force at the base from

$$V_{wall,base} = \omega_v^* \phi_{o,w} V_{wall,code} \quad (11)$$

and

$$\omega_v^* = 1 + (\omega_v - 1)\psi \quad (12)$$

where ω_v is the dyanmic shear magnification factor relevant to cantilever walls, obtained from

$$\omega_v = 0.9 + n/10 \quad \text{when} \quad n \leq 6 \quad (13a)$$

or

$$\omega_v = 1.3 + n/30 \leq 1.8 \quad \text{when} \quad n > 6 \quad (13b)$$

where n is the number of storeys above the base.

The approach developed for the shear design of walls in hybrid structures is an extension of the two stage methodology used for cantilever walls[1,9].

In the first stage, the design shear force is increased from the initial (Step 1) value to that corresponding with the development of a plastic hinge at flexural overstrength at the base of the wall. This is achieved with the introduction of the flexural overstrength factor, $\phi_{o,w}$, obtained in Step 15. In the next stage, allowance is made for the amplification of the base shear force during the inelastic dynamic response of the structure. While a plastic hinge develops at the base of a wall, due to the contribution of higher modes of vibration, the centroid of inertia forces over the height of the building may be in a significantly lower position than that predicted by the conventional analysis for lateral loads[9]. The larger the number of storeys, the more important is the participation of higher modes. The dynamic shear magnification for cantilever walls, ω_v, given in Eq. (13), makes allowance for this phenomenon[9]. The values so obtained agree with those recommended in NZS 3101.

It has also been found[3], that for a given earthquake record, the dynamically induced base shear forces in walls of hybrid structures increased with an increased participation of such walls in the resistance of the total base shear for the entire structure. Wall participation is quantified by the "shear ratio", ψ, obtained in Step 16. The effect of the "shear ratio" upon the magnification the maximum wall shear force is estimated by Eq. (12). It is seen that when $\psi = 1$, $\omega_v^* = \omega_v$.

Design criteria for shear strength[1] will often be found to be critical. At the base the thickness of walls may need to be increased on account of Eq. (11), and because of the maximum shear stress limitations of NZS 3101. Typically when using Grade 380 vertical wall reinforcement in a 12 storey hybrid structure, where the walls have been assigned 60% of the total base shear resistance, it will be found that with $\phi_{o,w} \simeq 1.6$, $\omega_v = 1.7$, $\psi = 0.6$ and $\omega_v^* = 1.42$, the ideal shear strength will need to be $V_{wall} = 2.27\ V_{code}$. In comparison, the ideal shear strength of a wall, proportioned with strength rather than capacity design procedures, would be $V_{wall} = V_{code}/0.85 = 1.18\ V_{code}$. Thus Eq. (11) implies very large apparent reserve strength in shear. Analyses in cases studied[11] consistently predicted, however, shear forces which are often 30% larger than those required by Eqn. (11). Of all the aspects of this proposed design strategy, the estimation of wall shear forces was found to be the least satisfactory. Some relevant issues are discussed subsequently in Section 4.4.

Step 18 - In each storey of each wall, provide shear resistance not less than that given by the shear design envelope of Fig. 10.

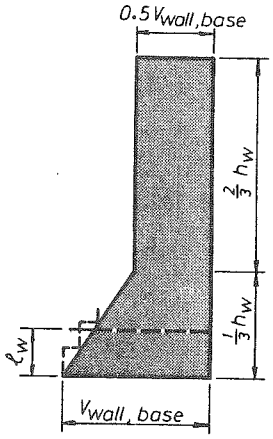

Fig. 10 Envelope for Design Shear Forces for Walls of Hybrid Structures

As Fig. 2(c) shows, shear demands predicted by analyses for static load may be quite small in the upper half of walls. As can be expected, during the response of the building to vigorous seismic excitations, much larger shear forces may be generated at these upper levels. A linear scaling up of the shear force diagram drawn for static load, in accordance with Eq. (11), would give an erronous prediction of shear demands in the upper storeys. Therefore from case studies the shear design envelope shown in Fig. 10 was developed. It is seen that the envelope gives the required shear strength in terms of the base shear for the wall, which was obtained in Step 17.

Figure 11 presents some results of the relevant study[11] of a 12 storey building. It is seen that the shear design envelope is satisfactory when structures with relatively slender walls, with $\psi \leq 0.57$, were subjected

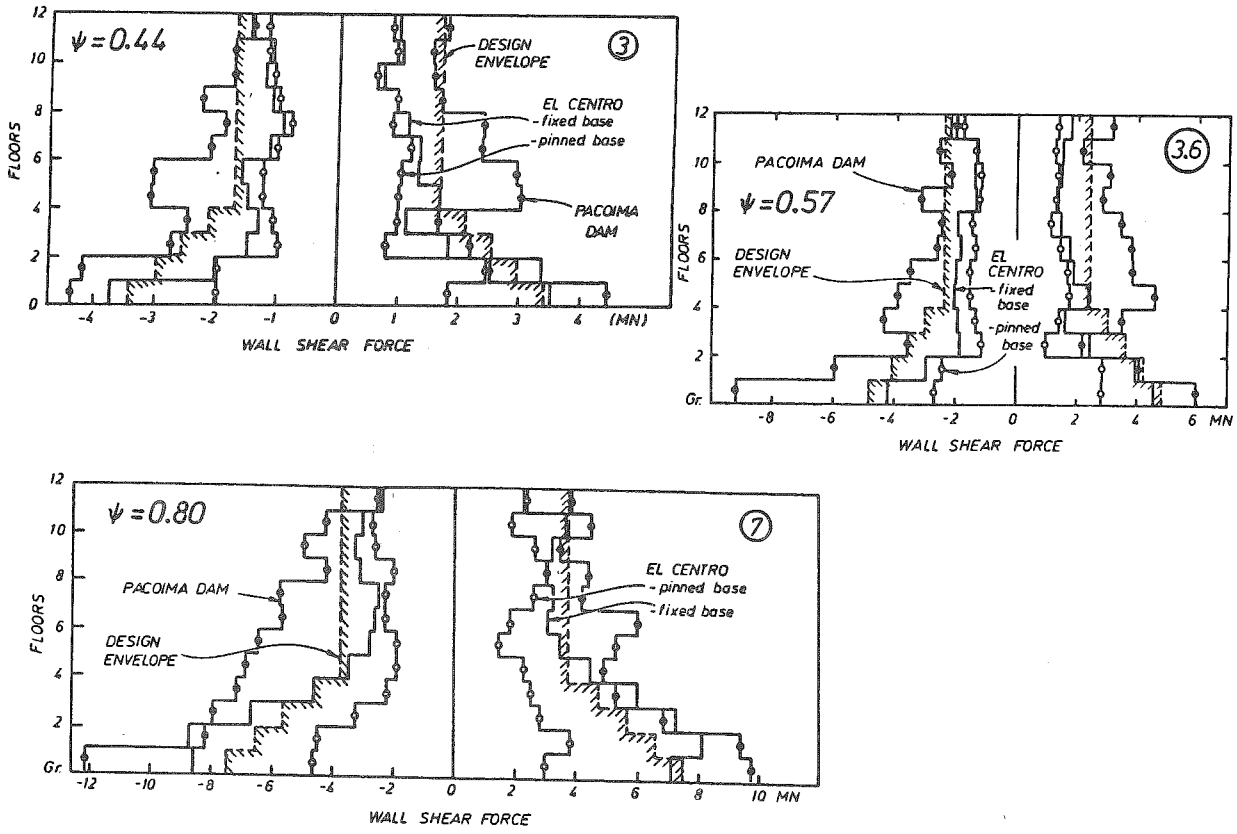

Fig. 11 Predicted Shear Demands for Different Walls in a 12 Storey Hybrid Structure.

to the El Centro excitation. The shear response of the structure with 7 m walls is less satisfactory in the lower storeys. As may be expected, the predicted demand for shear in pin based walls* is less, particularly as the length of the walls, ℓ_w, increases. Shear loads predicted for the Pacoima event were found to consistently exceed the suggested design values.

With the aid of the shear design envelope, the required amount of horizontal (shear) wall reinforcement at any level may be readily found. In this, attention must be paid to the different approaches used[1] to estimate the contribution of the concrete to shear strength, v_c, in the potential plastic hinge and the elastic regions of a wall. In the potential plastic hinge region, extending ℓ_w above the base, as shown in Fig. 10, the major part of the design shear, V_{wall}, will need to be assigned to shear reinforcement. In the upper (elastic) parts of the wall, however, the concrete may be relied on[1] to contribute significantly to shear resistance, allowing considerable reduction in the demand for shear reinforcement.

Step 19 - In the end regions of each wall, over the assumed length of the potential plastic hinge, provide adequate transverse reinforcement to supply the required confinement to parts of the flexural compression zone and to prevent premature buckling of vertical bars.

These detailing requirements for ductility are the same[1] as those recommended for cantilever and coupled structural walls. Recent experimental studies[11] indicated, however, that current code requirements, relevant to the region of confinement within wall sections, should be amended. For this reason, although presented elsewhere[10], the suggested improvement in the procedure is restated here.

The proposed approach to the confinement of wall sections rests on the precept that concrete should be laterally confined wherever compression strains, corresponding with the expected curvature ductility demand on the relevant section, exceed 0.004. The strain profile shown shaded in Fig. 12 indicates the ultimate curvature, ϕ_u, which might be necessary to enable the estimated displacement ductility, μ_Δ, for a particular hybrid structure to be sustained, when the concrete strain in the extreme compression fibre theoretically reaches the magnitude of 0.004. This strain profile is associated with a neutral axis depth, c_c. An estimate for this critical neutral axis depth, c_c, may be made[1] with

$$c_c = 0.10\ \phi_o^*\ S\ \ell_w \qquad (14)$$

*Note that the shear ratio, ψ, given by Eq. (10), is not applicable to pin based walls.

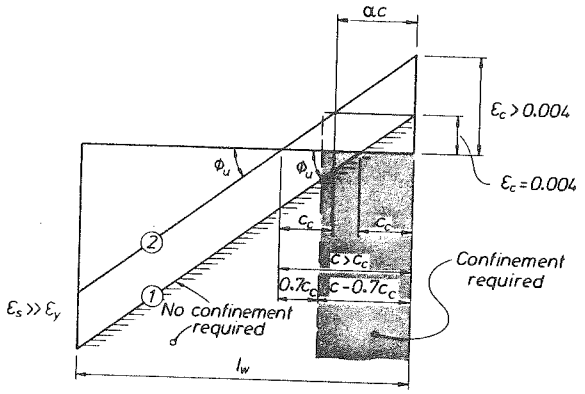

Fig. 12 Strain Profiles for Wall Sections.

where ℓ_w = length of wall,
S = structural type factor[2], and
ϕ_o^* = global overstrength factor, which is the ratio of the total resistance of the hybrid structure to overturning moment, including the contributions of axial forces in columns and walls and those of plastic hinges at the base of all columns and walls, evaluated at levels of flexural overstrength, to the corresponding overturning moment due to code specified lateral static loading. When the total strength provided by yielding regions of the structure matches very closely that required by the lateral code loading, the value of ϕ_o^* will not be less than 1.4.

To achieve in a wall the same ultimate curvature when the computed neutral axis depth, c, is larger than the critical value, c_c, as Fig. 12 shows, the length of wall section subjected to compression strains larger than 0.004, becomes αc. It is this length over which the compressed concrete needs to be confined. From the geometry shown in Fig. 12, $\alpha = 1 - c_c/c$.

Because it has been found in tests[10,11] that, after reversed cyclic loading, observed neutral axis depths tend to be larger than those predicted by conventional section analyses, it is suggested that the length of confinement, αc, be derived from

$$\alpha = 1 - 0.7\, c_c/c \geq 0.5 \qquad (15)$$

whenever $c_c/c < 1$. When c is only a little larger than c_c, a very small and impractical value of α would be obtained. In line with current requirements[1], it is suggested that in such cases at least one half of the theoretical compression zone be confined.

The tests quoted[10] also indicated that the amount of confining reinforcement specified in the code[1] is likely to be adequate.

4. ISSUES REQUIRING FURTHER STUDY

The proposed capacity design procedure and the accompanying discussion of the behaviour of hybrid structures, presented in the previous section, are by necessity restricted to simple and regular structural systems. The variety of ways in which walls and frames may be combined may present problems to which a satisfactory solution will require, as in many other structures, the application of engineering judgement. This may necessitate some rational adjustments in the outlined 19 step procedure. In the following, a few situations are mentioned where such judgement in the application of the proposed design methodology will be necessary. Some directions for promising approaches are also suggested.

4.1 Gross Irregularities in the Lateral Load Resisting System.

It is generally recognised that the larger the departure from symmetry and regularity in the arrangement of lateral load resisting substructures within a building, the less confidence should the designer have in predicting likely seismic response. Examples of irregularity are when wall dimensions change drastically over the height of the building or when walls terminate at different heights, and when setbacks occur. Symmetrical positioning of walls in plan may lead to gross eccentricities of applied lateral load with respect to centres of rigidity.

4.2 Torsional Effects

Codes make simple and rational provisions for torsional effects. The severity of torsion is commonly quantified by the distance between the centre of rigidity (or stiffness) of the lateral load resisting structural system and the centre of mass. In reasonably regular and symmetrical buildings this distance (horizontal eccentricity), does not significantly change from storey to storey. Errors due to inevitable variations of eccentricity over building height are thought to be compensated for by code specified amplifications of the computed (static) eccentricities. The corresponding assignment of additional lateral load to resisting elements, particularly those situated at greater distances from the centre of rigidity (centre of horizontal twist), are intended to compensate for torsional effects. Because minimum and maximum eccentricities, at least with respect to the two principal directions of earthquake attack, need to be considered, the structural system, as designed, will possess increased translational rather than torsional resistance.

It was emphasised that the contributions of walls to lateral load resistance in hybrid structures usually change dramatically over the height of the building. An example was shown in Fig. 2(c). For this reason the position of the centre of rigidity may also change significantly from floor to floor.

For the purpose of illustrating the variation of eccentricity with height, consider the example structure shown in Fig. 2(a), but slightly modified. Because of symmetry, torsion due to variation in the position of the centre of rigidity, does not arise. Assume, however, that instead of the two symmetrically positioned walls shown in Fig. 2(a), two 6 m long walls are placed side by side at 9.2 m from the left hand end

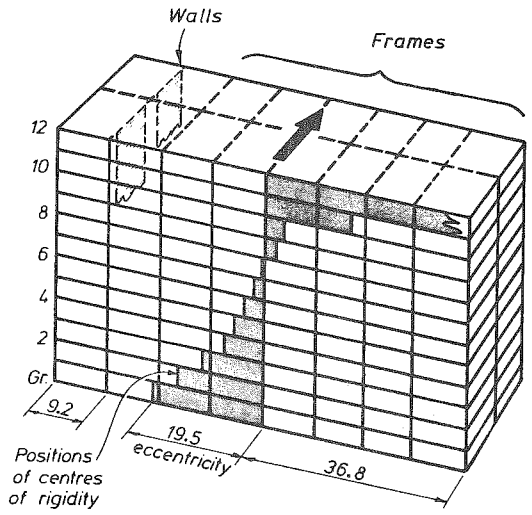

Fig. 13 The Variation of Computed Torsional Eccentricities in an Unsymmetrical 12 Storey Hybrid Structure.

of the building, as shown in Fig. 13, and that the right hand wall is replaced by a standard frame. Because the two walls, when displaced laterally by the same amount as the frames, would in this example structure resist 74% of the total shear in the first storey, the centre of rigidity would be 19.5 m from the centre of the (mass) building. In the 8th storey the two walls become rather ineffective, as they resist only about 12% of the storey shear i.e. approximately as much as one frame. At this level the eccentricity becomes negligible. As Fig. 13 shows, the computed static eccentricities would vary considerably in this example building between limits at the bottom and top storey. Note also the different senses. Torsional effects on individual columns and walls will depend on the total torsional resistance of the system, including the periphery frames along the long sides of the building.

4.3 Diaphragm Flexibility.

For most buildings, floor deformations associated with diaphragm actions are negligible. However, when structural walls resist a major fraction of the seismically induced inertia forces in long and narrow buildings, the effects of inplane floor deformations upon the distribution of resistance to frames and walls may need to be examined.

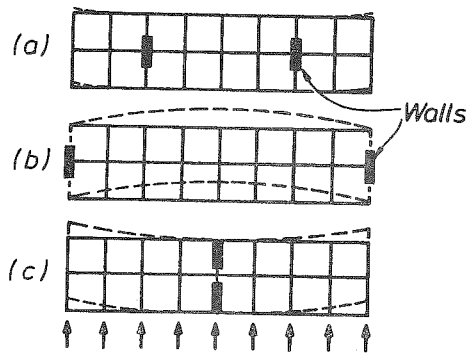

Fig. 14 Diaphragm Flexibility.

Figure 14 shows plans of a building with three different positions of identical walls. The building is similar to that shown in Fig. 2(a). The contribution of the two walls to total lateral load resistance is assumed to be the same in each of these three cases. Diaphragm deformations associated with each case are shown approximately to scale by the dashed lines. Diaphragm deformations in the case of Fig. 14(a) would be negligibly small in comparison with those of the other two cases. In deciding whether such deformations are significant, the following aspects might be considered:

(a) If elastic response is considered, the assignment of lateral load to some frames (Figs. 14(b) and (c)) would be clearly underestimated if diaphragms were to be assumed to be infinitely rigid. In-plane deformations of floors, even when derived with crude approximations, should be compared with interstorey drifts predicted by standard elastic analyses. Such a comparison will then indicate the relative importance of diaphragm flexibility.

(b) In ductile structures, significant inelastic storey drifts are to be expected. The larger the inelastic deformations the less important are differential elastic displacements between frames which would result from diaphragm deformations.

(c) As Fig. 2(c) illustrated, the contribution of walls to lateral load resistance in hybrid structures diminishes with the distance measured from the base. Therefore at upper floors, lateral load will be more evenly distributed among identical frames. This will greatly reduce diaphragm inplane shear and flexural actions. Hence diaphragm deformations at upper levels would diminish.

(d) Horizontal inertia forces are expected to increase with the distance from the base, while inplane bending and shear effects will diminish because of the decreasing participation of walls at upper floors. Hence it may be concluded that diaphragm flexibility is of lesser importance in hybrid structures of the type shown in Fig. 14, than in buildings where lateral load resistance is provided entirely by cantilever walls i.e. without the participation of any frames.

4.4 Prediction of Shear Demand in Walls.

A number of case studies for structures of the type shown in Fig. 2, typically with 3.0, 3.6 and 7.0 long walls, have indicated[11] that the capacity design procedure set out in Section 3, led to structures in which:

(a) Inelastic deformations during the El Centro event remained within limits currently envisaged in New Zealand. Typically storey drifts did not exceed 1% of storey heights.

(b) Plastic hinges in the columns of upper storeys were not predicted.

(c) Derived column design shear forces proscribed shear failure without the use of excessive shear reinforcement.

(d) Rotational ductility demands at the base of both columns and walls, remained well within the limits readily attained in appropriately detailed laboratory specimens[10].

(e) Predicted shear demands in the upper storeys of walls were satisfactorily catered for by the envelope shown in Fig. 10. However, maximum dynamic shear forces at the bases exceeded the design shear level (Fig. 11).

This latter feature was initially viewed with concern. Therefore a further study of the phenomenon, discussed previously with the description of design Steps 17 and 18, was undertaken. Some of the findings of this study are summarised in the following.

Firstly the incidence of the largest wall base shear forces and moments, analytically predicted for the El Centro event, was studied. This was achieved by recording the status of a wall base every 1/10 seconds

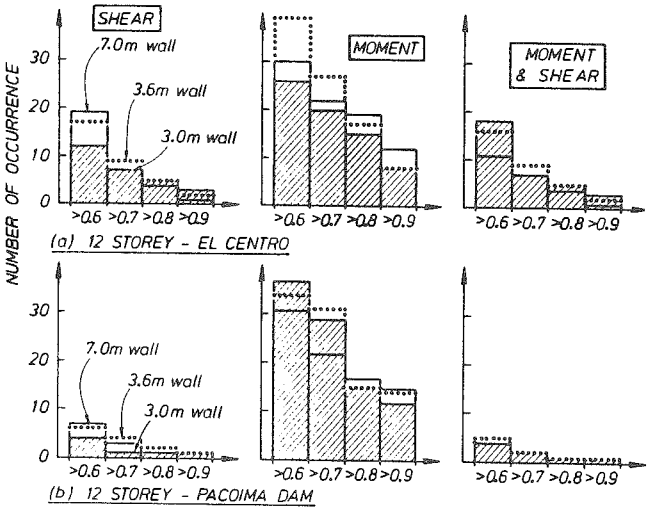

Fig. 15 Occurrence of High Shear Forces and Moments During the El Centro Event at the Base of the Walls of a 12 Storey Hybrid Structure.

during the first 10 seconds excitation. Figure 15(a) shows for the El Centro event the frequency of occurrence during these first 10 seconds of the record of ranges of normalized high shear or moment intensities, as well as the concurrent occurrence of both. Intensities of shear or moment were expressed in terms of absolute maxima encountered during the record and shown in Fig. 11. It is seen for example that when 7 m walls were used, the base shear in excess of 60% of the absolute maximum was encountered 19 times. Similarly shear load on the 3 m wall larger than 90% of the maximum, was encountered 3 times. In the 3.6 m long walls, base moments in excess of 90% of the maximum, were encountered 8 times during the 10 seconds of El Centro record.

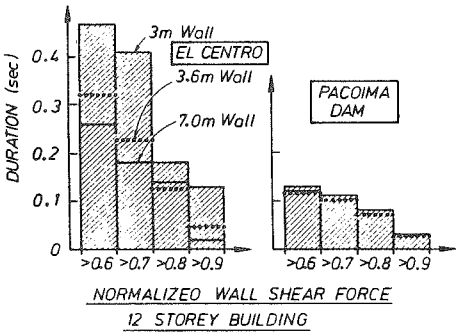

Fig. 16 Duration of Large Wall Shear Forces and Base Moments in Walls of a 12 Storey Hybrid Structure

As expected, such frequency distributions are strongly dependent on the characteristics of the earthquake record. As Fig. 15(b) shows, the pattern is different for the extremely severe Pacoima Dam record. While moment demands during the two different seismic events were comparable, the frequency of large shear forces and large concurrent shear and moment demands were significantly less during the Pacoima event. For reasons of computational economy, sampling was at 1/10 seconds intervals, even though the time step used in the analyses was 1/100 seconds. A sampling at 1000 instants would have yielded an increase in the number of occurrences of shear levels of concern.

Figure 16 provides additional useful information. Here the total time during which a certain intensity of shear, in terms of the maximum, was exceeded during the 10 seconds of two different earthquake records, is presented. This gives a more reassuring picture. When compared with Fig. 15(a), it is seen for example that during the El Centro event, the total time during which the predicted shear in the 3 m walls exceeded 90% of the maximum, (on three occasions) was only 0.12 seconds. Similarly the predicted duration of the 19 occurrences of shear in the 7 m walls, larger than 60% of maximum, was only 0.26 seconds. The computed duration of shears larger than 90% of the maximum, never exceeded 0.05 seconds during the El Centro event.

Although it is stressed that the prohibition of shear failure is of paramount importance in seismic design, it was concluded at the end of this study that the concern stemming from the less than satisfactory correlation between recommended design shear force levels for walls with maxima obtained from analytical predictions, could be dismissed because:

(a) Predicted peak shear forces were of very short durations. While there was no experimental evidence to prove it, it was felt that shear failures during real earthquakes could not occur within a few hundredths of a second.

(b) The probable shear strength of a wall, which could be utilized during such an extreme event, is in excess of the ideal strength (Eqn. (11)) used in design.

(c) Some inelastic shear deformation during the very few events of peak shear should be acceptable.

(d) Walls and columns were found not to be subjected simultaneously to peak shear demands. Therefore the danger of shear failure at the base, for the building as a whole, should not arise.

(e) The simultaneous occurrence during an earthquake record of predicted peak shear and peak flexural demands was found to be about the same as the occurrence of peak shear demands. This means that when maximum shear demand occurred, it did generally coincide with maximum flexural demands. Present code provisions[1] were based on this precept. While the relevant code provisions do not affect the amount of shear reinforcement to be used, they ensure that wall thickness is large enough to keep shear stresses during such events at moderate levels.

4.5 Variations in the Contribution of Walls to Earthquake Resistance.

The study of the seismic response of hybrid structures has shown, as was to be expected, that the presence of walls significantly reduced the dynamic moment demands on columns. This is because the mode shapes of relatively stiff walls, do not permit extreme deformation patterns in the inherently more flexible columns. Therefore moment increases in columns above or below beams, due to higher mode effects, as shown in Fig. 7, are much smaller. This was recognised by the introduction of a smaller dynamic moment magnification factor, $\omega = 1.2$, at intermediate floors, as discussed in design Step 11 and shown in Fig. 6. The applicability of appropriate values for ω was supported with a number of case studies[4,11], in which walls made a significant contribution to the resistance of design base shear.

The contribution of all walls to lateral load resistance was expressed by the wall shear ratio, ψ, introduced in design Step 16. The minimum value used in the example structure with two 3 m walls was 0.44.

The question arises as to the minimum value of the wall shear ratio, ψ, relevant to a hybrid structure, for the design of which the proposed procedure in Section 3 is still applicable. As the value of ψ diminishes, indicating that lateral load resistance must be assigned primarily to frames, parameters of the design procedure must approach values applicable to framed buildings[1]. At a sufficiently low value of this ratio, say $\psi < 0.1$, a designer may decide to ignore the contribution of walls. Walls could then be treated as secondary elements which would need to follow, without distress, displacements dictated by the behaviour of ductile frames.

The minimum value of ψ for which the procedure in Section 3 is applicable has not been established. It is felt that $\psi = 0.33$ might be an appropriate limit. For hybrid structures for which $0.1 < \psi < 0.33$, a linear interpolation of the relevant parameters, applicable to ductile frames and ductile hybrid structures, seems appropriate. These parameters are ω, ω_c, ω_v^* and R_m.

5. SUMMARY

(1) The methodology embodied in current capacity design procedures used in New Zealand, relevant to both ductile framed buildings and those in which seismic resistance is provided entirely by structural walls, has been extended to encompass hybrid structures. Appropriate values were suggested for governing design parameters.

(2) Regular 6 and 12 storey buildings with varying wall contents were designed using this approach, and subsequently subjected in analytical studies to the El Centro and Pacoima Dam accelerograms. The generally good performance of these buildings during the El Centro excitation suggested that prototype structures should exhibit good seismic performance.

(3) As intended, energy dissipation was found to occur primarily in beam and wall base plastic hinge zones.

(4) Columns were found to enjoy protection against flexural yielding except at the base and top floor levels, where hinge formation was expected. A dynamic magnification factor for column moments of $\omega = 1.2$ proved satisfactory.

(5) Column design shear forces were adequately predicted by the design procedure and generally found to be non-critical.

(6) The provisions of the linear design wall moment envelopes restricted significant inelastic wall deformations, even during the extreme Pacoima Dam event, to the base.

(7) Peak wall base shear forces encountered during analyses were somewhat underestimated by the proposed design procedure. In the context of uncertainties in the analysis, available reserve shear strength, and in particular the predicted very short duration of these shear forces, it was felt that this analytically predicted phenomenon should not be viewed with concern.

(8) The proposed envelopes for design wall shear forces adequately estimated upper level shear demands.

(9) It is believed that the methodology proposed is logical and straightforward. It should provide buildings so designed, and carefully detailed[1], with excellent seismic performance capability.

(10) Using engineering judgement, the approach is capable of being extended to other structural configurations not covered in this paper, but only by consistent application of capacity design principles.

(11) The excellent seismic behaviour of well balanced interacting ductile frame-wall structures, particularly in terms of drift control and dispersal of energy dissipating mechanisms throughout the structural system, should encourage their extensive use in reinforced concrete buildings.

6. ACKNOWLEDGEMENTS

This study, being part of a project which involved also considerable experimental work, would not have been possible without generous grants from the New Zealand Ministry of Works and Development and the University Grants Committee. Thanks are due to Mrs. V. Grey for preparation of illustrations, Mr. L. Gardner for photographic work and Mrs. J.Y. Johns for typing the text. The authors wish to acknowledge specially the invaluable assistance and advice received from Dr. A.J. Carr with respect to computational work.

7. REFERENCES

1. NZS 3101:1982, Parts 1 and 2, "Code of Practice for the Design of Concrete Structures", Standards Association of New Zealand, Wellington, 283pp.

2. Paulay, T. and Williams, R.L., "The Analysis and Design of and the Evaluation of Design Actions for Reinforced Concrete Ductile Shear Walls", Bulletin of the New Zealand National Society for Earthquake Engineering, Vol. 13, No. 2, June 1980, pp.108-143.

3. Goodsir, W.J., Paulay, T. and Carr, A.J., "A Study of the Inelastic Seismic Response of Reinforced Concrete Coupled Frame - Shear Wall Structures", Bulletin of the New Zealand National Society for Earthquake Engineering, Vol. 16, No. 3, Sept. 1983, pp.185-200.

4. Goodsir, W.J., "The Response of Coupled Shear Walls and Frames", Research Report No. 82-10, Department of Civil Engineering, University of Canterbury, Christchurch, New Zealand, 1982, 155pp.

5. NZS 4203:1984, "Code of Practice for General Structural Design and Design Loadings for Buildings", Standards Association of New Zealand, Wellington, 80pp.

6. Khan, F.R. and Sbarounis, J.A., "Interaction of Shear Walls with Frames in Concrete Structures under Lateral Loads", Journal of the Structural Division, ASCE, Vol. 90, No. ST3, June 1964, pp.285-335.

7. Rosman, R., "Laterally Loaded Systems Consisting of Walls and Frames", Tall Buildings, University of Southhampton, 1966, pp.273-289.

8. Paulay, T., "Moment Redistribution in Continuous Beams of Earthquake Resistant Multistorey Reinforced Concrete Frames", Bulletin of the New Zealand National Society for Earthquake Engineering, Vol. 9, Nol. 4, Dec. 1976, pp.205-212.

9. Blakeley, R.W.G., Cooney, R.C. and Megget, L.M., "Seismic Shear Loading at Flexural Capacity in Cantilever Walls", Bulletin of the New Zealand National Society for Earthquake Engineering, Vol. 8, No. 4, Dec. 1975, pp.278-290.

10. Paulay, T. and Goodsir, W.J., "The Ductility of Structural Walls", Bulletin of the New Zealand National Society for Earthquake Engineering, Vol. 18, No. 3, Sept. 1985, pp.250-269.

11. Goodsir, W.J., "The Design on Coupled Frame-Wall Structures for Seismic Actions", Research Report No. 85-8, Department of Civil Engineering, University of Canterbury, Christchurch, New Zealand, 1985, 383pp.

8. LIST OF SYMBOLS

A_g = gross concrete area of section
c = theoretical neutral axis depth
c_c = critical neutral axis depth
D = dead load
E = earthquake load
f'_c = specified compression strength of concrete (MPa)
h_b = depth of beam
I_a, I_b = second moment of area of beam sections
I_c = second moment of area of a column section
I_w = second moment of area of a wall section
ℓ = span lengths
ℓ_n = clear height of column
ℓ_w = length of wall, overall depth of wall section
L_R = reduced live load
M^o_{beam} = flexural overstrength of beam measured at column centre line
M_{code} = moment due to code specified lateral load
$M_{code,top}$ = column moment at the top of a column derived from lateral code loading
M_{col} = design moment for a column at ideal strength
M^o_{col} = flexural overstrength at a column section
M^o = moment developed at flexural overstrength
M_u = moment due to factored loads
n = number of storeys above a given level
P_D = axial load on column due to dead load
$P_{e,max}, P_{e,min}$ = design axial load on column including earthquake effects
P_{eq} = earthquake induced axial load in a column at the development of beam overstrengths
P_{LR} = axial load on column due to reduced live load
P_u = axial load due to factored loads
R_m = column design moment reduction factor

V_{code} = shear force for columns derived from code specified lateral static load

$V_{code,total}$ = total base shear for the entire structure derived from code specified lateral load

V_{col} = design shear force for a column at ideal strength

V_{oe} = displacement induced shear force in beam at the development of its flexural overstrength

$V_{wall,base}$ = design shear force for a wall at its base

$V_{wall,code}$ = shear force for a wall derived from code specified lateral load

U = ultimate factored load

μ_Δ = displacement ductility factor

ϕ = strength reduction factor

ϕ_o = overstrength factor

$\phi_{o,w}$ = flexural overstrength factor for a wall

ϕ_o^* = global overstrength factor

ϕ_u = ultimate curvature

ψ = wall shear ratio

ω = dynamic magnification factor in general

ω_c = dynamic shear magnification factor for a column

ω_v = dynamic shear magnification factor

ω_v^* = dynamic shear magnification for walls in hybrid structures

R_v = axial load reduction factor

S = structural type factor

S_{code} = dependable strength required by code specified lateral load only

S_i = ideal strength

S_o = maximum or overstrength that may be developed

v_c = ideal shear stress provided by concrete (MPa)

$^{\rightarrow}_{\leftarrow}$ = superscript indicating direction of earthquake attack

SOME ASPECTS OF THE SEISMIC DESIGN OF MOMENT RESISTING BUILDING FRAMES INCORPORATING PRESTRESSED CONCRETE

R. Park

SOME ASPECTS OF THE SEISMIC DESIGN OF MOMENT RESISTING BUILDING FRAMES INCORPORATING PRESTRESSED CONCRETE

by R. Park
University of Canterbury

ABSTRACT

Studies of the use of prestressed concrete in moment resisting frames designed for earthquake resistance have been conducted at the University of Canterbury in recent years. Aspects of that research work are described in this paper involving the seismic design of:

(1) Building frames incorporating precast prestressed concrete U-beam elements acting compositely with cast in situ reinforced concrete.

(2) Building frames composed of precast concrete members post-tensioned together for continuity.

1. SOME ASPECTS OF THE SEISMIC DESIGN OF BUILDING FRAMES INCORPORATING CAST IN PLACE REINFORCED CONCRETE AND PRECAST CONCRETE BEAM SHELLS

1.1 Introduction

The use of precast concrete in building frames has a number of attractive features such as better quality control of the product and savings in formwork and construction time. The basic problem in the design of earthquake resistant building structures incorporating precast concrete elements is in finding an economical and practical method for connecting the precast elements together. The connection between the elements should ensure satisfactory strength and stiffness against seismic loads and enable the structure to achieve the necessary ductility during cyclic loading in the inelastic range.

Composite systems of concrete buildings, combining precast and cast in situ reinforced concrete, have a number of advantages in construction. The incorporation of precast concrete elements has the advantage of high quality control and speed of construction, and the cast in situ reinforced concrete provides the structural continuity and the ductility necessary for adequate seismic performance.

A building system which has become popular in New Zealand involves the use of precast concrete beam shells as permanent formwork for beams. The precast shells are typically pretensioned prestressed concrete U-beams and are left permanently in position after the cast in situ reinforced concrete core has been cast. The precast U-beams support the self weight and construction loads and act compositely with the reinforced concrete core when subjected to other loading in the finished structure. The precast U-beams are not connected by steel to the cast in situ concrete of the beam or column.

The typical structural organisation of a building floor and frame system incorporating the precast pretensioned U-beam units is shown in Fig. 1. Current construction practice is to support the U-beam units on the cover concrete of the previously cast reinforced concrete column below, with a seating of 40 to 50 mm (1.6 to 2.0 in) and to place a proprietary precast concrete floor system between the U-beams of adjacent frames. Some propping may be provided under the ends of the U-beam units as a back-up measure in case the U-beam seating on the column should prove inadequate to carry the construction load. Once the floor system is in place, the reinforcement may be placed, and the in situ concrete cast, inside the beam units, the topping slab and the columns of the next storey. The section of the composite beam in the finished structure is shown in Fig. 2. Precast concrete columns have sometimes been used rather than cast in situ concrete columns.

The precast concrete U-beam illustrated in Fig. 1 has webs tapered from the bottom to the top, to ensure ease of removing internal formwork when precast. The inside surface is intentionally roughened, by the use of a chemical retarder and the removal of the surface cement paste, to facilitate the development of interface bond between the precast U-beam concrete and the cast in situ concrete core. The U-beams are pretensioned with seven wire strands and are designed to carry at least all of the self weight and imposed loads during construction. Note that the strands terminate in the end of the U-beam and hence are not anchored in the beam-column joint region.

To date in New Zealand precast concrete U-beams have been principally used in the construction of low rise buildings in which the lateral seismic loads are resisted primarily by other elements such as totally cast in situ reinforced concrete structural walls or frames. An early example of this type of construction is the Karioi Pulp Mill (see Fig. 3).

Recent trends have seen this form of composite beam construction used in multistorey moment resisting reinforced concrete framed structures. In this application, the composite beams will be required to act as the primary energy dissipating members during seismic loading. Doubts have been expressed by some designers and checking authorities concerning the ability of this form of composite construction to be able to fulfil that demand.

1.2 Seismic Design Considerations for Cast In Place Reinforced Concrete Frames Incorporating Precast Concrete Beam Shells

1.2.1 Flexural Strength of Beams

The negative moment flexural strength at the end of the beam will be aided by the presence of the U-beam since the bottom flange of the U-beam will bear in compression against the cast in situ column concrete. Hence the upper limit of the negative moment flexural strength at the ends of the beam will be that of the composite section. However should the beam end bearing on the column concrete and/or the interface bond between the cast in situ and precast beam concrete break down during seismic loading, the available negative moment flexural strength will reduce to less than the composite section value. The lower limit of negative moment flexural strength at the beam ends is that provided by the cast in situ reinforced concrete core alone. The negative moment flexural strength away from the ends will be that due to the composite section.

The positive moment flexural strength at the end of the beam will be provided only by the longitudinal reinforcement and the cast in situ concrete in the beam core and slab topping. Away from the beam ends there will be some contribution from the precast prestressed U-beam to the positive moment flexural strength, but a full contribution from the prestressing strands (and hence full composite action of the section) can only occur at a distance greater than approximately 150 strand diameters from the beam end, which is the order of length required to develop the tensile strength of the strand.

1.2.2 Plastic Hinge Behaviour of Beams

The length of the plastic hinge region in beams is of interest in seismic design since the plastic hinge length has a significant effect on the level of displacement ductility factor which can be achieved by frames. Longer plastic hinge lengths lead to greater available displacement ductility factors for a given ultimate section curvature [1]. In a conventional reinforced concrete frame the length of the beam region over which the tensile reinforcement yields is typically about equal to the beam depth and several flexural cracks will form in that region. In the composite system considered here, in which there is no connection by steel between the end of the precast U-beam and the column, the length of the region of reinforcement yielding at the end of the composite beam when the bending moment is positive will be less than for a beam in a conventional reinforced concrete frame. This is because when positive moment is applied the first crack to form will be at the contact surface between the end of the precast U-beam and the face of the column. It is possible that positive moment plastic rotations will concentrate at this one cracked section, since significant cracking may not occur in the flexurally stronger adjacent composite sections during subsequent loading. A consequence of a shortened plastic hinge length for positive moment would be higher beam curvatures in the plastic hinge region than for conventional reinforced concrete members. Also, if flexural cracking in the beam during positive moment does concentrate at the column face, the longitudinal reinforcement in the beam there would suffer high localised plastic tensile straining which would perhaps lead to bar fracture when significant plastic hinge rotation occurs. Further, the extensive widening of that crack at large plastic hinge rotations may mean that the shear resistance mechanism due to aggregate interlock along the (vertical) crack will break down, leading to sliding shear displacements along that weakened vertical plane. These opinions concerning the plastic hinge behaviour during positive moment have resulted in reservations being expressed by designers about the performance of this type of composite beam when required to act as primary energy dissipating members during seismic loading.

The possible shortening of the length of the region of reinforcement yielding only applies when the beam moment is positive. When the beam moment is negative the behaviour should be more like a conventional reinforced concrete beam, since the top of the cast in situ concrete core does not have the precast U-beam surrounding it and the plastic hinge should be able to spread along the beam.

One possible approach, aimed at improving the plastic hinge behaviour during positive moment, would be to construct a composite beam in such a manner that in the potential plastic hinge regions at the ends of the beam the bond at the interface between the precast U-beam and the cast in situ concrete core is intentionally eliminated. The effect of such a detail

would be to allow the plastic hinge region to spread along the cast in situ concrete beam core without hindrance from the U-beam, and so avoid the possible concentration of the beam plastic hinge rotation in the region close to the end of the beam.

In the plastic hinge regions of the beams the reinforced concrete cast in situ core should be detailed according to the seismic design provisions for ductile frames.

1.2.3 Shear Strength of Beams

In the plastic hinge regions at the ends of composite beams the cast in situ reinforced concrete core will need to resist all the applied shear force alone, if the bond at the interface between the precast U-beam and the cast in situ concrete breaks down or if the bond is intentionally eliminated. Away from the ends of the beam the whole composite section may be considered to provide shear resistance.

The design shear force for the beam should be calculated using the likely beam overstrength in flexure. For finding the likely upper limit of flexural overstrength of the beam, composite action should be assumed in plastic hinge regions where negative moment is applied, since the flange of the U-beam can act as the compression zone of the composite member, as previously discussed. However for positive bending moment in plastic hinge regions at the ends of the member, only the cast in situ reinforced concrete beam core need be considered. If positive moment plastic hinges form away from the beam ends, the composite section flexural strength should be used if the interface shear and strand development length requirements are satisfied.

1.2.4 Interface Shear Transfer Between the Precast U-Beam and the Cast in Situ Concrete Core

Composite action of the beam can only occur if shear can be transferred across the interface between the adjoining precast and cast in situ concrete surfaces with practically no slip. Shear stress is transferred across the interface of concrete surfaces by concrete adhesion, interlock of mated roughened contact surfaces, and friction. Friction is reliant on a clamping force orthogonal to the contact plane. In the composite beam detail, reinforcement does not cross the contact surface and therefore does not provide a clamping force. Some small clamping force may be generated on the side faces of the cast in situ concrete core by the U-beam webs resisting, by flexural action, the dilatancy caused by relative shear movement along the roughened contact surfaces. Nevertheless it would seem appropriate to ignore friction and to rely only on shear transfer by adhesion and interlock of the mated roughened contact surfaces.

The imposed shear stresses at the interface of the surfaces are the summation of stresses from a number of sources. The imposed horizontal shear stresses at the interface during positive bending moment arise from the transfer of the prestressing steel tension force from the U-beam to the cast in situ concrete core, and during negative bending moment arise from the transfer of the reinforcing steel force from the cast in situ concrete core to the U-beam flange. The horizontal interface shear stress could be found from $V_u/b_v d$, where V_u = vertical shear force at factored (ultimate) load, b_v = total width of interface (two sides plus bottom surface) and d = effective depth of composite section. This is a simplistic approach to the more complex real behaviour of the U-shaped interface. The imposed vertical shear stresses at the interface arise

from the self weight of the U-beam unit, the floor system weight, and the superimposed dead and live loads being supported by the floor system. These vertical loads need to be transferred from the U-beam unit, on which the floor system is seated, to the cast in situ concrete core by vertical shear stresses across the interface (see Fig.2). This transfer of vertical shear stresses across the interface may be particularly critical if the end support of the U-beam in the column concrete is lost during seismic loading.

In the New Zealand concrete design code [3] an interface shear of 0.55 MPa (80 psi) is permitted at the factored (ultimate) load for interfaces that have no cross ties, but have the contact surfaces cleaned and intentionally roughened to a full amplitude of 5 mm (0.2 in).

I 2.5 Beam-Column Joints and Columns

Normal procedures of capacity design to determine the required shear and flexural strength levels, and seismic detailing as for cast in place structures, apply to the beam-column joints and the columns. The design shear forces for joint cores can be based on the internal forces from the cast in situ reinforced concrete beam core acting alone.

1.3 Experimental Research Into the Behaviour of Cast in Place Reinforced Concrete Frames Incorporating Precast Concrete Beam Shells Subjected to Simulated Seismic Loading

1.3.1 The Test Units

Three full scale composite beam-exterior column units have recently been tested [4]. The overall dimensions of the units are shown in Figs. 4, 7 and 8. For ease of construction of the units the T beam flanges typically resulting from the presence of the cast in situ concrete floor topping were not modelled.

Figs. 5 and 6 show the loading arrangements and test rig. By alternating the directions of the load at the end of the beam earthquake loading was simulated. The loading cycles were applied statically. The axial load on the column during the tests was held constant at $0.1f'_cA_g$, where f'_c = concrete compressive cylinder strength and A_g = gross area of column cross section. Superimposed dead loads were also applied to the beams to represent a 200 mm (7.9 in) thick precast concrete voided slab floor with 65 mm (2.6 in) thick concrete topping spanning between frames in the prototype building at 6.6 m (21.6 ft) centres. The positioning of the superimposed dead load was organised so that this load was applied only on the top horizontal surface of the precast U-beam webs, which is how the slab system in a real structure would be supported.

The reinforcement in the three units is shown in Figs. 7 and 8. Grade 275 ($f_y \geq 40$ ksi) steel was used for the beam longitudinal reinforcement and all transverse reinforcement; Grade 380 ($f_y \geq 55$ ksi) steel was used for the column longitudinal reinforcement. The concrete compressive strength was about 30 MPa (4,400 psi) for the cast in situ concrete and about 50 MPa (7,300 psi) for the precast concrete. At the level of column axial load applied, $0.1A_gf'_c$, the sum of the ideal flexural strengths of the column sections above and below the beam was 1.59 times the beam section ideal flexural strength, based on actual material strengths.

Unit 1 was detailed for seismic loading, with a potential plastic hinge region in the beam. Unit 2 was not detailed for seismic loading. Unit 3 was detailed for seismic loading and was identical to Unit 1 in all respects except that the interface between the precast concrete and the cast in situ concrete in the potential plastic hinge region of the beam was deliberately debonded in an attempt to improve the plastic hinge behaviour. The debonding in Unit 3 was achieved by fixing a 3.5 mm (0.14 in) thick sheet of foam rubber to the inside face of the precast U-beam, over a length equal to the depth of the cast in situ core, before casting the in situ concrete core. The seismic provisions of the New Zealand concrete design code [3] were used where possible. The provisions do not cover all aspects of the seismic design of composite systems.

1.3.2 Test Results

The beam and load versus beam end deflection hysteresis loops measured for the units are shown in Fig. 9. The loading consisted of two cycles to a displacement ductility factor of $\mu = \pm 1$, four cycles to $\mu = \pm 2$, four cycles to $\mu = \pm 4$, and two cycles to $\mu = \pm 6$. In the figure the dashed lines marked $+P_i$ and $-P_i$ represent theoretical flexural strengths based on the beam core alone, and $-P_i'$ is the theoretical flexural strength based on the composite section. Views of the units at the end of testing are also shown in Fig.9. At the final stages of testing there was spalling of concrete at the column face in the region of the beam seating. This damage could have been prevented if a gap had been formed between the sides and bottom of the precast U-beam and the cast in situ column concrete.

Fig. 9 shows that Units 1 and 3, which were designed for seismic loading, exhibited very satisfactory strength and ductility characteristics. In addition the hysteresis loops were not pinched and indicated satisfactory energy dissipation characteristics. In Unit 1 there was a tendency for the plastic hinging to spread along the cast in situ reinforced concrete core within the precast concrete U-beam, even during positive bending moment, and hence the plastic hinge rotation did not concentrate in the beam at the column face and no undesirable concentration of curvature resulted. In Unit 1 the precast concrete U-beam became extensively cracked during the tests. In Unit 3 the deliberate debonding of the interface concrete resulted in a longer plastic hinge length in the cast in situ concrete core and the precast concrete U-beam was not damaged during the testing. Although both Units 1 and 3 displayed satisfactory ductile behaviour during seismic loading, it may be considered that the debonded construction used in Unit 3 is to be preferred, in order to reduce the damage to the precast concrete U-beam shell during seismic loading.

Unit 2 was not designed for seismic loading. That is, the potential plastic hinge region was not detailed with closely spaced stirrup ties for ductility. Extensive sliding shear displacements occurred in the plastic hinge region of the beam and resulted in pinched hysteresis loops with low included area. In Unit 2 the spacing of stirrup ties in the potential plastic hinge region was 250 mm (9.8 in) compared with the 100 mm (3.9 in) spacing in Units 1 and 3. Evidently that spacing in Unit 2 was too large to assist dowel action of the longitudinal beam bars to prevent sliding shear from occurring at the column face. Also in Unit 2 the area of longitudinal reinforcement in the bottom of the cast in situ concrete core was only 0.47% of the core bd, where b = beam core width and d = beam core effective depth, and hence the positive moment flexural strength

of the core was insufficient to cause cracking of the precast U-beam. As a result, in Unit 2 the plastic rotation in the beam during positive bending moment was undesirably localised at a single crack at the column face. Therefore the area of the bottom steel in the core should be higher than used in Unit 2 (it was 1.4% of the core bd in Unit 1) in order to improve the plastic hinge behaviour.

It was concluded that Units 1 and 3 would be satisfactory for use in seismic resisting ductile frames, but that Unit 2 as designed would be suitable for non-seismic resisting frames where seismic loads are carried by walls or other structural systems.

2. SOME ASPECTS OF THE SEISMIC DESIGN OF BUILDING FRAMES INCORPORATING PRECAST CONCRETE MEMBERS AND POST-TENSIONING

2.1 Introduction

Codes in the past have discouraged the use of prestressed concrete for primary seismic resisting members. However the New Zealand concrete design code [3] now contains seismic design recommendations for prestressed and partially prestressed concrete frames based on information from theoretical and experimental studies which has become available in recent years.

An appealing use of prestressing in frames is as a means of achieving continuity between precast concrete members. The precast concrete beams and columns can be post-tensioned together on the site to form continuous seismic resistant frames. Combinations of cast in place and precast concrete members can also be made continuous by post-tensioning. Post-tensioned connections do not appear to have found favour in some countries because of extra materials, tolerance problems, and small amount of post-tensioning work required, and the unfamiliarity of the techniques by the trades. Also, in design account needs to be taken of movements caused by the volume changes of the concrete due to temperature, shrinkage and creep. However these connections generally perform well if care is taken in their detailing.

2.2 Seismic Design Considerations for Prestressed Concrete Frames

2.2.1 The Available Curvature Ductility of Prestressed and Partially Prestressed Concrete Members

A suspicion that exists concerning prestressed and partially prestressed concrete in seismic design is whether the plastic hinge section in a member can achieve the required curvature ductility factor.

Studies of the theoretical moment-curvature response of prestressed and partially prestressed concrete sections in New Zealand have concluded that design provisions can be developed to ensure ductile behaviour [5]. The theoretical moment-curvature (M-ϕ) relationships were computed using idealised stress-strain relationships for concrete and steel by satisfying the requirements of strain compatibility and equilibrium for the sections while incrementing the extreme fibre strain. The stress-strain relationships for the steel were obtained by fitting equations to measured stress-strain curves. The stress-strain relationship used for the confined core concrete was that proposed by Kent and Park [1] which allows for the effect of transverse steel content on the ductility of the concrete. For the cover concrete (outside the transverse steel) a stress-strain curve was used which was closer to that for uncofined

concrete. Note that for the concrete the parameter Z defines the slope of the falling branch of the stress-strain curve. Reasonable agreement was obtained between the theoretical M-ϕ curves when checked against measured experimental curves, providing the appropriate model for the behaviour of the cover concrete was selected [5].

Fig. 10 shows theoretical M-ϕ curves obtained for a section eccentrically prestressed by a bonded tendon near the extreme tension fibre. The stress-strain relation for the concrete assumes the presence of stirrup ties as in a plastic hinge region of a beam of a ductile frame. The reduction of the available curvature ductility shown in Fig. 10 with increasing content of prestressing steel has led to the recommendation [5] that for seismic design the following requirement should be observed

$$a/h \leqq 0.2 \qquad (1)$$

where a = depth of equivalent rectangular concrete compressive stress block and h = overall depth of member. This recommendation has now been included in the New Zealand concrete design code [3]. For the section shown in Fig. 10, Eq. 1 leads to the requirement that $A_{ps}/bh \leqq 0.0046$. It is evident from the curves of that figure that this requirement should ensure adequate curvature ductility.

It is also of interest to compare the theoretical moment-curvature (M-ϕ) relationships for sections with different arrangements of prestressing steel. In seismic design moment reversals will require many sections to have both negative and positive moment strength and hence tendons will often exist near both extreme fibres of the section and near mid-depth. Fig. 11 shows theoretical M-ϕ curves for the section with up to five bonded tendons symmetrically placed down the depth. The total prestressing steel content is the same for each of the five cases, being 0.00696 of the gross concrete section. For the case of all steel concentrated in a single central tendon, N = 1, the moment capacity is more sensitive to a deterioration of the compressed concrete and a significant reduction of moment capacity occurs at high curvatures. However there is little difference in the moment capacity for two or more tendons at high curvatures. Therefore two or more tendons, with some tendons near both extreme fibres of the section, are to be preferred.

The theoretical study also showed that the presence of nonprestressed longitudinal reinforcement in the compression zone increased the available ductility of the section. Thus partially prestressed sections can be used to advantage in seismic design.

Theoretical moment-curvature relations under cyclic (reversed) loading for prestressed concrete, reinforced concrete, and partially prestressed concrete sections, ranging from fully prestressed to reinforced, subject to cyclic loading in the inelastic range, have also been derived previously [6, 7]. These theoretical analyses have been based on idealised models for the stress-strain behaviour of concrete and steel. The effect of spalling (crushing) of the concrete cover outside the stirrups was considered. Fig. 12 shows the agreement between theoretical and measured cyclic moment-curvature relationships obtained for a partially prestressed concrete section [7]. For the section in Fig. 12 the nonprestressed longitudinal reinforcement had a total area (top plus bottom) of 1.09% of the concrete sectional area and was of Grade 275 steel ($f_y \geqq 40$ ksi). The prestressing

tendons were grouted and the uniform concrete compressive stress due to prestress at transfer was 4.66 MPa (675 psi).

The section in Fig. 12 was partially prestressed and it is evident that the energy dissipation as represented by the area within the hysteresis loops is significant. For "fully" prestressed sections (without nonprestressed longitudinal reinforcement) the hysteresis loops are more pinched, resulting in smaller energy dissipation. This is because for fully prestressed concrete the initial elastic tensile strain in the tendons due to prestress cause a large deflection recovery, even after large deflections. The theoretical and measured moment-curvature behaviour for cyclically loaded members confirmed that the introduction of nonprestressed reinforcing steel into a prestressed concrete section reduces the stiffness degradation and significantly increases the energy dissipation capacity of the section when subject to cyclic flexure in the inelastic range. It was found that the energy dissipation capacity of a fully prestressed concrete member, as measured by the area within the cyclic moment-curvature hysteresis loops, may be as little as 0.15 times that of a reinforced concrete section of comparable size and flexural strength.

2.2.2 Dynamic Response of Prestressed Concrete Systems

A further suspicion that exists concerning prestressed and partially prestressed concrete in seismic design is whether the energy dissipation at the plastic hinge regions of members is adequate to prevent very large displacement responses of the structure to severe earthquake ground motions.

Studies have been conducted on the nonlinear dynamic response of prestressed, partially prestressed, and reinforced concrete single-degree-of-freedom systems to severe earthquake ground shaking [8,9]. The moment-curvature loops in the study by Thompson and Park [9] were idealised as shown in Fig. 13 for prestressed concrete, reinforced concrete and partially prestressed concrete. As expected, it was found that the lower hysteretic energy dissipation of a prestressed concrete system, compared with that of a reinforced concrete system of similar strength and initial stiffness, generally resulted in a greater deflection response of the prestressed concrete system to a severe earthquake. This difference in deflection response for code designed single-degree-of-freedom structures of similar strength, initial stiffness and viscous damping, responding nonlinearly to the 1940 El Centro and synthetic earthquakes was found on average to be approximately 30%. The New Zealand loadings code [2] requires the design seismic load used for prestressed concrete to be 25% greater than that used for a similar reinforced concrete structure to account for this difference.

2.3 Some Structural Configurations for Frames Utilizing Precast Partially Prestressed Components

In New Zealand some prestressed concrete frame buildings designed for earthquake resistance have been constructed, typically three storeys or less. Fig. 14 shows such a building structure in which the columns were pretensioned and precast without joints, in lengths equal to the full height of the building. The beams were lightly pretensioned and were precast in lengths to occupy the clear spans between columns. Therefore the jointing faces between adjacent precast members were at the beam ends and the column faces. Moist pack sand-cement mortar joints 25 mm (1 in)

thick were formed between the faces of the elements. The frame was made continuous by post-tensioned tendons which were placed in the beams and extended through the columns. The tendons were grouted. The tendons in the beams were draped so as to load balance the gravity loads which were considered to be present at the time of the earthquake (dead load plus a proportion of the live load). At the joints at the ends of the beams the prestress was generally close to concentric with the tendons spread down the depth of the section in order to resist the negative and positive moments caused by seismic load reversals.

There are many possible configurationa of precast concrete structural elements which can be used to form frames made continuous by post-tensioning. The tendons should be grouted to ensure that the ductility of the plastic hinge sections is as large as possible. Some possible structural configurations for interior beam-column connections of precast partially prestressed frames with plastic hinge regions located in the beams are shown in Figs. 15, 16 and 17. The jointing material between the connecting faces of the adjacent components can be cement-sand mortar or other suitable material. The connecting faces should be roughened or keyed to ensure good shear transfer and the retention of the jointing material after cracking. Special transverse steel, in the form of stirrup-ties in the beams and hoops or spirals in the columns, is necessary in the potential plastic hinge regions. Such steel is essential to provide concrete confinement, to prevent buckling of compression bars,and to act as shear reinforcement.

System 1 shown in Fig. 15 is that used for the building of Fig. 14. The jointing faces between the precast components are in the potential plastic hinge regions of the beams. The columns may be pretensioned and/or reinforced with nonprestressed steel. The beams, precast to occupy the clear span between columns, may be lightly pretensioned and/or reinforced with nonprestressed steel for handling purposes.

System 2a shown in Fig. 16 is an alternative scheme which removes the jointing faces between precast components from the plastic hinge regions in the beams. This system enables the presence of nonprestressed steel in the plastic hinge region in the beams, thus achieving better ductility and energy dissipating characteristics. The columns are precast in lengths to occupy only the clear height between floors. The beams are jointed within the spans. The frame is made continuous by post-tensioning the beams and by using coupled post-tensioned tendons or coupled nonprestressed reinforcement in the columns. System 2b shown in Fig. 16 is a further improvement on System 2a in that the additional nonprestressed reinforcement in the beam ends is designed to shift the critical moment sections away from the column faces and thus allow easier detailing of the joint core for shear and bond.

System 3a shown in Fig. 17 consists of cruciform shaped precast components, thus allowing plastic hinging to occur in the beams adjacent to the columns but away from the jointing faces. The frame is made continuous by post-tensioning the beams and by using coupled post-tensioned tendons or coupled nonprestressed reinforcement in the columns. System 3b shown in Fig. 17 is a further improvement on System 3a in that the additional non-prestressed reinforcement at the beam ends is designed to shift the critical moment sections away from the column faces to ease the detailing of the joint core for shear and bond. Both Systems 3a and b allow the presence of nonprestressed reinforcement in the plastic hinge zones of the beams. Another variation on System 3 is to joint the columns at each alternate

storey or the beams at each alternate span to give double cruciform shape units. This variable is only possible if the crane capacity is sufficient to lift the larger units into place. System 3 can be used to advantage when the beam spans are small.

There are many other variations on the systems shown in Figs. 15, 16 and 17 which can be used.

Small building frames in which plastic hinges are permitted to occur in the columns (that is, in which column sidesway mechanisms are allowed) can also be designed by choosing an appropriate system. Systems 1 and 3 appear to be the best for such frames.

2.4 Experimental Research into the Behaviour of Precast Concrete Frames Made Continuous by Post-Tensioning

Tests on four full-scale precast prestressed beam-column subassemblies under cyclic loading of high intensity have been previously reported [10]. The subassemblies were representative of exterior beam-column joints and the section sizes were similar to those of the existing building frame shown in Fig. 14. A subassembly under test is shown in Fig. 18. The columns were pretensioned, the beams were lightly pretensioned, and the subassembly was made continuous by post-tensioning the beams with tendons which passed through the columns into an exterior anchor block and were grouted. Moist pack joints 25 mm (1 in) thick existed between the column faces and the ends of the beams. Either two or three post-tensioned tendons existed in each beam, arranged concentrically with one in the top, one in the bottom and, when a third tendon existed, one at mid-depth of the section. This post-tensioning arrangement is similar to that used in the prototype structure. Static cyclic loading was used to simulate seismic loading. The relative flexural strengths of the beams and columns were such that when the sub-assemblies were subjected to simulated severe seismic loading the plastic hinges formed in either the beams or the columns. In two subassemblies (Units 3 and 4) the plastic hinges occurred in the columns at the joint, and in the other two subassemblies (Units 1 and 2, shown in Fig.19) plastic hinges occurred in the beam at the joint.

The tests showed that large post-elastic deformations can be available in prestressed members with bonded tendons. Probably the most interesting result was from the subassemblies in which plastic hinges formed in the beams at the column faces (Unit 1 and 2 of Fig.19) since the mortar joint was in the plastic hinge region in this case. Some concern had been expressed about the behaviour of mortar joints between precast members when subjected to seismic load reversals since it was felt that when wide cracking occurred at the mortar-precast concrete interface some of the mortar could fall away leaving the joint in poor condition when the moment reversed and the cracks attempted to close. In these tests the surfaces of the precast members at the joint had been roughened to a depth of approximately 16 mm (0.63 in) to help hold the mortar. In addition, two of the assemblies (Units 2 and 4) had a light wire stirrup in the mortar to help prevent loss of material. It was found that when the plastic hinge formed in the beam at the mortar joint the mortar was held in place even when the stirrup was not present. The plastic curvature extended well along the beam and did not concentrate only in the mortar. The plastic hinge region behaved in a similar manner to that expected of a monolithic joint, except that cracking occurred at the mortar-precast concrete interface earlier because of the lack of tensile strength.

Fig. 20a shows for one assembly (Unit 2) the measured beam plastic hinge moment versus beam end displacement curves, Fig. 20b shows the state of the joint at the end of the final loading run with beam negative moment applied, and Fig. 20c shows the state of the joint at the final loading run with beam positive moment applied.

In the assembly shown in Fig. 20b and c (Unit 2) a bond failure did not occur between the grouted prestressing duct and the column. However in Unit 1 a bond failure did occur in the column region, and the compressed tendon punched through the column and pushed off one end of the anchor block. Smooth metal ducts had been used. It is recommended that grouted corrugated metal ducts should be used to minimize the possibility of tendons being pushed through the column. Note that bond is important since at very large deformations the tendon in the compression zone aids the ductility of the section by acting as compression reinforcement. Thus grouting and corrugated ducts are necessary in fully prestressed members in order to improve the ductility of the sections at large inelastic deformations.

2.5 Unbonded Tendons in Frame Members

The use of unbonded tendons in frame members in seismic design has caused considerable controversy. It is considered that the use of unbonded post-tensioned tendons in prestressed concrete frames is undesirable for the following reasons:

(a) Unbonded tendons remain in the elastic range and therefore total reliance is placed on the concrete for energy dissipation and compressive strength.

(b) The ductility of a member with unbonded tendons is likely to be provided by inelastic flexural strains associated with a single wide crack at the critical section. The reduced equivalent plastic hinge length, in comparison with that for a bonded tendon, may significantly reduce the available displacement ductility factor.

(c) It is difficult to accurately predict the ultimate moment capacity of sections with unbonded tendons under reversed loading. Consequently, column moments induced by beam overstrength are equally difficult to predict.

(d) Fluctuation of tendon forces during seismic load reversals could cause failure of the anchorages of unbonded tendons with the catastrophic result of release of prestressing force.

(e) Grouted tendons in the concrete compression zone can act as compression reinforcement and improve the ductility of the member at large curvatures, whereas unbonded tendons cannot act as compression reinforcement.

These arguments are less valid when the prestress is used to balance gravity loads, with nonprestressed steel reinforcement providing the bulk of the seismic resistance. Under these circumstances unbonded tendons may be permitted, provided that the nonprestressed reinforcement provides the major part of the design resisting moment for earthquake plus gravity load combinations and that the anchorages are detailed so that anchorage failure or detensioning cannot occur under seismic loads.

There would appear to be no real objection to the use of unbonded tendons in floor or roof systems not contributing to the seismic strength of the frame.

3. CONCLUSIONS

The use of precast concrete in buildings has a number of attractive features. Composite frame systems combining precast concrete beam shells and cast in place reinforced concrete can be designed to perform in a ductile manner. Similarly, precast concrete beams and columns can be post-tensioned together on the site to form continuous frames. Tests have shown that design provisions can be developed to enable such systems to be used for primary seismic resisting structures.

ACKNOWLEDGEMENTS

The author acknowledges the research work conducted by Dr. R.W.G. Blakeley, Dr. K.J. Thompson and Mr. D.K. Bull while graduate students at the University of Canterbury.

REFERENCES

1. Park, R. and Paulay, T., "Reinforced Concrete Structures", John Wiley and Sons, New York, 1975, p.769.

2. "Code of Practice for General Structural Design and Design Loadings for Buildings NZS 4203:1984", Standards Association of New Zealand, Wellington, 1984.

3. "Code of Practice for the Design of Concrete Structures NZS 3101:1982", Standards Association of New Zealand, Wellington, 1982, p.127.

4. Park, R. and Bull, D.K., "Behaviour of Cast In Situ Reinforced Concrete Frames Incorporating Precast Concrete Beam Shells Subjected to Seismic Loading", Bulletin of the New Zealand National Society for Earthquake Engineering, Vol. 17, No. 4, December 1984, pp.223-250.

5. Thompson, K.J. and Park, R., "Ductility of Prestressed and Partially Prestressed Concrete Beam Sections", Journal of the Prestressed Concrete Institute, Vol. 25, No. 2, March-April 1980, pp.46-70.

6. Blakeley, R.W.G. and Park, R., "Prestressed Concrete Sections With Seismic Loading", Journal of the Structural Division, American Society of Civil Engineers, Vol. 69, St8, August 1973, pp.1717-1742.

7. Thompson, K.J. and Park, R., "Moment-Curvature Behaviour of Cyclically Loaded Structural Concrete Members", Proceedings of Institution of Civil Engineers, Part 2, Vol. 69, June 1980, pp.317-341.

8. Blakeley, R.W.G. and Park, R., "Response of Prestressed Concrete Structures to Earthquake Motions", New Zealand Engineering, Vol. 28, No. 2, February 1973, pp.42-54.

9. Thompson, K.J. and Park, R., "Seismic Response of Partially Prestressed Concrete Systems", Journal of Structural Division, American Society of Civil Engineers, Vol. 106, No. ST8, August 1980, pp.1755-1775.

10. Blakeley, R.W.G. and Park, R., "Seismic Resistance of Prestressed Concrete Beam-Column Assemblies", Journal of the American Concrete Institute, Proc. Vol. 28, No. 9, September 1971, pp.677-692.

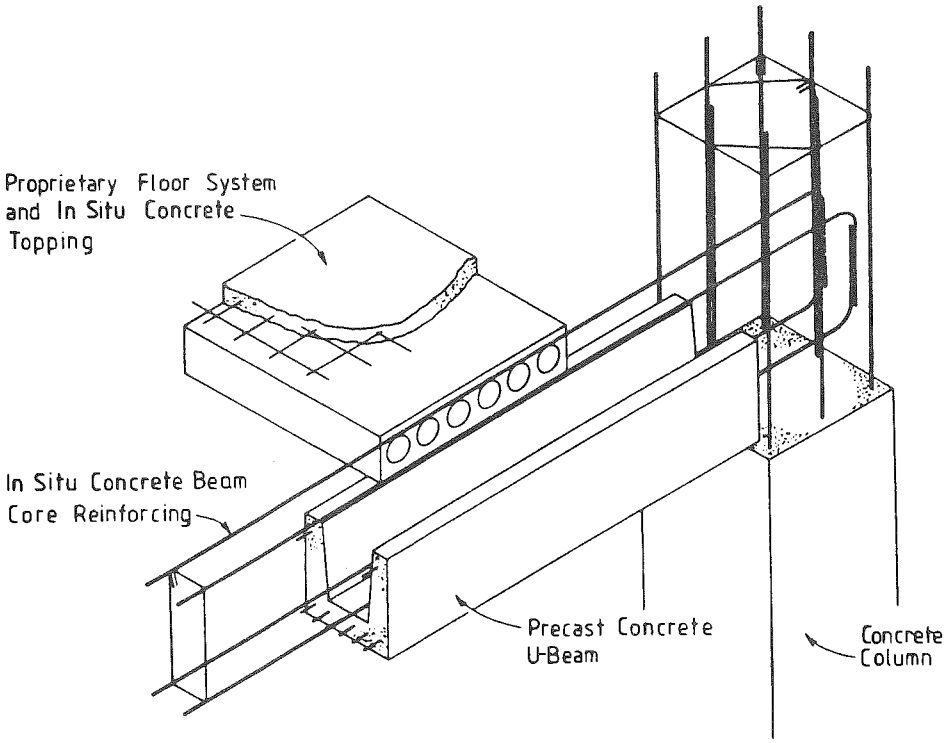

Fig. 1 Construction Details of a Composite Structural System (not all reinforcement shown).

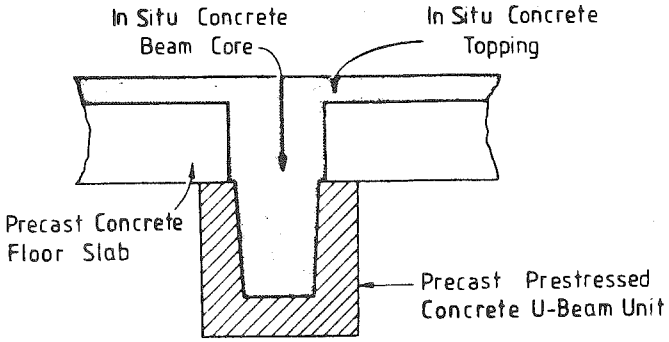

Fig. 2 Section of Composite Beam in Finished Structure (Reinforcement not shown).

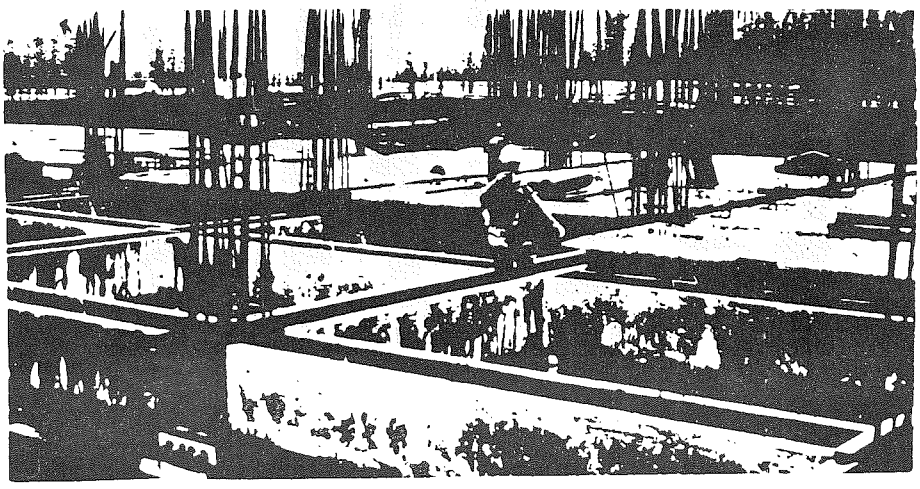

Fig. 3 Precast Concrete U-Beams Used as Permanent Shuttering for Cast-in-Place Reinforced Concrete Frames (Karioi Mill Building, New Zealand).

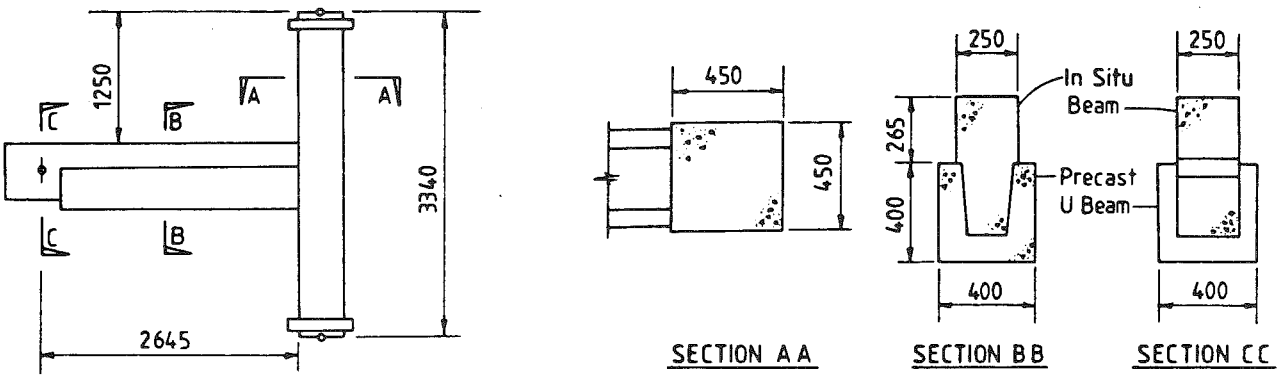

Fig. 4 Elevation and Sections of Test Units (Dimensions in mm) [4].

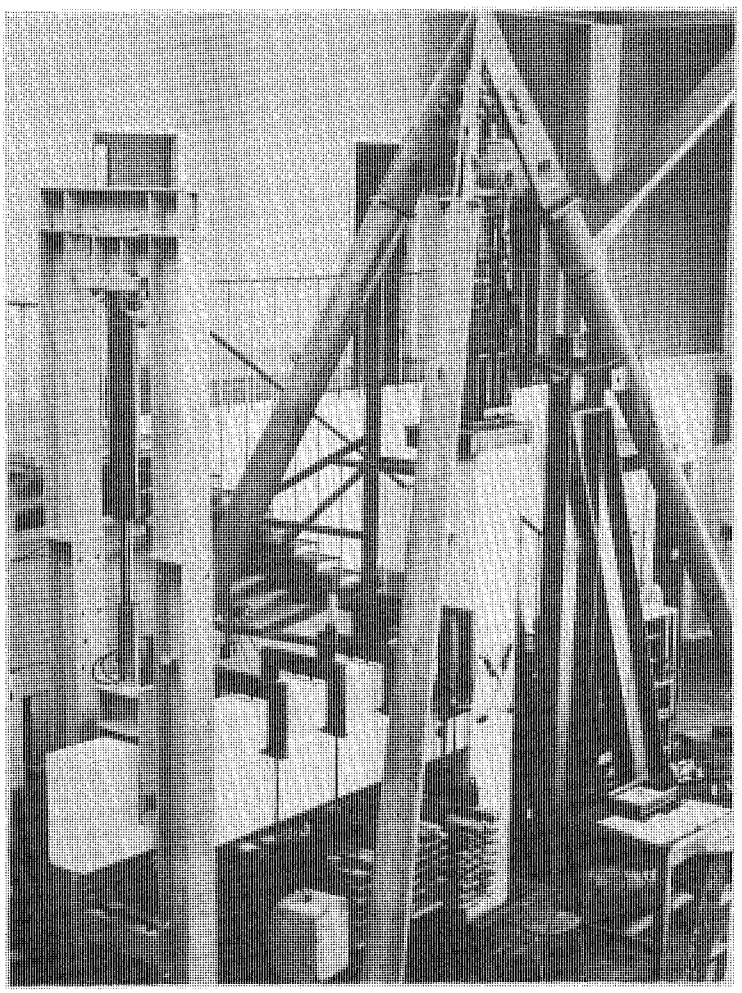

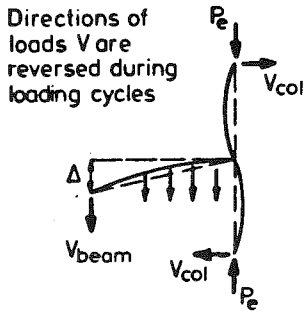

Fig. 5 External Loads Applied [4].

Fig. 6 View of Test Rig [4].

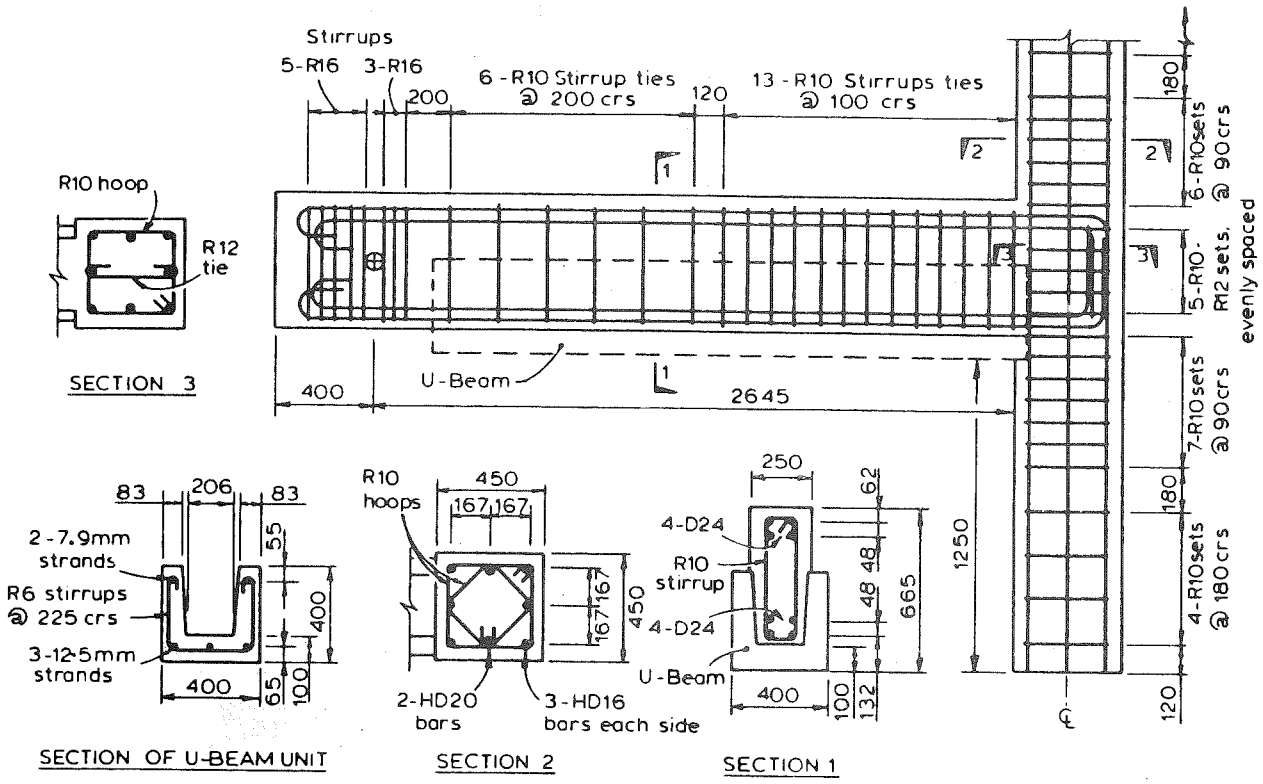

Fig. 7 Details of Reinforcement of Units 1 and 3 [4].

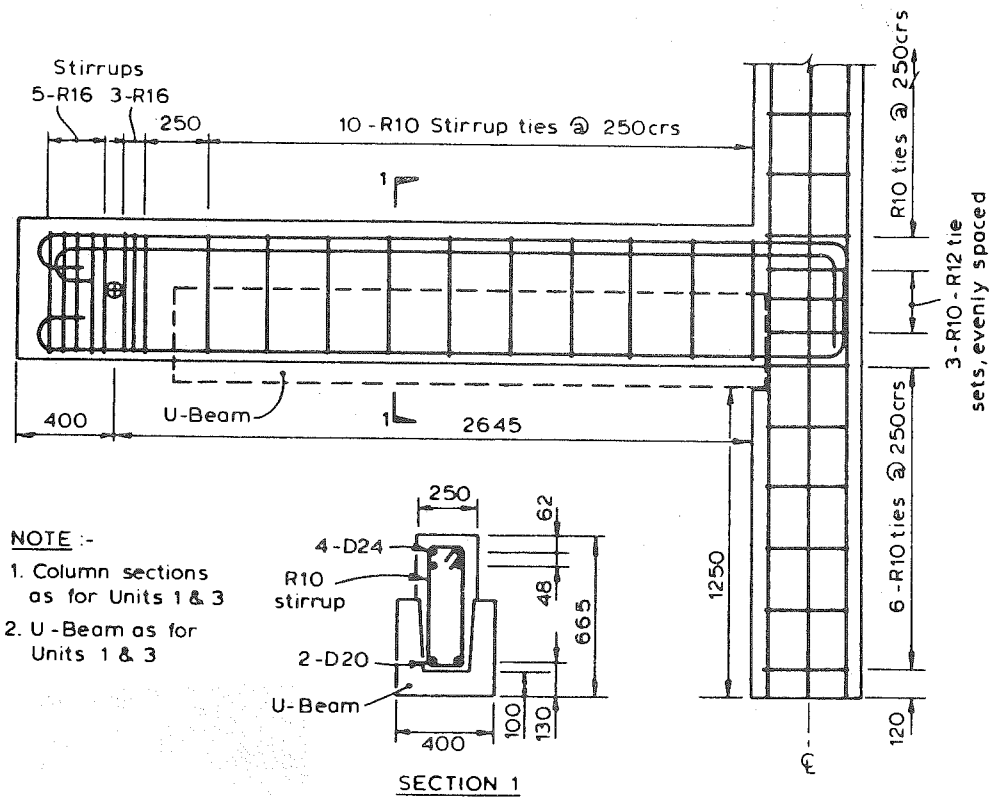

Fig. 8 Details of Reinforcement of Unit 2 [4].

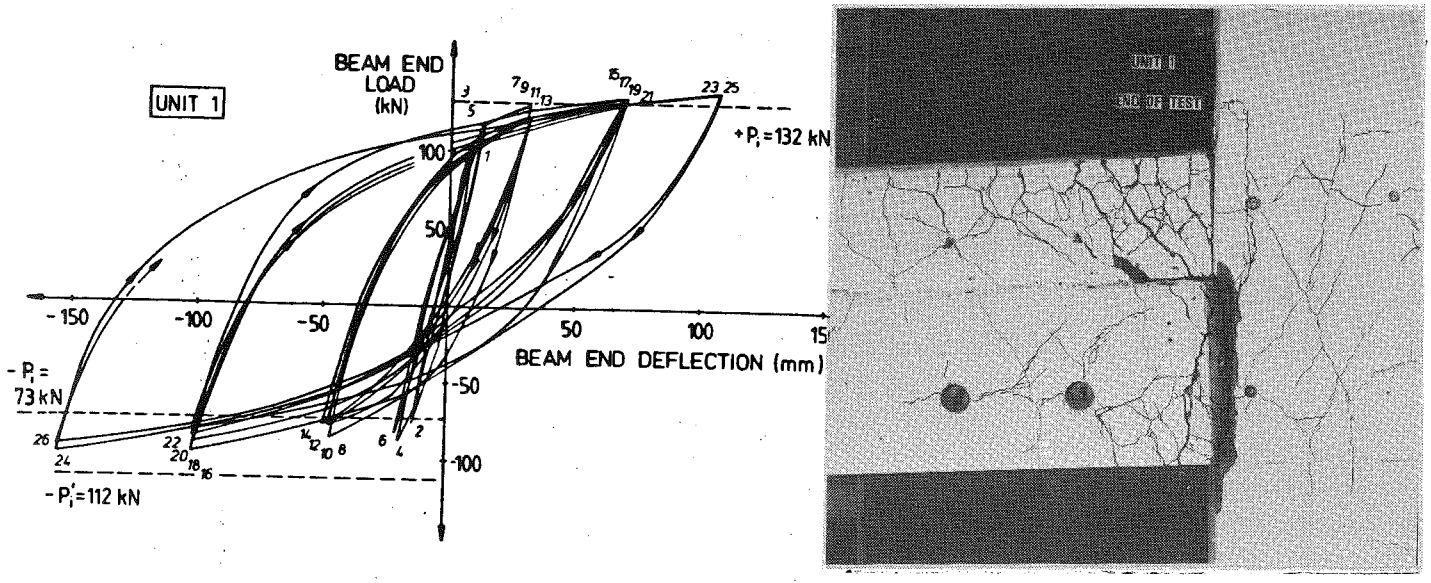

(a) Unit 1

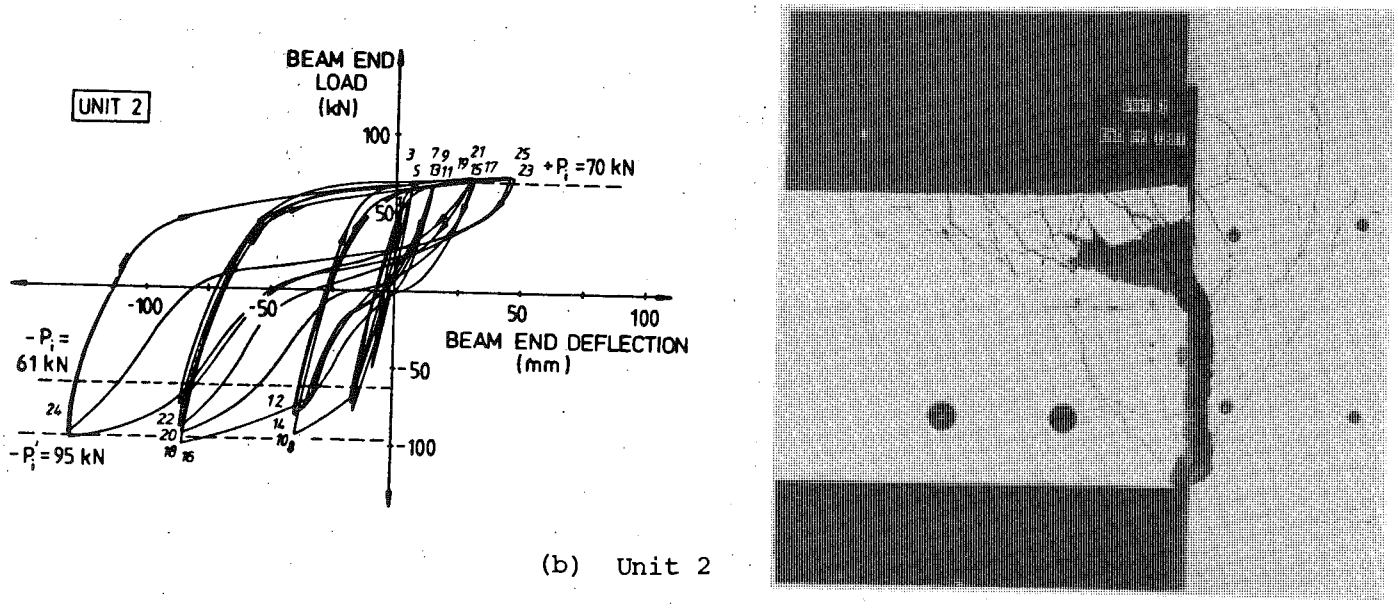

(b) Unit 2

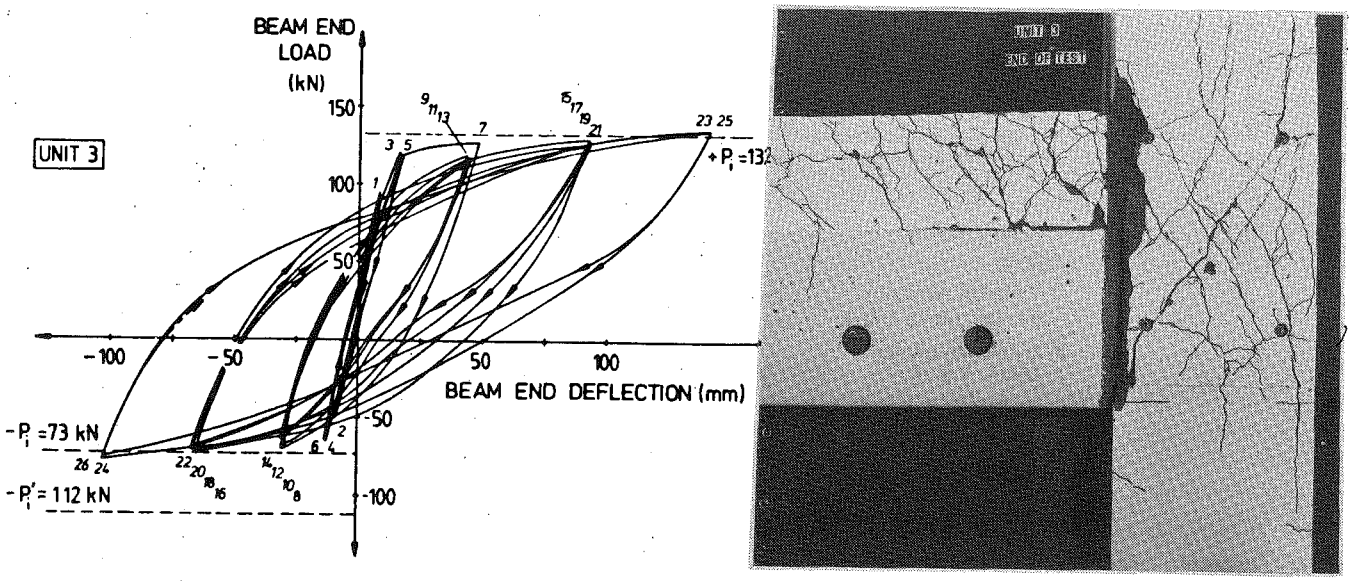

(c) Unit 3

Fig. 9 Beam End Load Versus Beam End Deflection and View of Units at End of Testing [4].

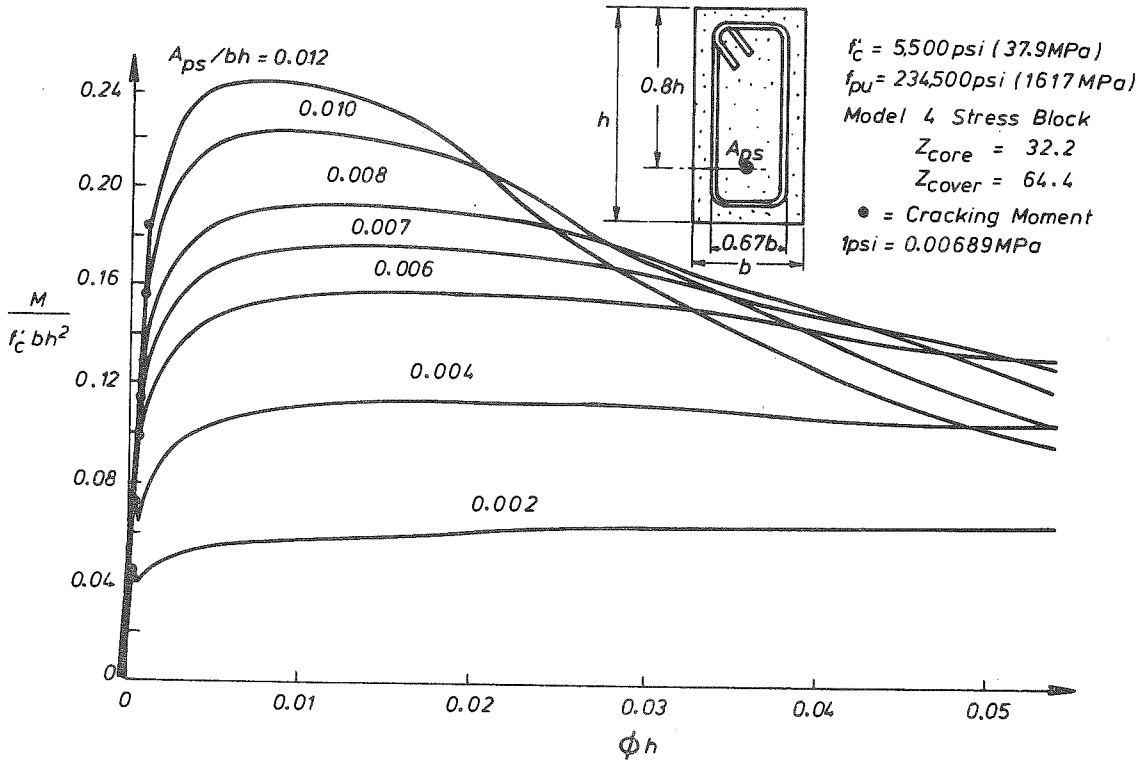

Fig. 10 Effect of Content of Prestressing Steel on Analytical Moment-Curvature Relation with One Tendon Position [5].

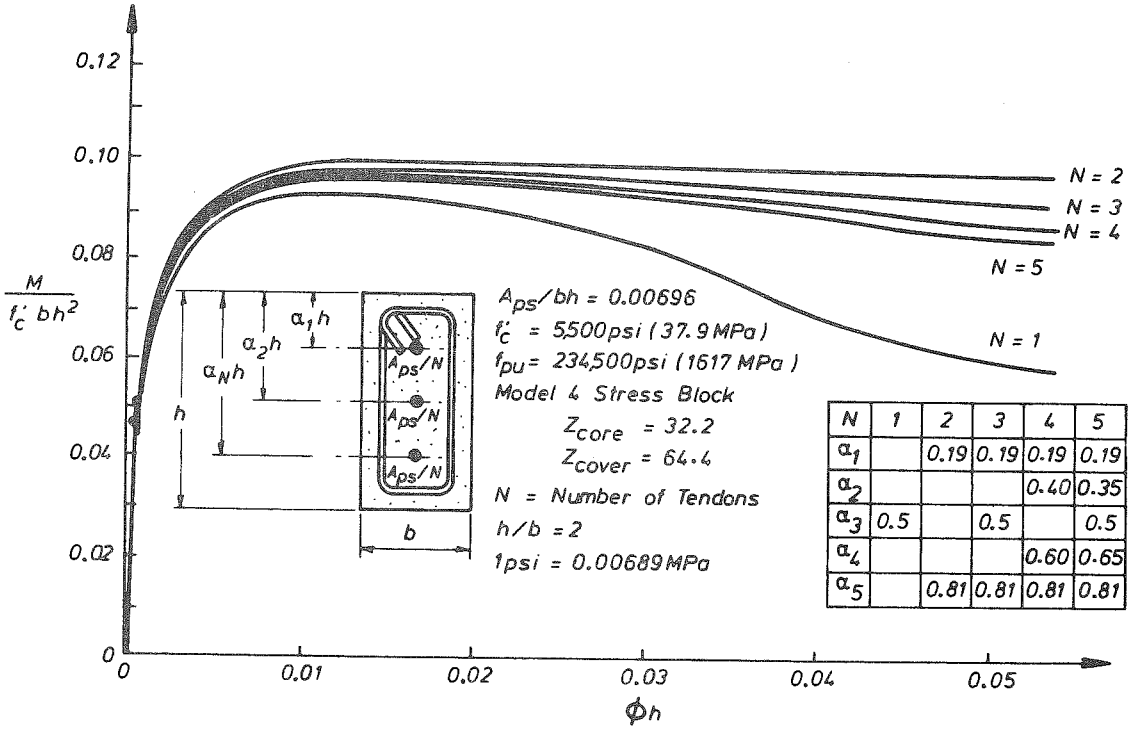

N	1	2	3	4	5
α_1		0.19	0.19	0.19	0.19
α_2				0.40	0.35
α_3	0.5		0.5		0.5
α_4				0.60	0.65
α_5		0.81	0.81	0.81	0.81

Fig. 11 Effect of Distribution of Prestressing Steel on Analytical Moment-Curvature Relation [5].

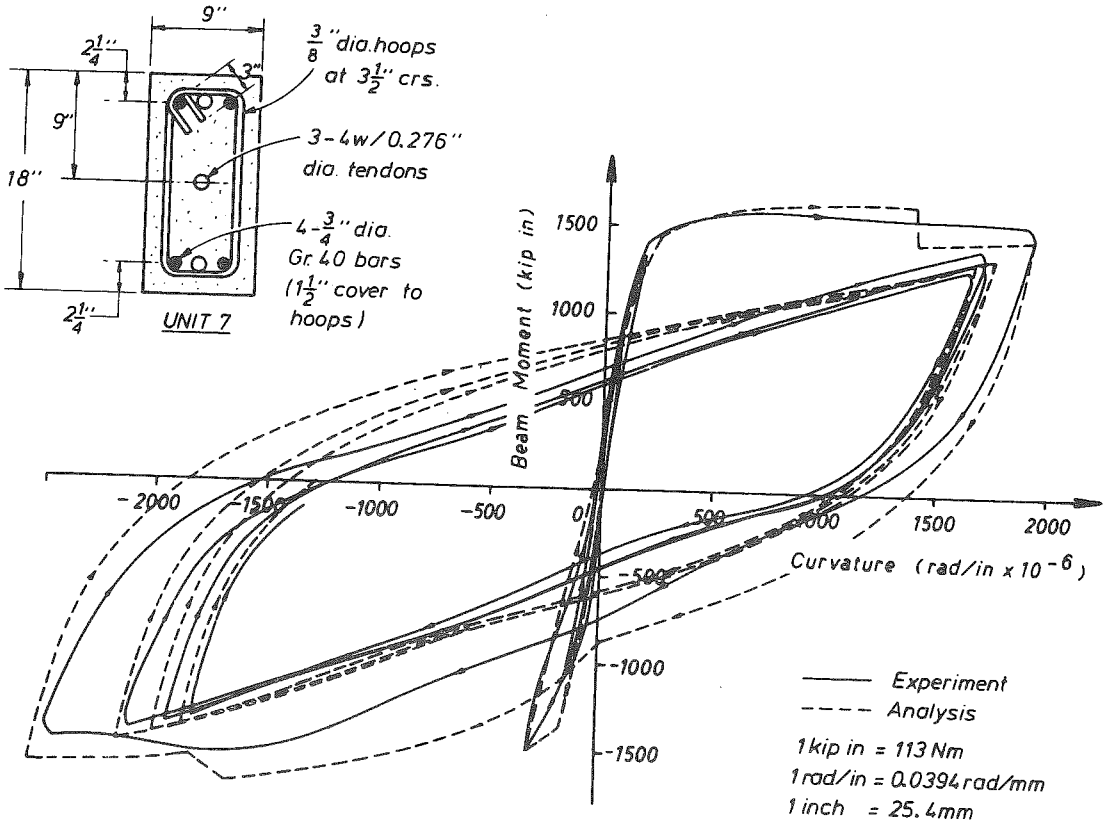

Fig. 12 Theoretical Moment-Curvature Relation Compared with Experimental Relation for Partially Prestressed Concrete Beam of Unit 7 [7].

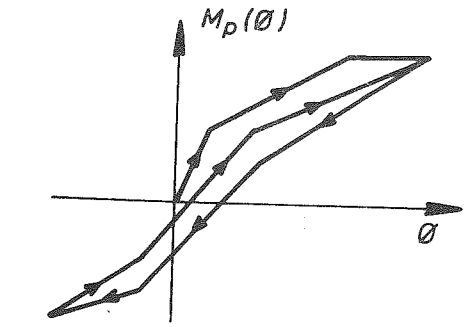

(a) Prestressed Concrete System

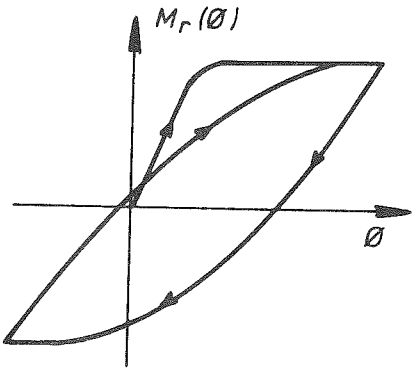

(b) Reinforced Concrete System

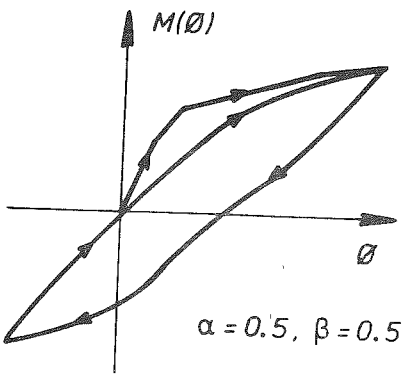

(c) Partially Prestressed Concrete System

Fig. 13 Moment-Curvature Idealizations [9].

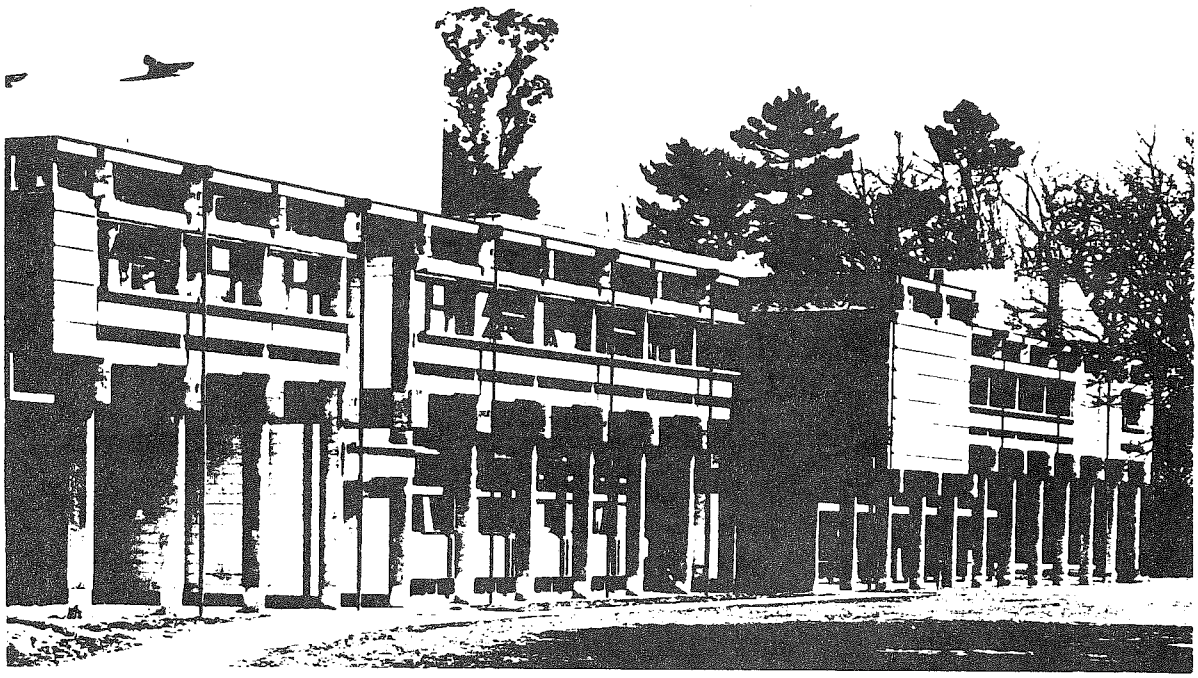

Fig. 14 Precast Post-Tensioned Prestressed Concrete Building Frames (Students Association, University of Canterbury, New Zealand.

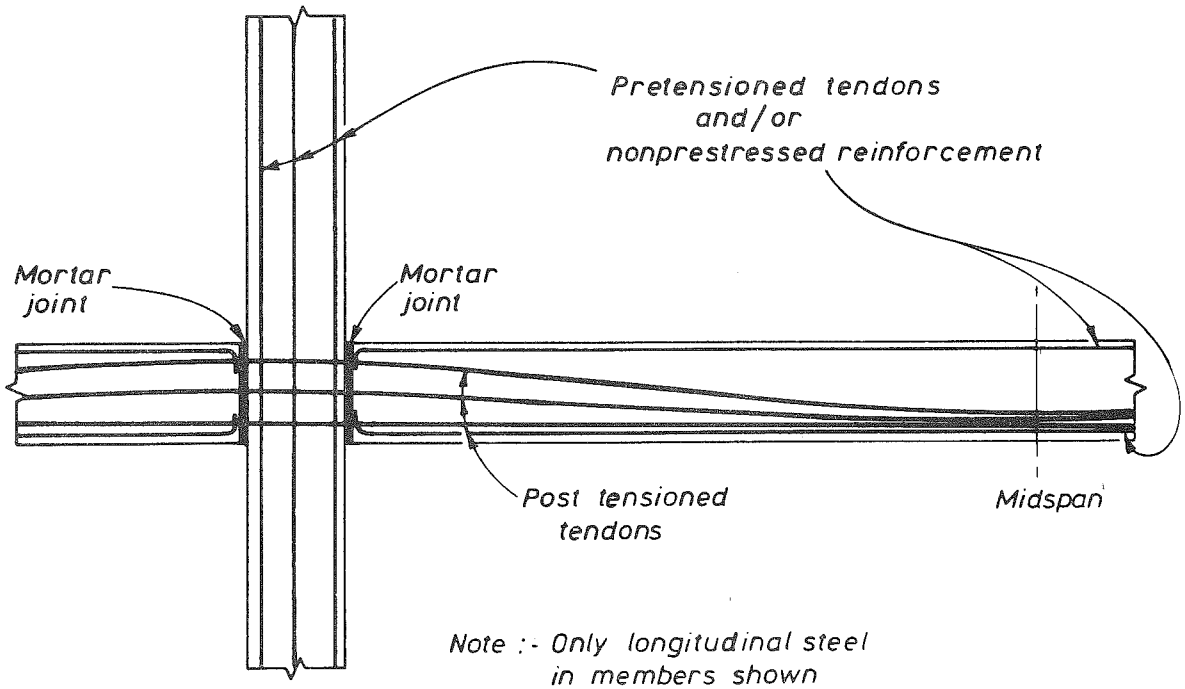

Fig. 15 System 1 Structural Configuration for Constructing Continuous Frames from Precast Concrete Elements.

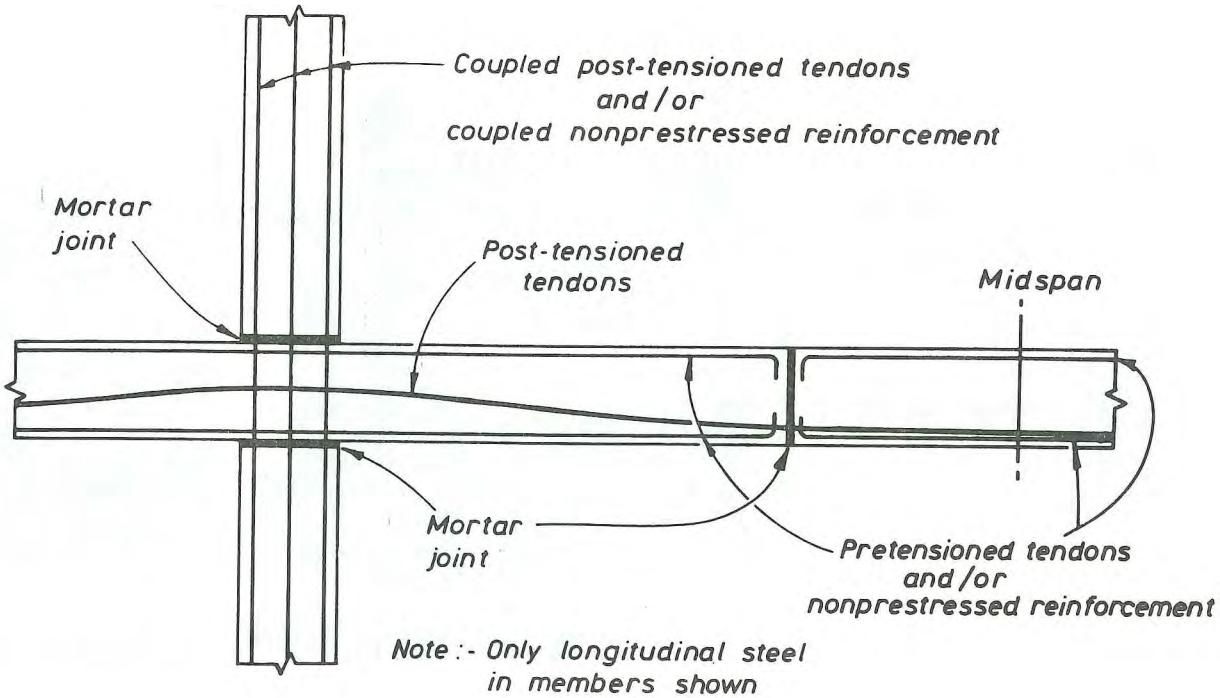

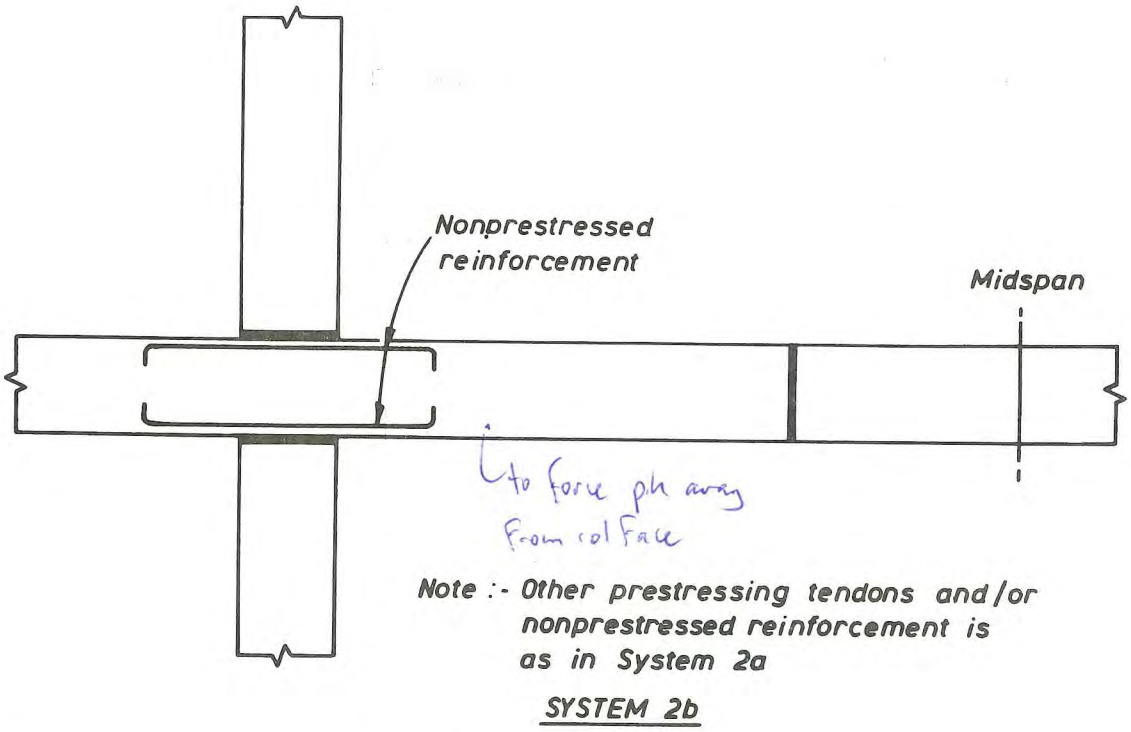

Fig. 16 System 2 Configurations for Constructing Continuous Frames from Precast Concrete Elements.

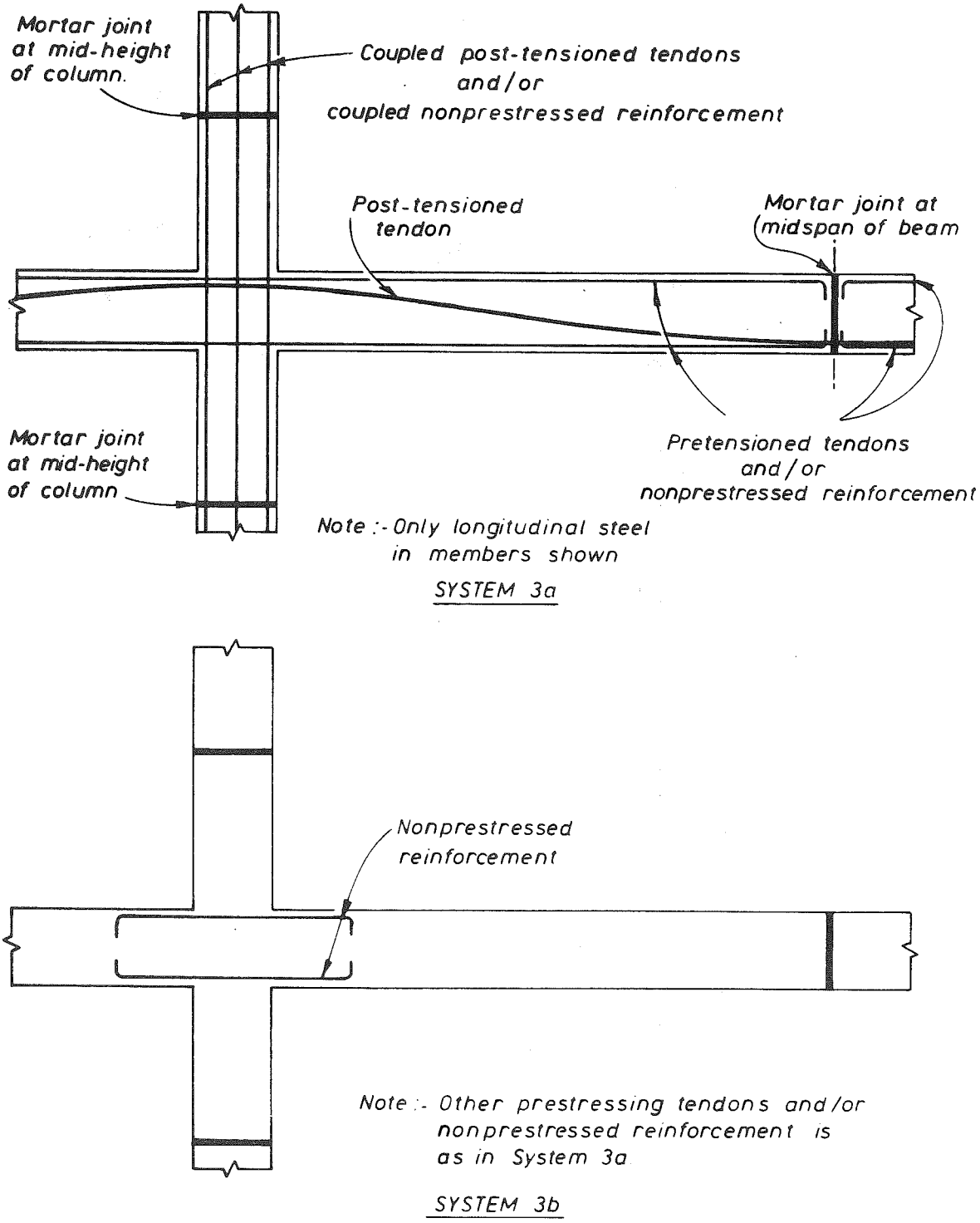

Fig. 17 System 3 Structural Configurations for Constructing Continuous Frames from Precast Concrete Elements.

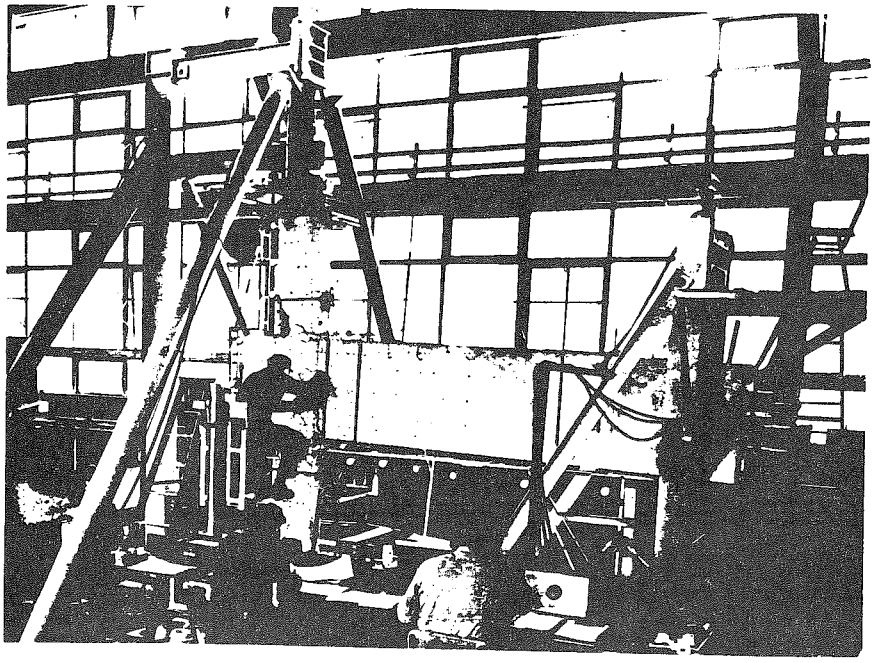

Fig. 18 Precast Post-Tensioned Prestressed Concrete Beam-Column Frame Subassembly Under Test [10].

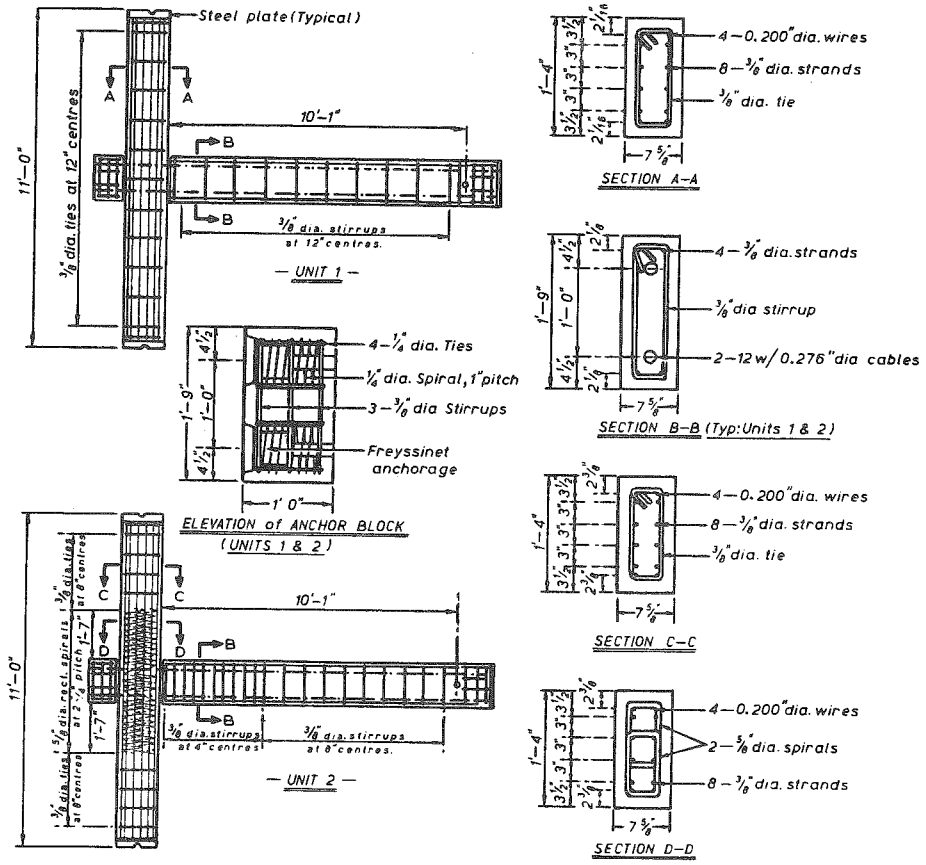

Fig. 19 Details of Precast Post-Tensioned Prestressed Concrete Beam-Column Frame Subassemblies (Units 1 and 2) [10].

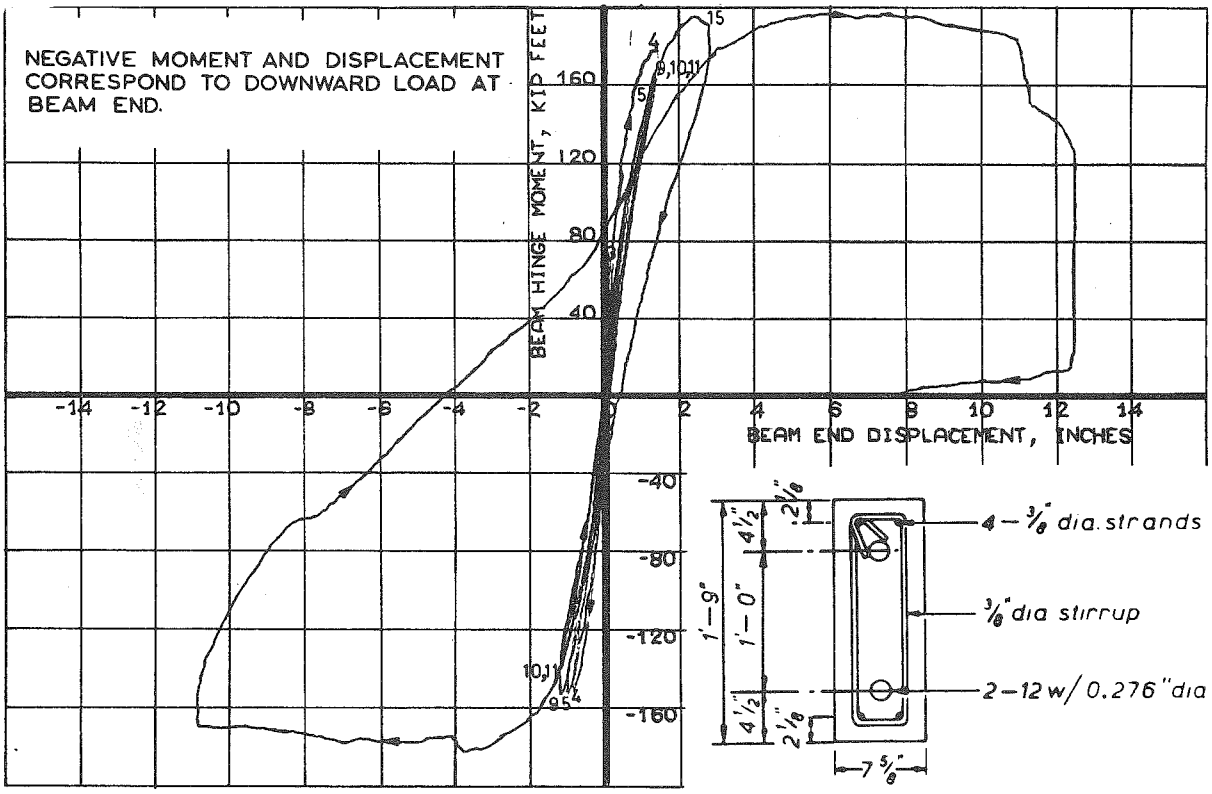

(a) Measured Beam End Displacement Versus Beam Plastic Hinge Moment.

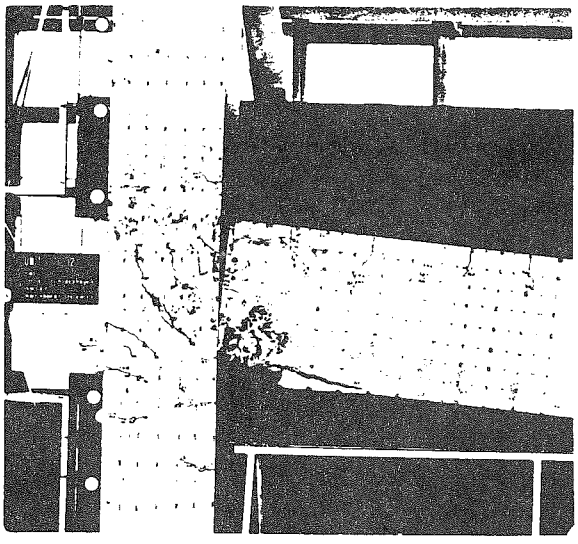

(b) Joint at End of Downward Loading on Beam

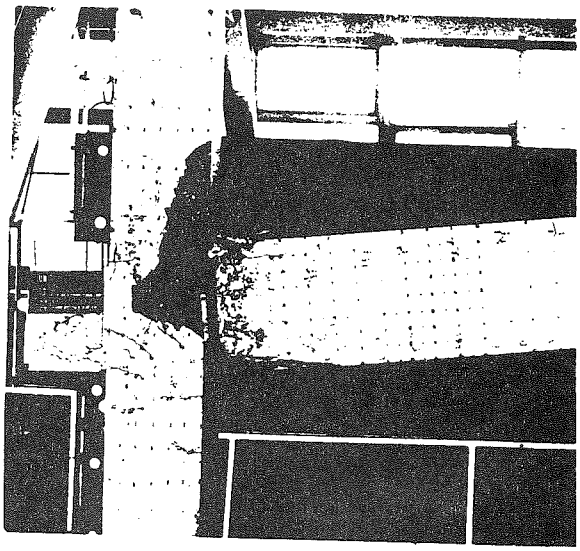

(c) Joint at End of Upward Loading on Beam

Fig. 20 Precast Post-Tensioned Prestressed Concrete Beam-Column Subassembly Test (Unit 2) [10].

CONCRETE STRUCTURES FOR THE STORAGE OF LIQUIDS

M.J.N. Priestley, J. Vessey and P.J. North

CONCRETE STRUCTURES FOR THE STORAGE OF LIQUIDS

The New Draft SANZ Code

by M.J.N. Priestley, J. Vessey and P.J. North

Background to provisions of the new draft code is given, with particular emphasis on thermal, seismic, creep and shrinkage effects. The significance of different aspects is assessed by reference to a design example involving a 7500 m^3 circular tank.

1. INTRODUCTION

In 1978, two documents entitled 'Code of Practice for Concrete Structures for the Storage of Liquids' Parts 1 and 2 were promulgated, intended to replace the technical requirements of NZS 1900:Chapter 11.1:1964[1]. The first of these, NZS 3106P Part 1:1978[2], a provisional standard, represented comparatively minor changes to the approach and substance of the 1964 document. The second document, published by SANZ as DZ 3106 Part 2[3], a draft for comment, contained a radically different 'crack control' approach, where design was basically controlled by calculated crack widths under service load conditions. This second document also contained much more detailed advice on seismic loading, temperature stresses, and effects of creep and shrinkage.

A small committee was formed in 1983 to reconcile the two approaches, and produce a new, single draft for comment, replacing both the earlier publications. In doing so, the committee was mindful of considerable resistance in the design profession to the 'crack control' approach. One of the reasons for this resistance was the uncertainty of crack control equations : different available equations result in a wide range of predicted crack widths, and the applicability of any of the equations to cracking of, for example, circular shell structures has yet to be established experimentally. For this reason, the 1984 draft code[4] reverts to the earlier concept of governing design by specifying limiting stress levels under service loads.

It is significant that this approach is contrary to the current trend to design structures in accordance with ultimate strength theory. However, ultimate strength design using factored loads is seen to be inappropriate when the basic design load (that of the contained liquid) is known to a comparatively high precision. Thus a load factor reflecting the uncertainty of magnitude of fluid loading would be close to unity. Similar conclusions are arrived at when thermal loading is considered. Design to realistic load factors ensuring a satisfactory probability of failure would inevitably result in an unserviceable structure under normal conditions. On the other hand, specification of unrealistically high load factors, to ensure adequate service load behaviour, is a negation of the whole ultimate strength design philosophy. For fluid storage tanks, it is seen that performance under service loads is of prime importance, and a detailed control of service conditions is essential.

The committee also recognised that the approach presented in NZS 3106P Part 1:1978 was largely outdated, and did not reflect advances in the state of knowledge of behaviour of concrete liquid retaining structures,

made over the past 20 years. In particular, the concept of 'resistance to cracking' as applied to reinforced concrete storage tanks is dropped, as it is recognised that the influence of thermal gradients, shrinkage strains and construction joints will make cracking inevitable. The effect of this relaxation will be to allow thinner, but more heavily reinforced walls for reinforced concrete tanks. Also, the 1984 draft code contains detailed requirements for consideration of seismic loading, and the effects of temperature, creep and shrinkage. Because much of the basis for their requirements is not readily available in standard texts, the commentary to the code contains extensive explanatory information, and even some design aids. The purpose of this paper is to further discuss the less well understood aspects of the code, and to establish the significance of certain provisions by specific design examples. Although it is intended that the paper be comprehensible as a 'stand-alone' document, its clarity will be enhanced if read in conjunction with the new draft code.

2. DESIGN LOADING

The draft code requires consideration of Dead Load (D), Live Load (L), Backfill Loading (EP), Construction Load (C), Liquid Load (F), Prestress (P), Wind (W), Temperature (T), Earthquake (E), Shrinkage (SL) and Swelling (SW). Ideally the design magnitude of the loads should be quantified in the Loadings Code, NZS 4203[5]. However, where detailed information is lacking (temperature and shrinkage effects) or was felt to be inadequate (seismic loading), DZ 3106 contains specific requirements.

To aid in the discussion of the significance of various load cases, reference will be made to stresses induced in a 7500 cu.m prestressed circular water reservoir, whose dimensions are: inside radius of walls, a = 16.8 m, maximum water height H = 8.4 m, and wall thickness t = 190 mm. The wall base is pinned.

Fluid Loading

For reference purposes, the wall surface stresses resulting from the design fluid loading are shown in Fig. 1a, plotted against fraction of wall height x/H. Vertical bending stresses are a maximum of about 4 MPa at x/H = 0.13, and hoop tension stresses reach about 5 MPa and 6 MPa on inside and outside surfaces respectively. Note that the biaxial nature of the stress field results in interaction between vertical bending and hoop tension, resulting in circumferential bending moments of

$$M_c = \nu M_v \qquad (1)$$

where ν = Poisson's ratio for concrete, and M_v = vertical bending moment. Thus surface stresses in the hoop direction contains a proportional component from the vertical bending stresses, as shown in Fig. 1a.

Thermal Loading

Thermal loading may result from ambient heating or cooling of the wall surface, or by containment of hot or cold fluids. Recent research[6] on prestressed concrete water reservoirs has indicated that under extreme weather conditions the outside surface of the wall may be as much as 30°C hotter, or 20°C colder than the inside surface. When the contained fluid is heated or cooled, much higher temperature gradients are possible.

Stresses are induced by restraint of the free thermal expansion resulting from temperature change. In Fig. 2a, a typical linear temperature gradient from θ_i on the inside to θ_o on the outside is shown. It is assumed that a uniform temperature θ_r can be identified at which the tank is thermal stress free. For water reservoirs θ_r may be taken as the water temperature. The temperature change from the reference temperature is divided into an average change

$$\theta_A = \frac{\theta_i + \theta_o}{2} - \theta_r \qquad (2)$$

and a differential change

$$\theta_D = \pm \frac{\theta_o - \theta_i}{2} \qquad (3)$$

The effect of a positive average temperature change will be to cause all wall dimensions to attempt to expand. At the wall base radial expansion will generally be restrained, causing circumferential compression, and vertical bending moments due to the vertical curvature associated with the deflected shape (see Fig. 2b). Differential components of temperature change tend to cause vertical and circumferential curvature, as shown in Fig. 2c. Restraint of these curvatures by geometric considerations induces circumferential and vertical bending moments causing tension on the inside surface, and compression on the outside surface when $\theta_o > \theta_i$. A full description of the behaviour of circular tanks under ambient thermal loading is given elsewhere[6].

The draft code specifies design temperature distributions for empty tanks, and tanks containing fluid at ambient temperatures. In these cases it is assumed that $\theta_i = \theta_r$, and outside surface temperature may vary between +30°C and -20°C from θ_r for a full tank. Lower gradients are specified for empty tank conditions. For heated or cooled fluids the code requires specific study to establish suitable design gradients.

Design tables developed in Ref. 6 for thermal stresses in circular reservoirs are reproduced as an Appendix to the draft code. Thermal stresses are presented in the form

$$f_t = K E_c \alpha\theta \qquad (4)$$

where E_c and α are modulus of elasticity, and coefficient of thermal expansion of concrete respectively, and K is a coefficient dependent on the shape factor H^2/Dt, position up the wall, wall base connection detail, and type of temperature effect (i.e. average, differential, or combined). The tables give inside and outside surface stresses for circumferential and vertical directions. Fig. 1b plots the stresses for the 7500 m^3 example tank corresponding to the positive design gradient of $\theta_o = \theta_i + 30^oC$, assuming E_c = 30 GPa and $\alpha = 10^{-5}/^oC$. It will be seen that maximum stresses are similar to, or higher than those from water load, and affect a greater extent of the wall.

It is important to note that the thermal tables of DZ 3106 assume uncracked section stiffness. Stresses induced by thermal effects are caused by restraint of free thermal deflections and curvatures and are consequently proportional to the stiffness of the section, which is reduced by cracking. For reinforced concrete circular tanks, the influence of cracking may be found by multiplying the moments and axial forces corresponding to the uncracked-section surface stresses by a reduction factor F_T.

For example, let circumferential stresses given by the tables be f_i and f_o for the inside and outside surfaces respectively. Then the thermal moments and axial forces for the uncracked section will be

Moment:
$$M_\theta = \left(\frac{f_i - f_o}{2}\right) \frac{t^2}{6} \text{ /unit height} \qquad (5)$$

Axial force:
$$C_\theta = \left(\frac{f_i + f_o}{2}\right) t \text{ /unit height} \qquad (6)$$

where t is the local wall thickness. The corresponding moment and force in the cracked state will be $F_T M$ and $F_T C_\theta$, where F_T is the ratio of cracked-section stiffness to uncracked-section stiffness. Exact analysis is extremely difficult, as F_T will be different for axial force and moment, and will be influenced by interaction between M_θ and C_θ, and other section forces. However, a reasonable approximtation may be obtained by using the flexural stiffness values of Fig. 3, which are related to wall thickness and reinforcement content, and include an estimate of the tension stiffening effect between cracks, based on 100% increase at ρ = 0.005, 30% increase at ρ = 0.02, and a linear interpolation between these values.

Fig. 3 indicates that if the 7500 m^3 example tank was constructed with reinforced, rather than prestressed walls, of 190 mm thickness and with $\rho = \rho' = 0.01$, then the appropriate value of F_T would be approximately 0.36. It must be realised that Fig. 3 only applies to moments and forces resulting to strain-induced actions, and must not be applied to those resulting from force-loading such as fluid or seismic loading.

The draft code only gives thermal tables for circular walls. Rectangular tanks will, however, also be affected. In the absence of a detailed analysis based on the principles outlined above, thermal moments of

$$M_\theta = F_T \cdot \frac{E_c \alpha \theta_D t^2}{6(1 - \nu)} \text{ per m} \qquad (7)$$

should be assumed to apply vertically and horizontally throughout the wall. A maximum thermal axial force of

$$C = F_T \cdot E_c \theta_A t \text{ per m} \qquad (8)$$

should be assumed to apply in the horizontal direction at the base of the tank, decreasing to zero at ¼ of tank height if adversely affecting design. If beneficial, C_θ should be ignored. In Eqns. 7 and 8, F_T is given by Fig. 3.

Shrinkage and Swelling

The influence of shrinkage and swelling on the stress state in reservoir walls is similar to thermal effects. If the walls shrink due to loss of moisture before filling, there will be a tendency for inwards movement which will be restrained at the base, unless it is free to slide. For circular tanks, restraint will be in the form of a radially outward base reaction inducing hoop tension and vertical bending in the lower parts of the wall. Since shrinkage develops slowly, the stresses induced are subject to some creep relaxation. Fig. 4 shows the development of shrinkage strain over a period of 100 days after casting, as line 1. If the wall is monolithically constructed with the base, the creep-compensated (or equivalant elastic) strain is shown by line 2. A rate-of-creep analysis gives the creep-compensated strain as

$$\varepsilon_c = \left(\frac{1 - e^{-\phi}}{\phi}\right) \varepsilon_{sh} \qquad (9)$$

where ϕ is the value of the creep function at the time considered. If the wall is initially free to slide radially, no stress results from shrinkage until the wall base is pinned, subsequent to stressing. Assuming this occurs when the concrete of the walls is 50 days old, line 3 represents the development of shrinkage-induced creep-compensated strain.

When the tank is filled, the concrete absorbs water and regains its shrinkage very rapidly. The effect is a swelling strain that is again resisted at the base, inducing hoop compressions near the base, and vertical bending moments of opposite sign to those resulting from shrinkage. Although the initial swelling may be considered an 'elastic' strain because it occurs so quickly, the stresses induced are gradually relaxed by creep. The relationship that applies in terms of equivalent elastic strains, can be shown to be

$$\varepsilon'_c = e^{-\phi'} \varepsilon_{sh} \qquad (10)$$

where ϕ' is a new creep factor relating to the age of the concrete at time of filling the reservoir.

The net effect of shrinkage followed by swelling is illustrated in Fig. 4 by an instantaneous creep-compensated strain change of ε_{sh} from line 2 to 4, or line 3 to 5, followed by a gradually decrease of effective strain.

Values for the creep-compensated shrinkage strain ε_c, and the net swelling strain ε_{sw} (see Fig. 4) are given in the draft code for typical environmental conditions and different wall thicknesses, based on New Zealand research data[7].

Stresses induced by these strains may be calculated by analogy to an equivalent average temperature change of

$$\theta_s = \varepsilon_c/\alpha \qquad (11)$$

since both θ_s and ε_c will produce identical effects. Thus the thermal tables provided in the draft code may be used to calculate shrinkage and swelling stresses. For the example tank, the code gives shrinkage and effective swelling strains as 47×10^{-6} and 166×10^{-6} respectively, assuming the walls to be precast or initially free to slide. Taking $\alpha = 10^{-5}/^{o}C$, the equivalent average temperature changes are $-4.7^{o}C$ and $+16.6^{o}C$. Fig. 1c shows the circumferential and vertical stresses induced by the thermal tables for the $16.6^{o}C$ swelling case.

It should be noted that Fig. 4 indicates that the peak swelling strains will decrease rapidly with time. It would thus be inappropriate to use full swelling strain in conjunction with other transient loads, such as thermal or seismic loading.

Where the tank is conventionally reinforced rather than prestressed, cracking will again reduce the moments and forces. The approach outlined above for thermal loading may be used in conjunction with Fig. 3 to calculate the appropriate reduced values.

Seismic Loading

Seismic loading of storage tanks can be considered to consist of three main components:

1. Horizontal inertia loading: A portion of the tank contents will displace with the tank walls as though rigidly attached to the walls.
2. Convective (slosh) loading: A portion of the tank contents will be excited to displace relative to the tank walls in the first anti-symmetric sloshing modes. Higher slosh modes may be excited, but will contribute little to seismic pressures on the walls.
3. Vertical inertia loading: The entire tank contents will be subjected to vertical accelerations which will cause changes in wall pressures from values applying under acceleration due to gravity (hydrostatic loading).

The method required by the draft code may be summarised as follows.

Horizontal response: Fig. 5 shows the proportions of total fluid weight W_o/W_f and W_c/W_f that respond in the inertia and convective modes respectively, and the heights h_o/H and h_c/H of the corresponding seismic forces above the wall base. The curves apply for both circular and rectangular tanks where ℓ is half the tank length in the direction of loading.

The maximum horizontal seismic force corresponding to the inertia mode is then

$$V_I = C_I \left[\left(\frac{W_o}{W_f}\right) W_f + W_s + W_R\right] \qquad (12)$$

where W_s and W_R are weight of walls and roof respectively, and C_I is the impulsive coefficient, discussed below. The line of action of V_I will be at the resultant height of W_o, W_s and W_R.

The maximum convective horizontal force will be

$$V_c = C_c \left(\frac{W_c}{W_f}\right) W_f \qquad (13)$$

where C_c is the convective coefficient.

For the example tank, with a/H = 2, Fig. 5 gives $W_o/W_f = 0.32$, $W_c/W_f = 0.67$, $h_o/H = 0.38$, $h/H = 0.53$. For a 7500 m^3 tank, $W_f = 73.6$ MN. With a total wall height of 8.9 m and a conventional 75 mm thick dome roof, W_s and W_R will be about 4.22 MN and 1.9 MN, at heights 4.45 m and 10.3 m respectively. With this data, Eqn. 12 and 13 respectively give

$$V_I = 29.7\ C_I \text{ MN at } h_I = 3.84 \text{ m}$$

$$V_c = 49.3\ C_c \text{ MN at } h_c = 4.45 \text{ m}$$

The current loadings code[5] design spectra should not be used to calculate C_I and C_c because they are very conservative at both very short and very long periods. For a ground supported tank the natural period of the inertia mode will typically be less than 0.05s, whereas the natural period of the convective mode will typically be longer than 5.0s. This later period, T_c, may be found from Fig. 6 which relates dimensionless period to the tank aspect ratio for both circular and rectangular tanks.

Response of a ground supported tank to seismic loading must be elastic, since a ductile hinging mechanism would appear to be difficult, if not impossible, to achieve. Fig. 7 shows the Loadings Code[5] Zone A spectrum multiplied by an SM = 5 factor, as required by Ammendment A3 for elastically responding prestressed concrete structures. Also shown in Fig. 7 are elastic spectra given in DZ 3106[4], based on recommendations of the NZNSEE study group on Seismic Design of Storage Tanks[8]. These include a 2% damped spectrum for the impulsive mode and a ½% damped spectrum for the slosh mode, which is very lightly damped. These spectra are based on peak ground accelerations of 0.4 g (in Fig. 7), 0.3 g and 0.2 g for Zones A, B and C respectively, and are to be multiplied by the appropriate risk factor in accordance with NZS 4203 Ammendment A3.

For the example tank, with a/H = 2.0 and a = 16.8 m, Fig. 6 yields

$$T_c = 5.3 \sqrt{\frac{16.8}{9.81}} = 6.94 \text{ s}$$

Calculations for the natural period of the inertia mode, with the tank deforming as a squat cylinder yield T_I = 0.03 s. Hence from Fig. 7, DZ 3106 gives C_I = 0.4 and C_c = 0.08, compared with the much more severe NZS 4203 requirements of C_I = 0.75 and C_c = 0.375. The above values correspond to a risk factor of R = 1.0, though generally R = 1.6 will be appropriate for water supply tanks.

For elevated tanks, a ductile support system is possible. In such cases the current loadings code recommendations for C_I, corresponding to the structural type and materials factor used, may be adopted.

Because the periods of inertia and convective response are generally widely separated, near simultaneous occurrence of peak values could occur, and direct superpositions of the effects is thus recommended for typical ground supported tanks. Thus for the example tank, adopting R = 1.6 and Zone A loading, we have

$$V_I = 0.4 \times 1.6 \times 29.7 = 19.0 \text{ MN at } h_I = 3.84 \text{ m}$$

$$V_c = 0.08 \times 1.6 \times 49.3 = 6.3 \text{ MN at } h_c = 4.45 \text{ m}$$

Hence, the resultant of V_I and V_c is

$$V_h = 25.3 \text{ MN at } h_e = 3.99 \text{ m.}$$

Fig. 8 shows the circumferential and vertical distribution of the seismic pressure distributions. In the circumferential direction, both impulsive and convective pressures are distributed according to a cosine distribution (Fig. 8a). Vertical distribution of seismic pressures, shown in Figs. 8b and 8c may be reasonably approximated by linear distributions. Consequently at the location of maximum seismic pressure ($\theta = 0$, Fig. 8a) the total linear pressure distribution may be defined by solution of the equations

$$F_{H\theta} = V_H/\pi a = (p_t + p_b)\frac{H}{2} \tag{14}$$

and

$$h_e/H = (2p_t + p_b)/3(p_t + p_b) \tag{15}$$

Solution of these equations for the example tank yields $p_t = 48.8$ kPa and $p_b = 66.0$ kPa. Analysis of the tank under the linear pressure distribution defined by p_t and p_b gives the maximum wall stresses resulting from horizontal seismic attack.

Vertical Response: Vertical accelerations in DZ 3106 are taken as 2/3 of the peak horizontal ground acceleration. Stresses induced by these may be directly scaled from the fluid stresses (Fig. 1a). Thus for the example considered above, the peak vertical acceleration is

$$a_v = 0.67 \times 0.4 \times 1.6 = 0.43 \text{ g}$$

The stresses will thus be 43% of those given in Fig. 1a. Peak vertical and horizontal response are unlikely to occur simultaneously, and direct superposition is unwarrented. As recommended by the NZNSEE study group[8], the draft code requires combination in accordance with the relationship

$$E = \sqrt{E_H^2 + E_v^2} \tag{16}$$

where E, E_H and E_v are the final, horizontal and vertical earthquake stress sets. Fig. 1d shows the results for 7500 m^3 example tank. Comparison with Fig. 1a shows that stresses are of similar magnitude to water load stresses.

The above discussion relates mainly to curcular ground supported tanks. However, the draft code also provides guidance for rectangular, and elevated tanks.

LOAD COMBINATIONS

Two categories of load combinations are considered in DZ 3106: Group A loads, consisting of permanent loads and loads of long duration, and Group B load combinations, which consist of permanent loads plus transient loads (e.g. temperature and earthquake).

Group A loads for wall design are

$$A = D + EP + P + (S_h \text{ or } 0.5\ S_w) \quad \text{(LC1)}$$

$$A = D + F + EP + P + 0.5\ S_w \quad \text{(LC2)}$$

EP will only apply for buried or partly buried tanks. Both prestress (P) before and after losses should be considered to ensure the more adverse condition is incorporated in design. The load factor associated with swelling accounts for the creep relaxation appropriate if long term loading is considered.

Group B loads for wall design are

$$B = D + F + EP + P + 0.8\ E + 0.5\ S_w \quad \text{(LC3)}$$

$$B = D + F + EP + P + 0.7\ S_w + T \quad \text{(LC4)}$$

$$B = D + EP + P + T + (0.7\ S_h \text{ or } 0.35\ S_w) \quad \text{(LC5)}$$

Discussion of these load combinations is adequately covered in DZ 3106.

Stress levels for both concrete and reinforcing steel are increased for Group B cases. For example, under Group A combinations prestressed walls must have residual compressions of at least 0.7 MPa, and maximum compressions no greater than $0.4\ f'_c$. Under Group B combinations, tension stresses up to $0.5\ \sqrt{f'_c}$ and compression stresses up to $0.55\ f'_c$ are permitted.

Fig. 9 compares the implications of the above load combinations to the prestress requirements for the 7500 m^3 example tank. If we consider circumferential prestress, this may be effected by rearranging load cases LC2, LC3 and LC4 to give

$$\text{LC2} : P_f > F + 0.5\ S_w + 0.7 \text{ MPa}$$

$$\text{LC3} : P_f > F + 0.8\ E + 0.5\ S_w - 0.5\sqrt{f'_c} \text{ MPa}$$

$$\text{LC4} : P_f > F + 0.7\ S_w + T - 0.5\sqrt{f'_c}$$

In these equations D is ignored, as no significant circumferential stresses are induced, and swelling only included where not beneficial (it has little influence on this design). Fig. 9 indicates that thermal loading dominates circumferential design on the inside surface and seismic loading is

critical for most of the outside surface. Total circumferential prestress will need to be about 25% higher than a design based solely on stress due to fluid load (i.e. design to the old code (1)).

Vertical prestress is governed by load case 2. Thus neither thermal nor seismic load considerations cause an increase in the level of vertical prestress required. It should be noted that Fig. 9c does not include vertical stresses induced by circumferential prestress, which would be critical in load cases LC2 and LC5. However, for typical circumferential prestress designs, these cases will be less critical than those shown.

REDISTRIBUTION OF CIRCUMFERENTIAL PRESTRESS

Figs. 9a and 9b indicate a requirement for circumferential prestress at the wall base. This cannot be achieved if the prestress is applied with the wall base pinned or fixed, since radial, and hence circumferential strain cannot develop. Consequently it has been common practice to stress some or all of the circumferential cables with the wall free to slide radially, and then pin the base to improve performance under fluid, and particularly seismic loading.

It is not often recognised that the action of pinning the base after prestress is applied causes a redistribution of prestress due to restraint of creep deflections. Consider the radial deflection of the walls under circumferential prestress, as shown in Fig. 10a. If all the prestress is applied with the base free to slide, an initial elastic radially inwards displacement occurs. If the walls remain free to slide, creep effects would gradually increase the displacements as shown. However, if the base is pinned after stressing, further radial displacement at the base cannot occur, while creep displacements higher up the wall are largely unaffected. The consequence is the development of a radially outwards reaction which will cause vertical bending and a reduction in circumferential prestress at the base.

The problem of creep redistribution due to structural modification can be solved by a rate-of-creep analysis[9]. The solution indicates that the final behaviour can be considered to be identical to that which would result from an elastic analysis considering a portion β_i of the prestress to be applied in the initial structural form (sliding base) with the remainder $\beta_f = 1 - \beta_i$ of the prestress being applied in the modified form (pinned base). From the rate-of-creep analysis,

$$\beta_i = e^{-(\phi_\infty - \phi_\rho)} \qquad (17)$$

where ϕ is the creep function set up at time of prestressing, and ϕ_ρ and ϕ_∞ are the values of ϕ at time of pinning the base and after all creep has occurred. Typically, $\phi_\infty - \phi_\rho \simeq 0.9$, giving $\beta_i = 0.40$ and $\beta_f = 0.60$. That is, final prestress will be as though 60% of the prestress was applied in the pinned base condition, and only 40% in the initial sliding base condition.

ANALYSIS

Modelling of Cylindrical Walls

Guidance on analysis methods is not a normal function of a design code. However, as already noted, specific design aids are included in DZ 3106[4] in the form of thermal stress tables, and design charts for seismic analysis.

Generally, stresses induced by 'conventional' load cases, such as fluid loading, and the equivalent radially inwards presssures of circumferential prestress will be found from published design tables and charts, such as those prepared by Creasy[10]. An alternative approach for cylindrical walls that enables more complex load cases, and variable wall thicknesses to be considered is to analyse using a computer frame analogy, as illustrated in Fig. 11. Fig. 11a models a strip of wall 1 m wide in the circumferential direction. The tank wall is divided into a number of vertical beam elements (typically 10 is adequate) whose connecting nodes are supported by lateral pin-ended struts from a rigid foundation. Beam members are given the local vertical bending stiffness properties of the section of wall represented, while strut properties model the hoop stiffness of that portion of wall extending midway to adjacent modes above and below, as shown in detail in Fig. 11b. Equating unrestrained deformations of the acutal wall and the equivalent strut under radial pressure requires the strut and wall properties to be related in accordance with

$$\frac{A_i}{\ell_i} = \frac{(t_1 + t_2)}{2a^2} \cdot \Delta h \qquad (18)$$

where a = tank radius. Note that Eqn. 18 assumes the strut modulus of elasticity is that of the concrete walls. Loads applied to the vertical beam must be appropriate for the width of wall adopted for analysis (e.g., unit width in the above simulation).

Vertical bending moments induced in the beam members are identical to those in the wall, and average hoop stresses f_h are found from the radial displacement y of the wall nodes, as

$$f_h = E_c \left(\frac{y}{a}\right) \qquad (19)$$

This method of simulation can be extended to model noncylindrical elevated tanks[11].

Non-Symmetrical Loads

Ambient thermal loading, and seismic loading, are not rotationally symmetric, and hence standard tables (and the frame simulation developed above) do not strictly apply. To obtain complete results, a full three-dimensional analysis would be required. However, for typical cylindrical concrete tank proportions, maximum stresses may be found by assuming the maximum loading effect (i.e. maximum thermal gradient, or maximum seismic pressure) to be distributed round the tank with rotational symmetry, enabling existing charts, or simplified analyses to be used. Justification for this approach is provided by Fig. 12[11] which compares maximum seismically induced stresses in the walls of a 10,000 m^3 water reservoir predicted by a frame analogy, as above (i.e. assuming rotational symmetry) with those from a full 3-D finite element analysis which assumed the peak seismic pressure distribution of Fig. 12a reduced with angle from the critical location in accordance with the cosine variation shown in Fig. 8a. It will be seen that agreement is excellent.

CONCLUSIONS

Space limitations have precluded a full discussion of the new draft code, and several important aspects have not been mentioned. Amongst these, the removal of a minimum thickness requirement for reinforced walls and floors, related to water head, and the provision of a rational method of analysis for floor slab shrinkage reinforcement will have a significant influence on design.

The draft code has attempted to incorporate aspects of an improved understanding of behaviour of storage tanks, without causing a significant increase in computational effort. Because some of the requirements of the code will be new to designers, it is hoped that the design profession will take the opportunity to comment fully on the draft code. Hopefully this paper will assist in interpretation.

REFERENCES

1. - NZS 1900:Chapter 11.1:1964, Concrete Structures for the Storage of Liquids, S.A.N.Z., Wellington, 1964.

2. - NZS 3106P Part 1:1978, Provisional Code of Practice for Concrete Structures for the Storage of Liquids, Design Based on 'Resistance to Cracking' approach, S.A.N.Z., Wellington, 1978.

3. - DZ 3106 Part 2:1978, Draft Code of Practice for Concrete Structures for the Storage of Liquids, Design Based in 'Crack Control' Approach, S.A.N.Z., Wellington, 1978.

4. - DZ 3106:1984, Draft Code of Practice for Concrete Structures for the Storage of Liquids, S.A.N.Z., Wellington, 1984.

5. - NZS 4203:1976 (plus Ammendments), General Structural Design and Design Loadings for Buildings.

6. PRIESTLEY, M.J.N., 'Ambient Thermal Stresses in Circular Prestressed Concrete Tanks', Jour. ACI Vol. 73, No. 10, Oct. 1976, pp.553-560.

7. VADHANAVIKKIT, C. and BRYANT, A.H., 'Creep and Shrinkage of Concrete', Rept. 334, School of Engineering, University of Auckland, March 1984, 144pp.

8. - 'Recommendations for the Seismic Design of Storage Tanks', Bulletin of the NZNSEE (to be published).

9. NEVILLE, A.M., 'Creep of Concrete : Plain, Reinforced and Prestressed', PITMAN, London.

10. CREASY, L.R., 'Prestressed Concrete Cylindrical Tanks', WILEY, New York, 1961, Appendix, pp.204-212.

11. PRIESTLEY, M.J.N., 'Analysis of Circular Prestressed Storage Tanks by Frame Analogy', Submitted to Jour. P.C.I.

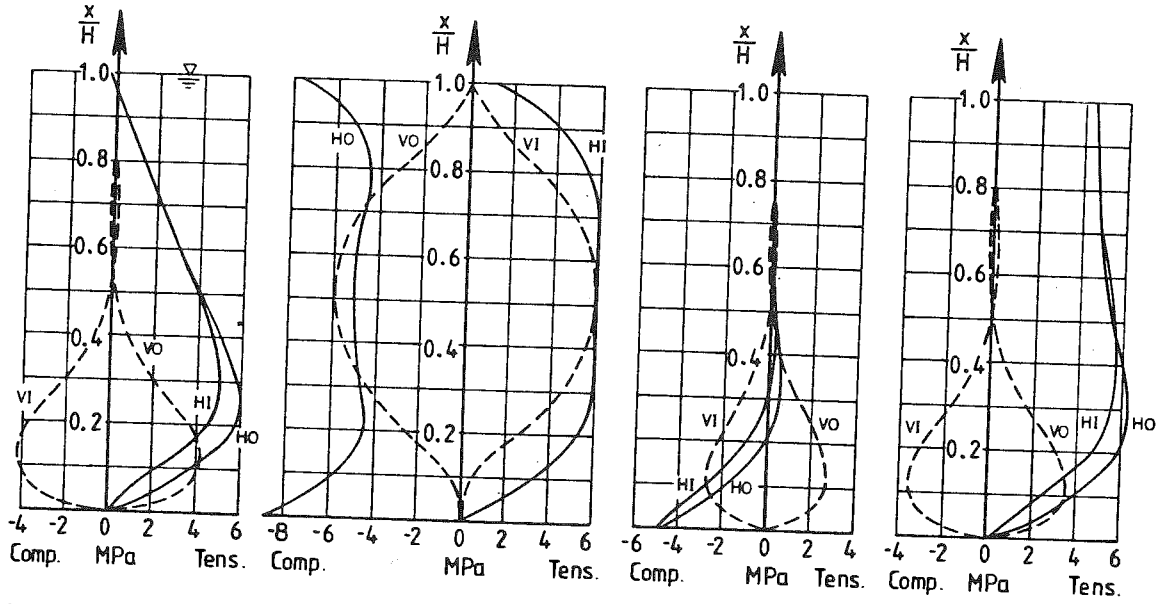

FIG. 1 Wall Stress Distributions for 7500 m^3 Prestressed Circular Tank (HO = Hoop, Outside Surface; HI = Hoop, Inside; VO = Vertical, Outside; VI = Vertical, Inside)

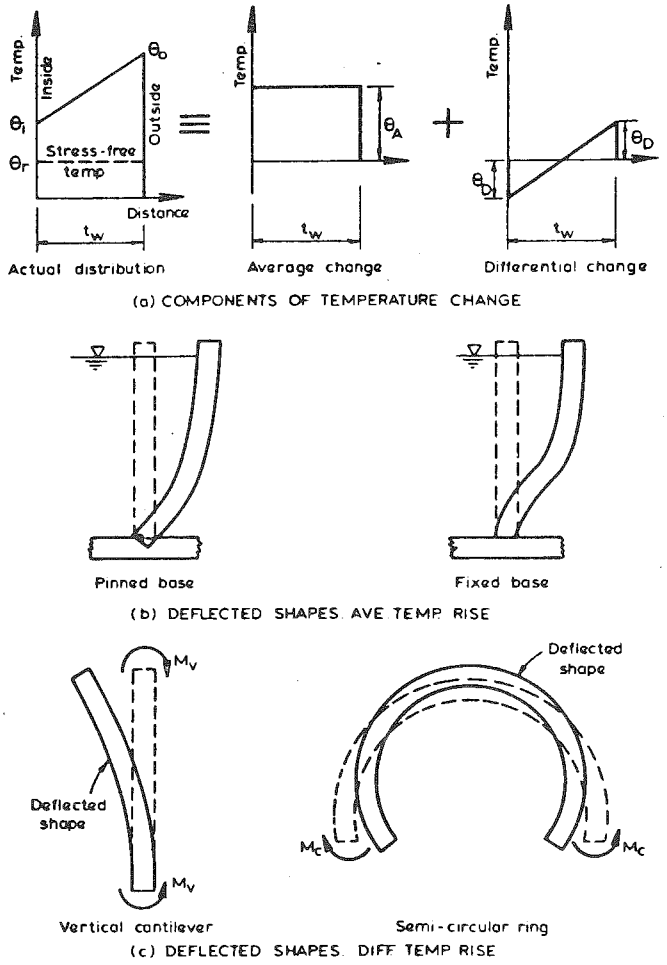

FIG. 2 Effects of Average and Differential Temperature Change for Circular Tank

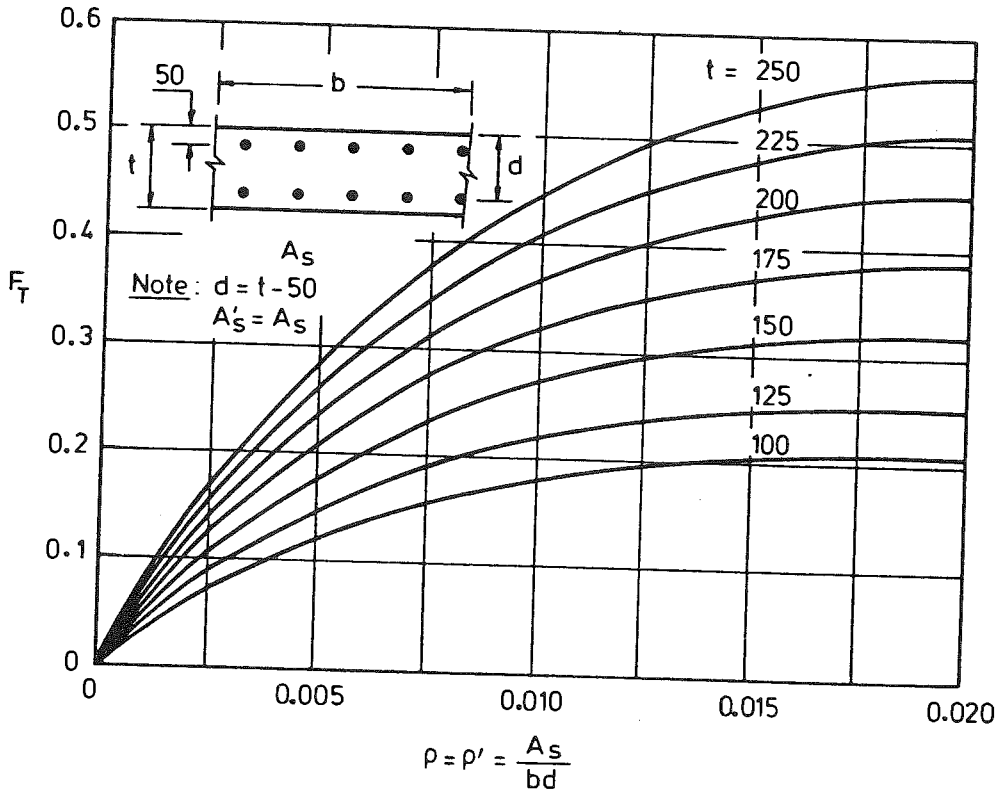

FIG. 3 Reduction of Stiffness of Doubly Reinforced Wall on Cracking (Including Tension Stiffening Effect)

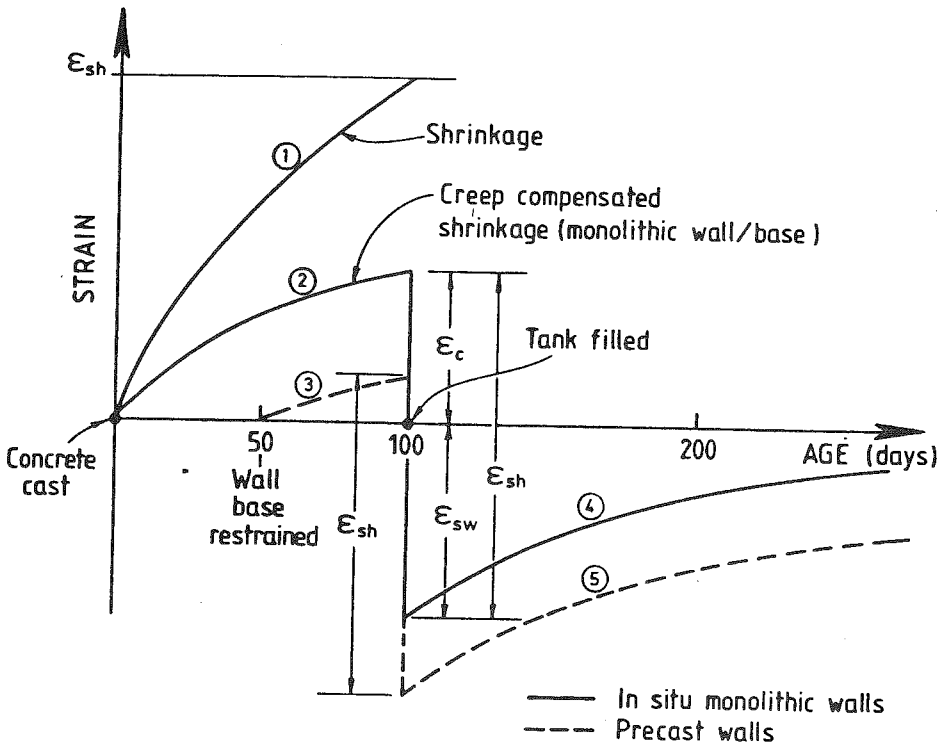

FIG. 4 'Effective' Shrinkage and Swelling Strains for Tank Walls

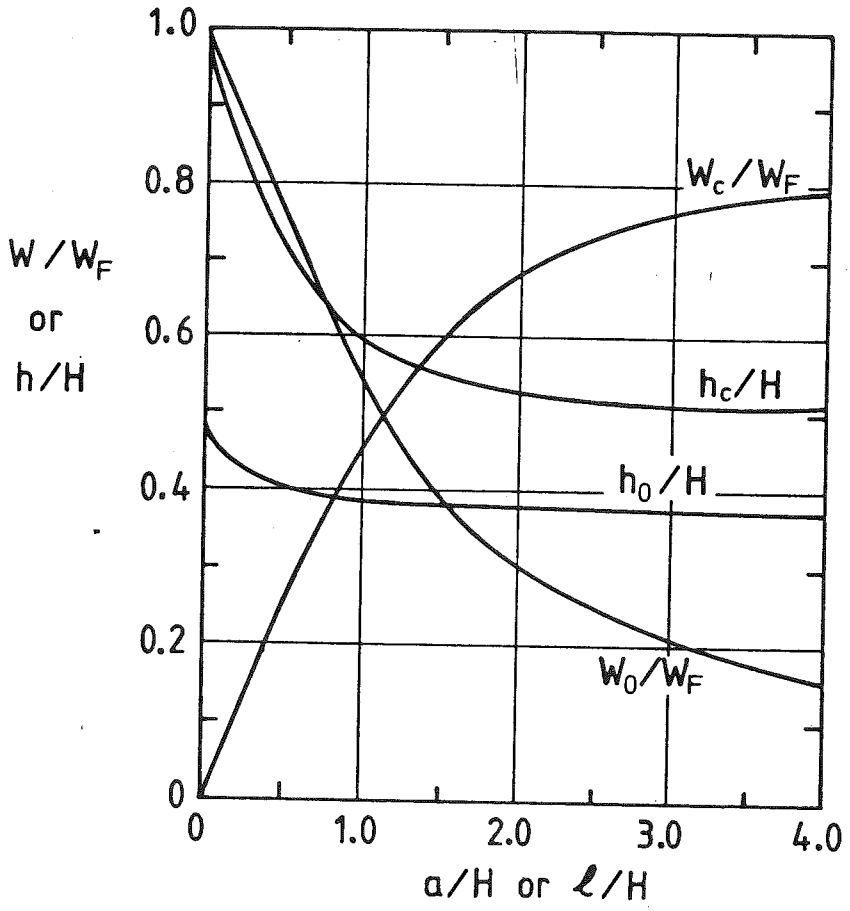

FIG. 5 Impulsive and Convective Components of Seismic Response for Contents of Circular and Rectangular Tanks[8]

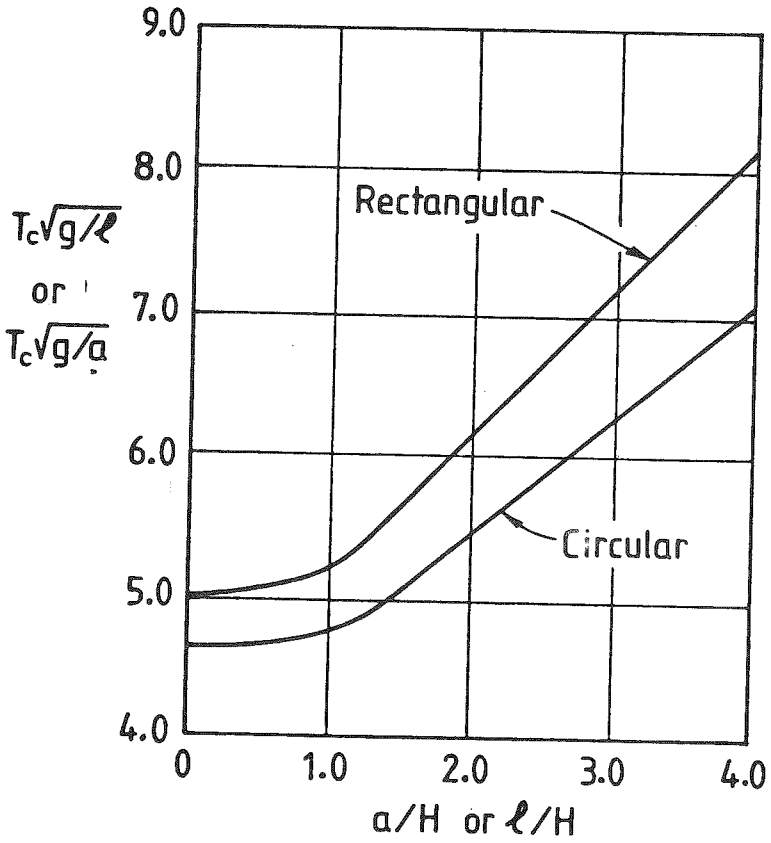

FIG. 6 Periods of Fundamental Sloshing Mode [8]

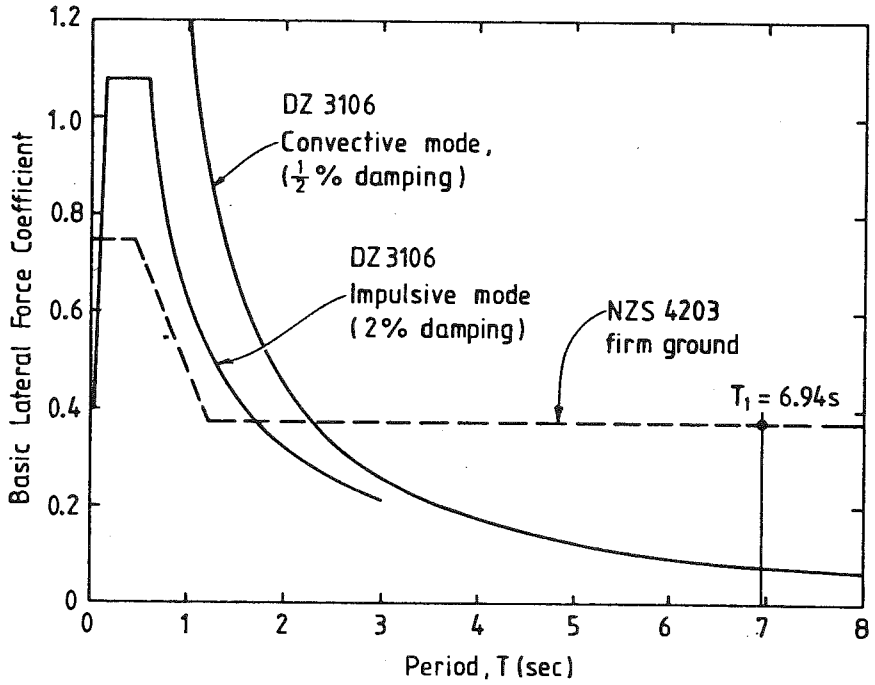

FIG. 7 Elastic Seismic Horizontal Force Coefficients for Zone A (R = 1.0)

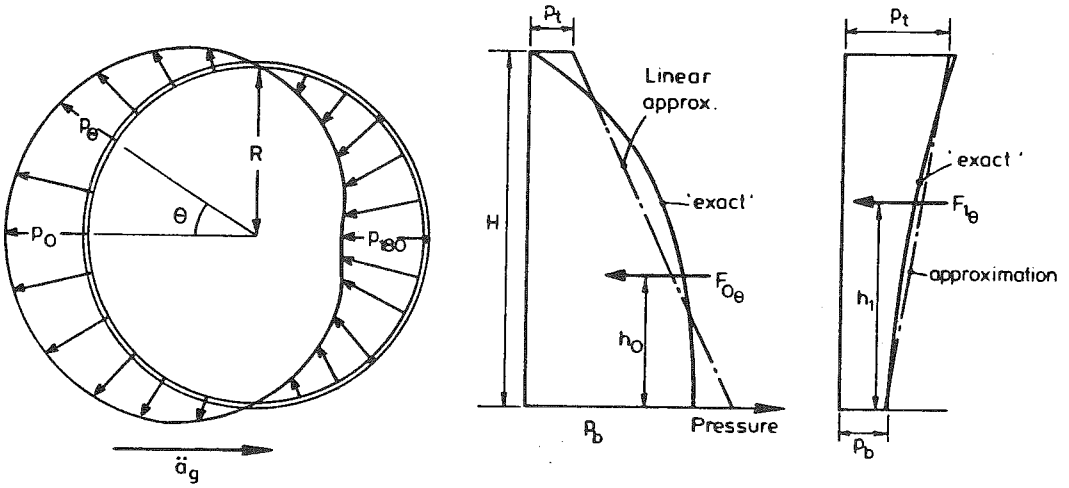

(a) Circumferential Distribution
$p_\theta = p_0 \cos\theta$

(b) Vertical Distribution, Impulsive Pressure

(c) Vertical Distribution, Convective Pressure

FIG. 8 Seismic Pressure Distributions in Cylindrical Tanks (8)

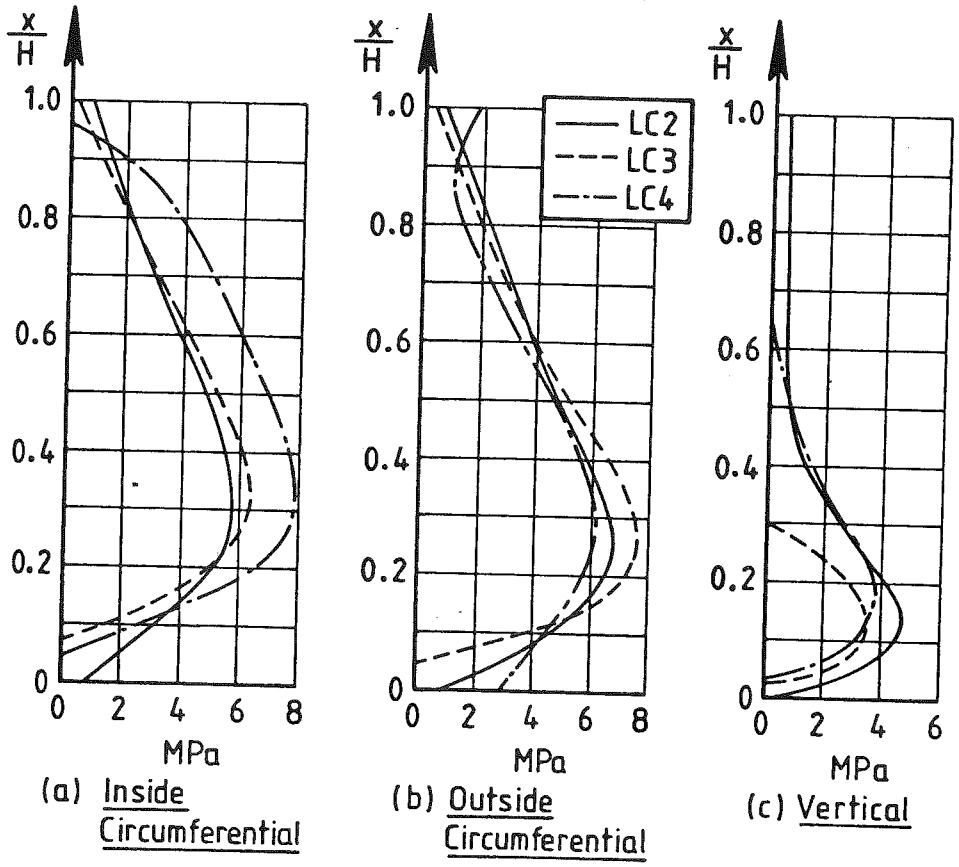

FIG. 9 Prestress Requirements for 7500 m^3 Circular Tank

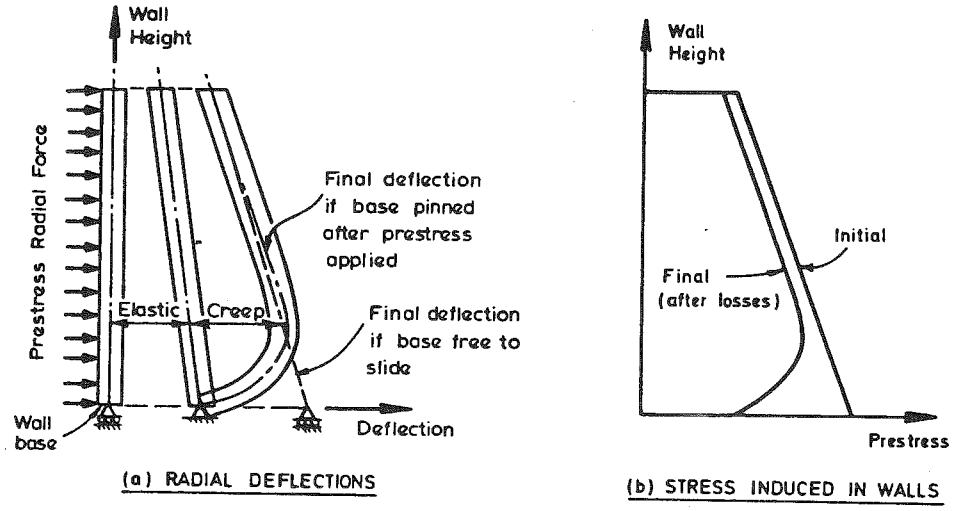

FIG. 10 Redistribution of Circumferential Prestress Due to Structural Modification

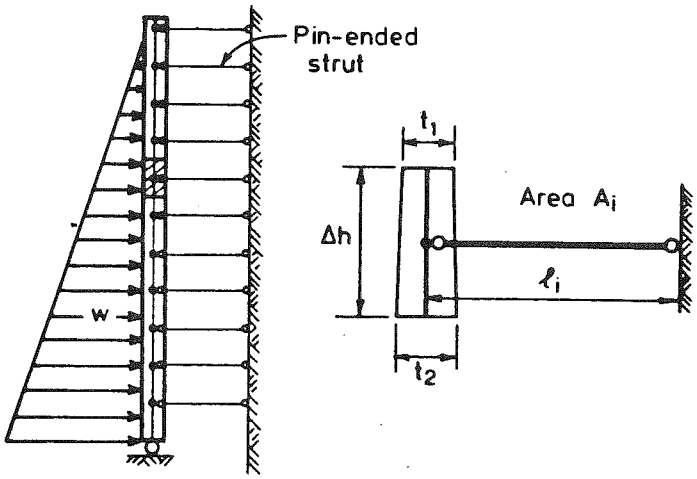

(a) Discretised Foundation - Frame Analogy

(b) Detail of Equivalent Strut

FIG. 11 Frame Simulation of Circular Tank Walls

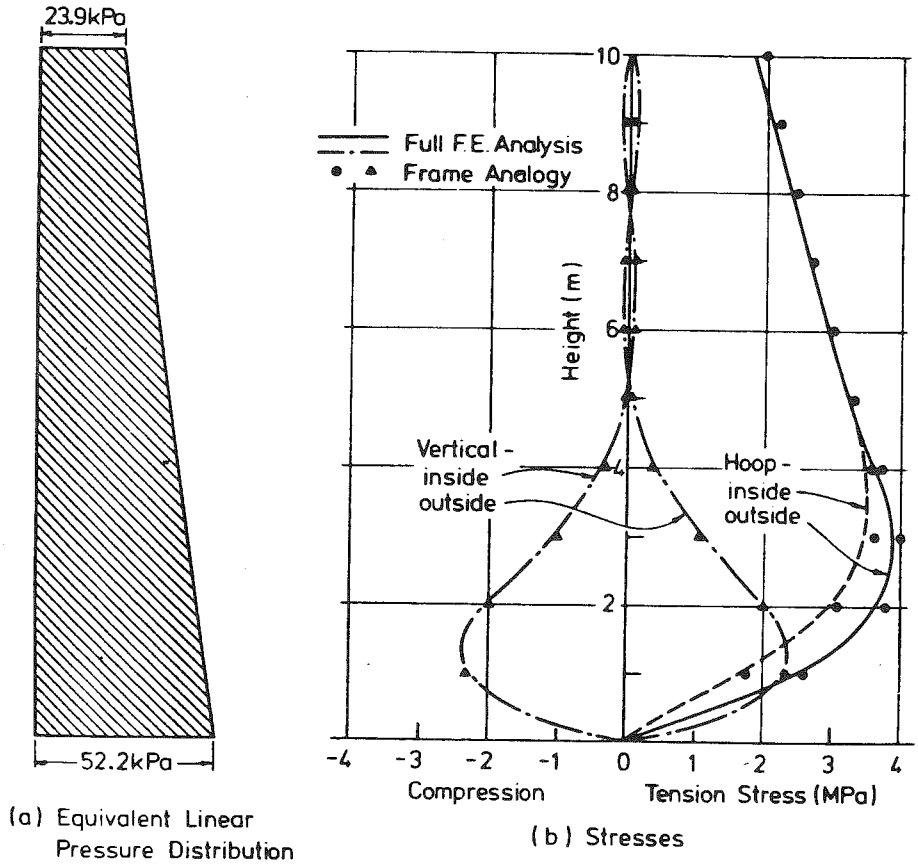

FIG. 12 Seismic Stresses Predicted by Frame Analogy and Full 3D Finite Element Analysis

SEISMIC DESIGN PHILOSOPHY FOR MASONRY STRUCTURES

M.J.N. Priestley

SEISMIC DESIGN PHILOSOPHY FOR MASONRY STRUCTURES

M.J.N. PRIESTLEY[1]

SUMMARY

A seismic design philosophy for masonry structures is developed. The basic tenets involve the choice of a suitable structural system, the dissipation of seismic energy by flexural action in carefully chosen plastic hinge regions, and the avoidance of undesirable modes of inelastic deformation. The aspects are described by example and by reference to recent experimental work.

1. University of Canterbury, New Zealand.

1. INTRODUCTION

'Design Philosophy' - a somewhat grandiose term for the fundamental basis of design. It covers reasons underlying our choice of design loads, our analytical techniques, our preferences for particular structural types and materials.

The significance of design philosophy becomes paramount when seismic considerations dominate the design. This is because we accept higher annual probabilities of damage under seismic loading than under other comparable extreme loads, such as maximum live load, or wind loading. For example, modern seismic loading codes typically specify design earthquakes with a return period of 100-500 years for ordinary structures such as office buildings. Where seismic lateral loads are based on ductile response to the design earthquake, this can imply that the ultimate load capacity (albeit with zero or limited ductility demand) can be achieved with an expected annual probability as high as $p = 0.01$ to 0.03. This compares with accepted annual probabilities for achieving ultimate capacity under gravity loads of perhaps $p = 0.0001$ to 0.001 per year. It follows that the consequences resulting from the lack of a rational seismic design philosophy are likely to be severe.

Great advances have been made over the last 20 years in the design philosophy of reinforced concrete and steel structures responding to earthquake loading. Despite evidence provided by poor performance of masonry structures in recent earthquakes [1], indicating the need for more rational design, the developments in masonry design have been less appreciable. The consequence has been that designers are often reluctant to use masonry elements in the major lateral load resisting system in regions of high seismicity, except for minor structures. The uncertainty about performance is incorporated in many design codes [2,3] which generally stipulate elastic design to low allowable stress levels in the belief that behaviour at service load levels is more predictable than at ultimate. Elastic design for seismic loading is also intended to protect masonry structures from inelastic action, and hence hopefully from damage under code-level ground excitation.

In fact, both of these premises are highly suspect. At service load levels, the influence of shrinkage, temperature, creep and settlement will often mean that stress levels predicted by elastic theory bear little resemblance to the true stresses. Further, the 'plane-sections-remain-plane' hypothesis may be invalid in many cases, particularly for squat masonry shear walls under in-plane loading. Ultimate strength behaviour is, however, rather insensitive to these aspects, so ultimate moments and shears can be predicted with comparative accuracy. There is now adequate test information [4-6] to support the application of ultimate strength methods developed for reinforced concrete, to reinforced masonry design.

The use of elastic design methods will not generally protect masonry structures from inelastic action under seismic loading. Consider the typical smoothed acceleration response

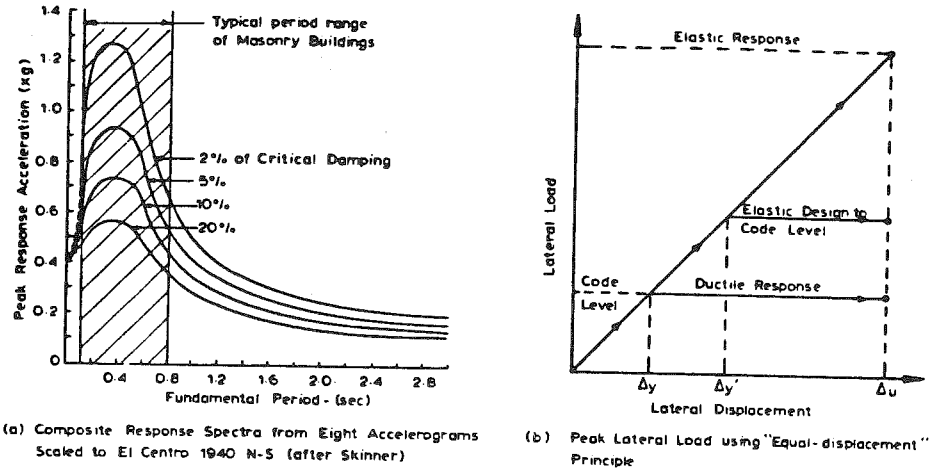

(a) Composite Response Spectra from Eight Accelerograms Scaled to El Centro 1940 N-S (after Skinner)

(b) Peak Lateral Load using "Equal-displacement" Principle

FIG. 1 - SEISMIC LOADS FOR MASONRY WALLS

spectra of Fig. 1a [7], which has been scaled to the intensity of the moderate El Centro 1940 N-S accelerogram. Masonry structures, being stiff, typically have fundamental periods in the range 0.1 - 0.8 s, thus spanning the frequency range of maximum response. Assuming a 5% equivalent viscous damping, peak elastic response of the order of 0.8 g can be anticipated.

Design for such high lateral force levels is not economically viable, and seismic coefficients included in most codes are reduced from the elastic response levels, typically by a factor of about 4, implying considerable ductility demand, as shown in Fig. 1b. Consequently it is to be expected that under the design level earthquake, the structure will attain its ultimate strength, and be required to deform inelastically in a ductile manner without significant loss of strength. The equal displacement rule, illustrated in Fig. 1b implies that the maximum displacement response $\Delta\mu$ is independent of the strength for structures of equal elastic stiffness. Thus if a masonry building is designed to allowable stress levels at the code level of lateral load, it will still attain its ultimate capacity under the design earthquake, but with a reduction in the required structure ductility, given by $\mu = \Delta u/\Delta y'$ in Fig. 1b. In fact, for short period structures, the equal displacement principles is known to be non-conservative, and ductility demand is likely to be higher.

Design to elastic theory in such cases is a 'head in the sand' approach, unless the structure is designed for the full lateral force level corresponding to elastic response. A more realistic approach is to accept that the ultimate capacity of the structure will be attained, and to design accordingly by ensuring that the materials and structural systems adopted are capable of sustaining the required ductility without excessive strength or stiffness degradation. This approach will be assumed for the remainder of this paper.

2. CHOICE OF STRUCTURAL FORM

Perhaps the most basic aspect of a successful design philosophy is the choice of a suitable structural form. This will dictate the location of areas of inelastic action (plastic hinges), and the relationship between local curvature ductility demand and overall structural ductility demand.

2.1 Cantilever Shear Walls

The ductility capacity of a masonry wall will depend principally on the structural form, and the ultimate curvature capacity of the wall. To ensure adequate ductility, the preferred structural form is the simple cantilever shear wall. Where two or more such walls occur in the same plane, linkage between them could be provided by flexible floor slabs (Fig. 2a) to ensure moment transfer between the walls is minimised. Openings within the wall elevation should be kept small enough to ensure that the basic cantilever action is not affected. Energy dissipation occurs only in carefully detailed plastic hinges at the base of each wall.

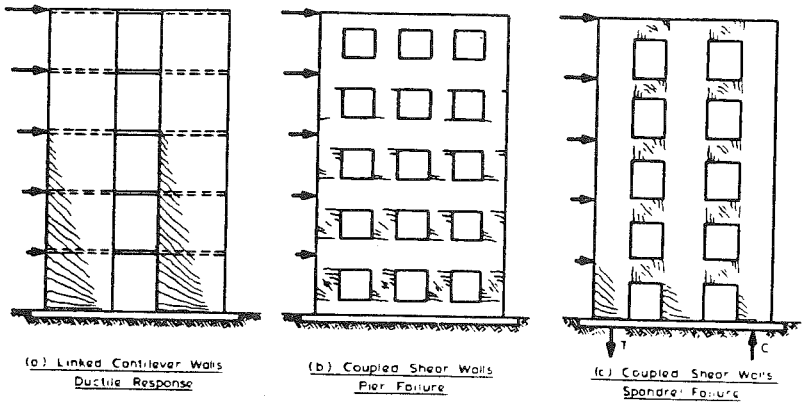

FIG. 2 - MASONRY SHEAR WALLS UNDER SEISMIC LOADING

Traditional masonry construction has generally consisted of peripheral masonry shear walls pierced by window and door openings, as idealised in Figs. 2b and c. Under inelastic response to lateral loading, hinging may initiate in the piers (Fig. 2b) or the spandrels (Fig. 2c). In the former, and more common case, the piers will be required to exhibit substantial ductility unless designed to resist elastically the displacements resulting from the design earthquake. Plastic displacement (flexural or shear) will inevitably be concentrated in the piers of one storey, generally the lowest, with consequential extremely high ductility demand at that level. It can be shown [8] that for a regular wall where pier height is half the storey height, the displacement ductility factor μ_p required of the piers is related to the structure ductility demand, μ, by the expression

$$\mu_p = 2n(\mu - 1) + 1 \qquad (1)$$

where n is the number of storeys. Thus for a 10 storey masonry shear wall designed for $\mu = 4$, the pier ductility demand would be $\mu_p = 61$. Extensive experimental research on piers at the University of California, Berkeley [6] has indicated extreme difficulty in obtaining reliable ductility levels an order of magnitude lower than this value. It is concluded that the structural system of Fig. 2b is only suitable if very low structural ductilities are required.

Occasionally, openings in masonry walls will be of such proportions that spandrels will be relatively weaker than piers, and behaviour will approximate coupled shear walls, with crack patterns as illustrated in Fig. 2c. Although well detailed coupled shear walls in reinforced concrete constitute an excellent structural system for seismic resistance, diagonal reinforcement of the spandrel beams is generally necessary to satisfy the high spandrel ductility demand. Such a reinforcement system is unsuitable for structural masonry, and strength and stiffness degradation of the spandrel is likely at moderate ductilities, causing the coupled shear wall to degrade towards the linked shear walls of Fig. 2a, with a consequential increase in the seismic forces on the walls.

2.2 Infilled Frames

It is a common misconception that masonry infill in structural steel or reinforced concrete frames can only increase the overall lateral load capacity, and therefore must always be beneficial to seismic performance. In fact there are numerous examples of earthquake damage that can be traced to structural modification of the basic frame by so-called non-structural masonry partitions and infill panels. Even if they are relatively weak, masonry infill can drastically alter the intended structural response, attracting forces to parts of the structure which have not been designed to resist them. Two examples are illustrated below to examine this behaviour.

Consider the floor plan of a symmetrical multi-storey reinforced concrete frame building with masonry infill panels on two boundary walls, as shown in Fig. 3. If the masonry infill is ignored in the design phase it may be assumed that each frame in each direction (i.e. frames 1, 2, 3 and 4 in the X direction, and frames a, b, c and d in the Y direction) are subjected to the same seismic lateral loads, because of the structural symmetry. The true influence of the infill on frames 4 and d will be to stiffen these frames relative to the other frames. The consequence will be that the natural period of the structure will decrease, and seismic forces will correspondingly increase. Further, the proportion of the total seismic shear at each floor transmitted by the infilled frames will increase because of the increased stiffness of these frames relative to the other frames. The structure will also be subjected to seismic torsional response because of the shift of centre of rigidity. Thus for seismic response along the X and Y axes respectively, the torsional moments will be

$$\text{X Axis} : M_T = M.e_y \qquad (2a)$$

$$\text{Y Axis} : M_T = M.e_x \qquad (2b)$$

where M is the total floor area.

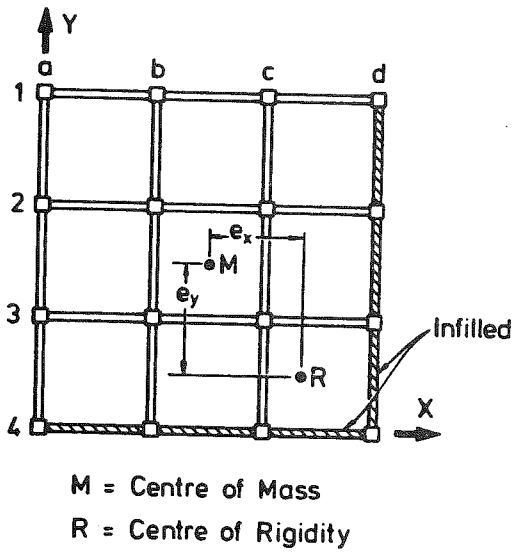

FIG. 3 - PLAN OF R.C. FRAME BUILDING WITH INFILL ON TWO BOUNDARIES.

The high shear forces generated in the infilled frames are transmitted primarily by shear stresses in the panels. Shear failure commonly results, with shedding of masonry into streets below, or into stairwells, with great hazard to life.

A second example is illustrated in Fig. 4, which shows masonry infill which extends for only part of the storey height, to allow for windows. Again the infill will stiffen the frame, reducing the natural period and increasing seismic forces. If the frame is designed for ductile response to the design level earthquake, without consideration of the effect of the infill, plastic hinges might be expected at top and bottom of columns. Because of the ductile design, these hinges would develop at a fraction of the full design level earthquake. The influence of the infill will be to stiffen the centre and right column (for the direction of lateral load shown) causing plastic hinges to form at top of the column and top of the infill, as shown in Fig. 4. The consequence will be an increase in column shears. The design level of shear force in the column will be

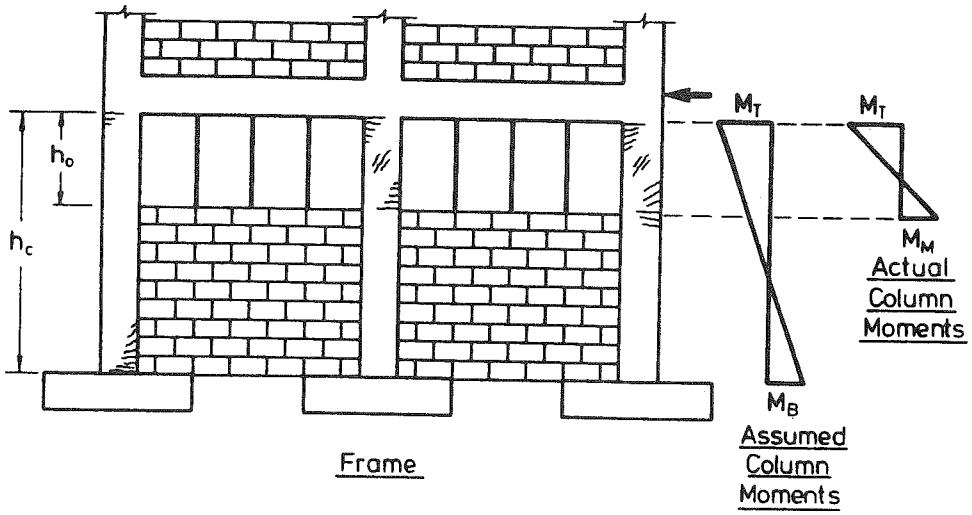

FIG. 4 - PARTIAL MASONRY INFILL

$$V_D = \frac{M_T + M_B}{h_c} \quad (3)$$

where h_c is the clear storey height. The actual shear force will be

$$V_A = \frac{M_T + M_M}{h_o} \quad (4)$$

where h_o is the height of the window opening. If the column is not designed for the higher shear force of Eqn. 4, shear failure can be expected. It should be noted that this higher shear force, corresponding to formation of plastic hinges as shown can develop because the original design was ductile. Hence the higher shear force will be developed, but at lower ductility, as shown in Fig. 1b.

When masonry infill is to be used there are two design alternatives. The designer may effectively isolate the panel from frame deformations by providing a flexible strip between the frame and panel, filled with a highly deformable material such as polystyrene. Alternatively the designer may allow the panel and frame to be in full contact, and design both for the seismic forces to which they will be subjected. The first option, of isolation, is not very effective as it is not possible nor desirable to provide flexibility at the base of the panel, and it is difficult to provide support against out-of-plane seismic forces.

2.3 Masonry Frames

An alternative reinforced masonry structural system that is suitable for ductile response, is the moment-resisting frame, whose proportions in terms of the ratio of bay length to storey height is more typical of reinforced concrete frames than those of Fig. 2c. Such an example is shown in Fig. 5. The system could be constructed from either reinforced grouted brick masonry (two wythes of solid bricks separated by a grouted, and reinforced cavity) or hollow unit concrete masonry. As shown in Fig. 5, the column units considered are constructed using standard units, rather than special pilaster units which effectively act only as permanent formwork, and which may be suitable for smaller structures than envisaged in this paper.

Provided such a frame is detailed in such a way as to ensure a suitable beam-hinging mechanism is developed with shear and column failures avoided by use of a capacity design approach, there is no reason why such a structural form should not perform well under seismic loading. This view point is confirmed by test results briefly summarised later in this paper.

2.4 Secondary Walls

Some shear wall structures do not lend themselves to rational analysis under lateral loading, as a consequence of the number, orientation and complexity of shape of the load

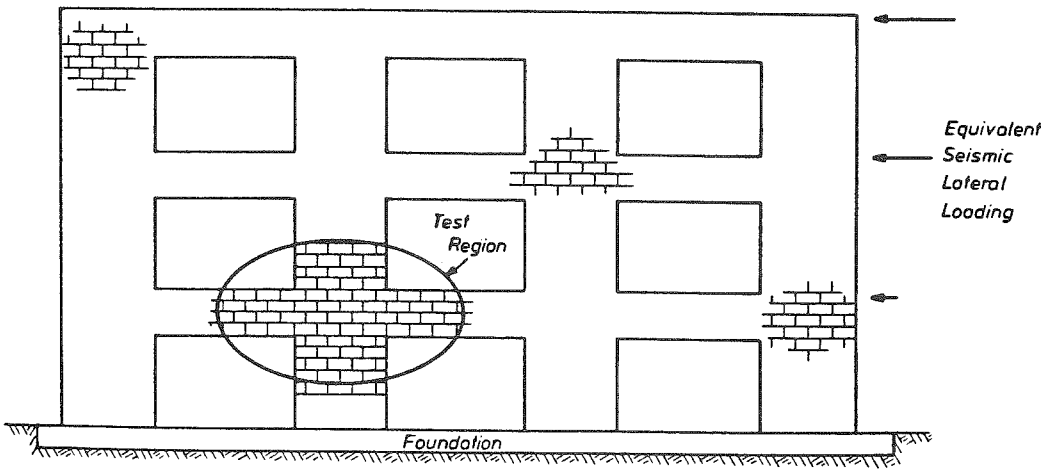

FIG. 5 - MASONRY FRAME UNDER LATERAL LOAD

bearing walls. In such cases the designer may consider the walls to consist of a primary system which carries gravity loads and the entire seismic lateral load, and a secondary system which is designed to support gravity loads and face loads only. This allows simplification of the lateral load analysis in cases where the extent of wall area exceeds that necessary to carry the code seismic loads. However, although it is assumed in the analysis that the secondary walls do not carry any in-plane loads, it is clear that they will carry an albeit indeterminate proportion of the lateral load. Consequently they must be detailed to sustain the deformation to which they will be subjected, by specifying similar standards as for structural walls, though code-minimum requirements for reinforcement will normally be adopted. To ensure satisfactory behaviour results, the natural period should be based on an assessed stiffness of the composite primary/secondary system.

No secondary wall should have a stiffness greater than about one-quarter that of the stiffest wall of the primary system. This is to ensure that the probability of significant inelastic deformation developing in secondary walls is minimised, and integrity of secondary walls for the role of gravity load support is maintained. Long stiff secondary walls may be divided into a series of more flexible walls by the incorporation of vertical control joints at regular centres. A further requirement in selecting the primary and secondary systems of walls is that the centres of rigidity of the two systems should be as close as possible to minimise unexpected torsional effects. Figure 6 shows acceptable and unacceptable division of a complex system of walls into primary and secondary systems.

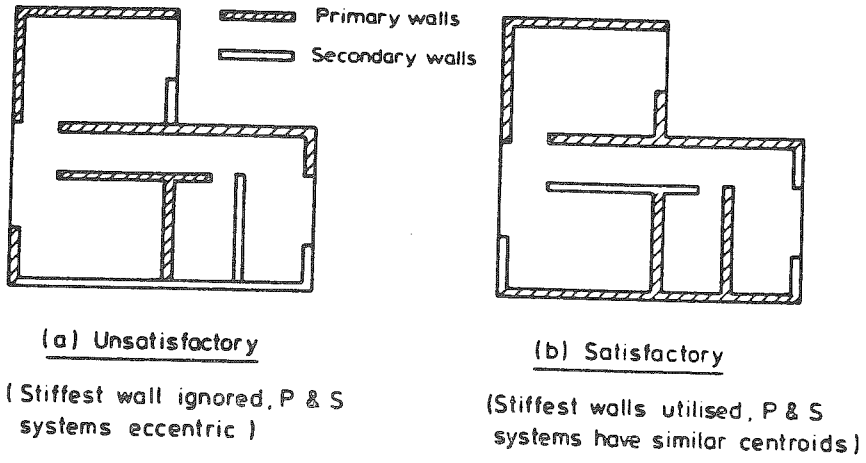

FIG. 6 - EXAMPLE OF SUBDIVISION OF WALLS INTO PRIMARY AND SECONDARY SYSTEMS

3. DESIGN CONSIDERATIONS

3.1 Ultimate Flexural Strength of Masonry Shear Walls. Compression Stress-Strain Curves for Masonry

Ultimate strength design of masonry requires knowledge of the complete compression stress-strain curve, including the crushing strength f'_m, the ultimate compression strain ε_{cu}, and the shape of both rising and falling-branch portions of the curve. From these, the parameters defining the shape of an equivalent rectangular stress block having the same area and centroidal location as the real stress block may be found, enabling flexural strength equations similar to those developed by the ACI for concrete structures to be used.

Recent research [9] on grouted concrete masonry prisms has indicated that the stress-strain curves for masonry in compression can be represented by suitably modified equations developed for reinforced concrete. Fig. 7 compares experimental results with theoretical curves found by modifying the Kent-Park curve for concrete [9,10]. Results are shown for unconfined concrete masonry, and for masonry with 3 mm steel plates laid in the mortar beds to provide a degree of confinement to the masonry. It was found that the compression of unconfined masonry could be represented by a stress-block defined by an average stress of $0.85f'_m$, with a depth $a = 0.85c$ (where c is distance from the extreme compression fibre to the neutral axis) and an ultimate compression strain of $\varepsilon_{cu} = 0.0025$. For confined masonry, the corresponding values were: average stress $= 0.9f''_m$, where f''_m is the compression strength of confined masonry, $a = 0.96c$, and $\varepsilon_{cu} = 0.008$.

Recent research in the U.S.A. by Atkinson [11] has indicated similar behaviour for hollow clay-brick masonry, though ultimate compression strains of about 0.003 appear to be more reasonable than the value of 0.0025 found in New Zealand for unconfined masonry.

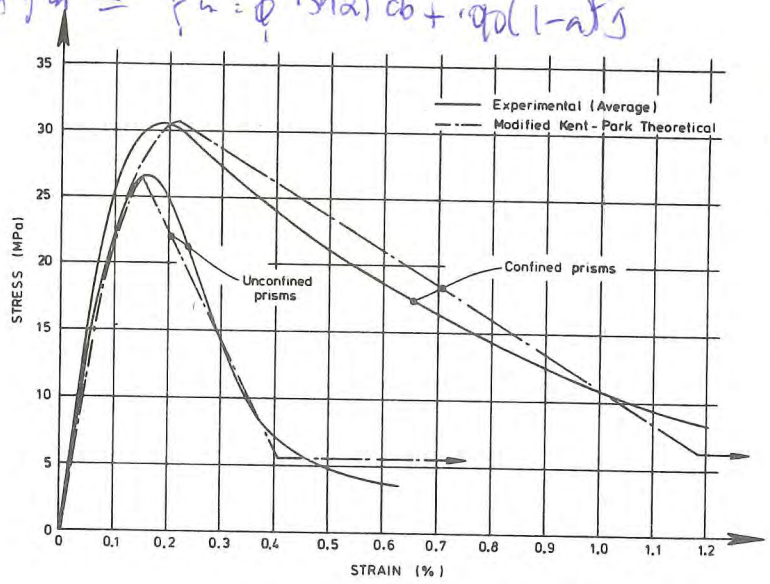

FIG. 7 - STRESS-STRAIN CURVES FOR CONCRETE MASONRY

The compression strength of confined masonry is given by the Kent-Park enhancement factor [10] as

$$f''_m = K f'_m \qquad (5)$$

where

$$K = 1 + \rho_s \frac{f_{yh}}{f'_m} \qquad (6)$$

ρ_s is the volumetric ratio of confinement provided by the confining plates, and f_{yh} is the yield stress of the confining plate material.

Distribution of Flexural Reinforcement

Using the information presented above, the flexural strength of a masonry shear wall can be calculated using the normal assumptions for reinforced concrete. It is of interest, however, to consider the influence of distribution of flexural reinforcement on flexural strength. Figure 8 shows two rectangular-section walls of identical dimensions and axial load level, reinforced with the same total quantity of flexural reinforcement, A_{st}, which is uniformly distributed along the wall length in Fig. 8a, but concentrated in two bundles of $A_{st}/2$, one at each end of the wall in Fig. 8b. Elastic theory indicates that the distribution of Fig. 8b results in a moment about 33% higher than for the distributed reinforcement of Fig. 8a. However, for the typically low steel percentages and low axial loads common in masonry construction, the ultimate flexural capacity is insensitive to the steel distribution. For uniformly distributed reinforcement (Fig. 8a) the small neutral axis depth will ensure tensile yield of virtually all vertical reinforcement, resulting in an ultimate capacity of

$$M_u \cong A_{st} \cdot f_y \frac{d}{2} + N_u \frac{\ell_w}{2} \qquad (7)$$

For reinforcement concentrated near the ends of the wall, the tension force, at $0.5A_{st} f_y$ is approximately half that for the distributed case, but at roughly twice the lever arm, so that flexural capacity again approximates to Eqn. 7.

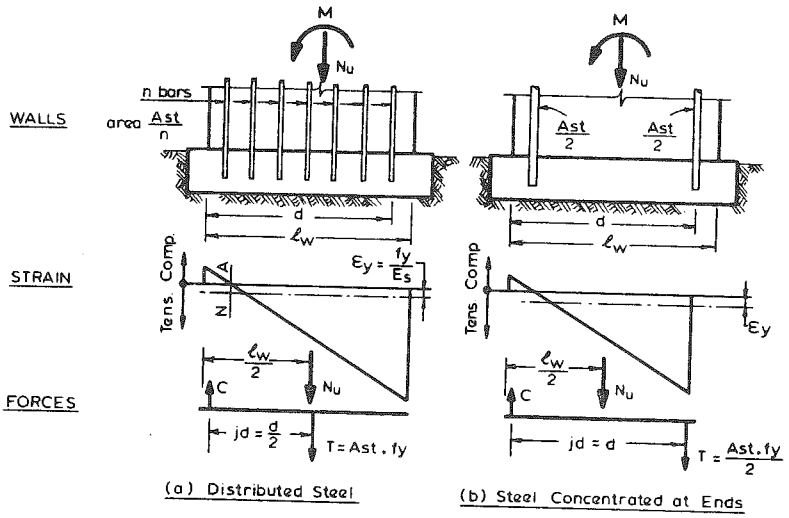

FIG. 8 - EFFECT OF STEEL DISTRIBUTION ON FLEXURAL CAPACITY

In fact there are strong reasons for adopting uniform distribution of the flexural steel along the wall when seismic loading is considered. Distributed reinforcement will result in a higher masonry flexural compression force, and therefore more efficient compression shear transfer, and provides a clamping force along the wall base joint, which is a region of potential sliding. Concentration of steel close to the wall ends results in congestion and difficulty with effective grouting, and causes high bond stresses on the limited grout area. Due to a potential for vertical splitting in the compression zone at ultimate, lateral stability provided by the masonry will often be inadequate to prevent the compression steel from buckling. This factor is less significant for walls with distributed reinforcement. Because of these factors, a recent New Zealand Masonry Design Code [12] requires that flexural reinforcement in shear walls be essentially uniformly distributed, and stipulates ultimate strength design.

Flexural Strength Reduction Factor

As with reinforced concrete design, a flexural strength reduction factor is necessary to allow for possible under-strength materials, dimensional errors, and inaccuracies in analysis. Values suggested for masonry shear walls [12] are

for $N_u = 0$ $\quad \phi_f = 0.85$

for $N_u \geq 0.1 f'_m A_g$ $\quad \phi_f = 0.65$

with linear variation between $\phi_f = 0.65$ and $\phi_f = 0.85$ as the axial load N_u decreases from $0.1f'_m A_g$ to zero.

3.2 Shear Strength of Masonry Shear Walls

Design Shear Force

Since shear failure is brittle, it must be avoided for masonry structures required to exhibit ductility under seismic loading. To ensure this, the shear strength must exceed the shear corresponding to maximum feasible flexural strength. Since flexural strength will be based on nominal (and therefore generally conservative) material strengths, and a strength reduction factor of $0.65 \leq \phi_f \leq 0.85$, the probable flexural strength will exceed the dependable strength by a substantial margin. Strain-hardening of tensile reinforcement at high flexural ductilities will further enhance the flexural strength, particularly for walls reinforced with high strength reinforcement, which typically exhibits early strain hardening. Figure 1 indicates that a wall designed for ductile response under seismic loading will develop its actual flexural strength, albeit at a lower ductility than that corresponding to dependable strength.

Consequently the maximum feasible shear V_D may be related to the shear corresponding to dependable flexural strength V_F by the relationship

$$V_D = \frac{\phi_o}{\phi_f} V_F \qquad (8)$$

where ϕ_o is a strength enhancement factor reflecting the influence of strain hardening, and higher than specified material strength. Typically for reinforcement with $f_y = 275$ MPa, $\phi_o = 1.25$ is appropriate [13]. For slender multistorey shear walls, a further shear amplification factor ω_v is advisable to allow for possible variations in the ratio of shear to flexure from that corresponding to a code distribution of lateral loads, resulting from higher mode response [14]. Typical values for ω_v are $1.2 \leq \omega_v \leq 1.8$.

Shear Carried by Masonry Shear Resisting Mechanisms

Within potential plastic hinge region, wide flexure-shear cracks and the effects of load reversals are likely to severely reduce the efficiency of the components contributing to masonry shear strength, namely compression shear transfer, aggregate interlock and dowel action. At present there are insufficient experimental data to quantify the reduction in shear strength of masonry with increasing ductility, though research planned in the USA as part of the Joint US-Japan study on behaviour of masonry structures [15] should provide useful data in the near future. Until then the conservative assumption should be made that all shear in potential plastic hinge regions should be carried by horizontal shear reinforcement.

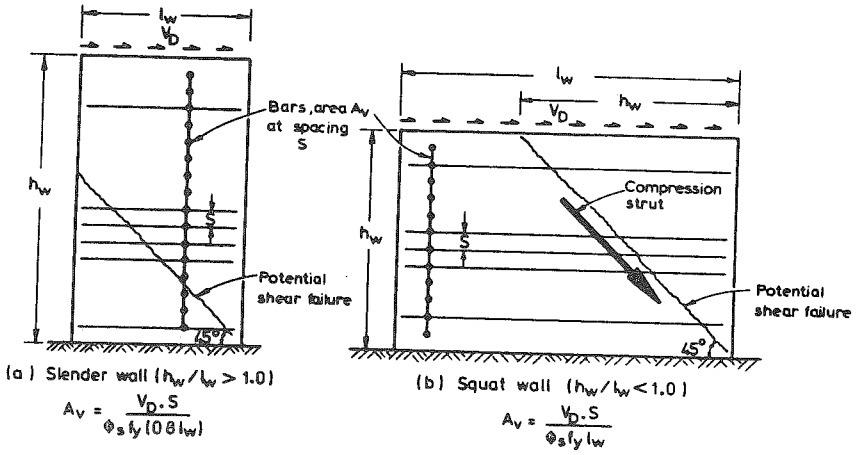

FIG. 9 - SHEAR CAPACITY OF HORIZONTAL REINFORCEMENT IN WALLS

Two possible situations are identified in Fig. 9 for the design of shear reinforcement. When the aspect ratio h_w/ℓ_w exceeds unity (Fig. 9a) a potential shear crack, inclined at 45° crosses the entire width of the wall. Normal reinforced concrete theory gives the required steel area A_v, at vertical spacing s, as

$$A_v = \frac{V_D \cdot s}{\phi_s \cdot f_y d} \qquad (9)$$

where ϕ_s is the strength reduction factor for shear, and d is the effective depth, normally taken as $0.8\ell_w$ for walls with distributed reinforcement.

When the aspect ratio is less than unity (Fig. 9b), the critical 45° crack intersects the wall top. Recent research on squat concrete walls [16] is applicable to masonry, and indicates that the shear entering the wall on the tension side of the 45° line from the compression toe can be transmitted by arch action involving the vertical flexural reinforcement, and inclined masonry compression struts. Shear reinforcement needs to be provided to transfer the shear entering the wall on the compression side of the potential inclined crack, back across the crack into the body of the wall. Thus in Fig. 9b, assuming that V_D is distributed evenly across the wall length, the required steel area is

$$A_v = \frac{1}{\phi_s} \cdot V_D \cdot \frac{h_w}{\ell_w} \cdot \frac{s}{f_y h_w} = \frac{V_D s}{\phi_s f_y \ell_w} \qquad (10)$$

When the design shear force V_D in Eqns. 9 or 10 is based on the capacity design approach described above, the strength reduction factor may be taken as $\phi_s = 1.0$ to avoid unnecessary conservatism. In all other circumstances, it should be taken as $\phi_s = 0.80$ [12].

Tests on a wide range of masonry shear walls have shown that if shear reinforcement is designed in accordance with the procedure outlined above, shear failure will be inhibited and a ductile flexural hinging mechanism will develop, even for walls with aspect ratios less than unity.

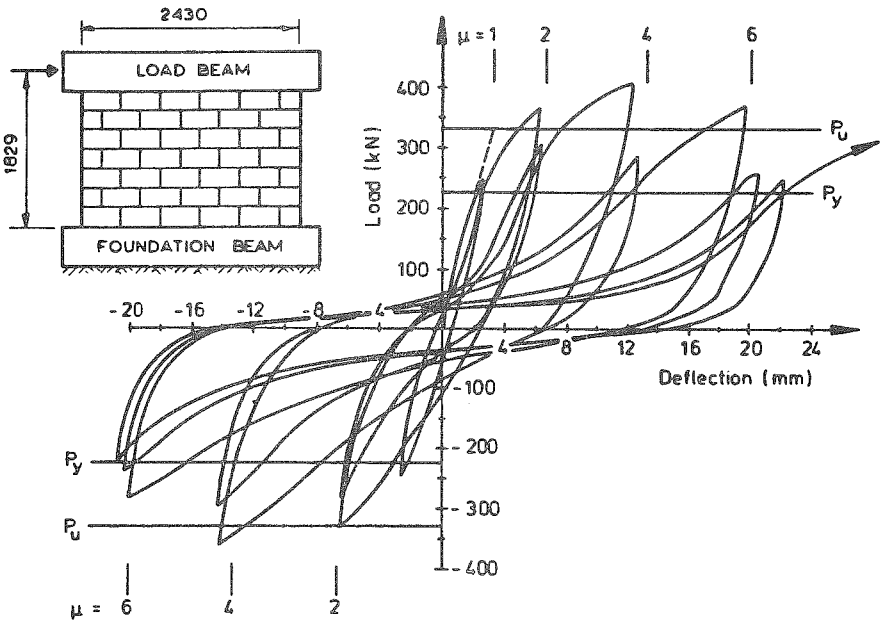

FIG. 10 - LOAD-DEFLECTION BEHAVIOUR OF A SQUAT CONCRETE MASONRY WALL

Figure 10 shows the load-deflection hysteresis loops for a typical squat wall of aspect ratio 0.75, tested under gradually increasing levels of displacement ductility factor. Also shown in Fig. 10 are the theoretical ultimate load P_u, and the first-yield load P_y, based on measured material strengths, and a strength reduction factor of $\phi = 1.0$. It will be seen that maximum experimental lateral loads exceeded P_u at the first peaks to $\mu = 2$ and 6. During subsequent cycles to the same level of displacement ductility significant load and stiffness degradation occurred as a result of a tendency of the wall to slide along the top of the foundation beam. However, on reloading to a higher level of displacement, the ultimate strength was again achieved. These results indicated that flexural failure modes with considerable ductility could be achieved from squat walls, but that energy absorption, as measured by area within the hysteresis loops was limited by the base slip. The results are very similar to those for squat reinforced concrete walls [16].

3.3 Ductility of Masonry Shear Walls

The maximum displacement, and hence the ductility capacity of a masonry structure, is a function of the ultimate curvature ϕ_u, which can be expressed as

$$\phi_u = \varepsilon_{cu}/c \qquad (11)$$

where ε_{cu} is the ultimate compression strain, and c is the distance from the extreme compression fibre to the neutral axis.

Based on an elastoplastic approximation of the load-deflection response of cantilever shear walls, and the equivalent stress block for masonry in compression, discussed above, it is a straightforward matter to calculate the displacement ductility capacity of a wall. Recent research [17] supports the use of a plastic hinge length for ductility calculations that is equal to half the section length, regardless of wall aspect ratio. Adopting this value, it can be shown [18] that the available displacement ductility is

$$\mu = 1 + \frac{1.5}{A_e}\left(\frac{\phi_u}{\phi_y} \cdot \frac{M_y}{M_u} - 1\right)\left(1 - \frac{1}{4A_e}\right) \qquad (12)$$

where A_e is the effective aspect ratio, based on height to the centre of lateral seismic force, rather than on wall height, ϕ_y is the curvature at the wall base when the extreme tension reinforcement is just at yield strain, and M_y and M_u are the base moments at first yield and ultimate respectively. Equation 12 indicates that μ will decrease as the aspect ratio (i.e. slenderness) of the wall increases. The other principal variable, namely the ratio of ultimate to yield curvature, ϕ_y/ϕ_y will depend on the material strengths, reinforcement ratio and axial load level.

Figure 11 compares ductility of cantilever shear walls of aspect ratio $A = h_w/\ell_w = 3$ with and without confining plates in the plastic hinge region [18]. As noted above, and illustrated in Fig. 7, confining plates greatly increase the effective ultimate strain (from about 0.0025 to 0.008) by inhibiting the characteristic vertical splitting failure mode. The design charts of Fig. 11 relate the ductility capacity μ_3 to the axial load ratio $N_u/f'_m A_g$, and the non-dimensionalised reinforcement ratio, ρ'. For unconfined masonry, (Fig. 10a),

$$\rho' = \rho \frac{8}{f'_m} = \frac{A_{st}}{\ell_w t} \frac{8}{f'_m} \qquad (13)$$

where A_{st} is the total area of flexural reinforcement, essentially uniformly distributed along the wall of length ℓ_w and thickness t, and f'_m is the masonry strength in MPa.

For confined masonry (Fig. 11b) the effect of confinement on crushing strength is incorporated in the dimensionless reinforcement ratio as

$$\rho' = \frac{10.42}{Kf'_m} \rho \qquad (14)$$

where K is given by Eqn. 5.

Figure 11 indicates that displacement ductility capacity reduces as the axial load ratio or the reinforcement ratio increases, but increases as f'_m increases. Comparison of

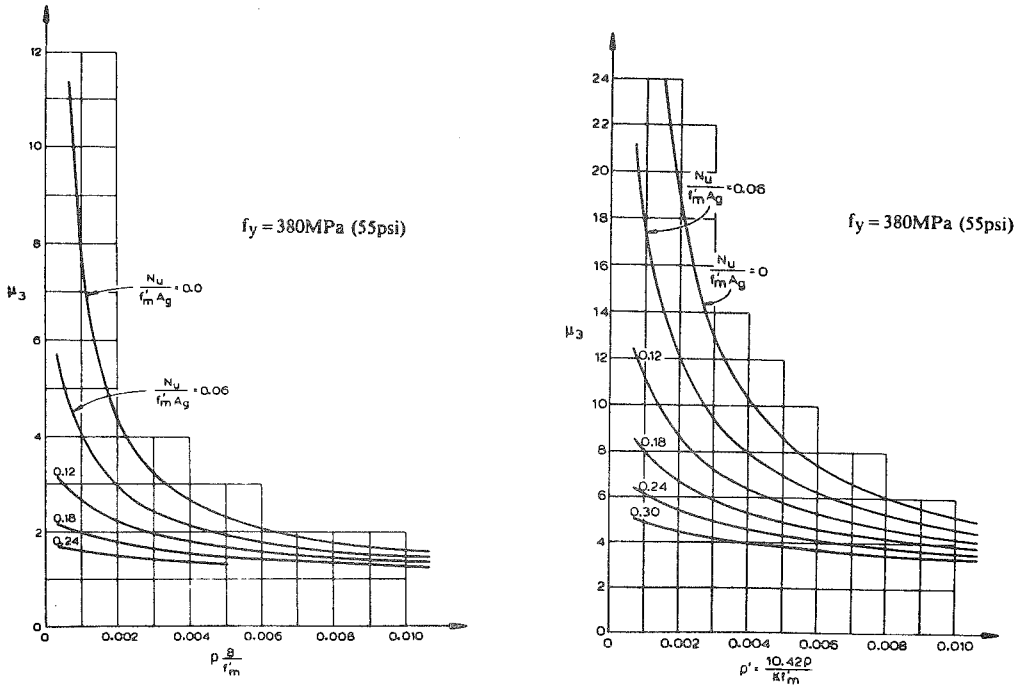

(a) Unconfined Masonry (b) Confined Masonry

FIG. 11 - DUCTILITY CAPACITY OF WALLS OF ASPECT RATIO $h_w/\ell_w = 3$

Fig. 11a and 11b indicates that using confining plates in plastic hinge regions can be expected to increase ductility capacity at least three-fold.

The curves of Fig. 11 apply for walls of aspect ratio $A = 3$. By manipulation of Eqn. 12, the ductility μ_A of a wall of aspect ratio A may be related to the ductility μ_3, given by Fig. 11 by the expression

$$\mu_A = 1 + \frac{3.43(\mu_3 - 1)(1 - .375/A)}{A} \qquad (15)$$

In Eqn. 15 (and Fig. 11) the aspect raio is related to the full wall height for simplicity, rather than using the effective aspect ratio of Eqn. 12. For regular walls, $A \cong 1.5A_e$. The ductility capacity found from Fig. 11 (or similar charts for different yield stresses [18] should be compared with that implied by the ratio of elastic response coefficient to code level lateral force coefficient, as illustrated in Fig. 1a. As noted above, a ductility demand of about $\mu = 4$ is typically implied. In the event that available ductility is less than this, redesign will be necessary. The most effective design options will be to increase f'_m, increase t, or use confining plates.

In order to investigate the theoretical reduction in ductility capacity with increasing slenderness implied by Eqn. 15, a series of tall slender concrete masonry shear walls of effective aspect ratio $A_e = 2.5$ has recently

been tested [5]. As well as testing the influence of wall aspect ratio on ductility capacity, the walls were intended to investigate the potential for lateral buckling of the compression end of the plastic hinge region under repeated cyclic loading, the influence of lapping flexural reinforcement within the plastic hinge region at the wall base, the use of confining plates in the plastic hinge region, and the influence of axial load level on seismic response.

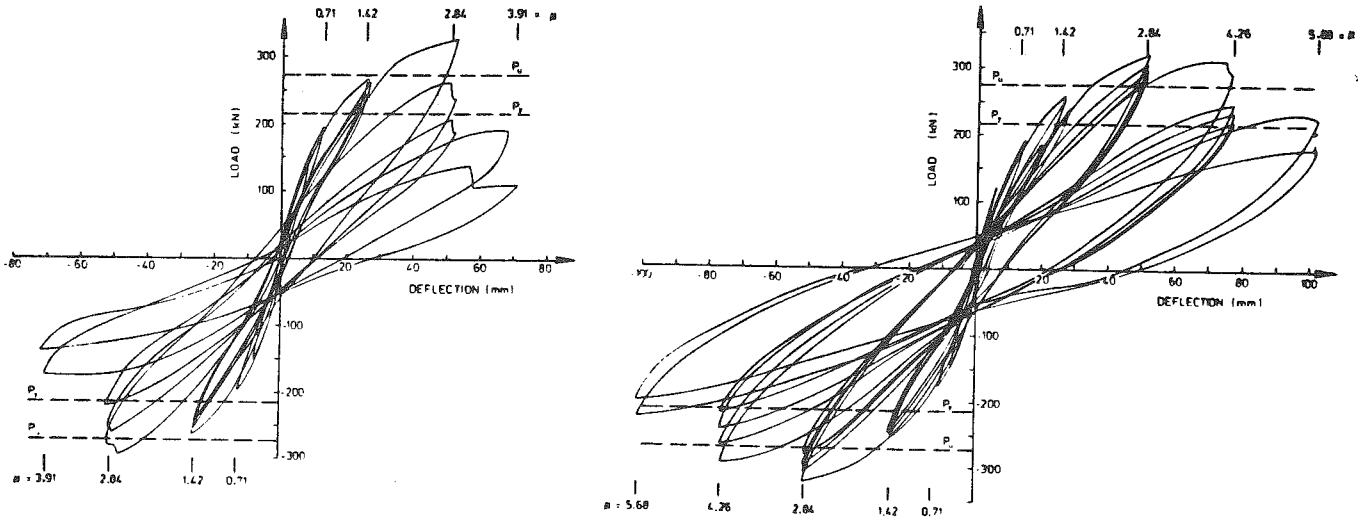

(a) Unconfined Wall (b) Confined Wall

FIG. 12 - LOAD DEFLECTION BEHAVIOUR OF CONCRETE MASONRY WALLS OF HIGH ASPECT RATIO

Figure 12 compares the load-deflection hysteresis loops for two walls with reasonably heavy axial load, identical except that Wall 2 contained confining plates in the critical mortar beds, while Wall 1 was unconfined. The confining plates in Wall 2 were 600 mm long and were placed at each end of the wall, only in the bottom 7 mortar courses.

During cycling of the unconfined wall to $\mu = 2.84$, crushing of mortar beds and vertical splitting of blocks within the compression zones near the wall ends occurred. The vertical splitting, which is characteristic of the failure mechanism of masonry in compression resulted in bond failure along the extreme tension reinforcement on reversal of load direction. This in turn caused degradation of load capacity, as is evident from the successive cycles at $\mu = 2.84$ in Fig. 10a. On increasing the displacement to a ductility factor of $\mu = 3.91$, further physical and load degradation occurred and the test was abandoned.

The companion confined wall exhibited much better behaviour. At a ductility of $\mu = 2.84$ the wall exceeded the theoretical ultimate strength for each peak displacement during 4 complete cycles. At a ductility of $\mu = 4.26$, some cracking and crushing of individual face shells in the

compression zones at the wall base occurred, but load degradation was not severe. Further testing to $\mu = 5.68$ resulted in extensive loss of face shells, and buckling of the extreme compression reinforcement.

The results of the test series confirmed the theoretical reduction in ductility capacity with increased aspect ratio. Using the design chart approach of Fig. 11, Wall 1 was estimated to have a ductility capacity of $\mu = 2.3$, which was in reasonable agreement with the observed degradation at $\mu = 2.8$.

3.4 Design of Structural Infilled Frames

Although beam theory can predict the elastic response of infilled frames with adequate accuracy, behaviour becomes more complex as deformations increase, and separation between frame and panel occurs due to differences between flexural deformations of the frame and shear deformations of the panel (see Fig. 13a). This separation may occur at 50-70% of the ultimate lateral shear capacity of the infill for reinforced concrete frames, and at very much lower loads for steel frames. After separation occurs, the panel acts as a diagonal strut with an effective width, w, less than that of the full panel, as shown in Fig. 13a.

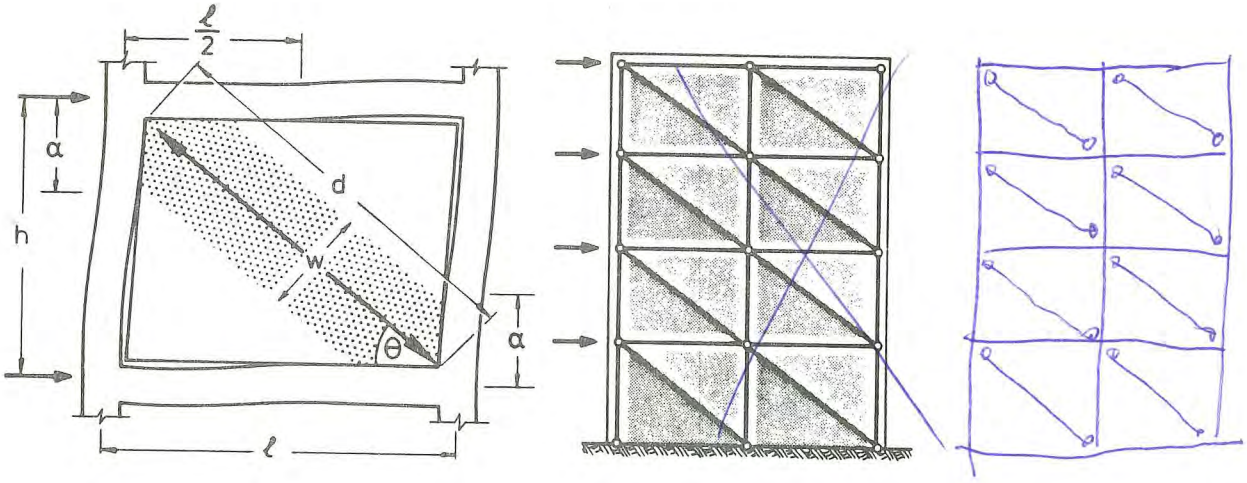

(a) Deformation under shear load

(b) Equivalent braced frame for 2 bay, 4 storey infilled wall

FIG. 13 - LATERAL STIFFNESS OF FRAME INFILLED WITH MASONRY

Natural period calculations should be based on the structural stiffness after bond separation. This may be found by assuming the frame members to be pin-jointed and braced by the equivalent diagonal masonry struts. Figure 13b shows the equivalent system for a 2-bay, 4-storey frame. Stafford-Smith and Carter [19] have developed analytical expressions based on a beam on elastic foundation analogy, modified by experimental results, showing that the effective

width w of the diagonal strut depends on the relative stiffnesses of frame and panel, the stress-strain curves of the materials, and the load level. However, since a high value of w will result in a stiffer structure, and therefore potentially higher seismic response, it is reasonable to take a conservatively high value of

$$w = 0.25\,d \qquad (16)$$

where d is the diagonal length, which agrees reasonably well with Smith and Carters' charts, assuming typical masonry infill properties and a load level of 50% of the ultimate capacity of the infilled frame.

Strength

There are several different possible failure modes for masonry infilled frames, including

(1) tension failure of the tension column resulting from applied moments,

(2) sliding shear failure of the masonry along horizontal mortar courses (generally at or close to midheight of the panel),

(3) diagonal tensile cracking of the panel. This does not generally constitute a failure condition, as higher lateral loads can be supported until:

(4) compression failure of the diagonal strut,

(5) flexural or shear failure of the columns.

In many cases the failure may be a sequential combination of some of the above failure modes. For example, flexural or shear failure of the columns will generally follow a sliding shear failure, or diagonal compression failure, of the masonry. For a particular infilled frame, the strength associated with the various possible failure modes should be calculated, and the lowest value used as the basis for design.

Tension failure mode

For infilled frames of high aspect ratio, the critical failure mode may be flexural, involving tensile yield of the tension column steel and of any vertical steel in the tension zone of the infill panel. Under these conditions the frame is acting as a cantilever shear wall, and a reasonably ductile failure mode can be expected. Design can then be in accordance with the recommendations for masonry shear walls given in 3.1 to 3.3 above.

Sliding shear failure

If sliding shear failure of the masonry infill occurs, the equivalent structural mechanism changes from the diagonally braced pin-jointed frame of Fig. 13a to a knee-braced frame shown in Fig. 14. The support provided by the masonry panel forces column hinges to form at approximately

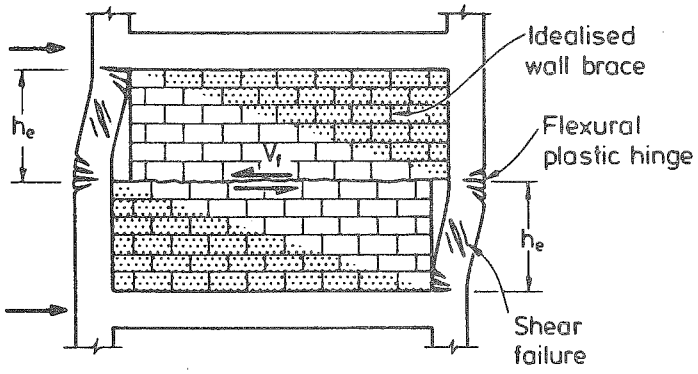

FIG. 14 - SLIDING SHEAR FAILURE OF MASONRY INFILL

mid-height and top or bottom of the columns, or may result in column shear failure. The lateral load capacity is initially governed by the combined actions of frictional resistance to sliding shear in the panel, and shear in the columns. Thus the failure load V_u for the panel in Fig. 14 may be estimated as

$$V_u = \frac{2}{h_c}(M_{ut} + M_{uc}) + V_f \qquad (17)$$

where M_{ut} and M_{uc} are the ultimate moment capacities of the tension and compression columns respectively, including the effects of axial forces resulting from gravity loads and overturning moments.

Shear friction force V_f degrades rapidly with cycling and should conservatively be ignored in calculating the shear capacity of this failure mode. The effective column height h_c between column hinges is approximately half the storey height h, both for exterior columns and for columns between adjacent infill panels, as in the latter case hinges tend to form close to the quarter points. Thus for a knee-braced frame of n bays wide, and $n + 1$ columns, the ultimate shear capacity is

$$V_u = \frac{4}{h} \sum_{i=1}^{n+1} M_{ui} \qquad (18)$$

where M_{ui} is the ultimate moment capacity of the ith column, including axial force effects. Column shear steel should be based on a capacity approach using overstrength column moments to avoid column shear failure.

The equivalent diagonal strut compression force to initiate horizontal shear sliding depends on the infill masonry type, the shear bond strength f_{bs} between the masonry and mortar, and the ratio between the maximum shear and the corresponding vertical stress in the panel. From these data, a conservative estimate of the diagonal strut force (Fig. 14a) when sliding initiates for masonry infill frames of typical dimensions and strength may be taken as

$$R_s = (0.9 + 0.3\,\frac{l}{h})\, f_{bs} h.t \qquad (19)$$

where l/h is the ratio of panel length to height, and t is the panel thickness. Equation 19 should be used to define the force required to initiate this failure mode, for comparison

with the flexural failure moment and the diagonal crushing force, as below, to establish the probable failure mode. However, for ductile response, the value predicted by Eqn 17 should be used as the design capacity.

Compression failure of diagonal strut

For typical masonry infill panels, Stafford-Smith and Carter show that diagonal tensile splitting will precede diagonal crushing. However, the final panel failure force will be dictated by the compression strength, which may thus be used as the ultimate capacity. Trigo [20] and Leuchars and Scrivener [21] found that the following modified form of the diagonal compression failure force predicted by Stafford-Smith and Carter gave a conservative agreement with test results

$$R_c = \frac{2}{3} \alpha t f'_m \sec \theta \qquad (20)$$

where f'_m = masonry prism strength and α defines the contact length between panel and column (see Fig. 13a) given by

$$\alpha = \frac{\pi}{2} \left(\frac{4 E_f I_f h_m}{E_m t \sin 2\theta} \right)^{\frac{1}{4}} \qquad (21)$$

where E_f and I_f are the modulus of elasticity and moment of inertia of the frame columns, E_m and h_m are the modulus of elasticity and height of the infill, and θ is the angle between the diagonal strut and the horizontal. On inelastic cycling the capacity of the diagonal strut will degrade, and behaviour will approximate the knee-braced frame of Fig. 14.

Ductility

The flexural failure mode involving tensile column yield possesses adequate ductility potential but is an uncommon failure mode. Klingner and Bertero [22] with work on carefully designed infilled frames with closely spaced vertical and horizontal reinforcement in the infill have shown that high ductilities can be obtained from panel shear mode failure, with good energy absorption characteristics. However, the knee-braced frame concept involves energy dissipation by column hinging in the bottom storey. To provide the required total structure ductility, the level of ductility required of the hinging 'soft storey' will be very large for frames more than two storeys high. It is thus recommended that infilled frames with either sliding shear failure or diagonal compression failure should be designed to respond elastically under seismic attack. A limited structural ductility would be appropriate for frames of moderate height provided well detailed and distributed horizontal and vertical reinforcement is placed in the infill panels, spliced to dowel starters in the frame columns and beams.

3.5 Design of Masonry Frames

It is now generally accepted that to obtain satisfactory inelastic seismic performance from multistorey building frames, it is necessary to force plastic hinges to form at the ends of beams, and to avoid plastic hinging in the columns. This is the so-called weak-beam/strong-column concept [23] and is adopted to avoid the formation of a soft-storey mechanism with high local ductility demand on lower storey columns. Other undesirable mechanisms such as beam or column shear failures, or joint failures must be avoided since these are brittle, and do not possess the fundamental requisite of ductile response, namely the ability to deform inelastically during repeated cyclic displacement response without significant strength or stiffness degradation.

The procedure adopted to ensure that inelastic action is concentrated only in flexural beam hinges is the so-called 'capacity-design' procedure [13]. The flexural reinforcement of the potential plastic hinge region is detailed to ensure a dependable flexural strength no less than that corresponding to the code distribution of lateral seismic loads, but all other parts of the structure are detailed to ensure their strength exceeds that corresponding to the maximum feasible strength of the potential plastic hinge regions. This maximum feasible strength is of course very much higher than the required dependable strength of the beam hinges, since the latter will include a strength reduction factor, and be based on conservative estimates of material strengths (masonry compression strength and reinforcement yield strength) rather than actual strengths. Further, at high ductility levels, flexural reinforcement in plastic hinge regions may be strained into the strain-hardening range, resulting in reinforcement stresses which exceed the actual yield stress. This procedure recognises that it is the actual flexural strength rather than the dependable strength that will be developed at the plastic hinges, as has already been noted above when discussing the shear design of cantilever shear walls.

Beam flexure

As shown in Fig. 15c, the beam flexural reinforcement should be uniformly distributed down the beam depth rather than attempting to follow conventional reinforced concrete beam design (Fig. 15a), which will produce excessive congestion in the typically narrow masonry beam (Fig. 15c).If hollow-unit masonry is used, this will imply the use of bond-beam units at all courses.

Beam shear

Beam shear design should be based on maximum feasible flexural strength being attained in the beam plastic hinges, and the conservative assumption that all beam shear force needs to be carried by shear reinforcement.

To ensure against column plastic hinges or shear failure, design column forces must be enhanced above the level

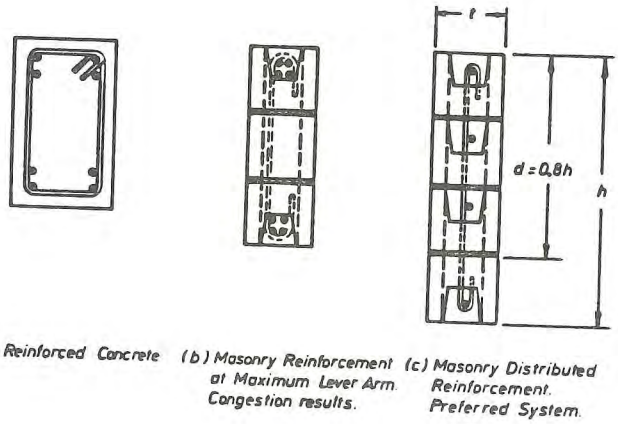

FIG. 15 - DISTRIBUTION OF BEAM FLEXURAL REINFORCEMENT

corresponding to development of dependable flexural strength in the beams, on the same basis as for beam shear. It is advisable to further enhance the design forces to reflect possible changes from the elastic distribution of forces corresponding to the code distribution of lateral loads, resulting from dynamic higher mode response effects. For structural frames with fundamental elastic period less than 0.7s, which will cover most masonry buildings, a dynamic amplification factor of 1.3 is appropriate [23]. As with shear, design to actions calculated by capacity design principles need not incorporate strength reduction factors.

Beam-column joint design

The design of the joint region between beams and columns requires special consideration. Two aspects are of particular importance: (1) the width of the joint (parallel to the beam axis) must be sufficient to allow the necessary change in beam reinforcement stress through the joint to be developed by bond, and (2) the dimensions and reinforcement of the joint must be adequate to carry the shear forces developed in the joint by the moment gradient across the joint.

Figure 16a shows the seismic forces and moments acting on a typical interior joint of a masonry frame, such as the critical region of Fig. 5. Because of the moment reversal across the joint, beam reinforcement may be yielding in compression at one side of the joint, and yielding in tension on the other side (Fig 16c). Consequently the joint width, which is equal to the column width h_c must be at least equal to the sum of tension and compression development lengths for the reinforcement. Typically this will require joint widths of

$$h_c \geqq 90 d_b \qquad (22)$$

where d_b is the diameter of the beam flexural reinforcement.

The moment gradient horizontally and vertically through the joint also enable the joint shear forces to be calculated. The relevant forces and moments for computation of the horizontal joint shear force V_{sh} are shown in Fig. 16b. Note that the moment $V.h'_c$ from the beam shear forces (assumed equal in this example) assist in effecting the change in column moment from M_T at the top of the joint to M_B at the bottom

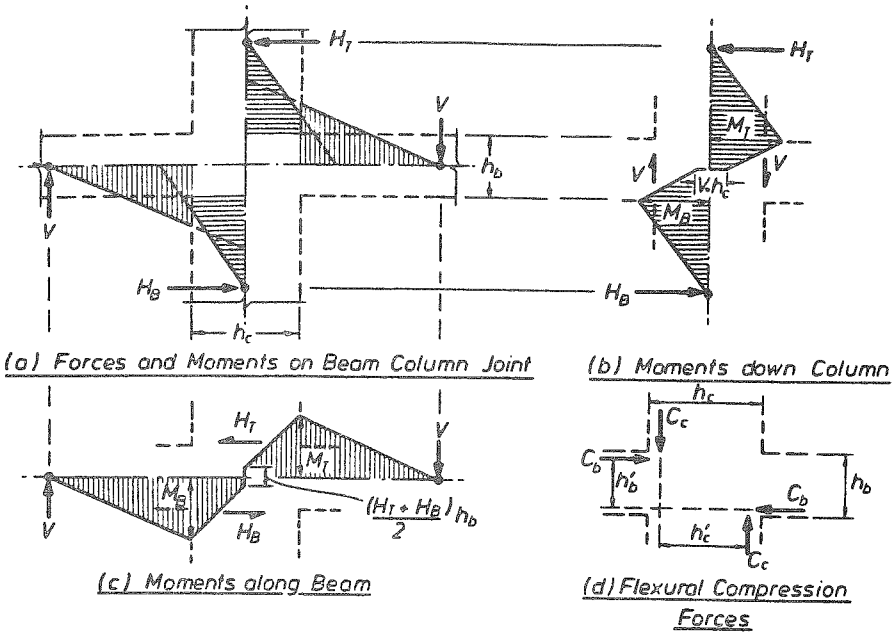

FIG. 16 - FORCE AND MOMENTS FOR COMPUTATION OF JOINT SHEARS

of the joint, and hence the horizontal joint shear will be

$$V_{jh} = \frac{(M_T + M_B - Vh'_c)}{h'_b} \qquad (23)$$

Conventional reinforced concrete joint design theory would require all of V_{jh} to be carried by horizontal joint reinforcement in the form of stirrups unless column axial load levels are high. Thus the required area of horizontal joint reinforcement, of yield strength f_{yh} parallel to the beam reinforcement will be

$$A_{jh} = V_{jh}/f_{yh} \qquad (24)$$

Similar calculations are necessary to determine the amount of vertical joint shear reinforcement, as has been explained in detail elsewhere [24].

Ductility

Inherent in the approach suggested above is the need to provide adequate ductility in the beam plastic hinges. No unique expression equivalent to Eqn 12 for cantilever shear walls is possible for masonry frames, as the relative contribution to elastic deformation from beams, columns and joint deformation depend on the overall frame geometry as well as beam and column section properties, while the inelastic deformation is dependent only on the plastic rotation of the beam hinges. However, based on the approximation that beam elastic deformation contributes 50% to the total yield displacement, the following expression, limiting the depth of the compression zone, c, in the beam plastic hinges will ensure

adequate ductility without exceeding the ultimate compression strain of $\varepsilon_{cu} = 0.0025$:

$$c \leq 1.2\, h_b^2/(\mu \ell_n) \qquad (25)$$

where h_b is the beam depth, ℓ_n is the clear beam span between column faces, and μ is the required structure displacement ductility factor.

Figure 17 shows details of a full size reinforced masonry beam column joint representing the region between column contra-flexure points and beam contraflexure points circled in Fig. 5, and designed to the above principles. The general test set up is shown in Fig. 17a, and details of the reinforcement in Fig. 17b. In this figure, the nomenclature 4D20 means 4 Deformed bars of nominal diameter 20 mm and yield strength 275 MPa, etc.

Lateral load-displacement hysteresis loops for the test units are plotted in Fig. 17c. Also included in this figure are the theoretical ultimate lateral load of $P_u = 121$ kN, the theoretical load P_y at which the extreme tension rebar in the beams first reached yield stress, and the design 'dependable' strength, $0.85P_u$.

Very satisfactory performance is indicated by Fig. 17c. Initial peak loads at $\mu = 2$, 3 and 4 are within ±5 of P_u, and load degradation during subsequent cycles at a given ductility level is comparatively minor. The loop shape is very stable, and indicates good energy dissipation capacity. At $\mu = 6$, the initial peak load exceeds P_u, but significant degradation occurs during the subsequent cycles, as a result of the physical degradation of the compression zones, and consequent buckling of the beam reinforcement.

The behaviour represented by Fig. 17c is as good as could be expected of well-designed reinforced concrete elements.

4. DETAILING

It could be argued that sound detailing is even more important than the provision of adequate shear and flexural strength. It is beyond the scope of this paper to deal with this topic in depth, and in consequence, only brief notes on matters of prime importance are included. These are based on requirements included in the recent New Zealand Masonry Design Code [12].

4.1 Wall Slenderness Ratios

Within plastic hinge regions, there is a danger of lateral instability of the wall if ratio of clear storey height to wall thickness is too high. This ratio should not exceed 13.3 unless the structure is less than three storeys high, or has a flexural compression zone (under combined axial load and bending moment) shorter than $c = 0.3\ell_w$ or $c = 4t$ where ℓ_w and t are the wall length and thickness respectively. This requirement is to prevent buckling of the compression end of the wall under inelastic cycling.

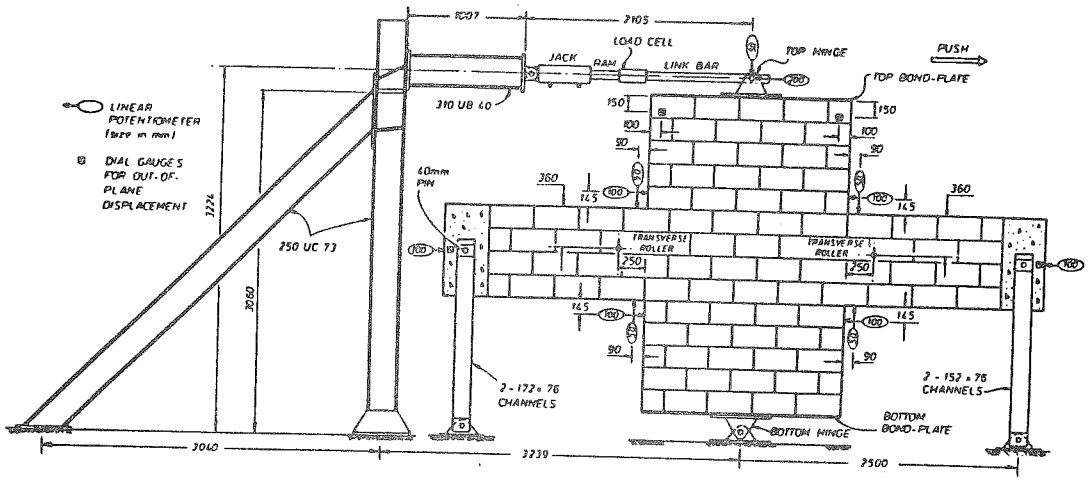

(a) Test Set Up

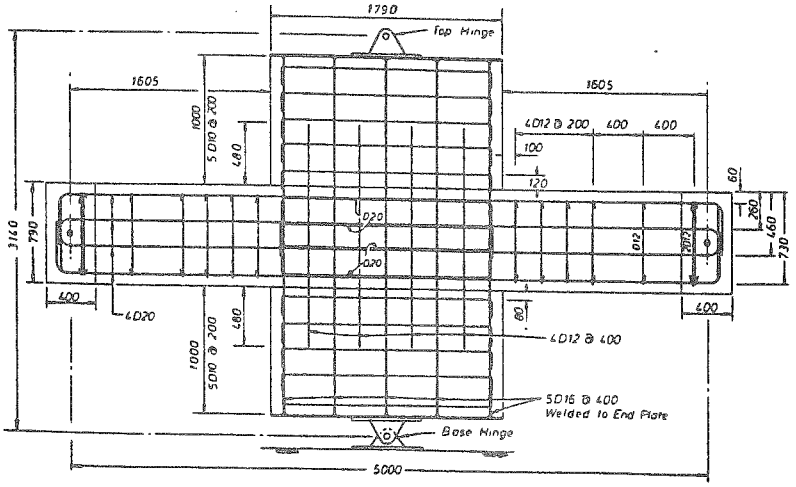

b) Dimensions and Reinforcement

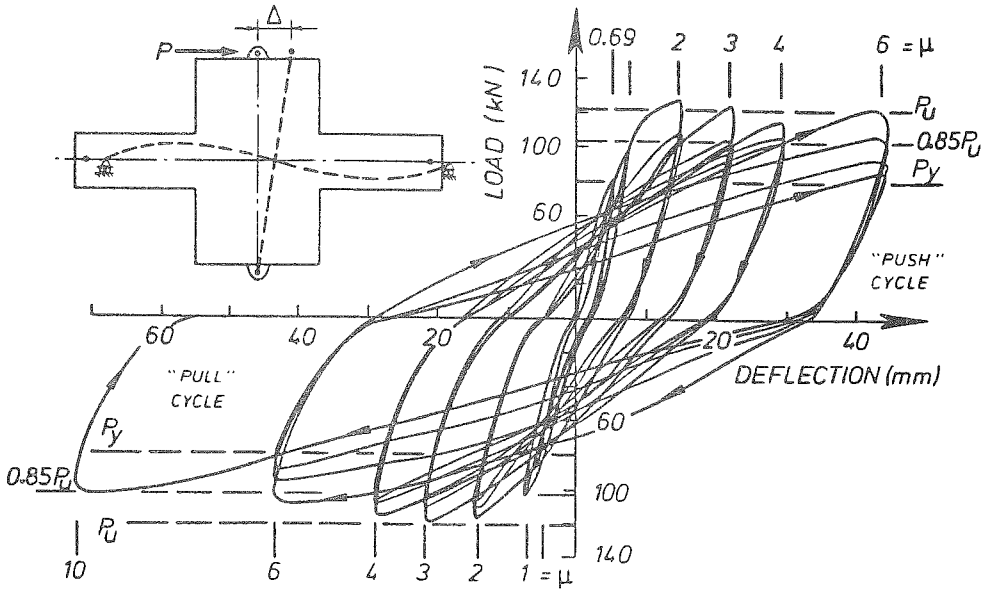

(c) Lateral Load-Displacement Hysteresis Loops

FIG. 17 - TESTING OF A CONCRETE MASONRY BEAM-COLUMN JOINT

4.2 Reinforcement Ratio

The sum of the horizontal and vertical reinforcement ratios for walls must be at least 0.2%, which can be divided up to 2/3, 1/3 in the two directions. Maximum reinforcement ratio is related to the cavity size, and must not exceed $\rho = 8/f_y$ (or $13/f_y$ at laps) at any part of the wall. Bar diameter must not exceed 1/4 of the cavity width. Maximum spacing between adjacent bars in both horizontal and vertical directions varies with the seismicity of the site and the importance of the building, and in the most stringent case is 400 mm each way. An exception to the requirement for two-way reinforcement is made for minor structures in the less seismically active regions of New Zealand, provided the structures are designed for the elastic response levels of seismic lateral force, and are subject to design shear stress which does not exceed the appropriate value for masonry shear mechanisms in which case horizontal reinforcement may be omitted.

4.3 Anchorage

Where possible, the designer should be encouraged to avoid lapping reinforcement within plastic hinge regions. Basic development lengths of $40d_b$ and $54d_b$ are recommended for bars of dia. d_b and yield strength 275 MPa and 380 MPa respectively. These should be increased by 50% where lapping within the plastic hinge region cannot be avoided. It should be noted that tests on unconfined slender walls indicate that even with the length of lapping, bond failure will eventually occur. The purpose of the increased lap length is to defer the bond failure for sufficient length of time to allow the structure to successfully 'ride out' the earthquake.

4.4 Non-structural Walls

Veneers and partitions, though considered non-structural, must be carefully designed to avoid the possibility of their collapse causing hazard to life. Sufficient separation between partitions and the structure's lateral load resisting system must be provided to prevent contact during the design level earthquake. This is to avoid loading of the partition, and structural modification of the primary seismic system. Partitions should be reinforced to provide sufficient out-of-plane load capacity, to withstand self inertia response.

Shedding of poorly connected masonry veneer into streets during earthquakes is a real hazard to life. On multistorey buildings, veneer should be vertically reinforced, and adequately tied back to the structural system with connections capable of allowing adequate relative lateral movement.

5. ASSESSMENT OF EXISTING MASONRY BUILDINGS

This paper has considered only the design philosophy appropriate to new masonry buildings. Because of the obvious advantages of reinforcement, the arguments have specifically excluded unreinforced masonry, which relies solely on gravity forces for stability. However, a topic that is becoming increasingly important is the assessment of potential seismic

performance of existing unreinforced masonry structures, often designed more than 50 years ago, and the development of economically viable strengthening strategies. In this area, the use of elastic design and allowable working shear calculations become excessively conservative. Analysis based on ultimate strength design is imperative, and considerations of stability based on assessing the level of seismic energy input required to destabilise a wall give more realistic results [25]. In many cases it will follow that, based on such calculations, adequate performance can be assured by providing sound connections between walls and floor, and walls and roof diaphragm, and removal of unstable elements such as unsupported parapets and chimneys. Much research is needed in this field.

6. CONCLUSIONS

This paper has attempted to outline a consistent design philosophy for masonry structures, based on the following tenets:

- the choice of a suitable structural system
- the use of ultimate strength theory for flexural design
- the use of a capacity design procedure to ensure brittle failure modes (shear failure) cannot occur
- the assessment of structural ductility capacity, and comparison with values implied by the lateral load level adopted
- careful detailing to ensure that the masonry elements can perform as the designer envisaged.

Adoption of this philosophy requires a major change to design practice currently common in masonry construction. However, unless we are prepared to treat masonry as a modern material capable of rational design, it will continue to demonstrate that masonry designed along conventional, traditional lines is a hazard under strong seismic attack.

7. REFERENCES

1. JENNINGS, P.C. (Ed) 'Engineering Features of the San Fernando Earthquake, Feb. 9, 1971' Rept. EERL 71-02, California Institute of Technology, June 1971, 512pp.
2. ACI COMMITTEE 531 'Building Code Requirements for Concrete Masonry Structures (ACI 531-79)(Revised 1981) and Commentary', American Concrete Institute, Detroit, 1981, 60pp.
3. 'Tentative Provisions for the Development of Seismic Regulations for Buildings', Special Publication No. 510, National Bureau of Standards, Washington D.C., 1978, Chapter 12 - Masonry, pp.111-166.
4. PRIESTLEY, M.J.N., 'Seismic Resistance of Reinforced Concrete Masonry Shear Walls with High Steel Percentages', Bulletin, New Zealand National Society for Earthquake Engineering (Wellington), Vol. 10, No. 1, March 1977, pp.1-16.

5. PRIESTLEY, M.J.N. and ELDER, D.M., 'Cyclic Loading Tests of Slender Concrete Masonry Shear Walls', Bulletin, New Zealand National Society for Earthquake Engineering (Wellington), Vol. 15, No. 1, March 1982, pp.3-21.
6. MAYES, R.L., OMOTO, Y. and CLOUGH, R.W., 'Cyclic Shear Tests of Masonry Piers", University of California, Berkeley, Report EERC 76-8, May 1976, 84pp.
7. SKINNER, R.I., 'Earthquake Generated Forces and Moments in Tall Buildings', Department of Scientific and Industrial Research (Wellington), Bulletin No. 166, 1964, 106pp.
8. PRIESTLEY, M.J.N., 'Seismic Design of Masonry Buildings - Background to the Draft Masonry Design Code DZ 4210', Bulletin, New Zealand National Society for Earthquake Engineering, Vol. 13, No. 4, pp.329-346.
9. PRIESTLEY, M.J.N. and ELDER, D.M., 'Stress-Strain Curves for Unconfined and Confined Concrete Masonry', ACI Journal, Proceedings, Vol. 80, No. 3, May/June 1983, pp.192-201.
10. SCOTT, B.D., PARK, R. and PRIESTLEY, M.J.N., 'Stress-Strain Behaviour of Concrete Confined by Overlapping Hoops at Low and High Strain Rates', ACI Journal, Proceedings, Vol. 79, No. 1, Jan/Feb. 1982, pp.13-27.
11. Atkinson, R.H. and KINGSLEY, G.R., 'A Comparison of the Behaviour of Clay and Concrete Masonry in Compression', US-Japan Coordinated Program for Masonry Building Research, Report 1,1-1, Atkinson-Noland & Ass. 1985, 151pp.
12. 'Code of Practice for Masonry Design', NZS 4203P, Standards Association of New Zealand, Wellington, 1984.
13. PARK, R. and PAULAY, T., 'Reinforced Concrete Structures', John Wiley & Sons, New York, 1975, 769pp.
14. BLAKELEY, R.W.G., COONEY, R.C. and MEGGET, L.M., 'Seismic Shear Loading at Flexural Capacity in Cantilever Wall Structures', Bulletin, New Zealand National Society for Earthquake Engineering, Vol. 8, No. 4, Dec. 1975, pp.278-290.
15. NOLAND, J.L., 'U.S. Research Plan', US-Japan Coordinated Program for Masonry Building Research, Atkinson-Noland Ass. Boulder, 1984, 22pp.
16. PAULAY, T., PRIESTLEY, M.J.N. and SYNGE, A.J.,'Ductility of Earthquake Resisting Squat Shear Walls', ACI Journal, Proceedings, Vol. 79, No. 4, July/Aug. 1982, pp.257-269.
17. PRIESTLEY, M.J.N. and PARK, R., 'Strength and Ductility of Bridge Substructures', RRU Bulletin 71, National Roads Board, Wellington, 1984, 120pp.
18. PRIESTLEY, M.J.N., 'Ductility of Unconfined and Confined Concrete Masonry Shear Walls', Masonry Society Journal, Vol. 1, No. 2, July/Dec. 1981, pp.T-28 to T-39.
19. STAFFORD-SMITH, B. and CARTER, C., 'A Method of Analysis for Infilled Frames', Proceedings, Institute of Civil Engineers, Vol. 44, 1969, pp.31-44.
20. TRIGO, J.d'A., 'Estructuras de Paineis sob a Accaó de Solicitacoes Horizontais', Laboratório Nacional de Engenharia Civil, Lisbon, 1968.
21. LEUCHARS, J.M. and SCRIVENER, J.C., 'Masonry Infill Panels Subjected to Cyclic In-Plane Loading', Bulletin, New Zealand National Society for Earthquake Engineering, Vol. 9, No. 2, 1976, pp.122-131.
22. KLINGNER, R.E. and BERTERO, V.V., 'Infilled Frames Aseismic Construction', Proceedings, Sixth World Conference on Earthquake Engineering, New Delhi, 1977.

23. 'Code of Practice for the Design of Concrete Structures', NZS 3101, Standard Association of New Zealand, 1982.
24. PRIESTLEY, M.J.N. and CHAI YUK HON, 'Seismic Design of Reinforced Concrete Masonry Moment Resisting Frames', The Masonry Society Journal, Vol. 5, No. 1, Jan/June 1985.
25. PRIESTLEY, M.J.N., 'Seismic Behaviour of Unreinforced Masonry Walls', Bulletin, New Zealand National Society for Earthquake Engineering, Wellington, Vol. 18, No. 2, June 1985, pp.191-205.

Classn:

DESIGN OF CONCRETE STRUCTURES
Joint University of Canterbury - New Zealand Concrete Society Seminar

R. Park, T. Paulay, M.J.N. Priestley and L. Gaerty

ABSTRACT: A collection of eight research papers and short state of the art reports, previously published, to serve as supplementary notes for a seminar. They cover seismic design aspects of reinforced concrete ductile frames, frames with limited ductility, beam-column joints, structural walls, hybrid structures, frames incorporating prestressed concrete and masonry structures. A draft code of structures for the storage of liquids is also included.

Department of Civil Engineering, University of Canterbury, Christchurch, New Zealand, 1986, Research Report 86-14

DESIGN OF CONCRETE STRUCTURES

Session 9:

Design Charts and Computer Programs for Reinforced Concrete

L.Gaerty, Assistant Director NZCRA

To Begin ..... A Timeless Message?

More than 50 years ago, Haddon C. Adams included the following remarks in the preface to the first edition (1933) of his classic text on The Elements of Reinforced Concrete Design:

> "In the design of complicated structures as a whole individual assumptions will have to be made which cannot be brought to the touchstone of general usage. In such cases individual judgment must be used, and care and imagination must be exercised in the consideration of possible variations in the finished structure from the conditions assumed in design.
>
> There is a further snare in the path of the unwary. As his experience increases the designer will embark upon new methods of dealing with complicated design. The most complicated method will not always yield the surest result. There is always a danger of being lulled into a false sense of security by abstruse mathematics - there is no magic charm in complicated and intricate computation; there is indeed some danger, and the safest guide in most matters is to cling fast to common sense.
>
> One word about the use of design charts. Until he has understood the methods and working which these are intended to replace the student has no business with them; they are useless in the learning stage, and useful only when applying knowledge to the solution of design problems. We must seek always first to understand, secondly to think constructively, and finally, when we have so to speak "found our feet", to use simple and direct methods of easing the tedious work of arithmetical solution.
>
> Reinforced concrete design is to those who pursue it from choice a fascinating study. It is a young science, and we have still much to learn."

Much has been learned and much has changed on the reinforced concrete scene in the interim since the words cited above were first written. However, the judgements and opinions expressed therein remain as viable in today's world of ultimate strength design, sophisticated analytical techniques, and electronic computing power as they ever were in their original context of working stresses, elastic analysis, and slide-rule calculations.

The Nature of Design Aids

Notwithstanding a multiplicity of possible forms, all design aids worthy of the name have the same primary function - namely, a reduction/easing of arithmetical tedium with consequent savings in time (and sanity!)

The presentation of locally comprehensive data sets is a recurrent (and very important) feature of many design aids. Consider, for example, tables of available reinforcement areas as against design charts showing viable combinations of axial load and bending moment for reinforced concrete columns. In both of these instances, the designer is confronted with relatively broad spectrum of would-be solutions from which to make a choice. The manner of presentation is different for each (numerical vs. graphical) but the two cases have much more in common than might appear to prevail at first sight.

Some users of design aids tend to express a personal preference for the diagramatic (as distinct from the tabular) mode - generally on the grounds that charts offer the designer greater overall perspective by way of their "shape". However, while the shape of interaction diagrams and the like undoubtedly carries useful information (from which important relational inferences may be drawn), the same is true of tabular assemblies of data providing the eye and mind of the observer are appropriately tuned (whether by training or natural inclination). The attribute of "shape" probably does not have the same visual immediacy in the context of tabular data presentations (as against diagramatic forms) but is nonetheless real.

Charts and diagrams do embody far greater potential for displaying large amounts of quantitative information within the confines of a single page than applies for numerical tables. If required, graphical data presentation can be extremely efficient in terms of minimum usage of space. Indeed, in the preparation of typical design charts, it is often the necessary provision of local titles (for the purpose of differentiating between particular curves) which serves to limit the number of separate curves able to be sensibly accommodated within any one diagram.

It is naturally important that design charts be easily "readable". (A would-be design aid which replaces the tedium of repetitive arithmetic with severe eye-strain serves no useful function!). The question of adequate readability also hinges on aspects of scale resolution. Some situations require only coarse resolution (e.g. the checking of relatively "safe" load combinations): others are somewhat more demanding (e.g. the checking of borderline cases and the taking of values for parameters to be used in subsequent calculations). If pushed to the limit, the readability of all design charts will be found wanting. This is not an indictment of design charts per se but rather a simple statement of associated fact. Those who might dismiss the worth of design charts on this basis could themselves be accused of losing sight of a proper perspective.

Having highlighted the matter of limited readability in the context of graphical data presentations, it must also be emphasised that tabular forms are rarely exempt from similar "deficiencies" if comprehensively tested. Here, the discrete items of numerical information actually listed are generally expressed to a level of precision deemed sufficiently "accurate" for the application in hand. The would-be problem (if it arises) concerns the status and/or reliability of interpolated values. As is the case for reading from graphs, different situations can engender quite different understandings as to how critical are considerations of local accuracy.

Left to their own devices, most structural designers will tend to assume that linear interpolation is valid unless positively notified to the contrary. Of course, the

immediate simplicity of linear mathematics has major appeal. It is commonly believed that the widespread espousal by concrete designers of the linear form (for interpolative and other purposes) carries over into the realms of graphical data presentations by way of a marked dislike for non-linear scales. Several compilers of reinforced concrete design charts make specific reference to having deliberately steered clear of non-linear scales (such as often feature in "scientific" nomograms) and cite the low opinion of structural concrete designers for anything other than linear scales as the reason for their having implemented this policy. To what extent the apparent aversion of designers to non-linear scales (and, indeed, to nomograms) applies in reality remains uncertain.

The code-dependency of design aids can vary in degree between nil and extensive. At one end of the scale lie items which owe no allegiance to specific codes of practice. Such items include general applied mechanics presentations and tables of enumerated mathematical parameters (e.g. second moments of area). Conversely, at the opposite extreme, the quantitative singificance of some design aids is closely tied to the particular code prescriptions employed in their generation. Column design charts which embody the constitutive influence of nominated stress-strain relationships, strength reduction factors, etc., fall into this category. In some instances, the code-related content of a design aid may only involve the superposition of upper and/or lower limits (whether tabulated or plotted), with these serving to define the "allowable" range of an otherwise unfettered parameter (e.g. area of reinforcement ratios).

Given two design aids which differ as to the degree of code-dependency manifest but are otherwise equivalent, that possessing the greater code content is likely to offer more advantage to the designer - providing, of course, that the actual code content is relevant to the case in hand. By the same token, the greater is the code content, the more susceptible becomes the design aid to potential obselescence as a consequence of code revisions. The employment of a design aid in circumstances outwith those for which the aid was originally developed requires due care on the part of the designer. This applies as much to perseverence with obsolete design aids (formulated around superseded code requirements) as it does to the borrowing of design aids from "foreign" sources. In either case, it is vital that the designer be fully aware of all pertinent distinguishing features.

Many reinforced concrete design aids (especially the simpler varieties) have formative roots which predate the coming of the electronic calculator and the subsequent growth in the "personal computing" field. While associated links with the by-gone era of the slide-rule do not serve alone as sufficient basis for questioning and/or discussing the worth of such design aids, the fact remains that the technological change which brought about the demise of the slide rule has also seen some forms of design aid suffer a marked denegration of relevance. Thus, it is often the case that information which was traditionally gleaned via reference to multiple arrays of tabulated coefficients and the like can now be generated at will by the use of a simple programmable calculator of fairly limited capacity (as judged against current norms).

Just as the electronic calculator overtook what might be termed "lower-order" design aids, so too the personal computer is challenging (and usurping!) the relevance of more complex items such as column design charts. This represents a quite natural progression, following up the computer-assisted compilation of design aids which first began seriously in the late 1960's and early 1970's. Thus, where designers were once content to work with second-hand presentations of computer output (when computing power was a good deal less accessible and/or affordable than it is today), benefits are now perceived in designers actually holding and running the appropriate software.

As for many other spheres of human endeavour, the coming of the computer age raises many interesting questions and possibilities in the context of concrete design. Not least among these questions is how far the process of automation should be taken. (The question as to how far it could be taken is limited only by the powers of imagination). Some designers feel distinctly uneasy about the prospect of computer software going "too far" and perhaps even threatening their own function. The writer does not share this unease, being of the opinion that there is much more to good design than efficient number-crunching processes and the demonstration of formal compliance with governing code requirements. Given the complexity of modern design codes, it perhaps is fitting that a computer be employed to keep track of the various demands.

The New Zealand Reinforced Concrete Design Handbook

Initiated in the late 1970's, when NZS 3101 was still in its draft stages, the New Zealand Reinforced Concrete Design Handbook presents an assortment of design information, covering several main areas:

Reinforcement Data
Members in Pure Bending
Combined Axial/Bending Load
Development

The original handbook - the first of its type in New Zealand - was compiled by the Development Engineering Section of the New Zealand Portland Cement Association with assistance from the Cement & Concrete Association of Australia and Morrison Cooper & Partners. The New Zealand Portland Cement Association, New Zealand Steel Ltd and Pacific Steel Ltd underwrote the costs of the project.

Inevitably the final version of NZS 3101, published in 1982, contained some variations that were not included in the original handbook.

In 1981 the technical section of the New Zealand Portland Cement Association was transferred to the New Zealand Concrete Research Association. The up-dating of the handbook became the responsibility of the NZCRA.

In 1984/85 a new underwriting partnership was formed principally between Pacific Steel Ltd and the New Zealand Concrete Research Association with additional support from the New Zealand Ready Mixed Concrete Association and the New Zealand Reinforcing Steel Fabricators Association Incorporated.

The policy of the partnership is that the handbook should be updated on a continuous basis and that this information be issued without charge to existing manual holders. At the same time the scope of the Handbook has been increased to include computer software such as design programs for rectangular (CONCOL 1) and circular (CONCOL 2) columns subject to axial load and uniaxial bending. Further software developments are planned.

REINFORCEMENT AROUND A LARGE OPENING IN A BEAM

Close to the midspan of the Beam 8-9 of the example 10 storey building, an opening as shown in the figure below is to be provided. The additional reinforcement in accordance with [7.5.6] is to be determined.

(1) The 600 x 200 mm opening is not in a potential plastic hinge region. [7.5.6.4].

(2) From previous analysis it was found that d = 715 mm and b_w = 350 mm.
Area of opening is:

$$600 \times 200 = 120000 > 0.004d^2 = 2045 \text{ mm}^2$$

Hence opening is to be considered as being large. [7.5.6.2].

(3) The maximum shear force at the opening due to the load combination $U = D + L_R + E^o$, i.e. with earthquake induced shear force considered at the development of the flexural overstrength of the beam, is V_u = 310 kN (see figure on page 44). Hence with ϕ = 1.0

(i) $v_i = 310000/(350 \times 715) = 1.24$ MPa $< 0.4\sqrt{f'_c} = 2.19$ MPa

(ii) and height of opening is 200 mm < 0.4d

(iii) and distance to compression edge is 400 > 0.33d.

Hence the opening may be used. [7.5.6.4)

(4) Following the arrangement shown in [Fig. C7.17] the shear stress in the part above the opening where d = 400 - 52 = 348 mm is

$$v_i = 310000/(350 \times 348) = 2.55 \text{ MPa} < 6.00 \text{ MPa}$$

According to [C7.5.6.5]

$$\frac{A_v}{s} = \frac{1.5 \times 2.55 \times 350}{275} = 4.87 \text{ mm}^2/\text{mm}$$

Using 4-R12 legs s = 4 x 113/4.87 = 93 say 90 mm

(5) At both sides of the opening provide full length stirrups to resist $2V_i$ [C7.5.6.6] so that

$$\Sigma A_v = 2 \times 310000/275 = 2255 \text{ mm}^2$$

Provide 5 sets of 4 legged R12 stirrups over a distance of 4 x 90 = 360 mm = 0.5d with total area of 5 x 4 x 113 = 2260 mm^2.

(6) The necessary longitudinal reinforcement arises from the need of having to resist a moment [Fig. C7.17] of:

$$1.5 \times 310 \times 0.5 \times 0.6 = 140 \text{ kNm}$$

Therefore $A_s \cong 140 \times 10^6/[275(348 - 52)] = 1720$ mm^2, use 4-D24 = 1810 mm^2

Development length for D24 bars (from page 46) with making use of heavy

transverse reinforcement, i.e.

$$k_{tr} = \frac{113 \times 275}{10 \times 90} = 34.5 > 24, \quad c = 40 \text{ mm}, \quad \ell_{db} = 784 \text{ mm},$$

is $\therefore \quad \ell_d = \frac{40}{40 + 24} 784 = 490 \cong 500 \text{ mm}$

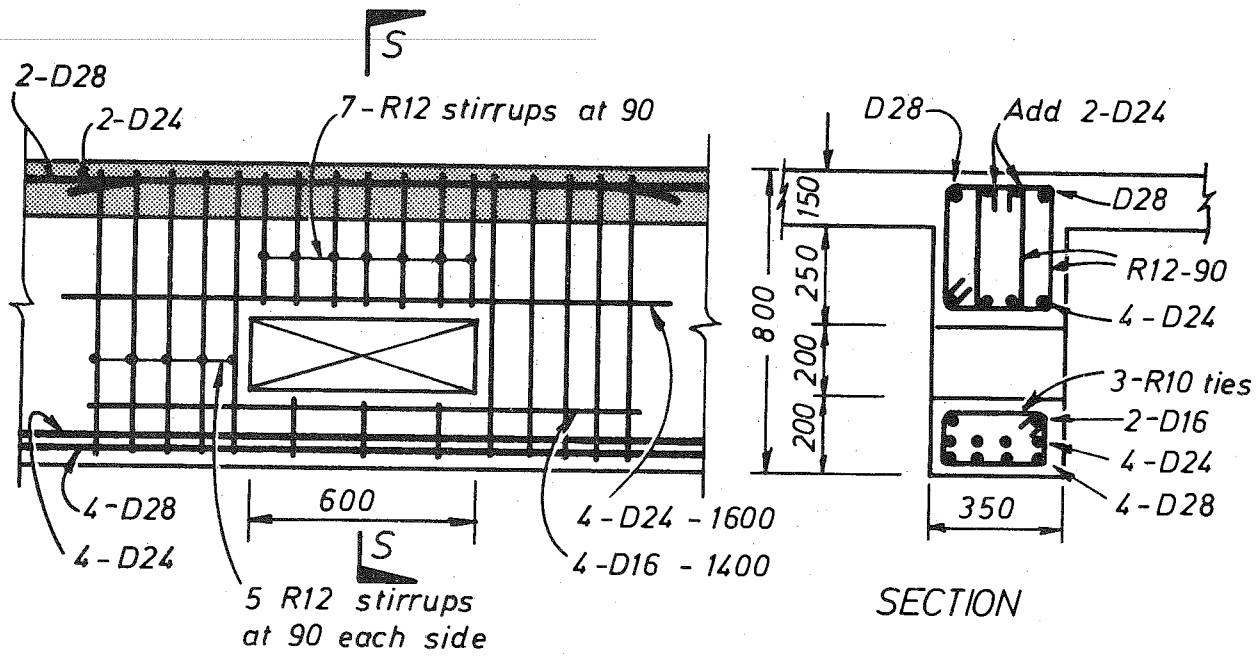

REINFORCEMENT AROUND A LARGE OPENING IN THE WEB OF A BEAM

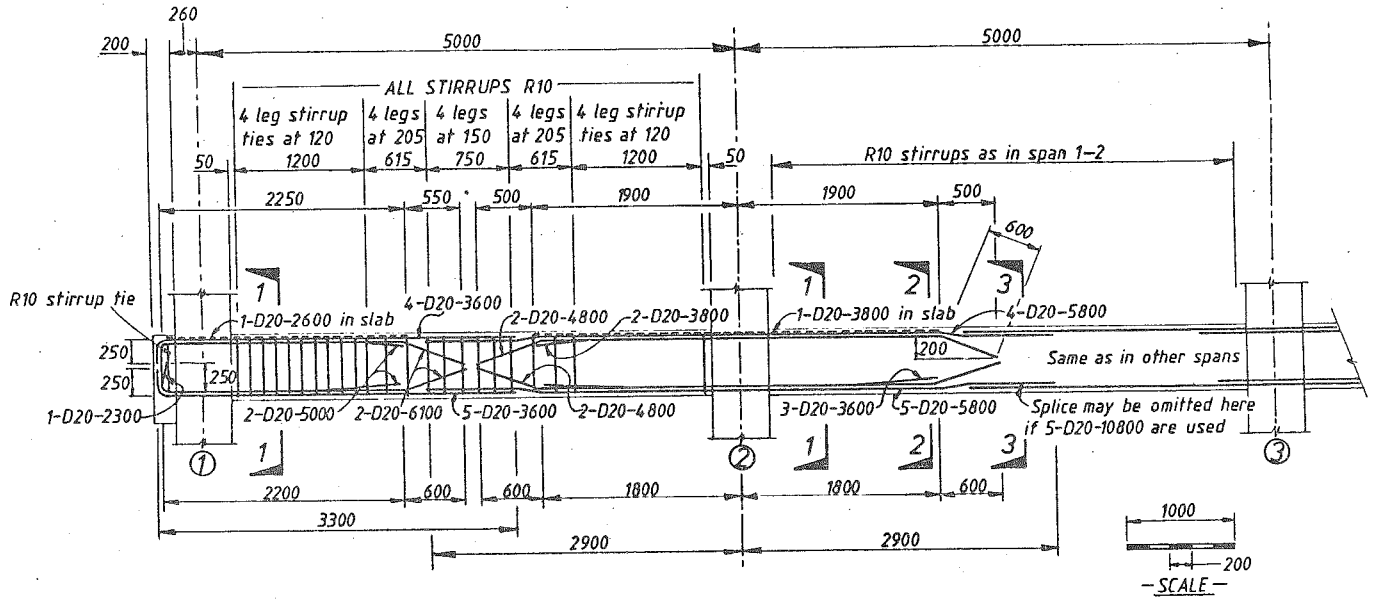

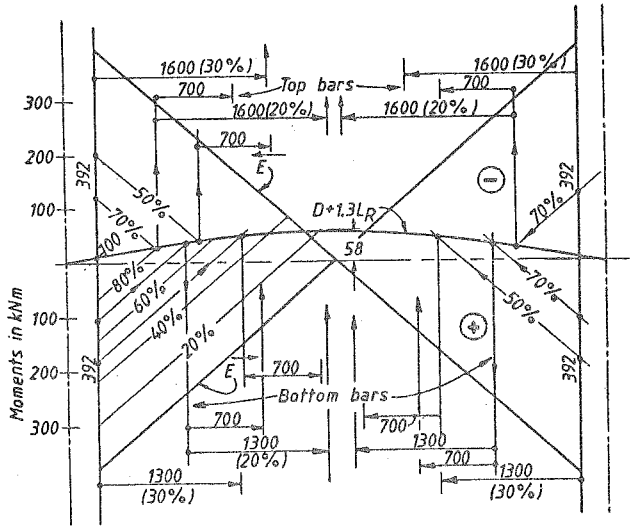

BENDING MOMENTS AND BAR CURTAILMENT

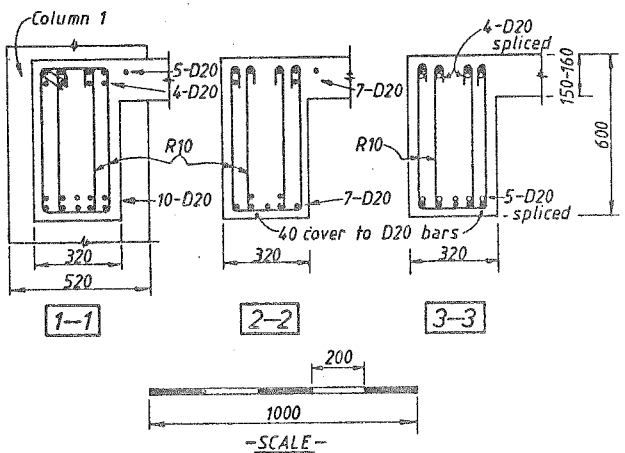

BEAM 1-2-3-4